

Durham E-Theses

CONTROLS ON FACIES DISTRIBUTION AND PROPERTIES IN THE NORTHWEST BORNEO DEEP WATER FOLD-AND-THRUST BELT

DAWING, SUDIRMAN,BIN

How to cite:

DAWING, SUDIRMAN,BIN (2022) *CONTROLS ON FACIES DISTRIBUTION AND PROPERTIES IN THE NORTHWEST BORNEO DEEP WATER FOLD-AND-THRUST BELT*, Durham theses, Durham University. Available at Durham E-Theses Online: <http://etheses.dur.ac.uk/14409/>

Use policy

The full-text may be used and/or reproduced, and given to third parties in any format or medium, without prior permission or charge, for personal research or study, educational, or not-for-profit purposes provided that:

- a full bibliographic reference is made to the original source
- a [link](#) is made to the metadata record in Durham E-Theses
- the full-text is not changed in any way

The full-text must not be sold in any format or medium without the formal permission of the copyright holders.

Please consult the [full Durham E-Theses policy](#) for further details.



**CONTROLS ON FACIES DISTRIBUTION AND
PROPERTIES IN THE NORTHWEST BORNEO DEEP
WATER FOLD-AND-THRUST BELT**

Sudirman Bin Dawing

This thesis is submitted in partial fulfilment of the requirements
for the degree of Doctor of Philosophy at Durham University

Department of Earth Sciences

University of Durham

2021

Abstract

The deep-water fold-and-thrust belt of NW Borneo contains a structurally complex region of active folds. The opening of the South China Sea during Oligocene to Middle Miocene times led to a Southeastward rifting of the continental crust of the Dangerous Grounds. Subduction of oceanic crust to the Southeast took place under the NW Borneo continental margin, with oceanic subduction ending at ~16 Ma. Collision between the Dangerous Grounds and the NW Borneo margin resulted in uplift and erosion of the Crocker Ranges, and shed large volumes of sediment Northwest into the adjacent sedimentary basins. The resultant fold-and-thrust belt hosts up to 8 km thickness of Mid-Miocene to Recent turbidites and submarine fan sediments, closely associated with fold growth. This study provides new interpretations of regional, three-dimensional (3-D), multichannel seismic-reflection profiles, and utilises data from 25 exploration and appraisal wells. The target of the wells is the fan system, located at the crestal part of the thrusting hanging walls of growth anticlines. This research studies the geometry and structural vergence of the folds, sequence stratigraphy, and burial history. Collectively, these are the controlling factors affecting the facies distribution and properties in the study area. Approaches include seismic analysis, well log analysis, petrology, and basin modelling. Fold-and-thrust belt evolution and syn-tectonic deposition were influenced by subduction and gravitational tectonic events, the proximity and variety of sediment provenance, and seabed topography during deposition. There was an important effect of overpressure generated by disequilibrium compaction, which preserved the porosity in the deeper formations. This study identified the individual fold growth magnitude, sediment provenances, depositional settings of the deep-water slope water environment, and accommodation space for the facies compartmentalisation seen in the wells, and models the depositional settings and the submarine channel pathways, with possible high quality reservoir distributions.

Table of Contents

Abstract	i
List of figures	vii
List of tables	xvi
Declaration	xvii
Acknowledgements	xviii
1. Chapter I: Introduction	1
1.1 Project rationale.....	2
1.2 Study aims.....	4
1.3 Thesis outline	5
1.3.1 Chapter II – Study area, data availability and methodology	6
1.3.2 Chapter III – Regional geology of NW Borneo and the study area	6
1.3.3 Chapter IV - Reversal in structural transport direction in the NW Borneo deep water fold-and-thrust belt	6
1.3.4 Chapter V – Depositional, and facies distribution in NW Borneo deep water fold-and-thrust belt	6
1.3.5 Chapter VI – Overpressure occurrence and impact on reservoir quality in submarine fan system of NW Borneo deep water fold-and-thrust belt.....	7
1.3.6 Chapter VII – Discussion, conclusion, and future work.....	7
2. Chapter II: Study area, data availability and methodology	9
2.1 Study area and data availability.....	10
2.2 Methodology	15

2.2.1	Well correlation	16
2.2.2	Sequence stratigraphy	16
2.2.3	2D Seismic and 3D Seismic interpretation and mapping	17
2.2.4	Structural analyses in defining the geometry, verge, and growth of the folds	18
2.2.5	Seismic facies and seismic attribute extraction analyses	18
2.2.6	1D Basin modelling	19
2.2.7	Pressure data, well logs and core properties analyses	20
3.	Chapter III: Regional geology of NW Borneo and the study area.....	21
3.1	Regional geology	22
3.2	Tectono-Stratigraphy	27
3.3	Petroleum system elements and potential	32
4.	Chapter IV: Reversal in structural transport direction in the NW Borneo deep water fold-and-thrust belt	35
4.1	Introduction	36
4.2	Regional Setting of NW Borneo.....	40
4.3	Tectono-Stratigraphy	41
4.4	Data.....	43
4.4.1	Three-Dimensional Multi-Azimuth Seismic Survey	43
4.4.2	Two Dimensional regional seismic lines	44
4.4.3	Well data and reports	45
4.5	Methodology	46

4.5.1	Well correlation	46
4.5.2	Seismic Interpretation and mapping	48
4.5.3	Qualitative and Quantitative Fold Dip Azimuth Analyses	49
4.5.4	Seismic Time Slice Geometry	50
4.5.5	Horizons flattening	51
4.5.6	Fold Expansion Index Quantification	56
4.6	Results	57
4.6.1	Tectonic and Depositional Control on Fold Geometry and Vergence Evolution	57
4.6.2	Evidence from Fold Dip-Azimuth Evolution.....	58
4.6.3	Fold Growth History	62
4.7	Discussion	63
4.7.1	Tectonic and Gravity-Driven Influences on Fold Vergence	64
4.7.2	Syncline Accommodation Space Control on Fold Growth History	65
4.8	Conclusions	66
5.	Chapter V: Depositional, and facies distribution in NW Borneo deep water fold-and-thrust belt	68
5.1	Introduction	69
5.2	Tectono-stratigraphy framework	71
5.3	Stratigraphy sequence framework of the study	73
5.4	Depositional settings and facies associations	77
5.4.1	Deposition accommodation.....	80

5.4.2	Deepwater depositional facies.....	87
5.5	Results.....	95
5.5.1	Well penetration: vertical stacking pattern	95
5.5.2	Characteristics of the basin fills	103
5.5.3	Seismic attribute and facies distribution.....	111
5.6	Discussion	129
5.6.1	Depositional settings and facies distribution controlling factor.....	129
5.6.2	Chronostratigraphic correlation.....	136
5.7	Conclusion.....	141
6.	Chapter VI: Overpressure occurrence and impact on reservoir quality in submarine fan systems of a NW Borneo deep water fold-and-thrust belt.....	143
6.1	Introduction	144
6.2	Tectono-stratigraphy	147
6.3	Overpressure and vertical effective stress.....	149
6.4	Methodology	152
6.4.1	One dimensional burial history modelling.....	153
6.4.2	Pore pressure history and wireline analysis	158
6.4.3	Petrography and sampling.....	161
6.5	Results.....	164
6.5.1	Well correlation and formation pressures	164
6.5.2	Burial history and overpressure evolution	170

6.5.3	Overpressure zones.....	176
6.5.4	NW Borneo DWFTB Overpressure mechanism	179
6.6	Discussion	192
6.6.1	Geopressure compartmentalization	192
6.6.2	Tectono-stratigraphy influence on overpressure	194
6.6.3	Pore fluid pressure and porosity	195
6.6.4	Implications for overpressure in NW Borneo Deep-Water Fold Belt	197
6.7	Conclusions	200
7.	Chapter VII: Discussion, conclusions, and future work	203
7.1	Synthesis	204
7.1.1	Structural evolution: control on reservoir distribution and quality	204
7.1.2	Sequences and associated facies in the study area	206
7.1.3	Depositional setting controls in the Deep-water NW Borneo fold-and-thrust belt:	208
7.1.4	Compartmentalization.....	209
7.1.5	Porosity preservation with overpressure.....	210
7.2	Conclusions	211
7.3	Implications of this study	212
7.4	Future work	214
8.	Appendices.....	218
9.	Bibliography	232

List of figures

Figure 1-1: (A) Regional simplified topography and bathymetry map of NW Borneo, showing the elevation deepening towards the Northwest from the Crocker Range to the Sabah Trough, and bounded by the Dangerous Grounds. Three dimensional (3D) seismic surveys and two dimensional regional seismic lines interpreted in this study cover the study area, with extensions to other geological provinces utilized for horizon correlations with regional tectonic and stratigraphic events. (B) Deep-water NW Borneo location at the South China Sea, to the southeast of Vietnam and to the southwest of Palawan Island, Philippines.	8
Figure 2-1: Offshore deep-water fold belt anticlines, interpreted from a mixture of regional surveys and seismic sections (Grant 2004; Gee et al, 2007, Hesse et al., 2009). Regional seismic cross section A-A' extends from the NW Borneo Trough and Sabah Platform to the NW Borneo (Baram-Balabac) Shelf, from merger of two-dimensional seismic line and three-dimensional seismic surveys (this study).....	14
Figure 3-1: Regional bathymetry map of Southeast Asia consist of the regional fault zone, basin, and sea (from Cullen, 2010) involved in deep-water NW Borneo fault-and-thrust belt tectonic (red dashed box). Abbreviations; Ailao Shan Red River Fault Zone (ASRR), Baram-Balabac Basin (BBB), Balabac Line (BAL), Celebes Sea (CS), Dangerous Ground (DG), East Vietnam Fault Zone (EVF), Lupar Line (LPL), Macclesfield Bank (MB), Mae Ping Fault zone (MP), North Makassar Straits (NMS), Palawan (PAL), ReedBank (RB), South China Sea (SCS), Sulu Sea (SS), Tinjar Line (TL), West Baram Line (WBL).....	23
Figure 3-2: Regional map of Borneo showing DWFTBs around the island modified from Morley et al (2010). The study area in NW Borneo DWFTB and the 3D seismic survey outline and 2D seismic lines are indicated.	24
Figure 3-3: Simplified comparison of regional tectonics (from Cullen, 2010) showing the comparison of (a) The extrusion model adapted from Replumaz et al., (2003); (b) The subduction model (modified from Hall, 2002); (c) The hybrid model of the extrusion and under thrusting at 20 Ma by Cullen (2010).....	25
Figure 3-4: Diagrammatic regional cross section of the Tertiary evolution of Sabah (from Hutchison, 2000 & 2004)	26
Figure 3-5: Source regions supplying sediment towards offshore Borneo. The NW Borneo deep-water fold-and-thrust belt received sediment supplied by the sandy Baram and Champion deltas, sourced by the Western Cordillera of the collision zone in Borneo (from Hutchison, 2000).	29

Figure 3-6: Regional stratigraphy of NW Borneo and key tectonostratigraphic events (adapted from Hutchinson, 2004; Franke et al., 2008; Lambiase et al 2008). Inset image of 2D seismic cross-section x-y (see Figure 2 1 for location) illustrating the key interpreted stratigraphic horizons; TWT—two-way time in seconds. DRU—Deep Regional Unconformity; TCU—Top Crocker Unconformity; SRU—Shallow Regional Unconformity, UIU- Upper Intermediate Unconformity, LIU- Lower Intermediate Unconformity, EOC – Eocene Unconformity, OB- ophiolitic basement; SB—sequence boundary.....	30
Figure 3-7: Merged 2D seismic section BGR-8622 with 3D seismic surveys (Four times vertical exaggeration) crossing all the fold thrust belt from the shelf at the Southeast towards the NW Borneo Trough and Dangerous Ground at the Northwest. The NW Borneo Trough extends to the Dangerous Ground to the NW seems to be higher until possibly Late Middle Miocene, suggesting sediment provenance from the NW. Fold geometry, especially at the buried toe thrust zone, is observed to be more symmetrical until Late Miocene, with vergence to the NW afterwards. The reconstruction of the seismic is by applying horizons flattening at the depositional level.	31
Figure 3-8: Petroleum system of NW Borneo deep-water fold-and-thrust belt showing the Late Miocene reservoir targets of the Kebabangan, Kinarut, Kamunsu and Pink fans (After Jong, et al., 2014).....	34
Figure 4-1: (a) Regional simplified topography and bathymetry map of NW Borneo, showing elevation dropping towards the Northwest from the Crocker Range to the Sabah Trough (b) Deepwater NW Borneo location at the South China Sea.....	38
Figure 4-2: Offshore deep-water fold belt anticlines, interpreted from a mixture of regional surveys (Grant 2004; Gee et al, 2007, Hesse et al., 2009). Regional seismic cross section A-A' extends from the NW Borneo Trough and Sabah Platform to the NW Borneo Shelf.....	38
Figure 4-3: Regional stratigraphy of NW Borneo and key tectonostratigraphic events (adapted from Hutchinson, 2004; Franke et al., 2008; Lambiase et al 2008). Inset: Image of 2D seismic cross-section x-y (see Figure 4 1 for location) illustrating the key interpreted stratigraphic horizons; TWT—two-way time in seconds. DRU—Deep Regional Unconformity; TCU—Top Crocker Unconformity; SRU—Shallow Regional Unconformity, UIU- Upper Intermediate Unconformity, LIU- Lower Intermediate Unconformity, EOC – Eocene Unconformity, OB- ophiolitic basement; SB—sequence boundary.....	39
Figure 4-4: Cross section A-B (shown on Figure 1) of the merged 2D seismic section BGR-8622 with 3D seismic surveys crossing the entire fold-and-thrust belt from the shelf at the Southeast towards the NW Borneo Trough and Sabah Platform (Dangerous Ground) at the Northwest. Horizons are correlated with the main events as compiled by Franke et al (2008). Cross section x-y of the study area shows the Lawa-Menawan and Bestari-Limbayong fold trends covered by the Multi Azimuth (MAZ) 3D seismic data.	52

- Figure 4-5: Depth maps of the interpreted horizons of the study area shows the fold and syncline geometry and vergence direction. 53
- Figure 4-6: Three-dimensional seismic survey time slices in the study area show fold geometry and vergence. The time slices are cut on flat surfaces and provide a surface deepening and younger towards the basin interior (Northwest). Even though it is not possible to specifically relate the geometry with the geological time, the vergence changes from Southeast at -5500 ms to Northwest at -3000 ms..... 54
- Figure 4-7: Merged 2D seismic section BGR-8622 with 3D seismic surveys (Four times vertical exaggeration) crossing all the fold thrust belt from the shelf at the Southeast towards the NW Borneo Trough and Dangerous Ground at the Northwest. The NW Borneo Trough which extends to the Dangerous Ground to the NW seems to be higher until possibly Late Middle Miocene. This might suggest the possible sediment provenance from the NW in addition to the Crocker Formation deposition in Sabah. Fold geometry, especially at the buried toe thrust zone, is observed to be more symmetrical until Late Miocene, with vergence to the NW afterwards..... 55
- Figure 4-8: (a) The 3D view surfaces give a direct observation of the geometry and verge direction of the folds. (b) The point selection for the measurement of the dip and azimuth are scattered randomly in the polygon areas, to represent the distribution. (c) Fold dip and azimuth streonet plots of each horizon are extracted from the gridded depth map bounded by the deepest synclines in both limbs of the fold. Both 3D views of the gridded horizons and dip azimuth measurements indicate vergence changes from mainly towards Southeast during the early Middle Miocene (DRU), becoming symmetrical in Late Miocene (SRU) and towards the Northwest during Pliocene until Recent times. 59
- Figure 4-9: Simple restoration by applying horizons flattening of cross section x-y (shown on Figure 4-1) using the MAZ 3D seismic depth gridded horizons in the study area. Restoration was performed by applying horizon flattening to better understand the fold geometry and vergence of each horizon. The NW Borneo Trough to the Dangerous Grounds to the Northwest seems to be higher, until possibly end of the early Middle Miocene, marked by the DRU. During the SRU event in the Late Miocene, gravity-driven influence on fold growth caused symmetrical folds as the sediment influx came from the Crocker Range. 60
- Figure 4-10: (a) Fold growth history measurement after Thorsen (1963) and Groshong (1993, 2006), for analysing the development of fold growth through time. The method uses the Expansion Index (E) measurement (flank thickness over crest thickness). (b) An E of 1 means no growth. An E value > 1 indicates upward growth of the anticlinal crest during deposition, whilst E < 1 indicate tectonic thickening. 61
- Figure 4-11: Summary of the identified phases of fold development and growth history in NW Borneo deep-water fold-and-thrust belt, with the tectonic and gravity-driven controlling mechanisms..... 67

Figure 5-1: The study area located in the middle part of the NW Borneo deep-water fold and thrust belt aligned parallel with Sabah coast. Borneo has at least 4 other deep-water fold-and-thrust belt all around the island. Modified from Morley et al. (2011).

71

Figure 5-2: Deep-water NW Borneo fold-and-thrust belt evolution and the horizons correlated in this study with the regional NW Borneo chronostratigraphic (Modified from Grant, 2004). 78

Figure 5-3: Log signature interpretation of the stratigraphic systems tracts and associated facies. Gamma-ray (GR) log is cut off at 80 API applied on to differentiate shale, and 70 API to separate silt from sand. The GR is calibrated with lithology description from cuttings and core sample. DTCO cross over with GR and density with Neutron log to confirm the lithology changes and shale baseline trend. 79

Figure 5-4: Various accommodation settings of seafloor profiles from the central Gulf of Mexico by Prather (2000, 2003). 83

Figure 5-5: Seabed topography of the study area showing the variety of accommodation space of the slope and intra-basin settings in deep-water fold-and-thrust belt of NW Borneo. 84

Figure 5-6: Accommodation space model of the study area based on the topography of the seabed. The model is applicable for the deposited fan systems from Middle Miocene to present-day as the process and depositional settings are the same. 85

Figure 5-7: Depth structural map figure (Pink, Kamunsu and Kinarut map) to show the well locations based on structural trap optimized location. This figure highlights the challenges in modelling the lateral depositional settings and facies particularly at the synclinal parts of the area. 86

Figure 5-8: Well log expression of the facies penetrated by well in the area and the lithology and facies types as classified by Mayall et al., 2006. 87

Figure 5-9: Seismic characterization of the facies based on Beaubouef et al., 2000 classifications of the facies in the deep-water submarine fan settings (Figure 5-9a, b, c & d) and the seismic cross section example from this study (Figure 5-9e). Abbreviations; Drape Complex (DC), Levee channel complex (LCC), Distributary channel-lobe complex (DLC), Channel Lag (CL) and Mass Transport Complex (MTC). 88

Figure 5-10: Well correlation of Menawan-1S1 and the wells in Limbayong structure with the correlated sequences and the maximum flooding surfaces (MFS) picked as the correlation marker in this study. The facies associated with the well log response and lithology description are defined and matched with the second order sequence stratigraphy system tract. 99

Figure 5-11: Well correlation of Lawa-1 and the wells in Bestari structure with the correlated sequences and the maximum flooding surfaces (MFS) pick as the correlation marker in this study. The facies associated with the well log respond and lithology description defined and matched with second order sequence stratigraphy system tract.	104
Figure 5-12: Seismic cross section of the Menawan-Limbayong-Petai structures with the sequences and interpreted horizons show the seismic amplitude characteristic differences defining the interlayering sequences in the synclinal area and the anticline of the fold- thrust structure.	107
Figure 5-13: Interpreted section of the Menawan-Limbayong section with the facies associated with the seismic characteristics calibrated with the facies defined from wells.	107
Figure 5-14: Seismic cross section of the Lawa-Bestari-Lumutan structures with the sequences and interpreted horizons show the seismic amplitude characteristic differences the interlayering sequences and between the synclinal area and the anticline of the fold- thrust structure.	110
Figure 5-15: Interpreted section of the Lawa-Bestari section with the facies associated with the seismic characteristics calibrated with the facies defined from wells. ...	110
Figure 5-16: (a and a') Seismic slices at 3760 ms at proven Kikeh and Gumusut-Kakap Fields seismic attributes at production reservoirs shows high amplitude at the field area. (b and b') and (c and c') show the Bestari and Limbayong cross sections with time slices at 2194 and 2658 ms each shows the RMS amplitude response at the reservoir penetrated by the wells in each structure high.	117
Figure 5-17: Seismic cross section with Sweetness attribute extraction, showing the horizons used to extract the RGB and RMS blending attributes (Figure 5-18 to Figure 5-24).	120
Figure 5-18: Seabed attribute of the blending of RMS, and sweetness attribute of the present-day seabed shows the submarine channels flowing down from the shelf-break in the southeast of the area. The obvious difference, between the southern area, with presence of bright yellowish attribute, represents the mixture, with coarser materials carried down in the MTC from the canyon complexes. In contrast the northern area with darker attribute indicates shale prone deposits.	121
Figure 5-19: MFS 2.6 horizon attribute blending, 500 m below the present-day seabed, shows an obvious difference between the unconfined and confined depositional settings. In the southern area of the Limbayong fan a series of submarine channels flowed down from the intra-slope canyons towards the basin in an unconfined setting and formed a submarine fan lobe further outboard. Whilst in the northern area at the Lawa-Bestari structures, confined accommodation spaces near the fold ridge caused the change in direction of the sediment flow towards the northeast, parallel to the fold trend.	122

Figure 5-20: Lingan submarine fan horizon attribute blending shows three dominant submarine channel systems flowing down to the basin from the southeast in between the fold highs. The sediment supply at this time is believed to be not huge, to accommodate and fill up the accommodation space available in the basin. Submarine channels flowing through the folds in Menawan and Limbayong could be seen making the high a bypass area, and deposited the sandstone in the footwall of the Limbayong structure. Lesser sediment in the Lawa-Bestari trend caused the sandstone to be deposited mainly in the footwall of Lawa fold; a small amount reached the northern flank of Bestari fold..... 123

Figure 5-21: The horizon attribute blending at the Yellow submarine fan displays the submarine flow around the Limbayong structural high, and forms a submarine fan in the intra-slope basin area. Increased sandstone deposition in the synclinal area of the Lawa footwall could be seen as the submarine channel flow across the bypass zone at the Lawa fold. A thinner submarine channel could reach the Bestari structural high, particularly at the Bestari-3 area, as shown by the amplitude colour response. 124

Figure 5-22: Pink submarine fan horizons attribute blending indicates increased sandstone at the Lawa and Bestari structures, with submarine fan lobes developed in the syncline in between the folds in the Lawa footwall inter-slope basin. However, the wells in Bestari might be receiving a different system of submarine channel sediment, as lateral continuity seems to be poor between Bestari-3 and Bestari-2. There is a sharp contact between the sand body and a possible MTC in the intra-slope basin at the footwall of Menawan. The sand prone submarine channel might be sourced from the southwest, and cut by the MTC deposition from the southeast. 125

Figure 5-23: Upper Kamunsu reservoir seems to be well developed on top of the Limbayong southwestern culmination, covering the Limbayong-1 well location, decreasing towards Limbayong-2 and totally separated from Limbayong-3/ST1/ST2. Even though the sand covers the crestal part of the structure, it still depends on individual submarine channel system deposition, making it laterally separated between the three well penetrations in those three areas in the Limbayong structure. In Bestari, the deposition was mainly in the intra-slope basin syncline area, and thins towards the crestal part of the structure..... 126

Figure 5-24: Lower Kamunsu reservoir is well developed on top of the Limbayong southwestern culmination, covering the Limbayong-1 well location, decreasing towards Limbayong-2 and totally separated from Limbayong-3/ST1/ST2. Even though the sand covers the crestal part of the structure, it still depends on individual submarine channel system deposition making it laterally separated between the three well penetration in those three areas in Limbayong structure. In Bestari, the deposition was mainly at the intra-slope basin syncline area, and thins towards the crestal part of the structure. 127

Figure 5-25: The horizon attribute blending of RMS and Sweetness attribute for the Kinarut submarine fan shows a rich reservoir sand being supplied to the basin, with

a good spread of the bright amplitude in the synclinal part, thinning towards the crest of Bestari but possibly developed better in the Limbayong structure. However, it is still difficult to prove the lateral continuity of the submarine channel system in between the wells drilled in Limbayong and Bestari, as each area was charged by different submarine channel system, except for possibly the sand deposited in the syncline, and flowed as one single huge stream in the southwest to northeast direction..... 128

Figure 5-26: Well correlation interpretation sections for the Lawa and Bestari wells, flattened at seabed, integrating information from the well log, lithology description, seismic facies and formation pressure. Data suggest a bypass zones dominated by either the MTC or “shale diapirs” at the Lawa-1 well, whilst at Bestari the sand encountered is proven to be charged by a different submarine channel stream. .. 134

Figure 5-27: Interpreted correlation of Menawan-1ST1 and the wells in the Limbayong structure, flattened at seabed. The sand deposition in Limbayong is thicker, with more layers as compared to Bestari due to the closeness to the source of the sediment. The upper part of Menawan-1ST1 and Limabyong-1 was dominated by MTC deposition from the multiple submarine canyons at the shelf-break. From below the Kamunsu reservoir and deeper, there are possibly the “shale diapirs” popping up from the deeper Setap Shale formation. 135

Figure 5-28: Interpretation from seismic section crossing (a) Lawa-1 and Bestari-1 and (b) Menawan-1ST1 and Limbayong-2 wells, showing the dominance of sand deposition at the synclinal area, forming a possible inter-pod depositional model, thick at the syncline and getting thinner towards the crest. The “Christmas tree” shaped of the possible shale diapirs could be seen in all structures, popped out higher at Lawa and Bestari, lower but wider at Limbayong and Menawan..... 138

Figure 5-29: Chronostratigraphic chart of Lawa and Bestari structures, summarizing information and analyses, results of the well logs, lithology, seismic facies, and attribute extractions..... 139

Figure 5-30: Chronostratigraphic chart of Menawan and Limbayong summarizing information and analyses result of the well log, lithology, seismic facies, and attribute extractions..... 140

Figure 6-1: The study area is in the middle part of the NW Borneo deep-water fold and thrust belt aligned parallel with Sabah coast. Offshore Borneo is the location of at least 4 other deep-water fold-and-thrust belts. Figure modified after Morley et al. (2011). 145

Figure 6-2: Depth structure map of Top Kamunsu shows the study area with the location of the thrust folds. The well data used in this study are located along the crest of the structures and are among the latest drilled in the deep-water fold and thrust belt province and the area covered by the 3D multi-azimuth seismic. 146

Figure 6-3: NW Borneo stratigraphy chart with the highlighted reservoir of interest in this study.	151
Figure 6-4: Burial history of Bestari-1 well located on the crest of the Bestari growth structure (See Figure 6 2 for locations). Three phases of the fold evolution from tectonic phase, symmetrical phase, and gravitational influence are recognised. Over 2000 m of submarine fan sediments have been deposited in the basin in the last 5 Ma. 155	
Figure 6-5: Model calibration for Bestari-1 well for the porosity, pressure, and temperature. The porosity calibration matches well with the model. However, even after optimization the pressure and temperature show a higher trend in the well as compared to the model.	156
Figure 6-6: The wireline logs as indicators of the top of overpressure in wells (modified after Bowers, 1994).	159
Figure 6-7: Response of formation acoustic velocity and density to effective stress (modified after Bowers, 1994). The same approach is used to analyse the dataset in the study area, to investigate the trend, and the possibility of generating overpressure other than disequilibrium compaction.	159
Figure 6-8: Density relationship with effective stress. Normal compaction or primary compaction profile, of the loading trend relationship shows increasing trend of effective stress to increase in density. The unloading profiles, however, display the opposite trend with increased density resulting in decreased effective stress. Multiple unloading profiles can potentially exist in one well (modified after Lahann et al., 2011).	160
Figure 6-9: Relationship between porosity with effective stress (Modified after Gouly et al., 2012).	160
Figure 6-10: Formation pressure divided into reservoirs (submarine fan systems).	167
Figure 6-11: Well correlation combining well log trends, seismic interpretation, biostratigraphy, and formation pressure data.	168
Figure 6-12: Schematic cross-section of the reservoir spatial and temporal distribution.	169
Figure 6-13: Burial history temperature plot for (a) Bestari-1 and (b) L3. Each model shows the folds have three phases of evolutions with the Limbayong structure seeming to be in the deeper part of the basin from the Eocene to Late Miocene. Both structures show temperature history of less than 100 °C for the reservoir level. .	174
Figure 6-14: Pressure and temperature (isoline) history of wells in the Bestari and Limbayong structures for the submarine fan reservoirs.	175

- Figure 6-15: Overpressure trend of the wells in both folds generally shows an increase with depth, with an exceptional trend of the Bestari-2/ST1/ST2 holes. Overpressure ramp-up from the Bestari-2/ST1/ST2 trend around 200 psia at 2200 m TVDSS and a significant 700 psia increment at 2400 m TVDSS. The Bestari-1 well, however, displays exceptional continuous increment of overpressure through depth as compared to the other wells..... 177
- Figure 6-16: Bestari-1 well logs (a) show changes in at least three depths in all the logs whilst Bestari-2/ST1/ST2 well logs (b) only show two possible trends throughout the well. 178
- Figure 6-17: Relationship between VES and acoustic/density of different overpressure mechanism and the acoustic velocity-density cross plot shows mainly a loading trend of disequilibrium compaction and an unloading trend in the Bestari-1 well..... 180
- Figure 6-18: Compressional velocity and density plots against vertical effective stress segregated by reservoirs for Bestari-2/ST1/ST2 and Limbayong-1ST1. Both wells are representative of wells in the Bestari and Limbayong structures, except for the Bestari-1 well, and show a disequilibrium compaction trend without any unloading trends as the overpressure generation mechanism. 181
- Figure 6-19: Bestari-1 well porosity, compressional velocity and density plots against vertical effective stress, showing both disequilibrium compaction and unloading curve. 185
- Figure 6-20: Temperature history of Bestari-1 and Bestari-2/ST1/ST2 wells for the deltaic fan reservoirs..... 186
- Figure 6-21: Bestari-1 well thin section and SEM (modified from Corelab Bestari-1 post evaluation report) sample, representative of the Kamunsu B sandstone and Kinarut sandstone. The black filled circle in (a) is the sample chosen to be looked in detail for the petrography, SEM and XRD for the clay mineralogy transformation. 190
- Figure 6-22: Bestari-2/ST1/ST2 well thin section and SEM micrographs (modified from Corelab Bestari-1 post evaluation report). Sample representative of the Pink sandstone and Kamunsu B sandstone. The black filled circle in (a) is the sample chosen for petrography, SEM and XRD analyses. 191
- Figure 6-23: Dip line seismic section crossing Bestari-1 and Bestari-2/ST-1/ST2 well locations, showing the gas pocket at the shallow level close to seabed migrated from the deeper level, through the thrust fault. 199

List of tables

Table 2-1: Wells utilised for the study.....	13
Table 6-1: Well data availability used in this study. A total of 10 wells were analysed across 4 growth folds.....	152
Table 6-2: Lithology type and respective thickness of the modelled layers for the 1D Basin Modelling input.....	157
Table 6-3: Samples from Bestari-1 and Bestari-2 wells were sampled for thin section, SEM, and XRD analyses by using side-wall core plugs and conventional core recovered from both wells.....	163

Declaration

I declare that this thesis, which I submit for the degree of Doctor of Philosophy at Durham University, is my own work, except where acknowledgement is made in the text, and not substantially the same as any work which has previously been submitted at this or any other university for any degree, diploma, or other qualification.

July 2021

© Copyright, Sudirman Bin Dawing, 2021

The copyright of this thesis rests with the author. No quotation from it should be published in any form without the author's prior written consent. All information derived from this thesis must be acknowledged appropriately.

Acknowledgements

In the name of Allah, The Most Beneficent and The Most Merciful. All praises and gratitude to the Almighty God for all the blesses to me, and with His permissions this research can be accomplished.

Special thanks to the Leadership Team of PETRONAS, for the opportunity given for me to pursue my PhD under the Staff Development Program. Appreciation to the Upstream Exploration in Petronas Carigali and Malaysia Petroleum Management for the permission in utilising PETRONAS data for the research.

I would like to thank my supervisory team for their support and guidance over the course of this research. I am personally grateful to Stuart Jones for his guidance, patience, and kindness. I sincerely appreciated the technical discussions, advise and motivations. Thank you to Mark Allen for always challenged me to look things from different perspective and bigger view. The critical thinking and guidance during the writing of the thesis highly appreciated. Thank you to Jonathan Imber, for the help at the early stage, your kindness and help was very helpful for me at the beginning of this research.

Thank you to the review team, Ken Mccaffrey and Fabian Wadsworth for the annual reviews. Enjoyed the discussion and appreciate the advice given during the review sessions.

I would also like to thank everyone in the Department of Earth Sciences at Durham University that has contributed in any form to making this PhD programme a success, from the fellow post graduate students, support staffs, to the administrative and finance offices.

Special thanks to Schlumberger for the PETREL and PETROMOD software. Thank you to ELIIS for the Paleoscan software academic license.

My high appreciation also goes to the PETRONAS Sponsorship, Student Management and Development department for the support during my 4 years journey in the UK. Special thanks to Kak Rozaini Rafar, Nizam Ahamad, Anes Juwita, Rohana Abu Jasman, Halim Rauf and the others in the HRM.

My special thanks also go to my mentors and coaches in PETRONAS for the advice, discussion, and support before and during my research, they are Suhaileen Shahar, Azli Abu Bakar, Nasaruddin Ahmad, Mahadir Ramly and the others not mentioned here.

To friends and colleagues in Malaysia for the technical discussion and moral support, Faizal Idris, Muiz Abidin, Shakila Mustaffa, Hishamuddin Ismail, Nizar Othman, Leng Chai's group, and all of the many others, thank you so much.

To my friends in Durham, the Malaysian Community, Indonesian Community, the DUISOC community and the others not mentioned, thank you for the friendship, support and help for the last 4 years.

My high gratitude to my parents, Hj. Dawing and Hj. Sufiah, who taught me everything about life, for the love and motivation for me to move forward every day. The same goes to all of my family members for the prayer and support.

Finally, I thank Yusnizar Julaidi, my beloved and beautiful wife, who has been with me in every step and junction, for always believe in me, and for the encouragement and support. It never easy with four kids, in foreign country and far from family, but you make everything easy for me and the kids. To my kids, Ilham Shirazy, Wiesha Nailah, Uwais Muhammad and Nairah Ruqayyah, thank you for always make me laugh and entertain me whenever I feel like drowning. Love you all, and thank you.

Chapter I:

Introduction

1.1 Project rationale

Interest in deep-water fold-and-thrust belts (DWFTBs) in areas such as the Gulf of Mexico, Niger Delta, Northwest Borneo, the Brazilian Margin, West Africa (Angola and Congo) and the South Caspian Basin has surged in the last few decades following advances in drilling technology by the oil industry in deep-water, and the associated anticlines (Morley et al., 2011). Thrust-related folds form hydrocarbon traps in many fold-and-thrust belts, from the subaerial fold belts such as in the Zagros of Iran and Iraq, and the sub-Andes, to deep-water fold belts such as in Northwest Borneo and Niger Delta fold-and-thrust belts (McClay (2011).

The development of thrust fault-related fold structures, the evolution of hanging wall folds, and their recognition in two-dimensional (2D) and three-dimensional (3D) data are vital in exploration and exploitation of hydrocarbons in deep-water fold and thrust belts (McClay (2011). The presence of thick, porous, and permeable reservoirs capable of sustaining high production rates is the critical subsurface factor determining the commercial success in deep-water hydrocarbon exploration ventures (Lambiase et al., 2013).

Recent advances in data acquisition and exploration for hydrocarbons in deep-water frontier areas have not only helped understand the depositional styles of the shelf-slope-basin-floor sedimentary deposits (Posamentier and Kolla, 2003; Sawyer et al., 2007; Kneller et al., 2016), but have also helped predict and mitigate the geohazards associated with such deposits (Ostermeier et al., 2002; Winker and Stancliffe, 2007a). Taking the deep-water exploration in the Gulf of Mexico (GOM) as an example, provides an

opportunity to understand the interactions among sediment supply, structural dynamics, sea-level changes, salt tectonics, and the resultant overpressure. Overpressure exists in the very rapidly deposited low permeability mudstones and is a precursor for large regional submarine landslides (Flemings et al., 2008).

In the Northwest Borneo deep-water fold-and-thrust belt, several substantial oil and gas discoveries prove the ideal combinations of structure, reservoir, charge, and seal in the structurally complex and actively deforming areas, such as the Kikeh, Gumusut, Kakap, Keabangan and Kamunsu East fields. These fields result in excess of 200 million barrels oil equivalent reserve (Ingram et al., 2004). Despite the discovery and proven petroleum system, the costly deep-water exploration drilling of the wells in the Bestari, Menawan and Lawa folds failed to find a commercial volume of hydrocarbons, with failure mainly associated with reservoir presence, lateral distribution and quality variations between wells drilled on the same structure.

This study was aimed to understand reservoir distribution and quality issues in NW Borneo deep-water fold-and-thrust belt, by analysing the fold-and-thrust belt evolution. and the depositional setting of the deep-water submarine sediments.

To get a better understanding of the reservoir distribution and effectiveness in these structural and depositional settings, the controlling factors of the facies deposition need to be understood. Therefore, in this research, the research questions to be addressed are:

- 1) Regional tectonic influences on fold-and-thrust belt evolution, as these are the main factors controlling the depositional setting regionally and the localization of fold-thrust structure.
- 2) Whether localized kinematic events had a greater influence on the accommodation space for deposition than the regional trends.
- 3) How multiple depositional provenances affect the variability of the facies distribution.
- 4) How vertical effective stress (VES) and high pore fluid pressures influenced the porosity preservation in the deeper and older formations.

1.2 Study aims

- 1) To establish the fold-and-thrust belt evolution phases by analysing the geometry and fold vergence of the folds, utilising a Multi-Azimuth (MAZ) three-dimensional (3D) seismic survey.
- 2) To use the interpreted seismic horizons from the 3D seismic survey in analysing the fold growth for each structure in the study area, and the impact on the deep-water submarine fan depositional settings.

- 3) To use well data, interpreted 2D and 3D seismic surveys and seismic attribute extractions in understanding the depositional setting variations of formations penetrated by the wells.
- 4) To use the well pressure, well logs and formation sample analyses to identify the overpressure generating mechanisms in each well. The mechanism of the overpressure generations will be used to establish relationships of the reservoir quality variations and connectivity between wells in the same and different structures.
- 5) To use the knowledge of the fold evolution, depositional settings and the geopressure relationship to model the reservoir lateral and vertical distribution in the NW Borneo deep-water fold-and-thrust belt.

1.3 Thesis outline

This thesis organized into six chapters to document the aims, objectives and outcomes of this study. This chapter (Chapter 1) outlines the contents of the thesis and provide the context of the study. Chapters are described individually below. Chapters 4, 5 and 6 are the main data sections of the thesis, have been written as standalone manuscripts to be submitted for publication in peer-reviewed journals. Therefore, the chapters contain specific introduction, background, discussion and conclusion and content-specific synopsis of the material in Chapter 2 and Chapter 3. Chapter 4 was presented at the 2020 AAPG Annual Convention and Exhibition (29 September – 1 October) and Chapter 6

was presented at Geopressure 2021 Conference (23-25 March 2021) hosted by Durham University and the Geological Society of London.

1.3.1 Chapter II – Study area, data availability and methodology

This chapter is an introduction to the study area and the available data used this study. A summary of the main methods used in the study is briefly explained in this chapter.

1.3.2 Chapter III – Regional geology of NW Borneo and the study area

This chapter provides geological background to the study, introduction to the study area and summary of the geology in the NW Borneo deep-water fold-and-thrust belt, based on published references.

1.3.3 Chapter IV - Reversal in structural transport direction in the NW Borneo deep water fold-and-thrust belt

This chapter uses three-dimensional (3D) seismic data to define fold-and-thrust belt evolution. There is documentation of an apparent reversal in structural transport direction between early and later mature stages of fold development, based on the geometry, fold vergence and fold growth analyses defined in detail in this chapter.

1.3.4 Chapter V – Depositional, and facies distribution in NW Borneo deep water fold-and-thrust belt

This chapter outlines the utilization of well data and 3D/2D seismic sections in identifying the depositional setting and associated facies of the formations penetrated by wells, and the wider distribution throughout the anticlinal and synclinal growth folds. The usage of sequence stratigraphy, seismic facies and seismic attribute extractions to classify the facies and model the depositional settings, is illustrated in this chapter.

1.3.5 Chapter VI – Overpressure occurrence and impact on reservoir quality in submarine fan system of NW Borneo deep water fold-and-thrust belt

Well data of the well logs, formation sample analyses and geopressure data are integrated in analysing the overpressure generation mechanism in the wells located along growth folds. Relationships between tectono-stratigraphy and the formation pressure trend are established in this chapter. The role played by overpressure and low vertical effective stress for arresting porosity loss and maintaining reservoir quality of the deep-water submarine fan sandstones is explored.

1.3.6 Chapter VII – Discussion, conclusion, and future work

This chapter synthesizes the discussion from the preceding chapters with implications for other deep-water fold-and-thrust belt settings globally. Conclusions for the thesis are presented and areas for future research are suggested based on the key findings developed in this thesis.

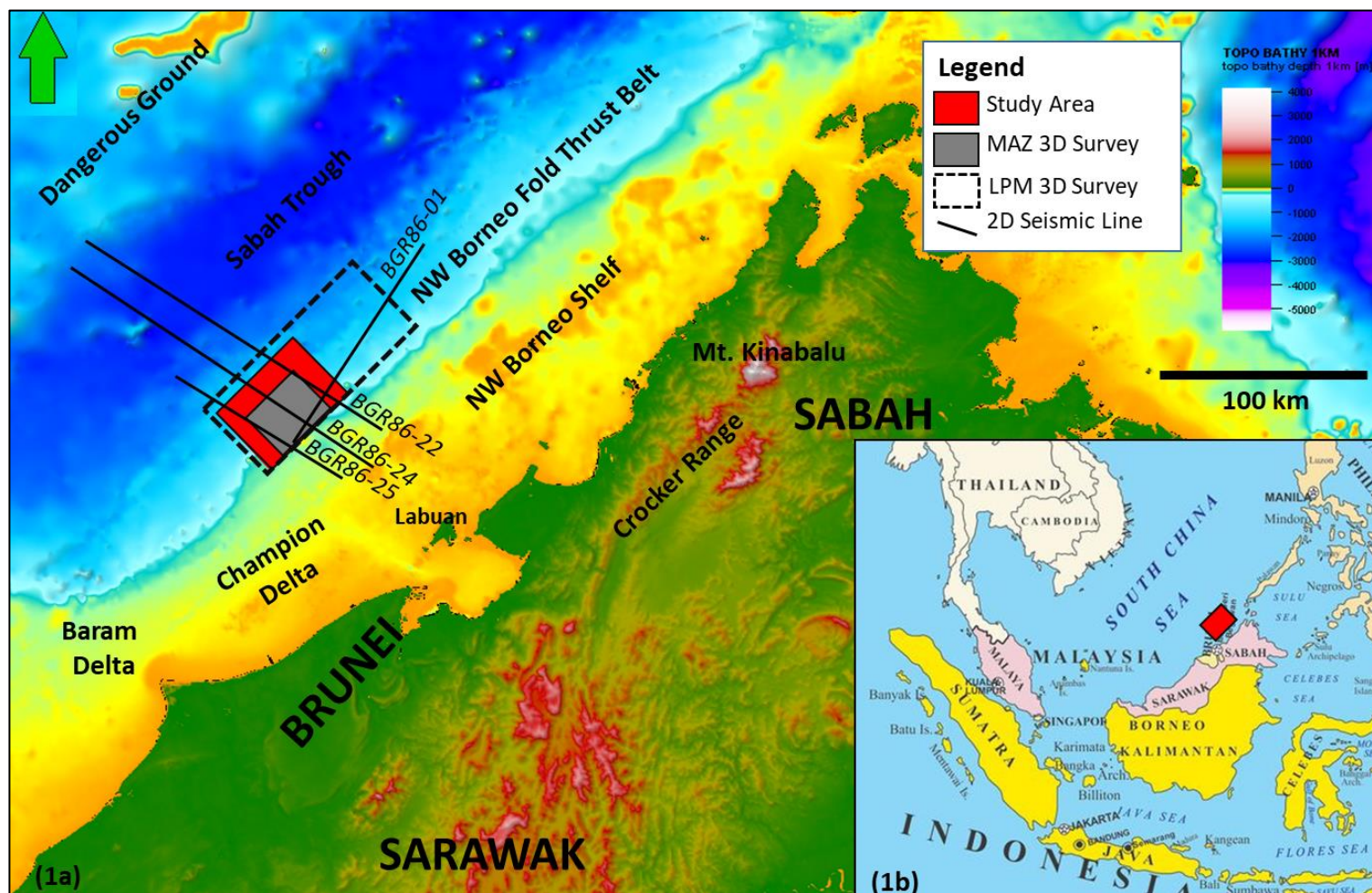


Figure 1-1: (A) Regional simplified topography and bathymetry map of NW Borneo, showing the elevation deepening towards the Northwest from the Crocker Range to the Sabah Trough, and bounded by the Dangerous Grounds. Three dimensional (3D) seismic surveys and two dimensional regional seismic lines interpreted in this study cover the study area, with extensions to other geological provinces utilized for horizon correlations with regional tectonic and stratigraphic events. (B) Deep-water NW Borneo location at the South China Sea, to the southeast of Vietnam and to the southwest of Palawan Island, Philippines.

Chapter II:

Study area, data availability and
methodology

2.1 Study area and data availability

Northwest Borneo Province is located offshore, to the west of Sabah (Borneo Island), in the east part of Malaysia consist of the Inboard and Outboard Belts. The Inboard Belt mainly on the shallow water part of the offshore, ranging from 10m to 150 m, whilst the Outboard Belt covering the deeper water, ranging from 150m to 2000 m (Figure 2-1).

The study area (Figure 2-1) covers a total of 1820 km², covering folds and underlying thrusts along the modern NW Borneo deep-water slope. Water depth ranges from 300 m to 2000 m, deepening towards the Northwest. The folds are elongated Northeast-Southwest, parallel to the Sabah coastline. The area selection is justified by the availability of the latest seismic survey, and the number of wells drilled in this part of the NW Borneo deep-water fold-and-thrust belt. This study focuses on the Lawa-Menawan and Limbayong-Bestari fold trends, as recent wells drilled in these two structures provide comprehensive data for detailed analysis and calibration.

All data utilized for the research are PETRONAS proprietary data. The data utilization is bounded by the Confidentiality Agreement between PETRONAS and Durham University for the purpose of this study.

The exploration, appraisal and development wells are available in the study area. All well data and reports were utilized for horizon correlation and lithology calibration. Eight wells drilled on the Bestari-Limbayong and Lawa-Menawan folds are the focus for detailed analysis, as these wells are the most recent, with complete data and reports available (Table 2-1). The total depths of the wells from sea level range from 1000 m to

the deepest of 4300 m. The data include raw and processed logs, drilling samples from cuttings, side wall core and conventional core, pressure data and drilling parameter data and logs. Most of the well reports including the pre-drill, operation and post-drill reports were available for this study. The reports from the wells are as follows:

1. Well proposal
2. Geological well completion report
3. Well evaluation report
4. Drilling end of well report
5. Mudlogging final report
6. Geopressure final report (including pressure data: RFT, DST, mud weights)
7. Wireline logging final report (e.g., ZVSP, Dual OBMI, Sonic Scanner etc.)
8. Core and geological sample report (e.g., Biostratigraphy, Sedimentological, Petrological, Petroleum geochemical etc.)

The wells were mostly drilled to target the Middle Miocene submarine fan system at a depth range from 1500 m to 3200 m from subsea, mainly located towards the crestal parts of the folds. Therefore, a limitation for this study is that there are no wells drilled in the synclinal part of the structures. The three-dimensional multi azimuth (3D MAZ) Q-Marine OBLIQ Pre-Stack Time Migration (PSTM) seismic survey was acquired in 2012 and processing was completed in 2014. The survey size is approximately 1500 km² full fold and 520 km² image coverage. The acquisition of the seismic was in multi-azimuth directions, which are namely Azimuth 1 in the North-South direction, Azimuth 2 in the Northwest-Southeast direction and Azimuth 3 taken from the existing Sabah LPM 3D seismic in the Northeast-Southwest direction. The seismic data were acquired in 2 ms

sample rate, 8000 ms record length with 72 nominal folds for the azimuths 1 and 2. The objective of the survey being acquired in multi-azimuth was to improve the imaging of the structures. The processed 3D MAZ OBLIQ PSTM data were then merged with the 2013 reprocessed Sabah LPM 3D seismic, to attain better coverage of the deep-water fold-and-thrust belt. For this study, the merged seismic survey area was cropped down to 1820 km², focusing on the folds with available wells. The polarity of the seismic follows the Society of Exploration Geophysics (SEG) convention, with an increase in acoustic impedance recorded as a negative number and as a minimum phase. The quality of the MAZ 3D seismic was variable depending on the area. The image and amplitude continuity are good to fair generally down to 5500 ms, especially at the synclinal areas. However, the images at fold crest in parts of the area can be poor, possibly due to gas seepages, and probably because of the complexity of the structure and distribution of lithologies.

The two dimensional (2D) seismic survey data used in the study are regional 2D multichannel seismic acquired by the Federal Institute for Natural Resources (BGR) in 1986. The seismic lines processed as Pre-Stack Time Migration with record length down to 12000 ms. The polarity follows the Society of Exploration Geophysics (SEG) convention, with increase in acoustic impedance as the minimum phase with negative value. 12 seismic lines were selected for interpreting the regional context of the area, especially Southeast-Northwest lines extending from the shelf in Sabah Inboard, towards the Sabah Trough and Dangerous Grounds. The main lines used for regional correlation are BGR8622, BGR8624 and BGR8625. (Figure 1-1 and Figure 2-1) The seismic quality is fair to poor, good to fair frequency content, very good vertical and horizontal resolution at the synclinal part of the coverage and poor to fair at the crestal part of the anticline,

however for regional interpretation and correlation they are satisfactory, especially considering the length of the line (177 km each for BGR8622 and BGR 8624).

No	Well Name	Well Label	Water Depth (m)	Total Depth (m TVDSS)	Total Depth (m MDDF)
1	BESTARI-1	BR-1	1156	2794	2845
2	BESTARI-2	BR-2	1106	2099	2125
3	BESTARI-2ST1	BR-2ST1	1106	2593	2620
4	BESTARI-2ST2	BR-2ST2	1106	2379	2543
5	BESTARI-3	BR-3	1096	2183	2233
6	LIMBAYONG-1ST1	LG-1ST1	959	2583	3274
7	LIMBAYONG-2	LG-2	926	2534	2767
8	LIMBAYONG-3	LG-3	1007	2766	2798
9	LIMBAYONG-3ST1	LG-3ST1	1007	2661	2815
10	MENAWAN-1ST1	MN-1ST1	398	3172	3492
11	LAWA-1	LW-1	666	3551	3583
12	AYA-1	AY-1	1365	3700	3700
13	GUMUSUT-1	GS-1	1079	1745	1767
14	GUMUSUT-2ST1	GS-2ST1	928	2666	2780
15	GUMUSUT-3	GS-3	1053	2989	2999
16	KAKAP-2	KP-2	1052	2951	2978
17	KERISI-1	KR-1	1413	3750	3750
18	KIKEH KECIL-1	KHC-1	1360	3568	3568
19	KIKEH-1	KH-1	1313	3576	3600
20	KIKEH-2	KH-2	1311	3450	3450
21	LUMUTAN-1	LT-1	1560	2845	2840
22	PETAI-1	PT-1	1244	3141	3204
23	PETAI-2	PT-2	1369	2536	2593
24	PISAGAN-1ST1	PS-1ST1	1466	1734	1734
25	SIKAP-1	SK-1	1360	3450	3541

Table 2-1: Wells utilised for the study.

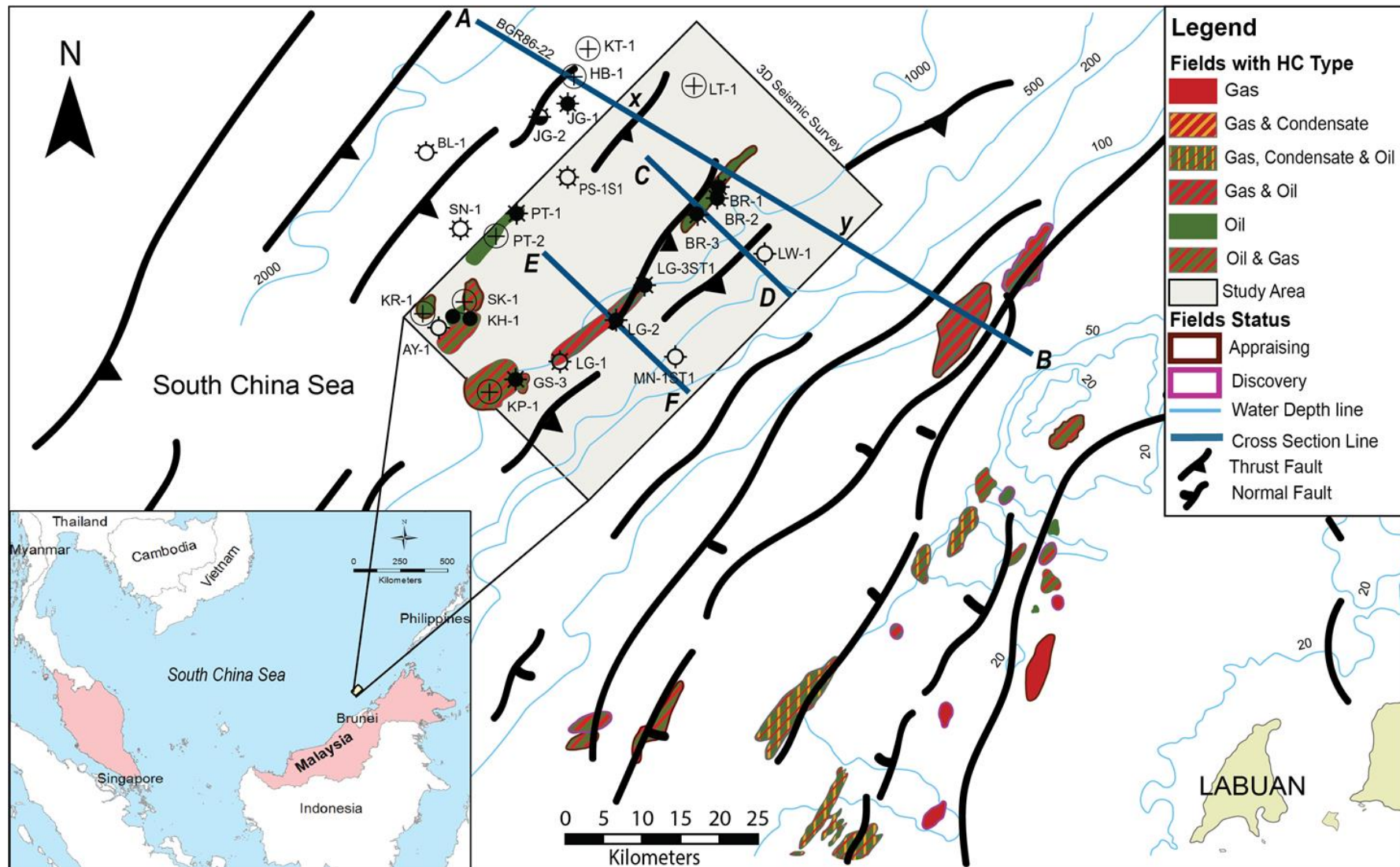


Figure 2-1: Offshore deep-water fold belt anticlines, interpreted from a mixture of regional surveys and seismic sections (Grant 2004; Gee et al., 2007, Hesse et al., 2009). Regional seismic cross section A-A' extends from the NW Borneo Trough and Sabah Platform to the NW Borneo (Baram-Balabac) Shelf, from merger of two-dimensional seismic line and three-dimensional seismic surveys (this study).

2.2 Methodology

In the exploration history and activities in the Sabah Outboard, especially in the study area, various regional and specialized studies were performed by different operators and contractors. All methods from the very basic practices and the advance technology have been performed for the exploration and development activities. However, the reservoir risk issues which have been realized since the earlier days of the exploration activities persist and are not well understood. Therefore, this study approaches the methodology in more integrated ways.

The study evaluated all the available data and information gathered from the drilled wells and acquired seismic, with integration of laboratory results and evaluation of the wells provided by PETRONAS.

Petrel E&P Software Platform 2018.2 by Schlumberger was used as the main interpretation software for the well and seismic correlation, interpretation, and modelling. All the digital data from well and seismic have been loaded into a Petrel project. The project coordinates reference system (CRS) is the UTM50_Timbalai, to match the data and reports provided by PETRONAS.

PetroMod 2018.2 software by Schlumberger was used for generating the burial history and one-dimensional (1D) basin modelling. For seismic attribute analyses, PETREL was used for the time slice and simple attribute extraction, but for the horizons attribute extractions and blending, PaleoScan 2019.2.1 courtesy of Eliis was used.

2.2.1 Well correlation

Prior to any interpretation in either using well data or seismic, well tops were gathered from the well reports. Final well tops from reports are usually very dependent to each operator, and their approach or understanding of the well location and depositional environment and timing of the formation. Different operators used different nomenclature and events in selecting the horizons for correlation. All well tops including biostratigraphy tops from Foraminifera, Nano-fossils and Palynology were compiled and compared throughout the area. Due to too many inconsistencies and miss-matches among the wells, a new correlation was performed using well log character and biostratigraphy information. Despite managing to have a good correlation from this method overall, there was an issue on time crossing while comparing the well correlation with seismic. Therefore, the correlation integrates horizons from seismic interpretation by anchoring the regional marker to the Maximum Flooding Surface (MFS) of the deep-water shale deposition to have a better control and confidence in the correlation. Formation pressure data established trends, based on the gradient in between the formations, vertically and between the well horizontally. These results were integrated with the stratigraphy correlation, to confirm the connectivity between the formations, especially the sand bodies, or possible compartmentalisation.

2.2.2 Sequence stratigraphy

Sequence Boundary (SB) and Maximum Flooding Surface (MFS) were identified based on Exxon's techniques by Van Wagoner et al., (1990), as a product of relative sea level

fluctuation. Seismic and well data were used to identify the major bounding surfaces and correlated with the regional lines, to be correlated with regional events in NW Borneo. Sequence stratigraphy system tracts were defined based on the seismic and well data to bound the facies into third order sequences, by using the SB and MFS. The system tracts were used in correlating the horizons in seismic and well data.

2.2.3 2D Seismic and 3D Seismic interpretation and mapping

Synthetic seismograms were generated for most of the wells to tie the well to seismic data e.g., Menawan-1, Lawa-1, Bestari-1, Bestari-2, Bestari-3, Limbayong-1, Limbayong-2 and Limbayong-3. Density and sonic log were used to construct the acoustic impedance (AI) and reflection coefficient (RC) logs. The series of Ricker wavelet (20, 25, 30 Hz) was used to convolve with the derived RC to generate the synthetic trace and correlated with seismic to obtain an optimum tie. The result of the synthetic seismograms indicates that the match between seismic and well data is good at the upper section, with simple, continuous, and horizontal reflectors, but uncertain when at deeper levels with dipping reflectors (Appendix 1). The analysis of the synthetic seismograms also concluded that the sandy formations are acoustically soft, while shale formations were represented by a hard-acoustic impedance kick. At least eight horizons are correlated and interpreted in this study. The horizon selection was mainly picked on the prominent event throughout the area, from seabed to the deeper traceable horizons coincident with the SB or MFS. The gridded time map was converted to depth map by using the single function of the combined time to depth relationship (Appendix 3), as the seismic velocity conversion is not reliable.

2.2.4 Structural analyses in defining the geometry, verge, and growth of the folds

Using the gridded maps in time and depth, the structure in the area was analysed to define the geometry, vergence, and growth of the individual folds in the study area. The methods selected are the (1) qualitative and quantitative fold dip azimuth analyses by using both 3D view and 2D view of the gridded horizons; (2) Seismic time slice geometry to look into the geometry surface cutting through a wide range of timelines; (3) Horizons flattening for simple structural restoration, to evaluate the vertical and temporal evolution of the structure; and (5) Fold expansion index quantification, adoptedg from Thorsen (1963) and Groshong (1993, 2006) methods in evaluating the fold growth history.

2.2.5 Seismic facies and seismic attribute extraction analyses

Seismic facies characteristics of the amplitude strength, frequency and continuity were used to classify the facies and interpret the depositional setting, with well log and lithology calibration (e.g., Beaubouef et al., 2000 and Mayall et al., 2000). Seismic attributes of the time slices and horizon slices were used to compare the seismic response between the proven reservoirs with high net to gross in the discovered field, with other areas.

The attribute blending of the horizons, using Root Mean Square (RMS) amplitude and Red Green Blue (RGB) frequencies colour blending, was performed to enhance the sediment pathway, with good confidence of lithology control throughout the area (Appendices 7A, 7B and 7C). The RMS amplitude attribute computes the root mean square of single trace sample over a specified vertical window with a length of samples

(Ismail et al., 2019. RMS amplitude extraction enables the detection of amplitude variations for channels with density changes compared with the surrounding area.

RGB colour blending enhance the geological features with richer visualisations (Henderson et al., 2008). In this study, the RGB blending by assigning the seismic attribute cube to one of the colour axes displaying the red, green and blue components. The red colour was using the 10Hz band pass, the green 20Hz and the blue cube 41 Hz (Appendix 8A). Each frequency of the colour displayed in the horizons and blended to enhance the submarine channel geometry.

Therefore, the blend of both RMS and RGB attribute extraction enables the sand filled submarine channels to be enhanced and imaged in the study area. The blending of the horizons attribute using RMS and RGB enhanced the geometry and most-likely lithological contrast of the submarine channel.

Other attribute extraction techniques used were Sweetness attribute (Figure 5-17). Sweetness is an attribute derived by combining instantaneous frequency and reflection strength (see Radovich et al., 1998). Shale dominated intervals tend to be characterised by low amplitudes and high frequencies whereas isolated sandy intervals, such as channel fills, correspond to higher amplitudes.

2.2.6 1D Basin modelling

One-Dimensional basin models were constructed with the PetroMod software. The modelling was constructed for all the wells, with the main objective to produce the burial

history of each well, and to identify if there is any variance between the wells or in between the folds. This will help to understand the present-day basin geometry and evolution.

The other important output of the model is to provide both depth and time evolution of the temperature, overpressure, and the porosity for each of the wells.

2.2.7 Pressure data, well logs and core properties analyses

Integration of pore pressure analyses, well logs (utilizing mainly the Gamma Ray (GR), resistivity, density and sonic logs) and core thin section analyses was performed to understand the generation mechanism of overpressure along the folds. Data from different sources acquired during well drilling, pre-drilling for pressure prediction and post-drilling analysis used to was obtained a comprehensive pressure data set for the structures. The fracture pressure obtained from well Leak of Test (LOT) and Formation Integrity Test (FIT), whilst formation pressures were obtained mostly from wireline logging operation of the Modular Formation Tester (MDT) and Repeat Formation Tester (RFT). The relationship between the tectono-stratigraphy and reservoir quality preservation with geopressure, particularly the vertical effective stress, was used to understand lateral discontinuity between the reservoir(s) encountered in the wells and the factor(s) causing the overpressure variation.

Chapter III:

Regional geology of NW Borneo and the study area

3.1 Regional geology

The Northwest Borneo Province is bounded by the Southwest Palawan Basin in the Philippines to the north and the Northwest Sabah Trough to the west. To the southern, the Northwest Borneo Provinces is adjacent to the Baram Delta Province, divided by the Jerudong-Morris Fault to the west and the Balabac Strait Fault to the east (Figure 3-1 and Figure 3-2). The NW Sabah Basin is a predominantly offshore Middle Miocene sedimentary basin that underlies the continental margin of western Sabah. The plate tectonic history of NW Borneo is complex, involving multiple extension and compressional episodes over a protracted period (Ingram et al. 2004). The deformation mechanisms for the region are still highly debated (e.g., Hall, 2011). NW Borneo's tectonic evolution has been discussed, with various models (Figure 3-3) including extrusion (e.g., Tapponnier et.al. 1986, 2003), a subduction-focused model (e.g., Hamilton 1979, Holloway 1982, Lee & Laver 1995, and Hall 1997, 2009, 2012) and a hybrid continental rifting model (e.g., Cullen 2010). Recently, further tectonic models have recognized the importance of the South China Sea seafloor spreading with counterclockwise rotation (up to 45°) of Borneo since the Late Eocene (e.g., Zahirovic et al., 2013, 2014; Teasdale et al., 2017; Wu & Suppe 2018).

During the early Cenozoic to late Early Miocene, NW Borneo was an active margin due to the southward subduction of the proto-South China Sea under Borneo (Hutchison, 1996, Hall, 1996; Hall et al., 2008). In the mid-Miocene, cessation of subduction led to the collision of the NW Borneo and the Dangerous Grounds continental crust, which is known as the Sabah Orogeny (Hutchinson et al., 2000). The collision led to extensive uplift and erosion of the interior of Borneo, providing sediment to the deltaic and shallow marine

Middle to Upper Miocene successions of the Meligan and Tanjong deltas (Balaguru et al, 2009). The Sabah Orogen has been linked to a prominent regional unconformity on seismic sections and named the Deep Regional Unconformity (DRU); Hutchinson et al., 2000, Balaguru et al, 2009). The DRU has been suggested to mark the end of folding and thrusting in the onshore Crocker Ranges, and mark the start of Baram Basin extension and sediment flux (Morley, 2016).

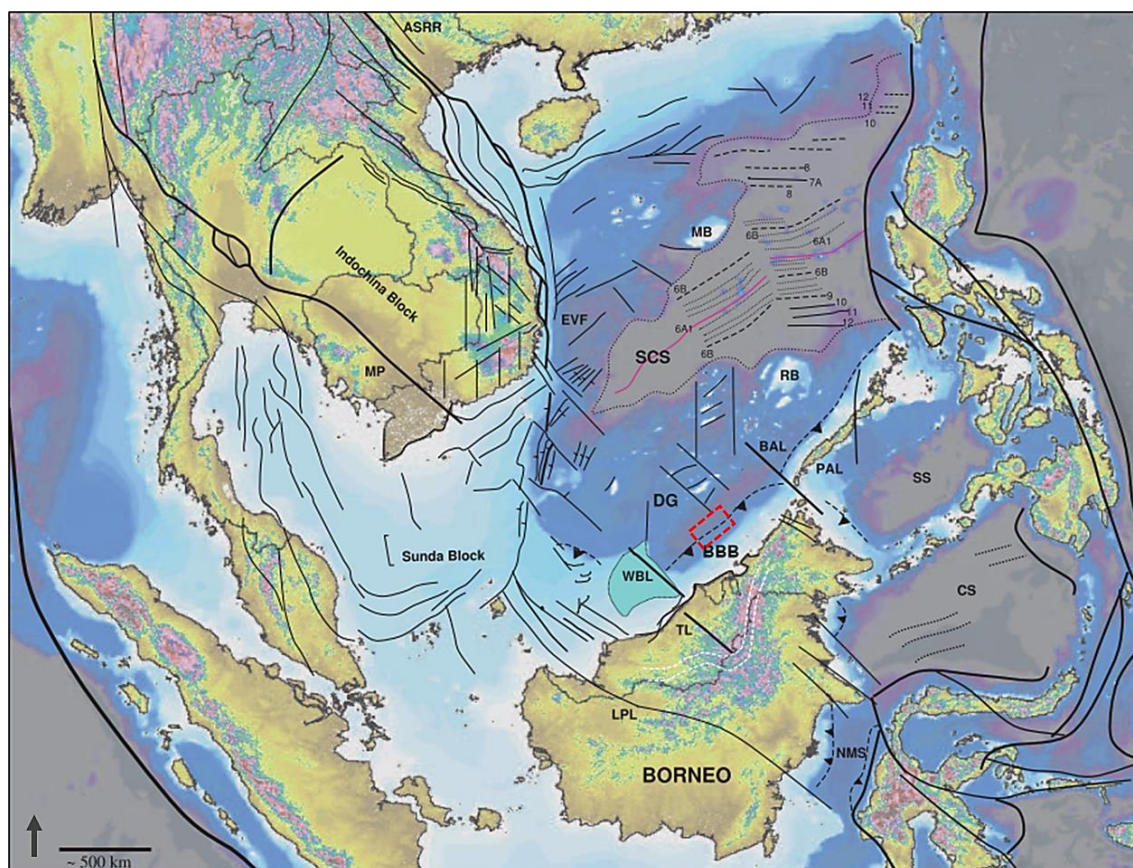


Figure 3-1: Regional bathymetry map of Southeast Asia consist of the regional fault zone, basin, and sea (from Cullen, 2010) involved in deep-water NW Borneo fault-and-thrust belt tectonic (red dashed box). Abbreviations; Ailao Shan Red River Fault Zone (ASRR), Baram-Balabac Basin (BBB), Balabac Line (BAL), Celebes Sea (CS), Dangerous Ground (DG), East Vietnam Fault Zone (EVF), Lupar Line (LPL), Macclesfield Bank (MB), Mae Ping Fault zone (MP), North Makassar Straits (NMS), Palawan (PAL), ReedBank (RB), South China Sea (SCS), Sulu Sea (SS), Tinjar Line (TL), West Baram Line (WBL).

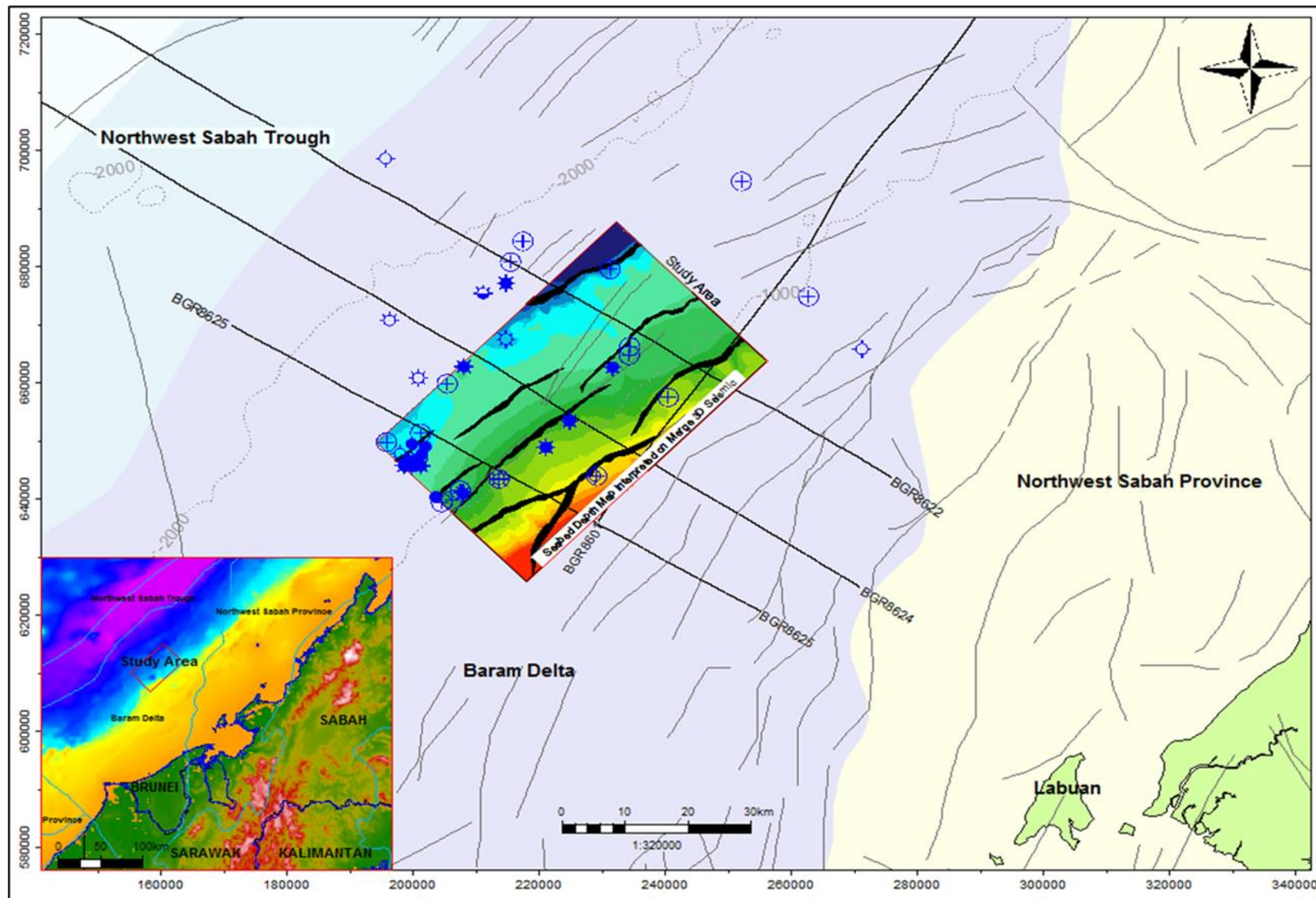


Figure 3-2: Regional map of Borneo showing DWFTBs around the island modified from Morley et al (2010). The study area in NW Borneo DWFTB and the 3D seismic survey outline and 2D seismic lines are indicated.

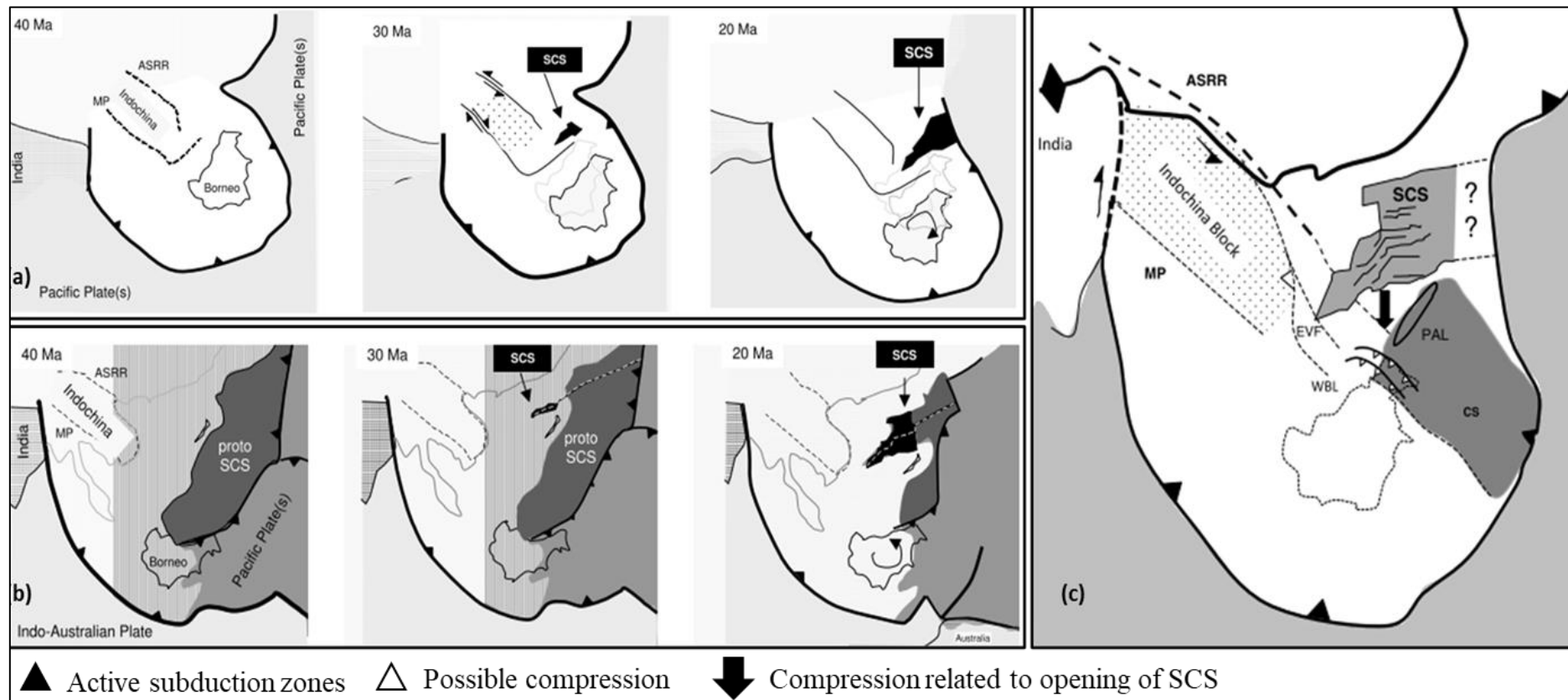


Figure 3-3: Simplified comparison of regional tectonics (from Cullen, 2010) showing the comparison of (a) The extrusion model adapted from Replumaz et al., (2003); (b) The subduction model (modified from Hall, 2002); (c) The hybrid model of the extrusion and under thrusting at 20 Ma by Cullen (2010).

Hutchison *et al.*, 2000 proposed a NW Borneo tectonic model based on extensive mapping of Sabah (see Figure 3-4). The model suggested the NW Borneo basement is not continental, but built over Mesozoic ophiolites, and that the West Crocker Formation was allochthonous and thrust out over the buried continental shelf and attenuated continental crust of the Dangerous Ground. From the Mid-Miocene, NW Borneo has experienced at least 8 km of uplift (Roberts *et al.*, 2018). Uplift occurred at the same time as rapid deposition of sediments along the NW Borneo margin, and wider circum-Borneo offshore sedimentary basins. The present-day NW Borneo continental margin is largely aseismic, with only a very minor, <1 cm/yr., westerly geodetic motion (Simons *et al.*, 2007). This motion is associated with gravity-driven failure of the uplifted Borneo margin, and high sediment flux into the deep-water regions in this study (e.g., Hall 2013).

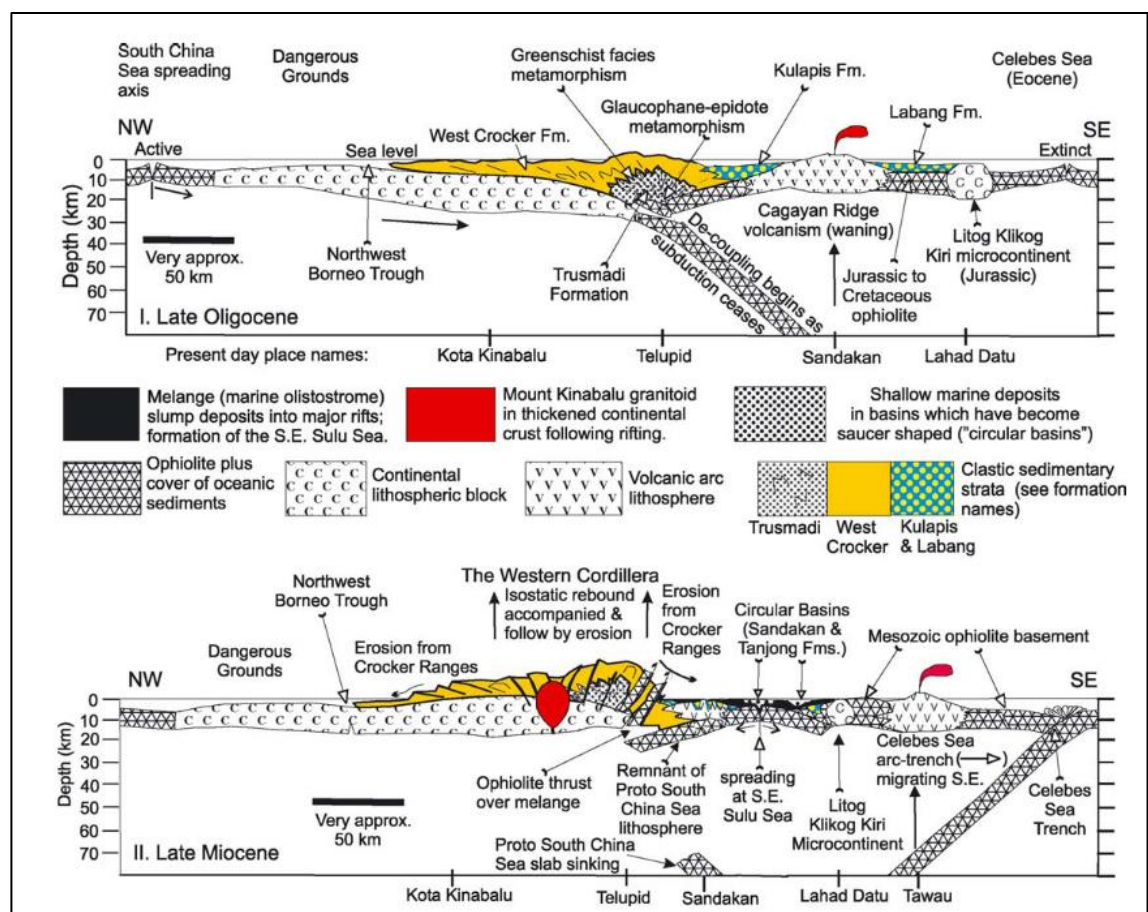


Figure 3-4: Diagrammatic regional cross section of the Tertiary evolution of Sabah (from Hutchison, 2000 & 2004)

3.2 Tectono-Stratigraphy

The compressional tectonic regime in SE Asia, including the deformation of the terrain in Sabah and Palawan, has been caused by collision between Australia and SE Asia (Early Miocene, ~21 Ma). An approximately 300 km wide new depocenter was developed in front of a major onshore fold and thrust belt (Rajang-Crocker), containing an imbricated pile of metasediments and ophiolites (Ingram et al., 2004) on the Northwest Borneo margin. Between the Middle to Late Miocene (15.5-10.8 Ma), renewed compressional deformation in an ESE-WNW orientation caused by ongoing northward movement of India and Australia resulted in deformation, partitioned by major NW-trending strike slip fault zones (Ingram et al., 2004). Subduction caused the trench and foreland loading, with development of accommodation space in the basins along the active NW Borneo margin; these basins were rapidly filled by sediments eroded from the uplifted basement lying on the east. The tectonic event is significant because it is coincident with the onset of major turbidite fans deposited in the NW Borneo trough (Casson et al. 1999). From the Late Miocene to Recent (10.8 Ma-Recent), the NW Borneo margin has been in a state of compression, resulting in the formation of a deep-water fold and thrust belt as well as inversion inboard along regional growth faults and the Sabah ridges (Grant, 2004). Fault propagation folding and reverse faulting, initiated in Middle Miocene, affected both shelf and slope domains, leading to the development of a pronounced unconformity above active structures. Major counter-regional normal faults formed at this time, possibly reactivating older basement thrusts. At about 5 Ma, Timor collided with the Sunda Arc, causing significant stress changes in SE Asia. At this time, a complex compressional 'indenter' terrain was formed in the Northwest Borneo margin, bounded by major NW trending strike-slip fault zones: (the dextral) Balabac Fault Zone in the northeast, and the

sinistral West Baram Fault Zone to the southwest. NW divergent thrusting in the Rajang-Crocker Allochthon over the attenuated lower plate began along a decollement that was located within over pressured early Miocene Setap Shale or its equivalents. Existing structures within the Northwest Borneo margin were variously reactivated depending on their location. Shortening was focused along the leading edge of the allochthon, where imbricated folds and thrust belts developed both within the allochthon itself, and within adjacent sediments of the Sabah Trough (Ingram et.al, 2004).

The tectono-stratigraphic models proposed for the NW Borneo deep-water submarine fan systems have been influenced by local and regional tectonics as well as eustatic events (Casson et al. 1999). Uplift and erosion across the inboard shelf and mountainous hinterland regions of Sabah have shed large volumes of sediment into the shallow marine domain of the NW Borneo Basin. Due to extensive regional uplift, sediments cascaded over the shelf edge through a system of upper slope feeder channels or canyons and were deposited in a system of fan lobes (Figure 3-5).

The Miocene to present-day stratigraphy associated with fold growth in NW Borneo forms the focus of this study. This sequence is better constrained than deeper units, due to the high-quality seismic data, well log correlation and biostratigraphy zonation across the NW Borneo shelf and deep-water regions (Figure 3-6 and Figure 3-7). Regional hiatuses and a chrono-sequence have previously been defined (e.g., Carigali and Krebs, 2004). The shelf part of the NW Borneo's lithostratigraphy, landward towards Borneo to the east, can be used for wider correlation (e.g., Bol et al., 1980; Levell, 1987; Noad et al., 1997; Morrison et al., 2003; Grant, 2003), including the deep-water fold-and-thrust belt.

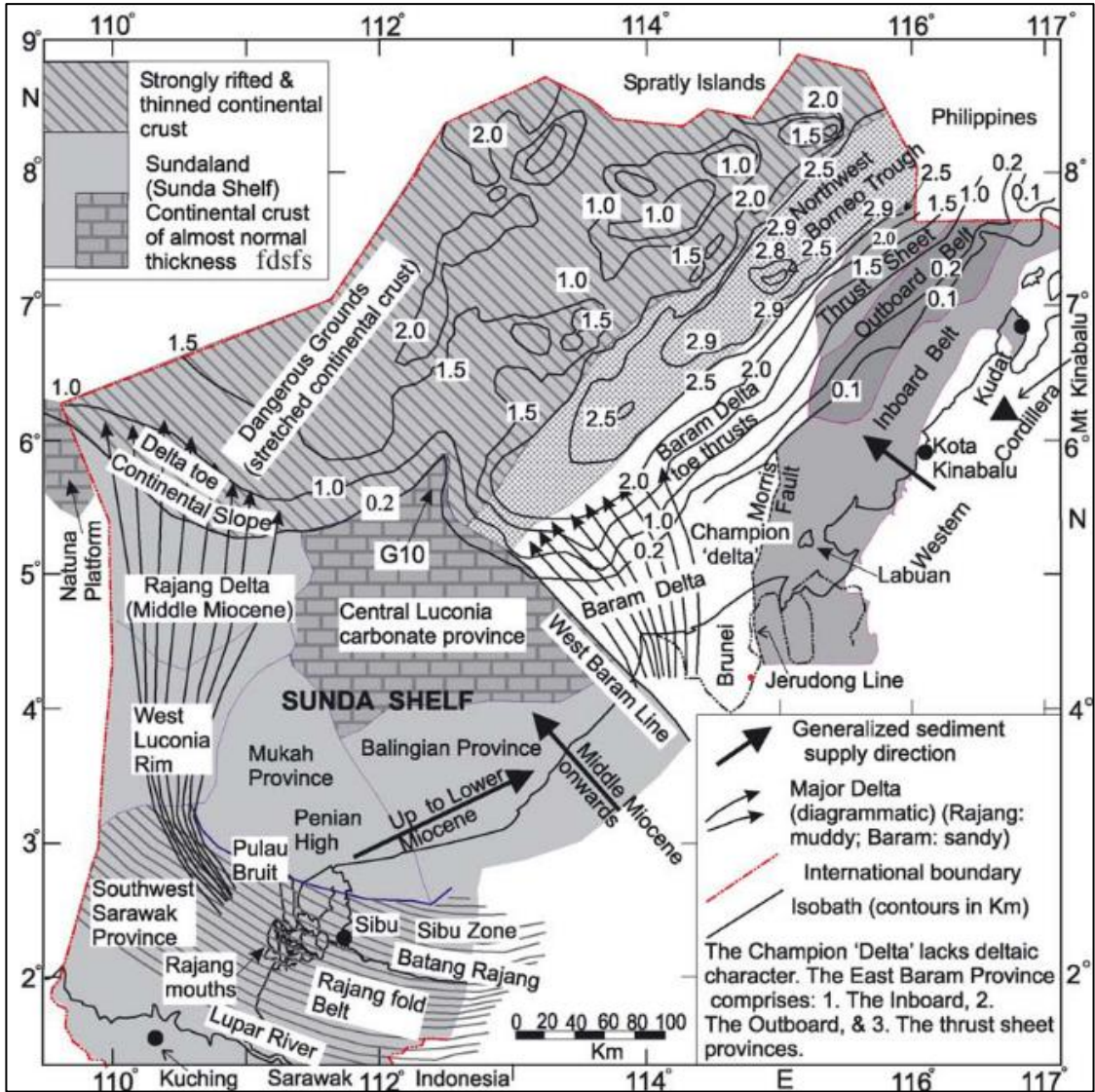


Figure 3-5: Source regions supplying sediment towards offshore Borneo. The NW Borneo deep-water fold-and-thrust belt received sediment supplied by the sandy Baram and Champion deltas, sourced by the Western Cordillera of the collision zone in Borneo (from Hutchison, 2000).

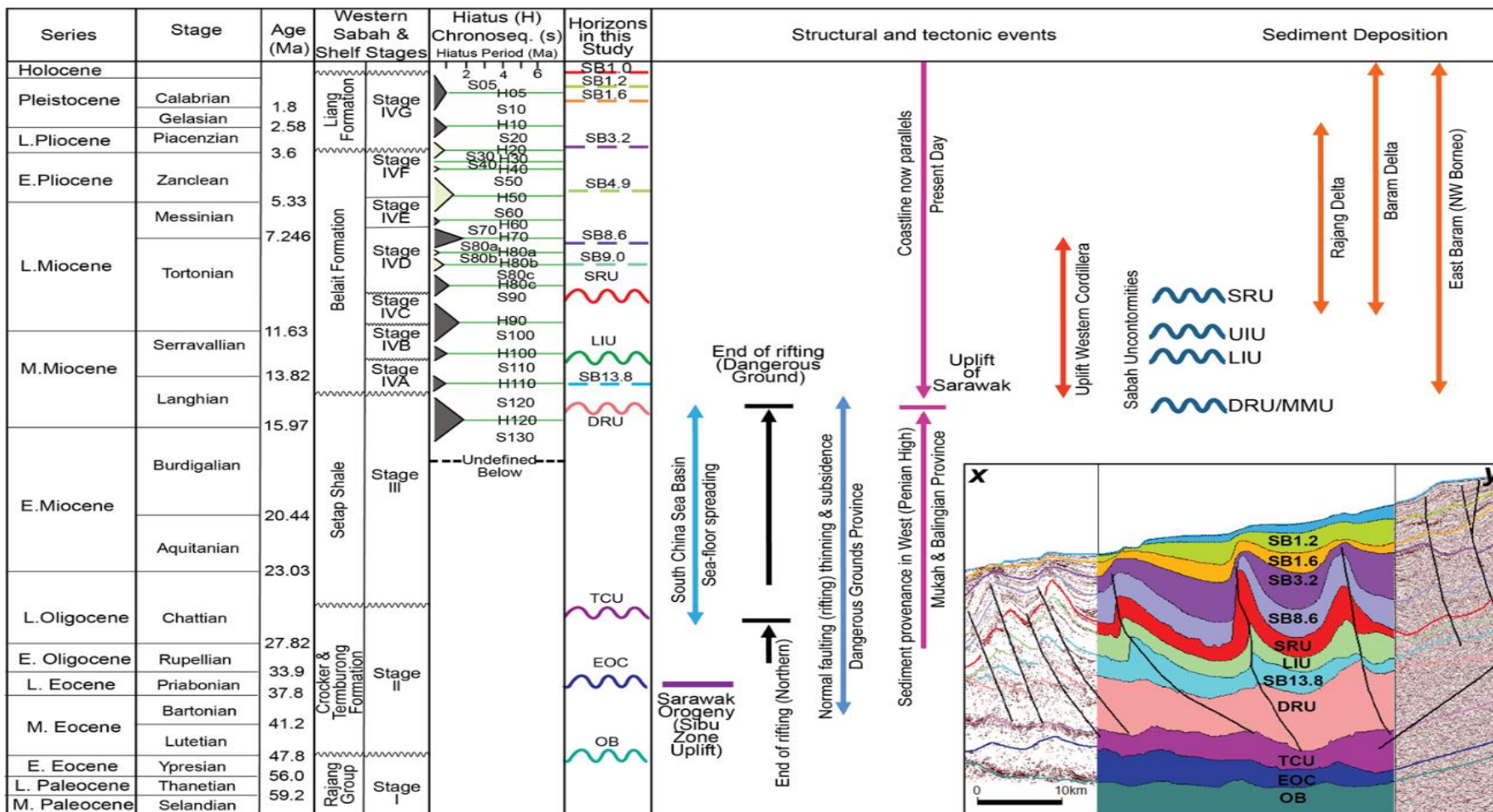


Figure 3-6: Regional stratigraphy of NW Borneo and key tectonostratigraphic events (adapted from Hutchinson, 2004; Franke et al., 2008; Lambiase et al 2008). Inset image of 2D seismic cross-section x-y (see Figure 2 1 for location) illustrating the key interpreted stratigraphic horizons; TWT—two-way time in seconds. DRU—Deep Regional Unconformity; TCU—Top Crocker Unconformity; SRU—Shallow Regional Unconformity, UIU- Upper Intermediate Unconformity, LIU- Lower Intermediate Unconformity, EOC – Eocene Unconformity, OB- ophiolitic basement; SB—sequence boundary.

Open

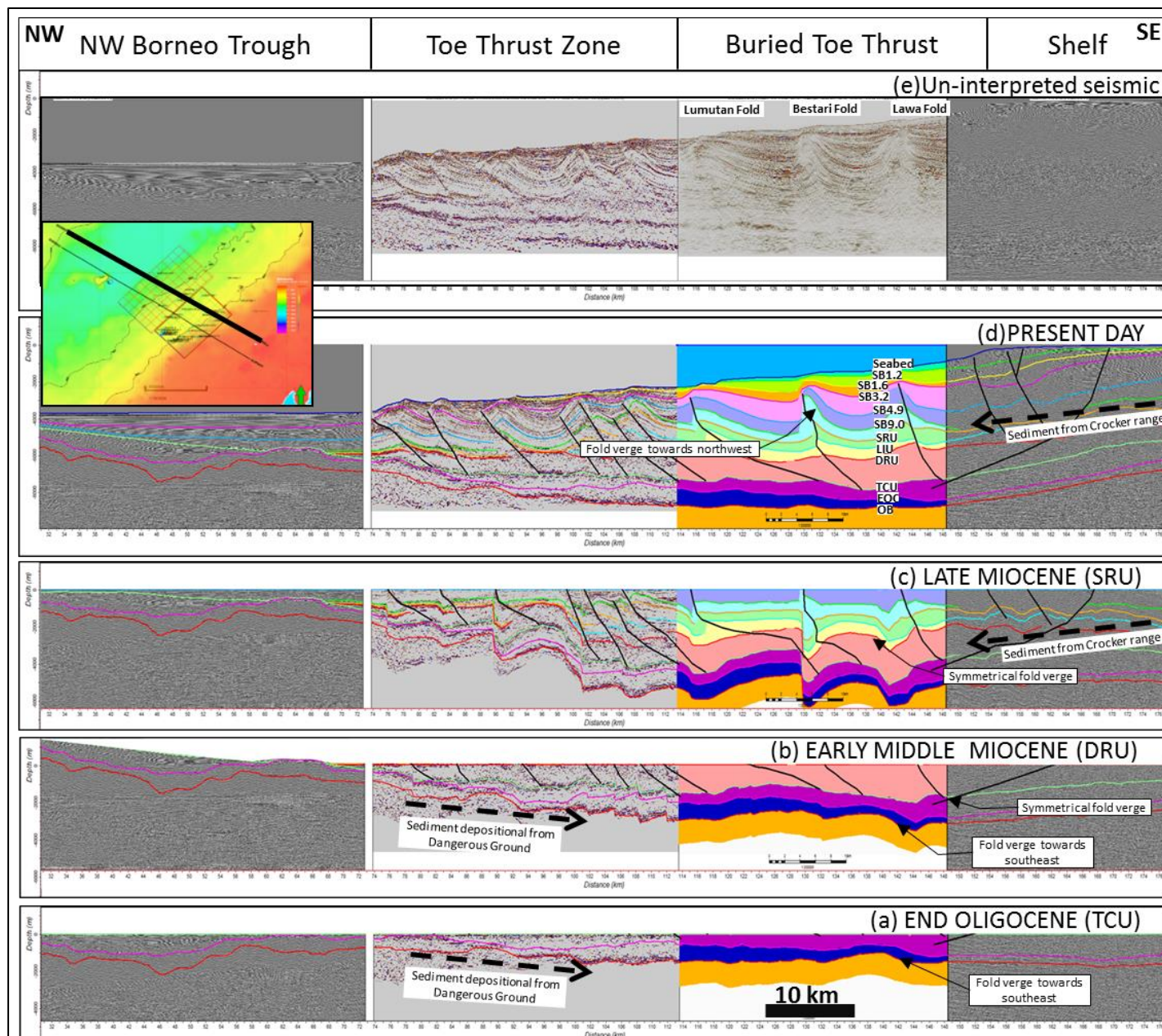


Figure 3-7: Merged 2D seismic section BGR-8622 with 3D seismic surveys (Four times vertical exaggeration) crossing all the fold thrust belt from the shelf at the Southeast towards the NW Borneo Trough and Dangerous Ground at the Northwest. The NW Borneo Trough extends to the Dangerous Ground to the NW seems to be higher until possibly Late Middle Miocene, suggesting sediment provenance from the NW. Fold geometry, especially at the buried toe thrust zone, is

3.3 Petroleum system elements and potential

The area remains the focus of oil and gas exploration, even-though the Northwest Borneo deep-water fold-and-thrust belt has already been the interest of various oil and gas operators since the 90's. This is proven by seven deep-water exploration and appraisal wells drilled in area in the last ten years - more than any part of the basin. The hydrocarbon exploration plays in the study area consist of the deep-water submarine fans in the hanging wall anticlines of thrust structures, with shale cores to the growth anticlines. The potential of stratigraphic trap plays is yet to be tested in the area; it would be an interesting target to drill to test the petroleum system in the synclinal part of the structures, targeting the submarine channels and fan lobes in the unconfined setting of the basin. The petroleum system elements (Figure 3-8) for the plays are summarized as follows:

1. Trap

The tested trap mechanisms in the study area were mainly the fault-bounded three-way dip-closure and the four-way dip anticline of the hanging walls of the thrust anticline (Scherer, 1980). Possible stratigraphic traps in the basin area in the intra-slope synclines between the anticlines, are yet to be tested.

2. Reservoir

The primary target is the submarine fan of the Middle to Upper Miocene of the Kebabangan (older), Kamunsu and Pink. The Yellow (younger) fan system is the secondary objective. The marine turbidites, consist of the submarine channel and submarine fan, form a thick, high-quality reservoir (Madon et al., 1999).

3. Source rock

The source rocks in this region contain terrigenous organic matter that has been redeposited with deep-water sands, silts and mudstones, of a similar age or older than the target reservoirs (Anuar et al., 1997). The slump mass transport deposits (MTD) in West Crocker Formation, the shaly facies have relatively high amount of organic matter (TOC > 2 wt.%), a fair to excellent source rock generation potential (Abdullah et al., 2016). However, potential source rock from the deeper shale of the Setap Formation is generally lean and thermally overmature (Madon et al., 1999).

4. Migration and Timing

The kitchen area for the source rock most likely in the syncline areas in between the anticlines, with migration pathways provided by lateral and vertical migration through the porous sand and silt layers of the submarine fans (Nor Azidin et al., 2011). Migration through faults from deeper source rocks in the footwalls, either from the Setap shale or source rock at the adjacent footwall, is very likely provided by the thrust faults and the juxtaposition of the porous formations.

5. Seal

For the fault bounded play, the thrust fault mostly acts as the lateral seal, For the stratigraphic play, the reservoirs pinch-out and are bounded by the mass-transit complexes and hemipelagic deep-water shales. The top seal mainly provided by intraformational shale and mudstone with effective top and flank seals in many proven hydrocarbon accumulations ((Madon et al., 1999) such as Erb West, Kinabalu, Kikeh and Gumust-Kakap fields.

It is the aim of this study to be able to explain the lithology and stratigraphic column penetrated by the wells in the thrustured folds. This is achieved by understanding the facies distribution, based on the most likely depositional models.

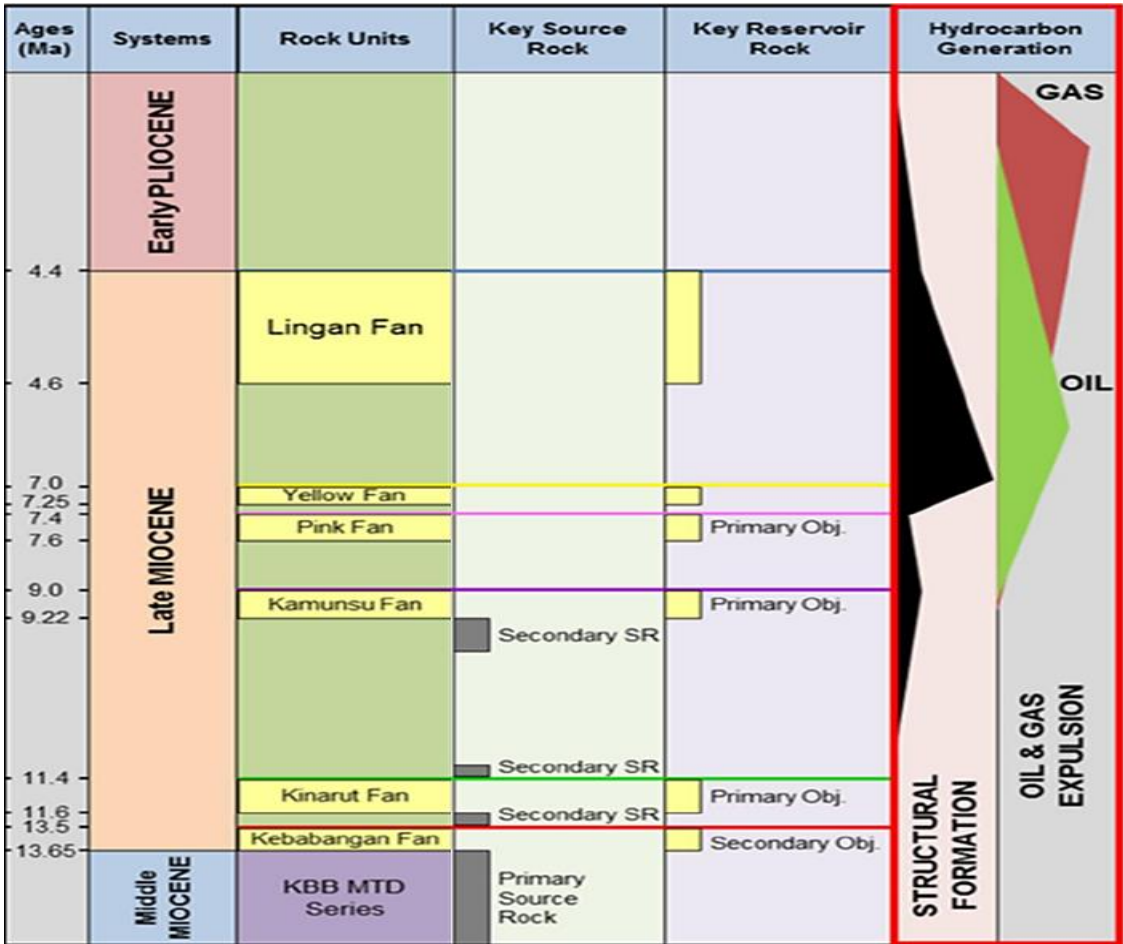


Figure 3-8: Petroleum system of NW Borneo deep-water fold-and-thrust belt showing the Late Miocene reservoir targets of the Keababangan, Kinarut, Kamunsu and Pink fans (After Jong, et al., 2014).

Chapter IV:

Reversal in structural transport
direction in the NW Borneo deep
water fold-and-thrust belt

*This chapter has been submitted to the Journal Marine and Petroleum Geology and is
in review.*

4.1 Introduction

The aim of this paper is to use 3D seismic data to better understand the long-term evolution of NW Borneo deep-water fold-and-thrust belt (Figure 4-1). This study reveals a previously unrecognized change in structural transport direction (vergence), that we relate to changing regional tectonics and the transition from a pre-collisional to a syn-collisional setting. The continental shelf and deep-water areas of NW Borneo are well known from drilling and seismic-reflection survey data (e.g., Multi Azimuth 3D Seismic).

The NW Borneo deep-water area is on the margins of a rapidly subsiding shelf, which has accumulated siliciclastic sediments from the Baram and Champion deltas since the Middle Miocene. Reworking of shallow-marine sediment into the deep water has produced a tapering wedge of late-Early Miocene–Holocene sediments from slope to deep-water environments. This wedge is >10 km thick near the shelf edge, and ~3–4 km thick at water depths of >3 km. The use of latest acquisition of the high-resolution three-dimensional (3D) seismic reflection survey data sets in this study reveals complex interactions between deep-water sedimentary processes and growing large-scale folds and thrusts (e.g., Morley 2009).

The extensional and compressional structural features (Figure 4-2) include kilometre-scale syn-sedimentary normal faults (growth faults), overpressure shale diapirs, and inversion-related anticlines (e.g., Imber et al., 2003; Morley et al., 2003, 2011; Wu et al., 2019). The growing anticlines are positive features on the seafloor and act as baffles to down-slope sediment transport, while synclines serve as localized depo-centres. Thrusting and folding along the slope is of Late Miocene–Holocene age and developed

as a result of both near field stresses related to gravity-driven deformation of the large deltas, and far-field stresses associated with the early stage of collision between the Dangerous Grounds continental fragment, and the NW Borneo margin. Despite significant research and exploration efforts in the deep-water NW Borneo in recent years, there are still uncertainties concerning the reservoir presence and effectiveness controlling mechanisms of deep-water fold-and-thrust systems.

This chapter presents new interpretations of regional seismic reflection data, with-full integration of well data covering the NW Borneo deep-water fold-and-thrust belt (Figure 4-1). The study uses a spatially extensive data set (2000 km²), high-quality petroleum industry 3-D seismic volume recorded to 7 s two-way travel time (TWT) and linked 2D seismic sections that image the full stratal growth record. Earliest evolution of the fold-and-thrust belt was in the Eocene, followed by gravitational slope collapse from the Middle Miocene to the present-day. This research is one of the first papers to use high quality 3D seismic reflection data sets, to characterize the changing geometry and vergence of the growth folds and associated faults from the Eocene to Recent. The study demonstrates two different sets of folds separated by the change from subduction of the Proto-South China Sea beneath Borneo to the gravitationally driven deep-water delta system. The results highlight the importance of changes in geometry for relating the history of fold development in each individual fold in the area.

This study will assist the understanding of facies distributions associated with fold development in NW Borneo deep-water fold-and-belt and will improve understanding of complex deep-water submarine fan depositional settings.

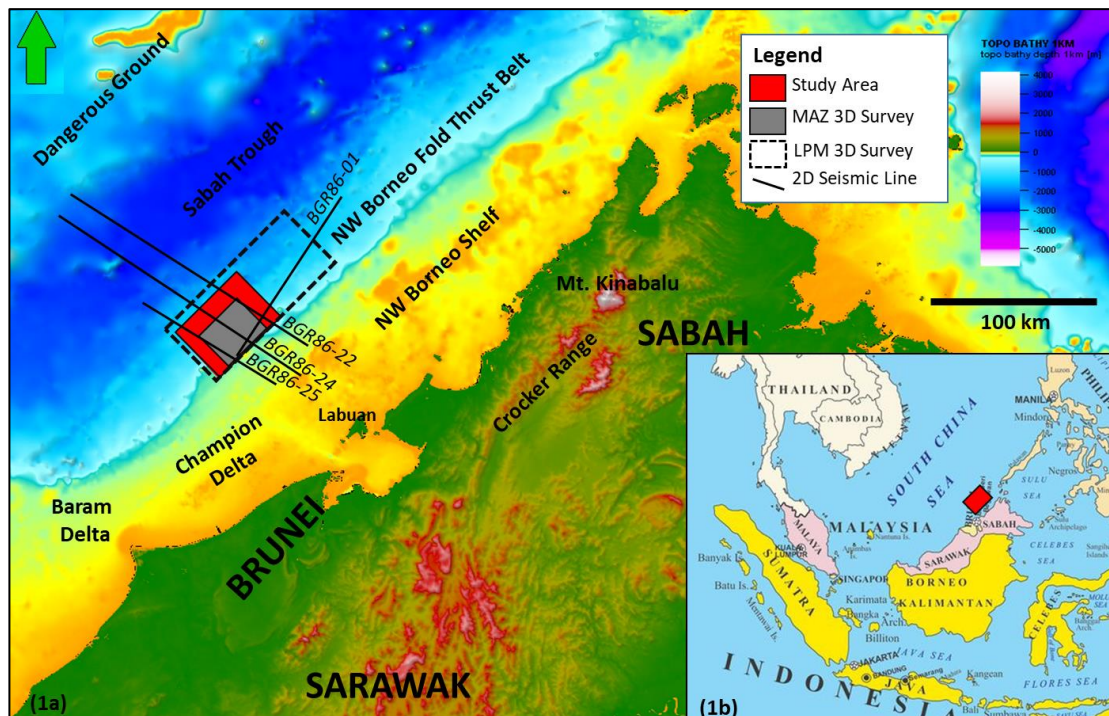


Figure 4-1: (a) Regional simplified topography and bathymetry map of NW Borneo, showing elevation dropping towards the Northwest from the Crocker Range to the Sabah Trough (b) Deepwater NW Borneo location at the South China Sea

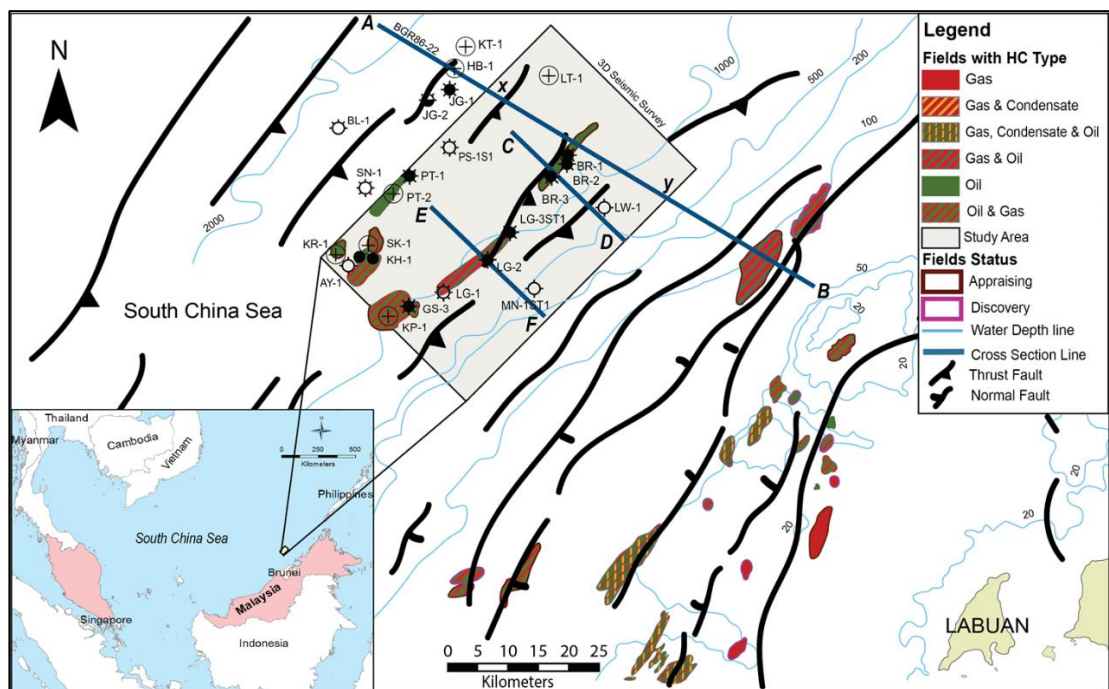


Figure 4-2: Offshore deep-water fold belt anticlines, interpreted from a mixture of regional surveys (Grant 2004; Gee et al, 2007, Hesse et al., 2009). Regional seismic cross section A-A' extends from the NW Borneo Trough and Sabah Platform to the NW Borneo Shelf.

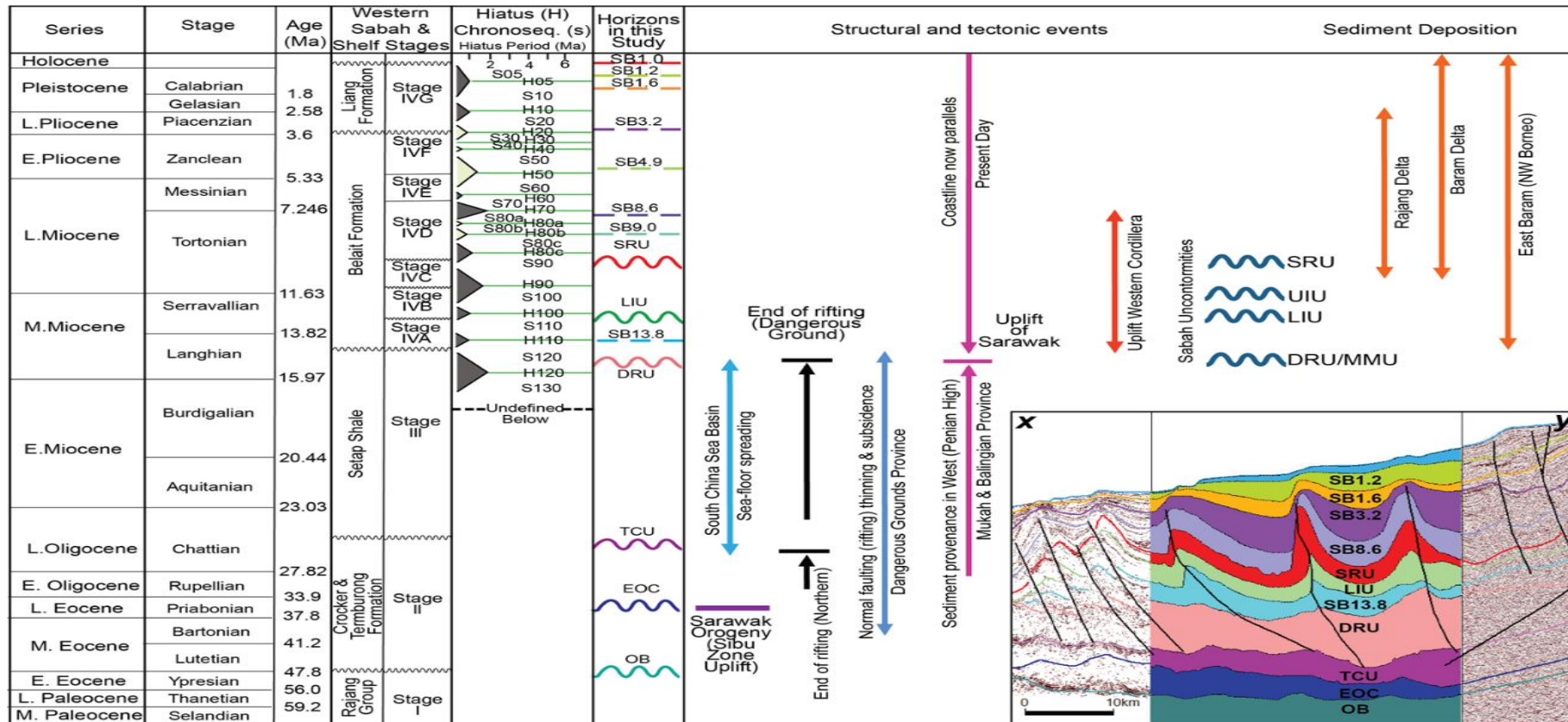


Figure 4-3: Regional stratigraphy of NW Borneo and key tectonostratigraphic events (adapted from Hutchinson, 2004; Franke et al., 2008; Lambiasi et al 2008). Inset: Image of 2D seismic cross-section x-y (see Figure 4 1 for location) illustrating the key interpreted stratigraphic horizons; TWT—two-way time in seconds. DRU—Deep Regional Unconformity; TCU—Top Crocker Unconformity; SRU—Shallow Regional Unconformity, UIU- Upper Intermediate Unconformity, LIU- Lower Intermediate Unconformity, EOC – Eocene Unconformity, OB- ophiolitic basement; SB—sequence boundary.

4.2 Regional Setting of NW Borneo

Geology of NW Borneo is still poorly constrained, and deformation mechanisms for the region are still highly debated (e.g., Hall, 2011). NW Borneo's tectonic evolution has been discussed, with various models including extrusion (e.g., Tapponnier et al., 1986, 2003), a subduction-focused model (e.g., Hamilton 1979, Holloway 1982, Lee & Laver 1995 and Hall 1997, 2009, 2012) and a hybrid continental rifting model (e.g., Cullen 2010). More recently, further tectonic models have recognized the importance of the South China Sea seafloor spreading with counterclockwise rotation (up to 45°) of Borneo since the Late Eocene (e.g., Zahirovic et al., 2013, 2014; Teasdale et al., 2017; Wu & Suppe 2018). During the early Cenozoic to late Early Miocene, NW Borneo was an active margin due to the southward subduction of the proto-South China Sea under Borneo (Figure 4-3; Hutchison, 1996, Hall, 1996; Hall et al., 2008). By the mid-Miocene, cessation of subduction led to the collision of NW Borneo and Dangerous Grounds continental crust, causing the Sabah Orogeny (Figure 4-3; Hutchinson et al., 2000). The collision led to extensive uplift and erosion of the interior of Borneo, providing sediment to the deltaic and shallow marine Middle to Upper Miocene successions of the Meligan and Tanjong deltas (Balaguru et al, 2009). The Sabah Orogeny has been linked to a prominent regional unconformity on seismic sections and named the Deep Regional Unconformity (DRU); Hutchinson et al., 2000, Balaguru et al, 2009). The DRU has been suggested to mark the end of folding and thrusting in the onshore Crocker Ranges, and mark the start of Baram Basin extension and sediment flux (Morley, 2016).

Hutchison *et al.*, 2000 proposed a NW Borneo tectonic model based on extensive mapping of Sabah. The model suggested the NW Borneo basement is not continental, but

built over Mesozoic ophiolites, and that the West Crocker Formation was allochthonous and thrust out over the buried continental shelf and attenuated continental crust of the Dangerous Ground (Figure 4-1). From the Mid-Miocene, NW Borneo has experienced at least 8 km of uplift (Roberts et al., 2018). Uplift occurred at the same time as rapid deposition of sediments along the NW Borneo margin, and wider circum-Borneo offshore sedimentary basins. The present-day NW Borneo continental margin is largely aseismic, with only a very minor, <1 cm/yr., westerly geodetic motion (Simons et al., 2007). This motion is associated with gravity-driven failure of the uplifted Borneo margin, and high sediment flux into the deep-water regions in this study (e.g., Hall 2013).

4.3 Tectono-Stratigraphy

NW Borneo margin forms part of an approximately 100 km wide foreland fold-and-thrust belt, that developed in front of the onshore fold-and-thrust belt of the Rajang-Crocker Ranges. The Rajang-Crocker Ranges contain an imbricated pile of metasediments and ophiolites (see Figure 4-1 and Figure 4-2; Ingram et al., 2004). The NW Borneo margin is not well constrained at depth but is floored by the Rajang Group, which is composed predominantly of marine sediments (Hutchison, 2005). From the Late Paleocene to Mid Miocene the Rajang Group marine strata were uplifted, deformed, and metamorphosed (Hutchison, 1996), and the West Crocker Formation and its shale-dominated offshore equivalents (e.g., Temburong Formation) were deposited (e.g., Lambiase et al., 2008). The Oligocene to mid-Miocene is the dominant phase of West Crocker Formation deposition, especially in the Inboard Belt. Neogene to present-day deep marine strata is observed in the Outboard Belt. The lithology is dominated by sand-rich turbidite facies. From the mid-Miocene deep-marine sediments were still dominated by sandy turbiditic

fans, but a series of prograding deltas became established with up to 12 km thickness of sediments rapidly deposited along the NW Borneo margin.

The tectono-stratigraphic models proposed for the NW Borneo deep-water submarine fan systems have been influenced by local and regional tectonics as well as eustatic events (Casson et al. 1999). Uplift and erosion across the inboard shelf and mountainous hinterland regions of Sabah have shed large volumes of sediment into the shallow marine domain of the NW Borneo Basin. Due to extensive regional uplift, sediments cascaded over the shelf edge through a system of upper slope feeder channels or canyons and were deposited in a system of fan lobes.

The structural and depositional history of NW Borneo can be divided into three episodes. Firstly, the Late Eocene tectonic deformation coincides with south-easterly subduction of the proto-South China Sea; this was followed by Early Miocene deformation that saw the development of a deltaic system in the basin, and thirdly there was a Middle Miocene event with continued subsidence and deposition of thick prograding post-rift sediments (Balaguru et al, 2009). Since the mid Miocene to the present-day there has been up to 12 km of marine sediments deposited along the NW Borneo shelfal margin and offshore sedimentary basins dominated by a series of prograding deltas (Morley et al., 2003; 2011). Two significant deltaic systems were established to the SW of the study area: The Champion Delta and younger Baram Delta. High sediment flux from the Crocker Ranges has caused continued rapid progradation of the deltas and sediment supply to the deep-water fold-and-thrust belt.

The Miocene to present-day stratigraphy associated with fold growth in NW Borneo forms the focus of this study. This sequence is better constrained than deeper units, due to the high-quality seismic data, well log correlation and biostratigraphy zonation across the NW Borneo shelf and deep-water regions. Regional hiatuses and a chrono-sequence have been defined (e.g., Carigali and Krebs, 2004). The shelf part of the NW Borneo's lithostratigraphy landward towards Borneo to the east can be used for wider correlation (e.g., Bol et al., 1980; Levell, 1987; Noad et al., 1997; Morrison et al., 2003; Grant, 2003), including the deep-water fold-and-thrust belt.

4.4 Data

The study area covers a total of 1820 km², covering folds and underlying thrusts along the modern NW Borneo deep-water slope. Water depth ranges from 300 m to 2000 m, deepening towards the Northwest. The folds are elongated Northeast-Southwest, parallel with the Sabah coastline. The area selection is justified by the availability of the latest seismic survey, and the number of wells drilled in this part of the NW Borneo deep-water fold-and-thrust belt. This study focuses on the Lawa-Menawan and Limbayong-Bestari fold trends, as recent wells drilled in these two structures provide comprehensive data for detailed analysis and calibration.

4.4.1 Three-Dimensional Multi-Azimuth Seismic Survey

The three-dimensional multi azimuth (3D MAZ) Q-Marine OBLIQ Pre-Stack Time Migration (PSTM) seismic survey was acquired in 2012 and processing was completed in 2014. The survey size is approximately 1500 km² full fold and 520 km² image

coverage. The acquisition of the seismic was in multi-azimuth directions, which are namely Azimuth 1 in the North-South direction, Azimuth 2 in the Northwest-Southeast direction and Azimuth 3 taken from the existing Sabah LPM 3D seismic in the Northeast-Southwest direction. The seismic data were acquired in 2 ms sample rate, 8000 ms record length with 72 nominal folds for the azimuths 1 and 2. The objective of the survey being acquired in multi-azimuth was to improve the imaging of the structures.

The processed 3D MAZ OBLIQ PSTM data were then merged with the 2013 reprocessed Sabah LPM 3D seismic, to attain better coverage of the deep-water fold-and-thrust belt. For this study, the merged seismic survey area was cropped down to 1820 km², focusing on the folds with available wells. The polarity of the seismic follows the Society of Exploration Geophysics (SEG) convention, with an increase in acoustic impedance recorded as a negative number and as a minimum phase. The quality of the MAZ 3D seismic was variable depending on the area. The image and amplitude continuity are good to fair generally down to 5500 ms, especially at the synclinal area. However, the images at fold crest in parts of the area can be poor, possibly due to gas seepages, and probably because of the complexity of the structure and distribution of lithologies.

4.4.2 Two Dimensional regional seismic lines

The two dimensional (2D) seismic survey data used in the study are regional 2D multichannel seismic acquired by the Federal Institute for Natural Resources (BGR) in 1986. The seismic lines processed as Pre-Stack Time Migration with record length down to 12000 ms. The polarity follows the Society of Exploration Geophysics (SEG)

convention, with increase in acoustic impedance as the minimum phase with negative value.

12 seismic lines were selected for interpreting the regional context of the area, especially Southeast-Northwest lines extending from the shelf in Sabah Inboard, towards the Sabah Trough and Dangerous Grounds. The main lines used for regional correlation are BGR8622, BGR8624 and BGR8625 (Figure 4-2). The seismic quality is fair to poor, however for regional interpretation and correlation they are satisfactory, especially considering the length of the line (177 km each for BGR8622 and BGR 8624).

4.4.3 Well data and reports

A total of 20 exploration, appraisal and development wells are available in the study area. All well data and reports were utilized for horizon correlation and lithology calibration. Eight wells drilled on the Bestari-Limbayong and Lawa-Menawan folds are the focus for detailed analysis, as these wells are the most recent, with complete data and reports available. The total depths of the wells from the sea level range from 1000 m to the deepest of 4300 m.

The data include raw and processed logs, drilling samples from cuttings, side wall core and conventional core, pressure data and drilling parameter data and logs. Most of the well reports including the pre-drill, operation and post-drill reports were available for this study. The wells were mostly drilled to target the Middle Miocene submarine fan system at an average depth range from 1500 m to 3200 m from subsea, mainly located towards

the crestal parts of the folds. Therefore, a limitation for this study is that there are no wells drilled in the synclinal part of the structures.

4.5 Methodology

Three-dimensional (3D) seismic cube, two-dimensional (2D) seismic lines and well data were all loaded into PETREL 2018.2 software for the analyses, such as well correlation, seismic well tie, seismic interpretation and mapping, attribute extraction, structural evaluation and stratigraphy modelling and reconstruction. The coordinate reference system (CRS) is UTM50 TIMBALAI, and the unit system is standardized to Metric. The project reference datum is set to Mean Sea Level for both depth and time. Uploaded 3D seismic cube and 2D seismic lines were conditioned by applying vertical adjustment, amplitude, and phase standardizing to the best possible fit among the vintages.

The standard well information and data were loaded to the PETREL project, such as the well survey for deviation, Checkshot or Vertical Seismic Profile (VSP) for time to depth relationship and Measurement While Drilling (MWD) for drilling parameters. For well evaluation data, the Logging While Drilling (LWD) and wireline logging data were loaded from different types of geological, geophysical, petrophysical and reservoir engineering data acquisition tools the well evaluation.

4.5.1 Well correlation

Prior to any interpretation of either well data or seismic, all well tops gathered from the well reports were gathered and compiled. Different operators used different nomenclature

and events in selecting horizons for correlation. All well tops including biostratigraphy tops from foraminifera, nano-fossils and palynology were compiled and being compared throughout the area. Due to the many inconsistencies and mismatches among the wells, this study constructed a new correlation by using well log character, adopting sequence stratigraphy concepts for deep-water depositional settings (Wagoner et al, 1990). The correlation basically ties mostly on the shale patterns, in relation to possible changes in sea level fluctuations. Biostratigraphy information from well sample evaluation and correlation were used in defining the age and the paleo-environment.

The correlation is challenging considering the diachronous nature of the deposition, with sediment deposition of up to 2500 m in less than 9 Myrs. The other issues of the biostratigraphy correlation are the uncertainty produced by the possible mix-up of in-situ and reworked samples, as most of the wells are located at the slope and might be affected by slope failure, deltaic progradation and erosion.

The main regional horizons from the well and seismic correlations were then correlated using the regional seismic lines for regional event ties with other established horizons, which mainly compiled by Franke et al (2008). Most of the major regional unconformities could be identified from seismic correlation and the log characteristics, despite difficulties with wells affected by sand deposition by the delta fan, or mass-transport-deposit chaotic facies.

The horizons or event nomenclature used in this paper adopts the biostratigraphy ages of the chrono-sequence boundaries (SB), or unconformities and hiatuses, or possible mass-flooding surface (MFS). The usage of well-known regional unconformities, such as the

Shallow Regional Unconformity (SRU), and DRU, allows easy correlation with the regional tectono-stratigraphy events.

4.5.2 Seismic Interpretation and mapping

Prior to the seismic interpretation, synthetic seismograms were generated for most of the wells to tie the well data to seismic data. Density and sonic logs were used to construct the acoustic impedance (AI) and reflection coefficient (RC) logs. The series of Ricker wavelets (20, 25, 30 Hz) was used to convolve with the derived RC to generate the synthetic trace and correlated with seismic data to obtain an optimum tie. The result of the synthetic traces indicates that the match between seismic and well data is good at the upper section, which has simple, continuous, and horizontal reflectors, whilst becoming uncertain at deeper levels and with dipping reflectors. The analysis of synthetic seismograms showed that the sandy formations are acoustically soft, while shale formations are represented by a hard-acoustic impedance kick.

Fifteen horizons were correlated and interpreted across the area. The horizon selection focused on main prominent events throughout the area, calibrated with the horizons based on well correlations, and regional unconformities marked by erosional surfaces or using seismic continuity termination patterns such as top lap, on lap and down lap. The horizon interpretations on regional 2D seismic lines mostly match with regional horizons compiled by Franke et al (2008).

Even though the seismic data used for the interpretation are among the latest vintage, correlating the horizons is challenging. This is mainly due to poor imaging of parts of the

seismic, especially in the crestal parts of the folds, which is mainly an effect of shallow gas clouds, Bottom Simulating Reflector (BSR) effects, thrust fault shadow, and highly faulted and collapsed crests. Confidence levels are considered very low to fair at the crest of fold structures but mainly fair to good at the synclinal areas. The confidence level is fair to good for the horizons above the thrust structures, up to the seabed, but mainly low for horizons affected directly by thrust faulting.

A total of eight folds were interpreted from the regional 2D seismic lines, trending from NNW to SSE (Figure 4-4). Some of the folds are separated by splays, dividing each long fold into two parts. Most folds are affected by thrust faults, but some have no associated faults, especially underneath the DRU, and the Setap Shale Formation, which is known to be mobile (Figure 5-13 and 5-14).

The gridded Two-Way Time (TWT) maps were converted to depth structure maps by using a single function with well top corrections, using a gridding convergent algorithm. Both time and depth maps were used for the structure and facies modelling, dip azimuth analyses, horizons flattening for simple structure restoration and the fold expansion index quantification.

4.5.3 Qualitative and Quantitative Fold Dip Azimuth Analyses

The 3D gridded horizons viewed in both 3D (Figure 4-5) and 2D view (Figure 4-8b) all directly display the geometry and vergence of the folds in the study area. The 3D depth horizon image with dip line cross sections (Figure 4-5 and Figure 4-8a) were generated from the depth structure modelling. Three main horizons with different geometry and

vergence trends were selected to represent the other horizons. The gridded horizons show a change in the structure geometry, and clearly indicate the vergence changes of the folds through time. This permits a good interpretation of the geometry of the anticlines and synclines along the fold trends, with the vergence direction of each fold.

The 2D gridded horizon depth map allows measurement of the dip azimuth and dip angle of the selected horizons. Two polygons were constructed for each Northeast – Southwest fold, one each for the Bestari – Limbayong and Lawa – Menawan fold trends (Figure 4-8b). The polygon was drawn to cover both side of the fold limb bounded by the deepest syncline to get the measurement of the dip azimuth and the dip angle. A total of 1000 random points then generated from each horizon map, which later were filtered to every 4th point to get a random point distribution in the polygon. Figure 4-8b is further filtered with only 50 to 60 points sampled, for better display purposes. The dip azimuth arrow as displayed on the depth map of the representative selected horizons; this gives a qualitative insight of the geometry and vergence of the individual fold. The dip azimuth measurements from the horizon depth maps in Figure 4-8b is plotted as streonet plots in Figure 4-8c. The dip azimuth measurements from both fold trends are plotted together for each horizon to get the relative overall fold trend in the study area and for comparison purposes.

4.5.4 Seismic Time Slice Geometry

The 3D seismic survey time slices in the study area are analysed for the fold geometry and vergence trend (Figure 4-6). The time slices are cut on flat surfaces, providing a surface with wide range of geological time, getting younger towards the synclines. This

was due to the quality of the 3D seismic clearly imaging the structure in the area, with a significant strong amplitude exposing the geometry and the fold vergence. Good time slice images were observed down to 6500 ms from mean sea level. Greater than this depth, the seismic image is considerably poorer, due to weak seismic amplitudes.

4.5.5 Horizons flattening

A simple gridded structural and stratigraphy model was constructed using the gridded depth maps and well top horizons. The result is a 3D structural model with layering and horizon thicknesses. The model was then used to perform a horizon flattening for simple structural restoration to see the vertical evolution of the structure, especially the fold vergence and geometry through time. Based on structure balancing and restoration of the regional seismic in deep-water portion of NW Borneo, Hesse et al. (2009) suggested shortening increases through time, with the present-day shelf growth as the main control of gravity-driven fold-and-thrust belt shortening in the study area, whilst basement-driven compression was not as dominant as compared to further North in NW Borneo. The suggestion, however, is more relevant to the dominant control of shortening in relation to lateral present-day trend, not to the trend through time at any one place.

Therefore, cross sections from the 3D structural modelling were located for the best possible seismic image coverage with the closest possible distance to well intersections (Figure 4-7). Horizon's flattening was performed by restoring each unit or sequence to their correct pre-deformation configuration, by reversing the displacements that formed the structure. The restoration is independent of the transport direction. The assumption used is that the transport direction is perpendicular to the fold axis.

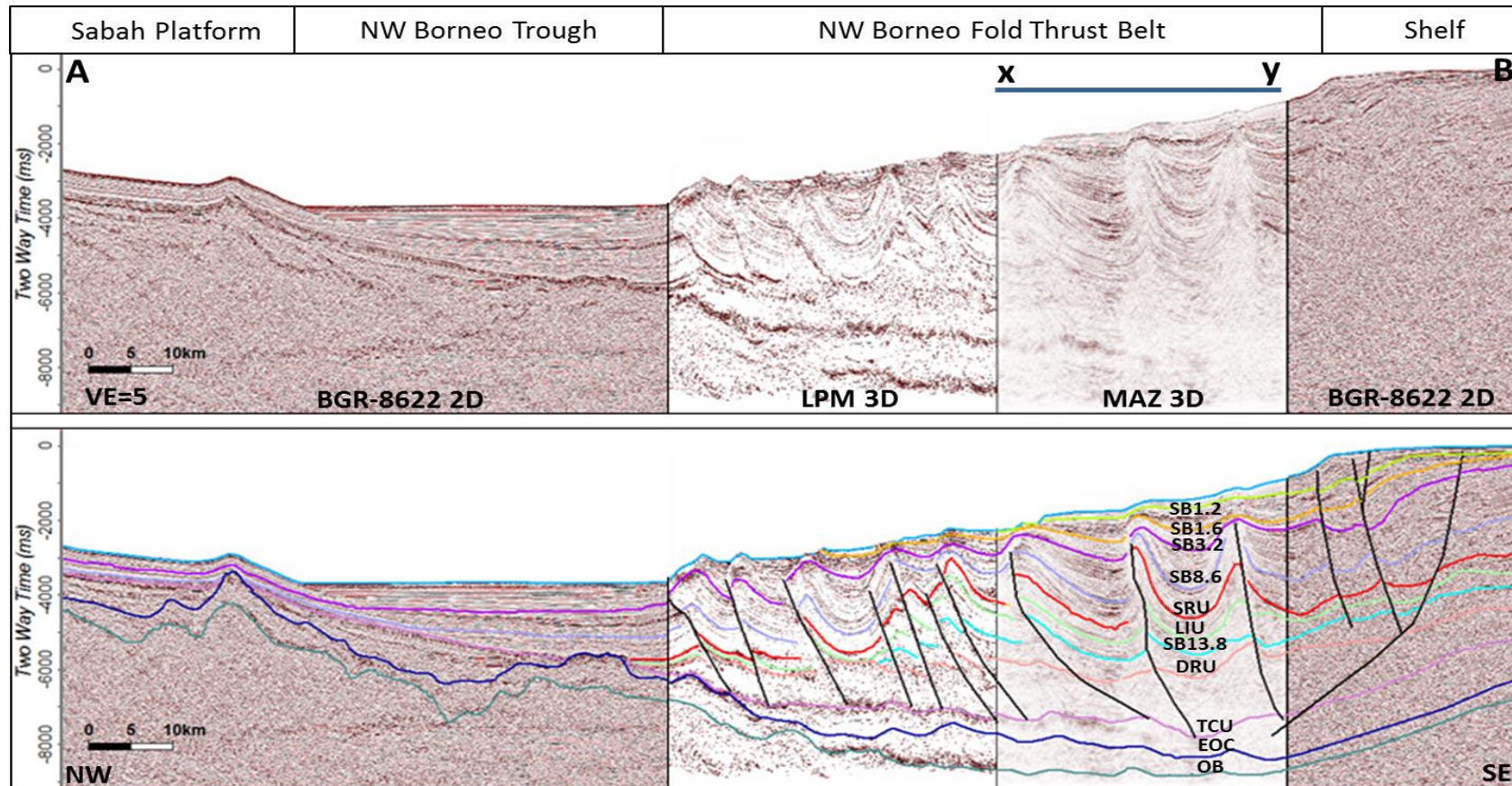


Figure 4-4: Cross section A-B (shown on Figure 1) of the merged 2D seismic section BGR-8622 with 3D seismic surveys crossing the entire fold-and-thrust belt from the shelf at the Southeast towards the NW Borneo Trough and Sabah Platform (Dangerous Ground) at the Northwest. Horizons are correlated with the main events as compiled by Franke et al (2008). Cross section x-y of the study area shows the Lawa-Menawan and Bestari-Limbayong fold trends covered by the Multi Azimuth (MAZ) 3D seismic data.

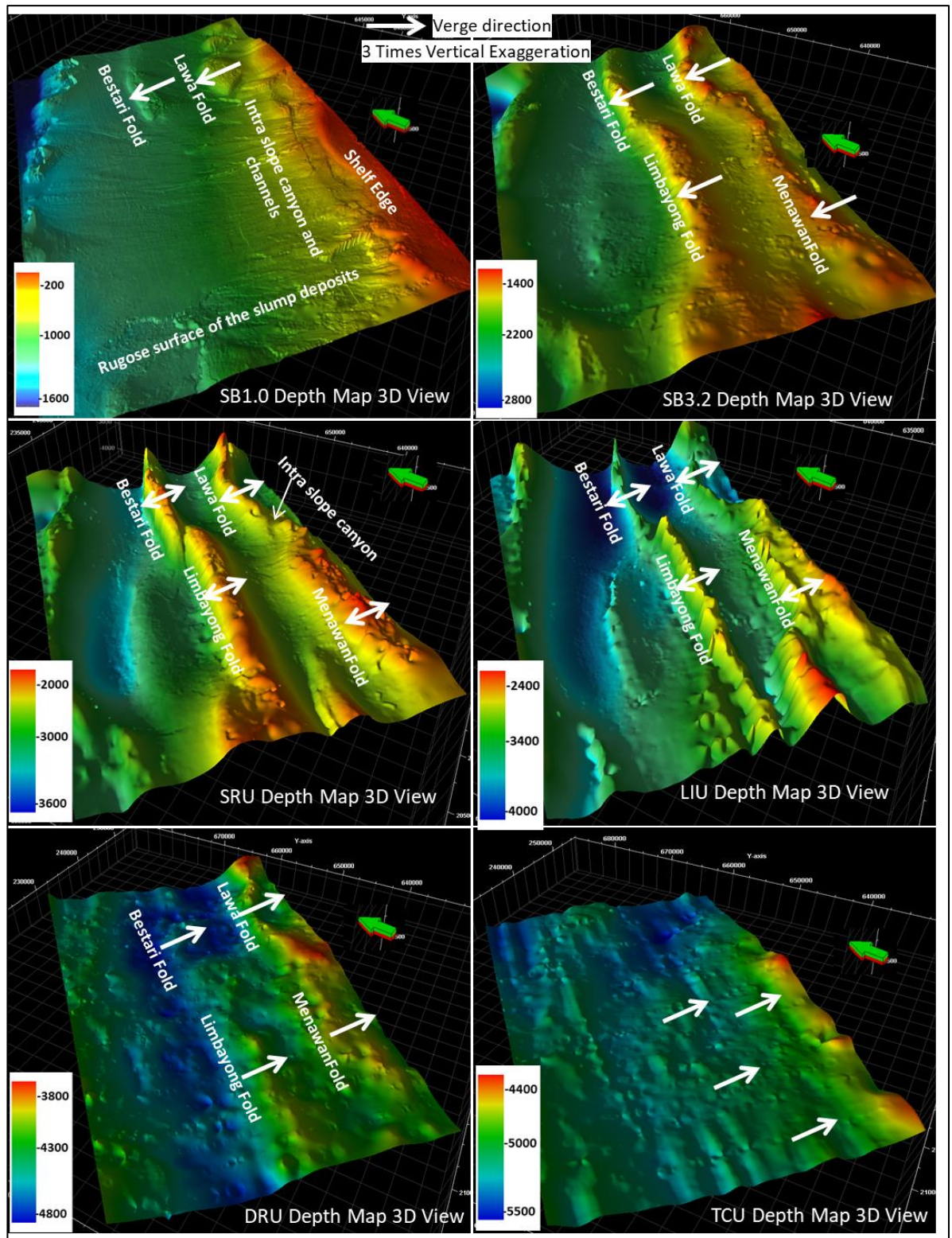


Figure 4-5: Depth maps of the interpreted horizons of the study area shows the fold and syncline geometry and vergence direction.

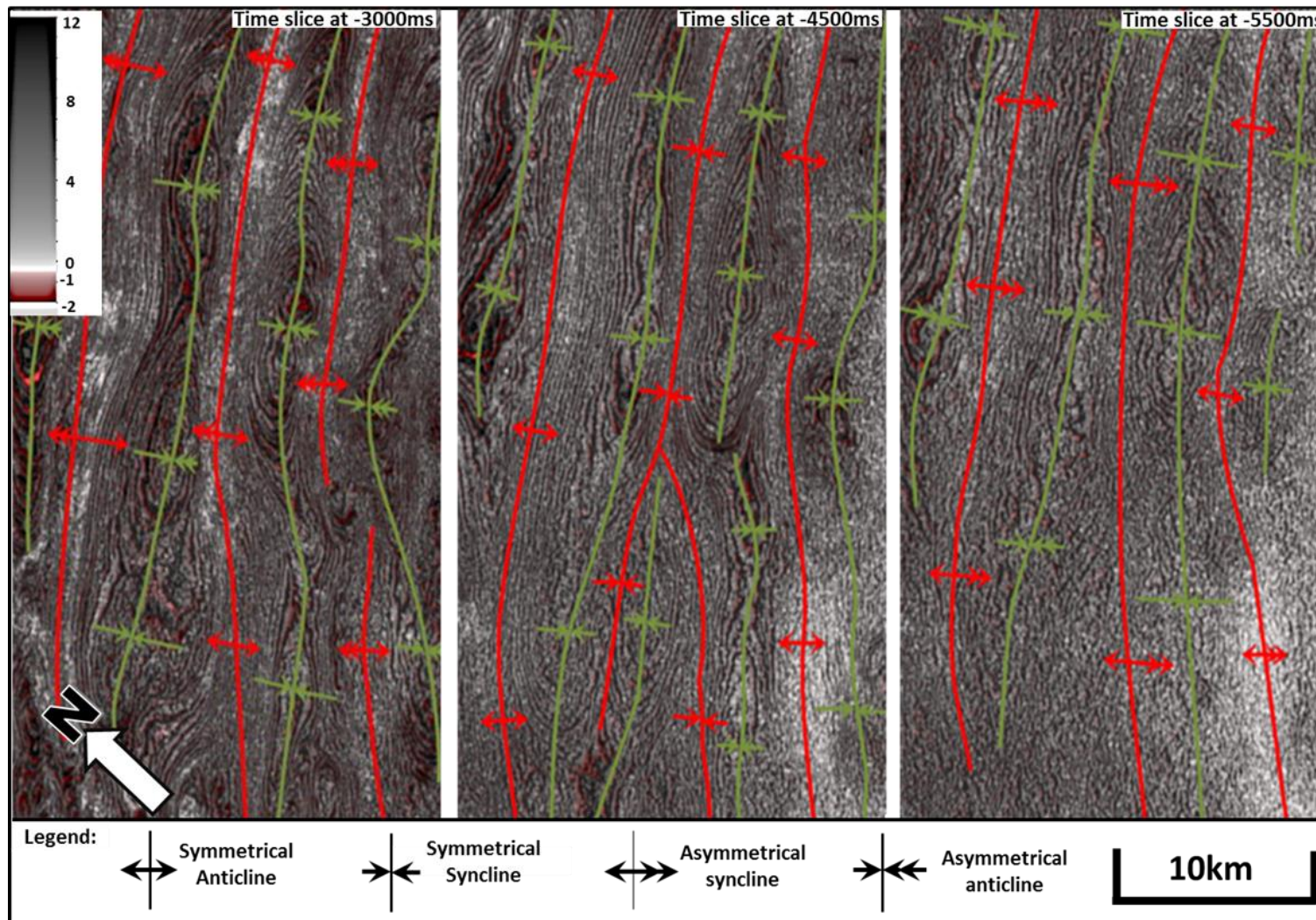


Figure 4-6: Three-dimensional seismic survey time slices in the study area show fold geometry and vergence. The time slices are cut on flat surfaces and provide a surface deepening and younger towards the basin interior (Northwest). Even though it is not possible to specifically relate the geometry with the geological time, the vergence changes from Southeast at -5500 ms to Northwest at -3000 ms.

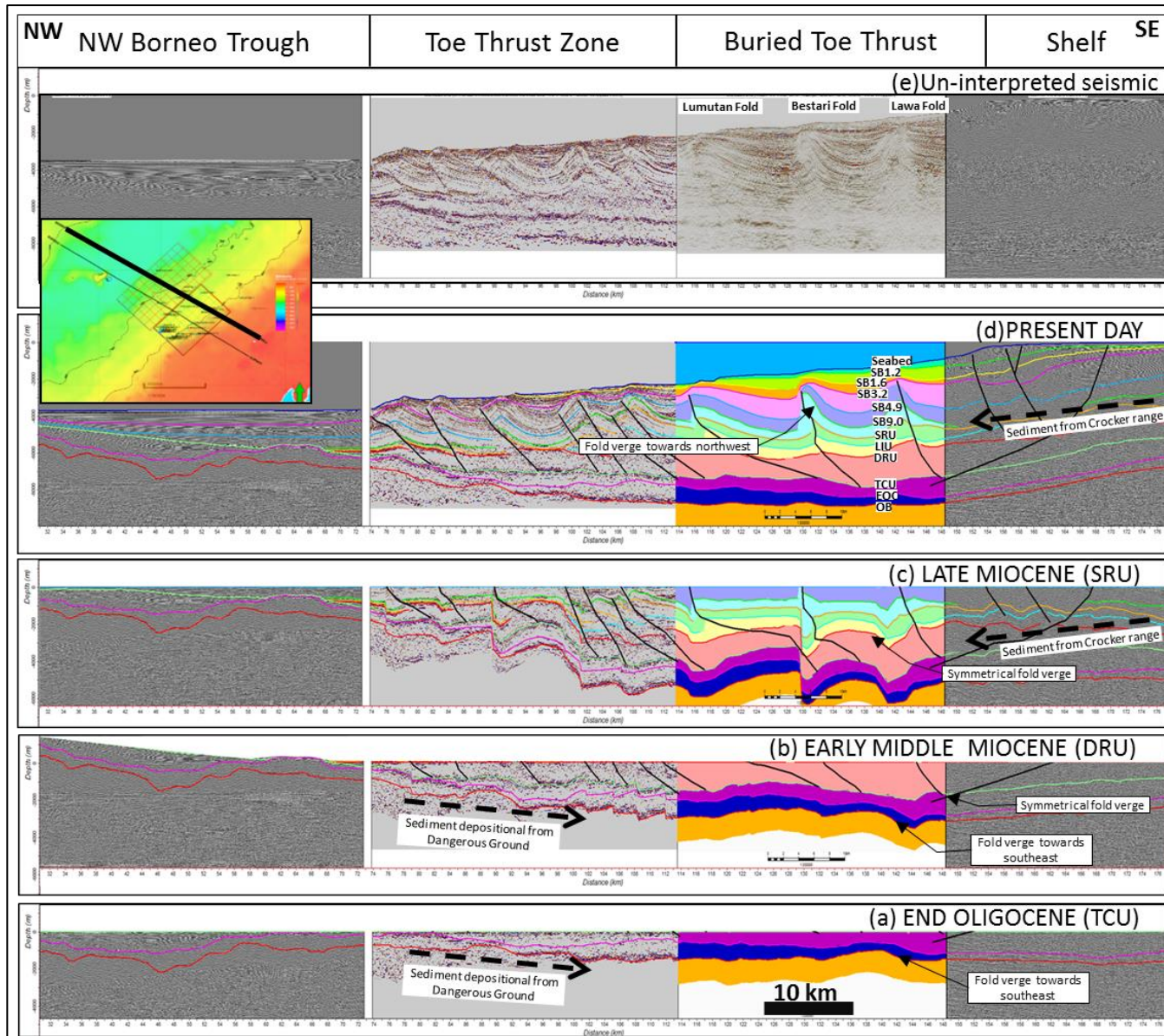


Figure 4-7: Merged 2D seismic section BGR-8622 with 3D seismic surveys (Four times vertical exaggeration) crossing all the fold thrust belt from the shelf at the Southeast towards the NW Borneo Trough and Dangerous Ground at the Northwest. The NW Borneo Trough which extends to the Dangerous Ground to the NW seems to be higher until possibly Late Middle Miocene. This might suggest the possible sediment provenance from the NW in addition to the Crocker Formation deposition in Sabah. Fold geometry, especially at the buried toe thrust zone, is observed to be more symmetrical until Late Miocene, with vergence to the NW afterwards.

4.5.6 Fold Expansion Index Quantification

In the study area, two dip-lines were selected (cross sections C-D and E-F in Figure 4-1) to lie perpendicular to the folds, with the depth converted gridded interpreted horizons from the seabed to the basement horizons (Figure 4-10). The depth cross sections were generated to analyse the fold growth history after Thorsen (1963) and Groshong (1993, 2006).

The selected dip-line cross section C–D crosses the Lawa and Bestari folds, to show the measurement method of the Flank Thickness (t_f) and Crestal Thickness (t_c) as inputs to calculate the Expansion Index (E) (Figure 4-10a). In this study, as the focus is in analysing the fold growth history, flank and crest thickness terms are used instead of the Upthrown and Downthrown terms used by Thorsen (1963) and Groshong (1993, 2006). Each horizon thickness was measured at the crest and flank parts of each fold section as inputs for the Expansion Index (EI) calculation. This procedure allows quantification of the growth fold and indirectly the thrust fault development during sediment deposition, by analysing the expansion index diagram (Figure 4-10b), where the expansion index, E is:

$$E = t_d / t_u \text{ (Equation 1)}$$

With t_d = the downthrown thickness (off structure) and t_u = the upthrown thickness (on the fold crest). The magnitude of the expansion index is plotted against the stratigraphic unit to give the expansion index diagram. The diagram illustrates the growth history of the fold. Tectonic thickening is represented by expansion index of <1 , and an index value of more than 1 indicates upward growth of the anticlinal crest during deposition. An

expansion index of 1 means no growth. Only three folds were measured for this exercise, as the Menawan fold from the E–F cross section has a limited seismic coverage at the flank area.

4.6 Results

The 3D seismic time slices, time, and depth cross sections, 2D and 3D map qualitative and quantitative analyses lead to the establishment of the geometry, vergence and growth history of the folds through time.

4.6.1 Tectonic and Depositional Control on Fold Geometry and Vergence Evolution

Even though the time slice surfaces cross age timelines, the different phases of fold development can be observed, and match the vergence direction, mainly guided by the synclinal dips and geometry. The fold development phases are based on the fold geometry and vergence on the cross sections. The structures mainly verge towards the Southeast at least until the early Middle Miocene as defined by the DRU. The next stage involves symmetrical folds. This stage affects strata younger than the DRU. At this stage, the basin possibly received sediment supply from both Dangerous Grounds and the Crocker Formation to the Northwest and Southeast respectively. Flattening the seismic data at the Late Miocene age of the SRU shows symmetrical fold trends present towards the present-day shelf, whilst vergence towards the Southeast is still recorded closer to the Dangerous Grounds. This pattern indicates the beginning of sediment being supplied from Crocker Ranges by the delta plain towards NW Borneo offshore regions. This could be taken as an evidence of the thrust and fold development becoming younger towards the present

basin, as sediment loading first influenced the proximal folds (in the Southeast) and then moved towards the distal folds to the Northwest. Vergence towards the Northwest is observed on nearly all folds in the study area, from Pliocene to present-day.

4.6.2 Evidence from Fold Dip-Azimuth Evolution

Qualitative observation from the 3D views of the DRU, SRU and SB3.2 depth-gridded horizons (Figure 4-8a) permits the classification of the geometry and vergence directions into the three phases. The DRU 3D view grid shows asymmetrical folds with vergence towards the Southeast, as there is a gentle dip towards the Northwest on the Northwest limbs and steeper dip to the Southeast at the Southeast limb of the folds. This pattern is consistently observed in most individual folds in the study area. This result gives a strong indication of the tectonic influence in the early stage of the fold development before and during the Early Middle Miocene. In Late Miocene times, as shown in the SRU 3D depth map view, the folds show symmetrical dip steepness in both sides with no obvious vergence towards any direction. The folds seem to be at the beginning of growth process, with wide and deep synclines on both flanks of the fold. The younger horizons, as shown by the 3D view of the SB3.2 horizon (Figure 4-8), shows evidence of the full influence of gravitational factors on fold development from the end of the Late Miocene until the present-day, as observed at the present seabed. The vergence direction is towards the Northwest. A huge sediment supply came from the Crocker Range via the Champion and East Baram deltas. The 2D structural map (Figure 4-8b) shows the accommodation space in regions closest to the sediment sources to the Southeast as being mostly shallower, compared to the distal synclines, with fold and thrust development becoming younger towards the deeper parts of the basin to the Northwest.

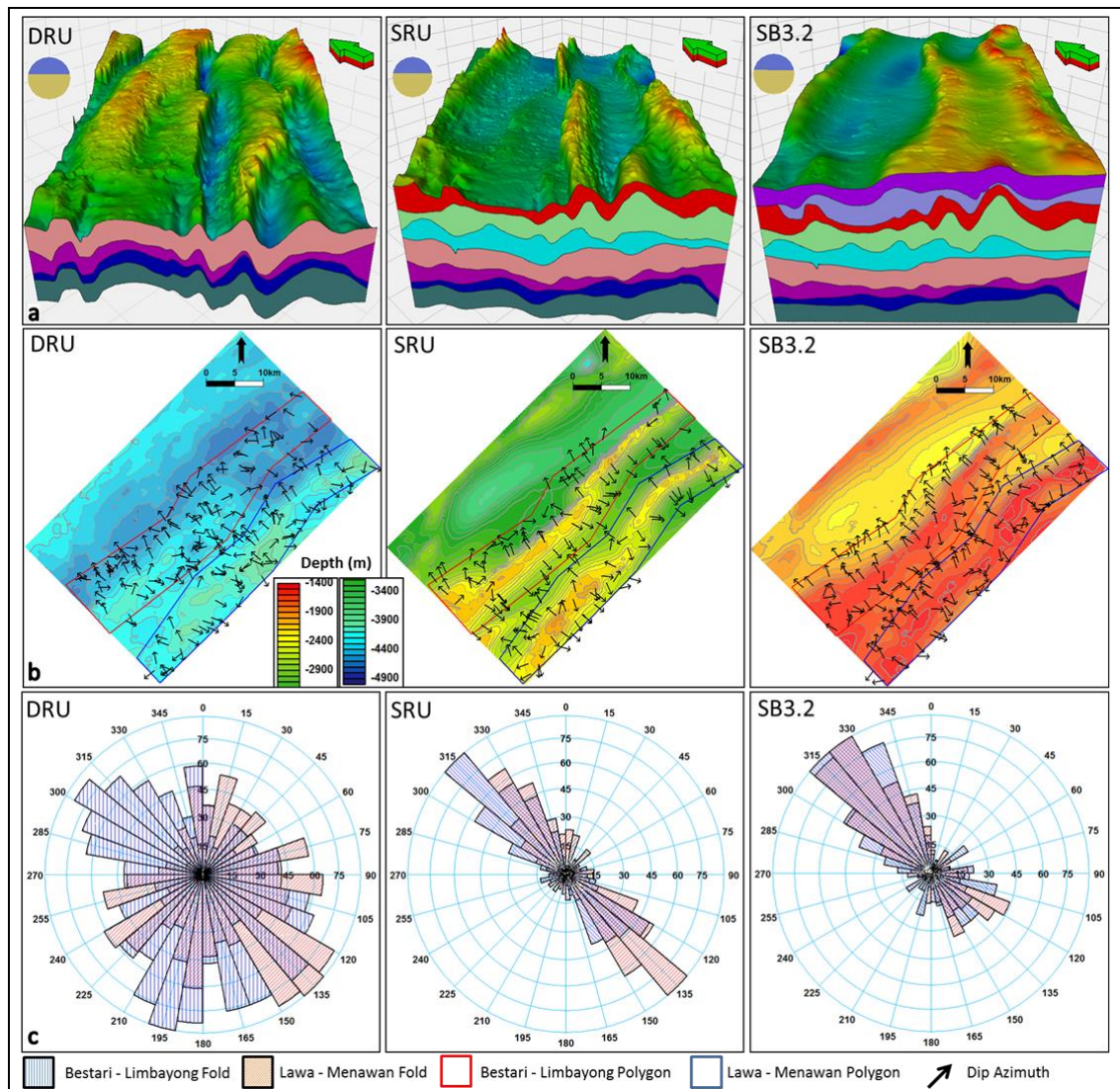


Figure 4-8: (a) The 3D view surfaces give a direct observation of the geometry and verge direction of the folds. (b) The point selection for the measurement of the dip and azimuth are scattered randomly in the polygon areas, to represent the distribution. (c) Fold dip and azimuth streeonet plots of each horizon are extracted from the gridded depth map bounded by the deepest synclines in both limbs of the fold. Both 3D views of the gridded horizons and dip azimuth measurements indicate vergence changes from mainly towards Southeast during the early Middle Miocene (DRU), becoming symmetrical in Late Miocene (SRU) and towards the Northwest during Pliocene until Recent times.

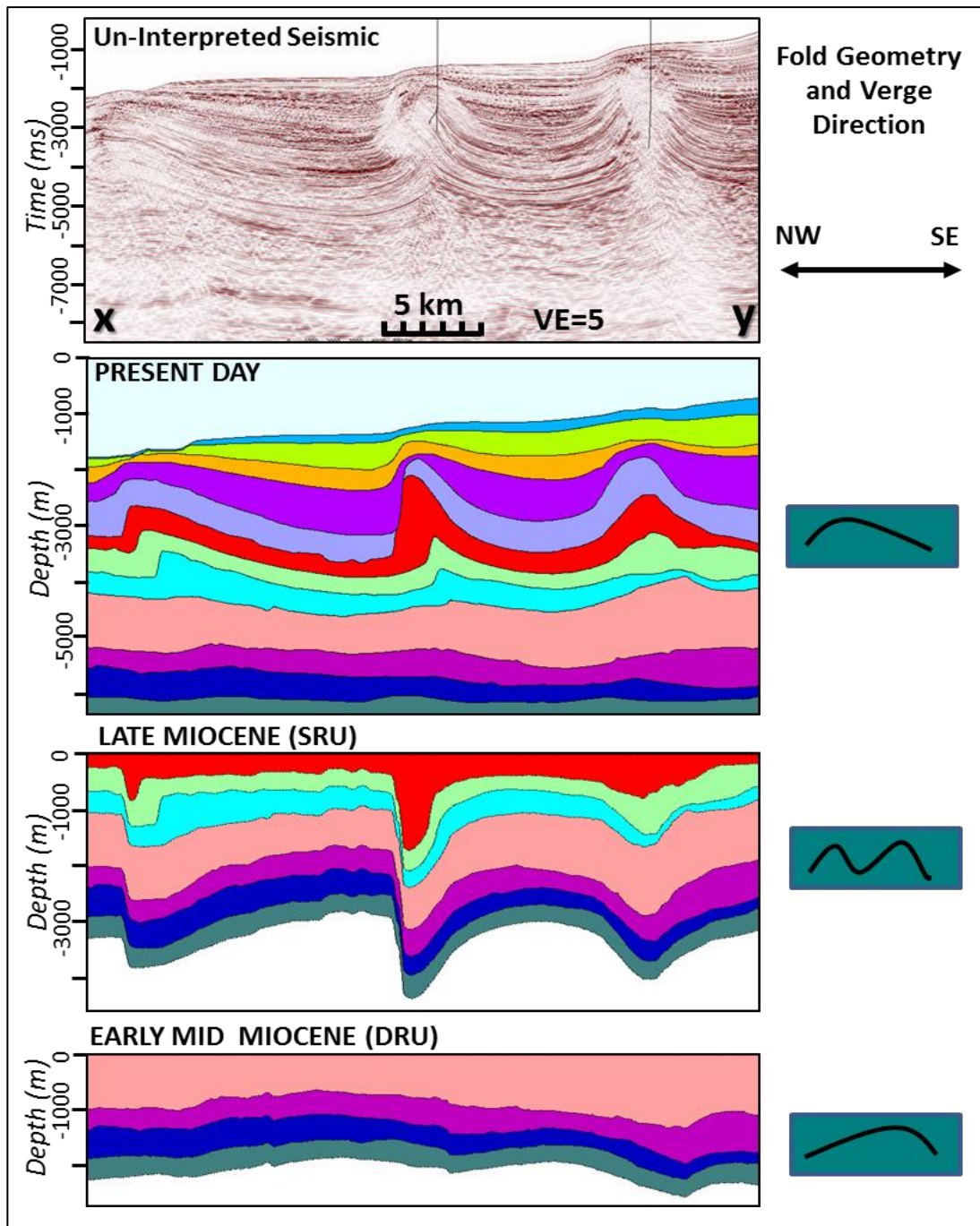


Figure 4-9: Simple restoration by applying horizons flattening of cross section x-y (shown on Figure 4-1) using the MAZ 3D seismic depth gridded horizons in the study area. Restoration was performed by applying horizon flattening to better understand the fold geometry and vergence of each horizon. The NW Borneo Trough to the Dangerous Grounds to the Northwest seems to be higher, until possibly end of the early Middle Miocene, marked by the DRU. During the SRU event in the Late Miocene, gravity-driven influence on fold growth caused symmetrical folds as the sediment influx came from the Crocker Range.

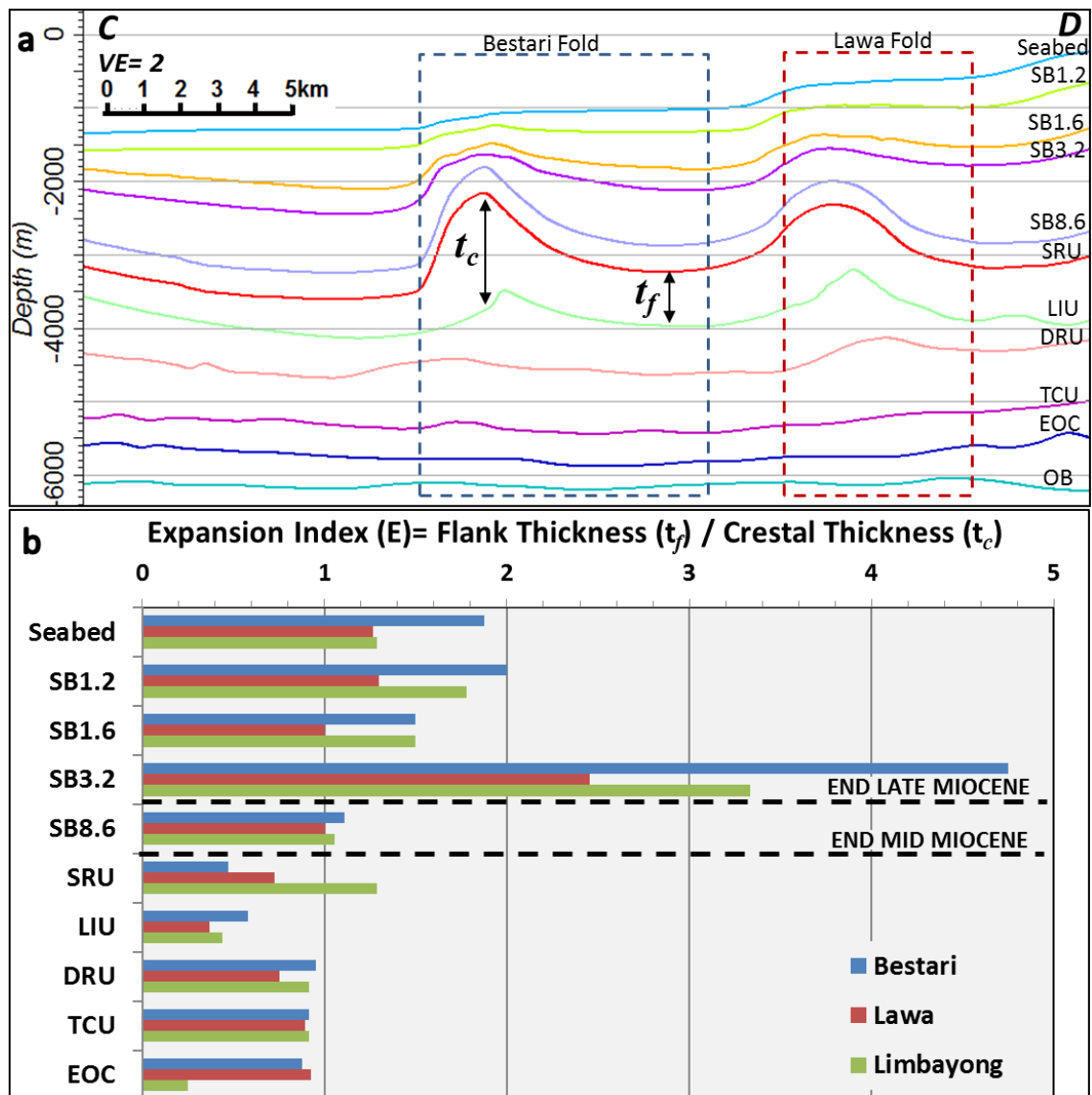


Figure 4-10: (a) Fold growth history measurement after Thorsen (1963) and Groshong (1993, 2006), for analysing the development of fold growth through time. The method uses the Expansion Index (E) measurement (flank thickness over crest thickness). (b) An E of 1 means no growth. An E value > 1 indicates upward growth of the anticlinal crest during deposition, whilst E < 1 indicate tectonic thickening.

The 3D seismic survey time slices also show the different geometries and vergences of the folds and confirm the three phases of structural evolution in the basin. In the deepest time slice from 6500 ms from subsea and deeper, the trend shows close to symmetrical anticlines, although in some parts a possible vergence to the Southeast can be seen in the Bestari and Lawa structures, despite the poor seismic image quality at this level. The geometry of the structures, especially the synclinal areas, improves in time slices at <5500 ms. All folds and synclines trend elongated parallel to the present-day coastline. Vergence is towards the Southeast in all anticlines at this structural level. Meanwhile time slices at <4500 ms demonstrate more symmetrical forms in both anticlines and synclines. The dips of the fold limbs are similar on either side of the fold, without vergence towards either direction. Closer to the seabed, at the -3000 ms time slice and upwards, the fold vergence is predominantly towards the Northwest. This pattern is observed in all folds. At this level, in between folds, the dip decreases from the centre of the syncline towards the Northwest.

4.6.3 Fold Growth History

The expansion index plot (Figure 4-10) provides a clear view of the time boundaries of the fold growth history, which also divides the fold growth into three different phases. From the Eocene to the Middle Miocene the strata were in pre-growth phase with tectonic thickening as the Expansion Index is generally below 1.

Interestingly, for the SRU horizon, during the Late Miocene, the Expansion Index is equal to 1 for all three folds (Bestari, Lawa and Limbayong), indicating a no growth phase. This

might be related to the phase when the gravitational effects began to influence fold development, as the tectonic thickening ceased.

The third phase, from the end of the Late Miocene until the Present-Day is represented by the SB3.2 horizons upwards and starts with an abrupt change of the expansion index from 2 to 4 during SB3.2 (Figure 4-10). This change suggests high upward growth, and sin-fold deposition of sediments in the synclines.

Another aspect observed by the expansion index values is the influence of accommodation space at the synclinal regions on fold development, as observed in the Bestari structure. The Bestari structure has the highest expansion index as compared to other folds, suggesting high accommodation space in the synclinal areas. Meanwhile, the Lawa fold is narrower and has a lower amplitude recording a lower expansion index (see Figure 4-10).

4.7 Discussion

The use of 3D seismic surveys in this study, in qualitative and quantitative analysis of the gridded horizons and dip-azimuth measurement, simple restoration by flattening the horizons and expansion index trend, enables the identification of tectonic and gravitational factors in controlling fold evolution in the NW Borneo deep-water fold-and-thrust belt. The 3D seismic image quality makes it possible to analyse fold evolution through time, tracking the growth history of the folds. This is critically important to understand the controlling factors, magnitude, and timing of the fold-and-thrust belt.

4.7.1 Tectonic and Gravity-Driven Influences on Fold Vergence

This study provides evidence of three phases of deformation, based on the nature of fold development in the study area over time. The timing of these phases matches regional events defined by Hutchison (2004) (Figure 4-3). The phases identified from the analysis of the fold geometry and vergence development, and the relationships with tectonic and/or gravity-driven shortening are as follows:

The first phase: A Late Oligocene to Early Middle Miocene event. No major elongated fold trend had yet formed, with the individual anticlines showing vergence towards the Southeast. We propose that this event was caused by tectonic movement of the Dangerous Grounds towards the Southeast. During this phase, the sediment was likely to have been provided by the Dangerous Grounds, with little supply from the Borneo mainland, as recognised in the regional seismic cross-section (Figure 4-7).

The second phase: Middle Miocene to Late Miocene. This phase is marked by the Lower Intermediate Unconformity (LIU) and the SRU. The generally symmetrical folds indicate the start of the gravity-driven control on the fold development, and the end of the Southeastward vergence that marked the first phase.

The third phase: Late Miocene to Present Day. This is the phase where folds actively developed with vergence towards the Northwest, the fold vergence and high sedimentation rates suggest the dominant control of gravity-driven deformation and sediment loading. At this time, the Western Cordillera uplift was almost at its peak (Hutchison, 2004). The Baram and East Baram deltas acted as the sediment sources.

4.7.2 Syncline Accommodation Space Control on Fold Growth History

The influence of the gravity-driven shortening on the existing folds are found to be affected by distance of the fold from the sediment source area. However, the accommodation space volume generated in the synclinal areas plays a major role in affecting the magnitude of fold growth.

The measured growth history of each individual fold indicates that the fold development is not only driven by regional shortening but is critically controlled by the distance from the sediment source area (Crocker Ranges) and the accommodation space in the synclinal areas. The expansion index of the folds in this study directly indicates the relationship between the fold growth magnitude and the contemporaneous sediments in the associated syncline. This has been clearly observed by the high expansion index in distally located Bestari fold compared to the proximal Lawa and Limbayong folds (Figure 4-10). This provides direct evidence for the high sediment yields transported to the basin from the Crocker Ranges via the Baram delta and shelf bypass into the deep-water NW Borneo.

The deep-water sedimentary systems have been deposited in less than 8 Myrs. and provide a first order control upon the gravity-driven fold growth. An additional control on sediment flux to the deep-water fold thrust belt is drainage diversion in response to the sin-depositional folding and thrusting, which can produce major shifts in the location and magnitude of sediment source points from the shelf. However, sediment is still temporarily stored in the synclinal regions where it intimately controls the fold growth development from the proximal to distal regions.

4.8 Conclusions

The analysis of the geometry, vergence and growth history of the NW Borneo deep-water fold-and-thrust belt in this study using three-dimensional (3D) seismic data, leads to the establishment of the three phases of fold development which related to the early fold development of the tectonic phase, the early phase of the gravitational sediment loading and the phase of the gravitational driven fold development.

The first phase begins with the controlling factor of subduction towards the Southeast, forming the initial anticline vergence towards Sabah, and sediment deposition from the Dangerous Grounds in the Northwest. The next phase involved the development of symmetrical structures in the Middle Miocene, as the Crocker Ranges started supplying sediment towards the basin. The final phase was gravity-driven development, causing thrusting and rapid growth of the folds as huge and continued sediment volumes were transported towards the basin to the Northwest.

The results presented in this research demonstrate that 3D seismic data can be a powerful tool in our understanding of deep-water fold and thrust belt systems, and that linking structural and stratigraphic investigations can provide new insights into the interactions between deformation and sedimentation.

The methods used in this study are applicable for other deep-water fold-and-thrust belt systems and especially those with a development history influenced by both tectonic and gravitational sediment loading.

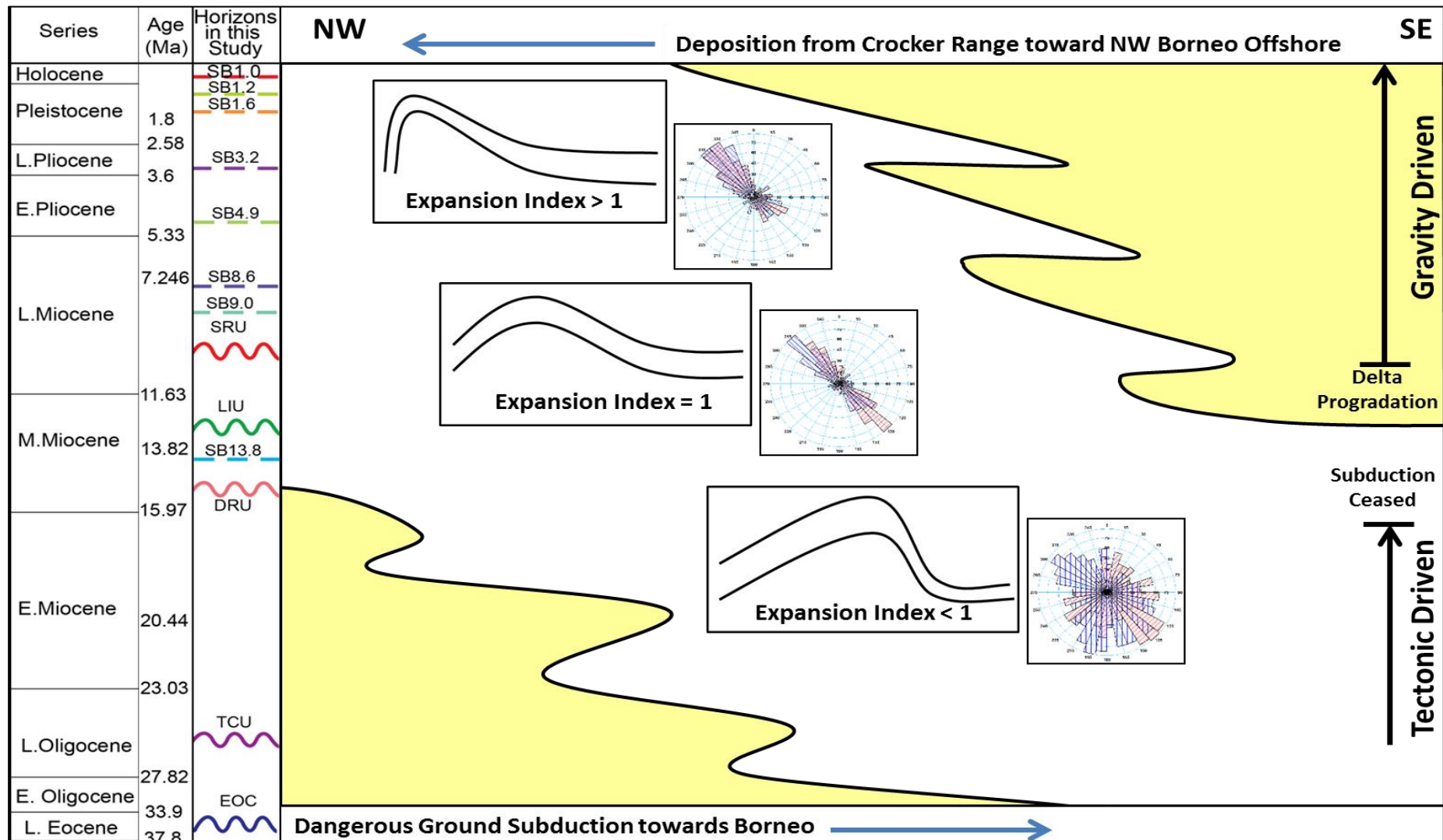


Figure 4-11: Summary of the identified phases of fold development and growth history in NW Borneo deep-water fold-and-thrust belt, with the tectonic and gravity-driven controlling mechanisms.

Chapter V:

Depositional, and facies

distribution in NW Borneo deep

water fold-and-thrust belt

5.1 Introduction

Submarine fan complexes and mass-transport deposits (MTD's) are the results of gravity induced sedimentary flows (e.g., turbidites) occurring mainly in deep water environments. They dominate sediment transport into many parts of the deep ocean and produce some of the most extensive and voluminous sediment accumulations on Earth (e.g., Bengal and Indus submarine fans). Because these deep-water sediments are widespread and have various drivers in diverse tectonic settings, deep-water sequences are generally characterised by complicated depositional architectures and poorly constrained stratigraphic correlations. Several studies have stressed the effect of tectonic forcing on the origin and trigger of MTDs and turbidite systems especially in tectonically active margins (e.g., Hodgson et al., 2018; Pickering & Corregidor 2005; Sweet and Blum, 2016).

In submarine fold-and-thrust belt settings, tectonic activities such as faulting and earthquakes cause submarine slope failures that move vast quantities of sediment down slope to the deeper basin portions and/or topographic lows via mass transport process (Ortiz-Karpf et al., 2018). Tectonic process also affects deep-water active margins because tectonically induced topography forms positive bathymetric barriers, or tectonism directly triggers the avulsion of submarine channels in submarine fan complexes. Therefore, it is essential to understand the tectonic control on deep-water deposition in tectonically active and fold-and-thrust belts.

Furthermore, the dynamic setting of a deep-water fold-and-thrust belt requires the application of detailed and robust stratigraphic correlation to allow for regional correlations and clear links to clastic input sites from the continental shelf and slope.

The deep-water fold-and-thrust belt of Northwest Borneo, to the Northwest of Sabah is the main focus of this study (see Figure 5-1). The study area is located at the edge of the Sabah shelf in the Northwest Sabah Province, to the North of Baram Delta and the Northwest Sabah Trough to the Northwest. Sediment is sourced directly from the Crocker Ranges of NW Borneo and transported directly to the continental margin via rivers (e.g., Blum and Hattier-Womack, 2009).

The high sediment supply via the Champion and Baram Deltas has supplied clastic sediments to the Sabah shelf over the last 12 Ma, but in particular the last 5 Ma. This sediment loading on the Sabah shelf edge has created instability. This instability, when combined with a trigger mechanism (e.g., tectonism), can result in collapse of the accumulated sediment downslope in the form of sediment gravity flows, specifically turbidity currents, debris flows and MTDs.

The recognition of the effect of a tectonic control on the MTD's and sediment gravity flows of the deep-water fold-and-thrust belt of NW Borneo have been widely acknowledged (e.g., Ingram et al., 2003). However, there still is a paucity of detailed analysis that provides robust stratigraphic correlation of the submarine fan sands and MTDs, and their correlation with the syn-depositional fold growth. This will be addressed in this chapter by using interpretations of well and seismic to explain the

submarine fan deposition and facies distribution and through the application of high-resolution sequence stratigraphy and advanced seismic attribute extraction techniques.

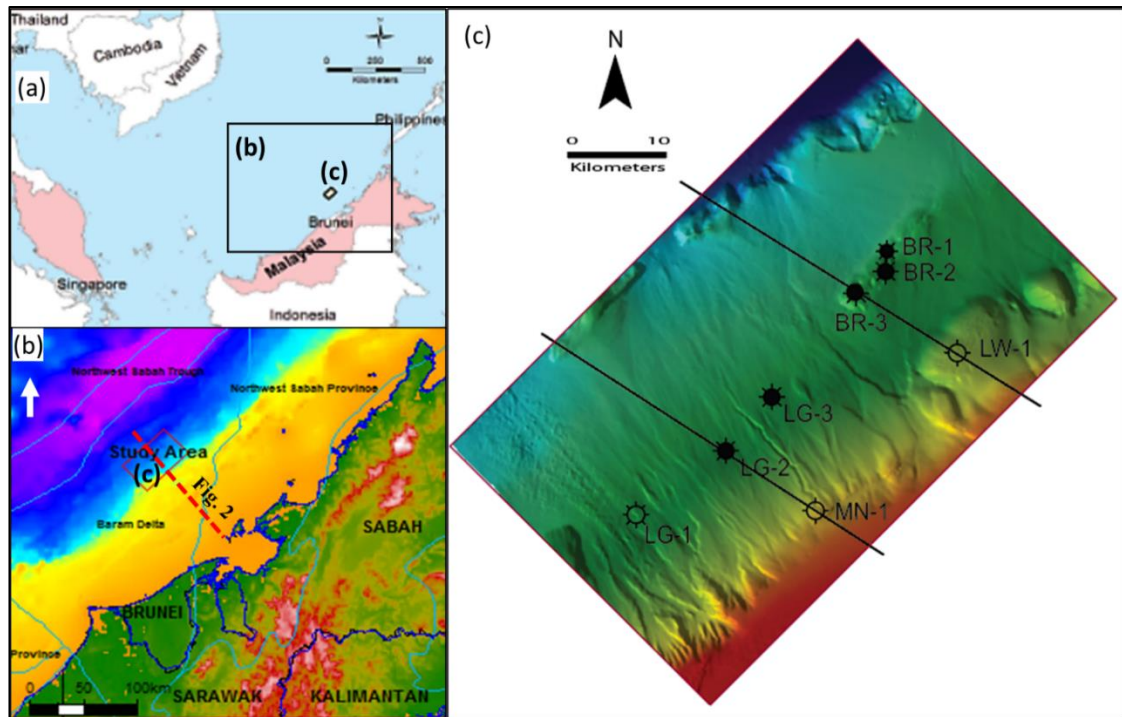


Figure 5-1: The study area located in the middle part of the NW Borneo deep-water fold and thrust belt aligned parallel with Sabah coast. Borneo has at least 4 other deep-water fold-and-thrust belt all around the island. Modified from Morley et al. (2011).

5.2 Tectono-stratigraphy framework

The deep-water NW Borneo fold-and-thrust as defined in the previous chapter of this thesis could be divided into three phases of fold development (Figure 4-11) with the first phase solely controlled by the tectonic activity of the dangerous ground subduction towards Borneo from Late Oligocene to Early Middle Miocene. During this phase, the sediment was likely sourced from the Dangerous Ground at the Northwest with little supply from the Borneo mainland. The second phase, from Middle to Late Miocene, the

ceased of the subduction towards Borneo and subsequent uplift of the Crocker Ranges caused huge amount of sediment being deposited from the mainland forming the Champion and Baram deltas and sourced the sediment towards the deeper part of the basin. The third phase, from Late Miocene to present-day, the continuous supply of sediment from the Crocker Ranges highly influences the development of the gravity-driven fold-and thrust belt in deep-water NW Borneo.

The NW Borneo inboard province, at the shelf of the Sabah shallow water was characterized by multiple deformation phases of extension, inversion, and compression, whilst the outboard provinces were largely dominated by the gravity-related delta and form a compressional fold belt further basinward (Ingram et al., 2003).

Casson et al (1998) identified a 7 km height differential between the highest peak of the Mount Kinabalu at 4,101 m and the 3000 m deepest water in NW Sabah trough in over just 200 km distance. The shelf is 80-100 km wide and comprised of mixed clastic and carbonate sedimentation and a steep continental slope towards the shelf break. The slope with an average of $>2^\circ$ is characterized by sediment by-pass features such as canyons, channels, and slump scars at the upper slope. Moving basin-ward, the fold-and-thrust belt setting is progressively dominated by under-filled ponded basins with ponded turbidites younging towards the basin floor of the Sabah Trough. Unconfined mixed sand and mud submarine fan systems have evolved and form the greatest accumulations of sediment in the deep-water environment.

The episodic uplift of the Crocker Ranges is recorded in the Middle Miocene as the Deep Regional Unconformity up to the Shallow Regional Unconformity in the Upper Miocene

which resulting in the north-westwards limit of tectonic deformation being progressively moved ocean-wards towards the continental slope (Hutchison 1996). The deformation resulted in the rapid deposition of a thick deltaic sequence around Borneo (Hall et al., 2002) such as Baram Delta built out onto the NW Borneo margin from the early Miocene to the present day (Hall et al., 2002 and Morley et al., 2008).

The short distance between the coastline of Borneo and the deep-water fold-thrust belt provides a narrow shelf with limited accommodation space for the clastic detritus supplied from the uplifting Crocker Ranges, even at present during a highstand. Shelf-slope instability from rapid sediment loading, monsoonal storm-wave loading, and seismicity leads to sediment from inland to cascade further down the slope through feeder canyons and submarine channels via mass flows, debris flows, and canyons periodically flushed by turbidity currents (Hutchison, 1995 and Grant, 2004). The turbidity currents and submarine fans are closely controlled by the submarine topography (growth folds), with which the submarine fans and turbidity currents interact.

5.3 Stratigraphy sequence framework of the study

The study area is located in the SW Sabah Ramp Margin as defined by Grant (2004). This margin is characterized as the less developed sand-prone deep marine fan systems, that are smaller in size and amalgamated locally which originated from multiple entry points along a linear ramp margin. This was due to the growth faulting within the deltas created much more accommodation space on the shelf as compared to the northern part of the basin limiting deep marine fan deposition towards the outboard (Figure 5-2).

At least seven turbidite complexes are identified and mapped regionally from inboard towards the shelf edge in the form of slope channels and bypass assemblages, further outboard to the deeper water was mainly deposited as mixed sand-mud and mud dominated basin floor fan systems (Ingram et al., 2004). The turbidite fan complexes are from youngest to oldest: the Lingan Fan, Pink Fan, Kamunsu Fan, Kinarut Fan and Keabangan Fan. The submarine fan complexes are correlated by seismo-stratigraphy with unconformities on the shelf with relation to sea-level changes.

The focus of the exploration activities in this region is mainly on the second and third phase of the fold development become the well penetration has mostly targeted the fan systems in the Middle Miocene to Late Miocene (Fig. 5-2). Therefore, the well data acquisition and evaluation has focused on the Pink, Kamunsu, Kinarut and Keabangan submarine fan systems.

This study identified six main sequences (I-VI) from the Middle Miocene to the present-day, bounded by six Maximum Flooding Surfaces (MFS) defined mainly using well log analysis by interpreting their vertical stacking patterns, mainly to determine system tracts and other stratal surfaces which could not be determined from seismic. In addition, well log was analysed to interpret depositional environments and predict lateral facies correlation and distribution between the well locations, supported by seismic data. The log stacking pattern is a manifestation the interplay between rate of deposition versus accommodation space created. A progradational stacking pattern is normally reflected by a coarsening upward succession observed on log responses. It could be associated with a higher rate of deposition relative to accommodation space or relative sea level rise. Aggradational stacking pattern is represented by a uniform log stacking pattern, reflecting

a balance between sediment supply and rate of accommodation space. Meanwhile, retrogradational stacking pattern shows fining upward succession reflecting rate of sediment supply is lower than accommodation space or relative sea level rise. By different type of stacking patterns described above, appropriate system tracts can be determined.

The well log analyses performed on Gamma Ray (GR) log, Compressional Density log (DTCO) cross over with GR, and Neutron (NPHI) and Density (DEN) logs cross over (Figure 5-3). The MFS was picked on the cleanest shale possible indicating possible deepest water before the sea level changes from Transgressive System Tract (TST) towards the Prograding Complex (PGC) of the slope and basin floor at the deeper water and Low stand System Tract (LST) at the shallower water closer to coastline. Biostratigraphy correlation of the nannofossils (NN) and pollen provided by PETRONAS from Corelab evaluation from Bestari-1, Bestari-2ST1 and ST2, Menawan-1ST1, Lawa-1 and Limbayong-1ST1 wells in the study area are used to confirm the MFS ages.

The picked MFSs from the well, correlated with the seismic and could be related directly to the seismic amplitude, continuity and frequency changes that directly provide details of the sedimentary facies (Figure 5-3). The seismic data has specifically been appraised in detail for recognition of the MFS's and sequence boundaries in the synclinal regions where submarine fan ponding and turbidite compensational stacking has taken place. Third order stacking patterns and sequences of the area generally shows a repetition of coarsening upwards (PGC) and fining upwards sequence (TST). These identified six sequences are as follows:

1. Sequence I, the deepest penetrated sequence by the well, bound by the MFS11.6 at the top of the sequence. The Keabangan Fan is the reservoir potential in this sequence with bright and continuous amplitude from the seismic could be related with the turbiditic sand. This sequence marked by the Upper Intermediate Unconformity (UIU) at the Upper Middle Miocene.
2. Sequence II extend from MFS11.6 to MFS9.0 is the Kinarut Fan associated deposition mark by dim and discontinuous seismic amplitude at the bottom part interpreted as possible Mass Transit Complex (MTC) and the continuous and bright amplitude of the turbiditic sand on the top of the sequence.
3. Sequence III, from MFS 9.0 at the bottom to MFS8.7, marked by the Shallow Regional Unconformity (SRU) right on top of the sequence and associated with the Kamunsu Fans depositions. The well penetration and seismic generally shows possible two or three turbidites sand packages deposited at this sequence separated by either pelagic shale or MTC.
4. Sequence IV associated with the Pink Fans extend from MFS8.7 to MFS6.7. The bottom of the sequence dominantly filled by pelagic shale as observed from the dim and continuous seismic amplitude. With possible thick turbidite sand at the upper part shown by the bright continuous seismic amplitude.
5. Sequence V, bounded by MFS6.7 at the bottom, MFS5.6 in the middle and MFS 4.1 at the top. This sequence is a combination of two sequence, the bottom part associated with the Yellow Fans and the top part with the Lingan Fans.

6. Sequence VI is the Pleistocene and Holocene sediment fill mainly by pelagic shale dominant with thin layers of sand.

This study will be focusing on the Sequence VI, V, IV and III with direct relationship to the Pink, Kamunsu, Kinarut and Keabangan submarine fan facies, respectively. These sequences are mainly the drilling exploration target in this area and proven to be prolific with production fields producing from this reservoir in the adjacent regions.

5.4 Depositional settings and facies associations

One of the fundamental concepts for appreciating the deposition of submarine fan systems is the importance of the balance between sediment supply and space for sediment accumulation, called "accommodation". When sediment supply is sufficient to overwhelm nearshore accommodation on the continental shelf, deposition can be focused on submarine fans in the deep sea. Accommodation creation and destruction have been tied to sea-level fluctuations, especially those caused by glacial eustasy. Hypothetically, when sea level falls, accommodation on the shelf is relocated basinward to the deep sea. Fluvial systems are able to cross the subaerially-exposed shelf and deliver their sedimentary loads to the heads of submarine canyon-channel systems, which funnel the sediment to deep-sea fans. This generates the 'classic' lowstand clastic wedges. It has been noted that sediment delivery to submarine fans and turbidite systems can occur during any stand of sea level, and especially if there are incised canyons cutting across the continental shelf and sediment is transported to the shelf edge.

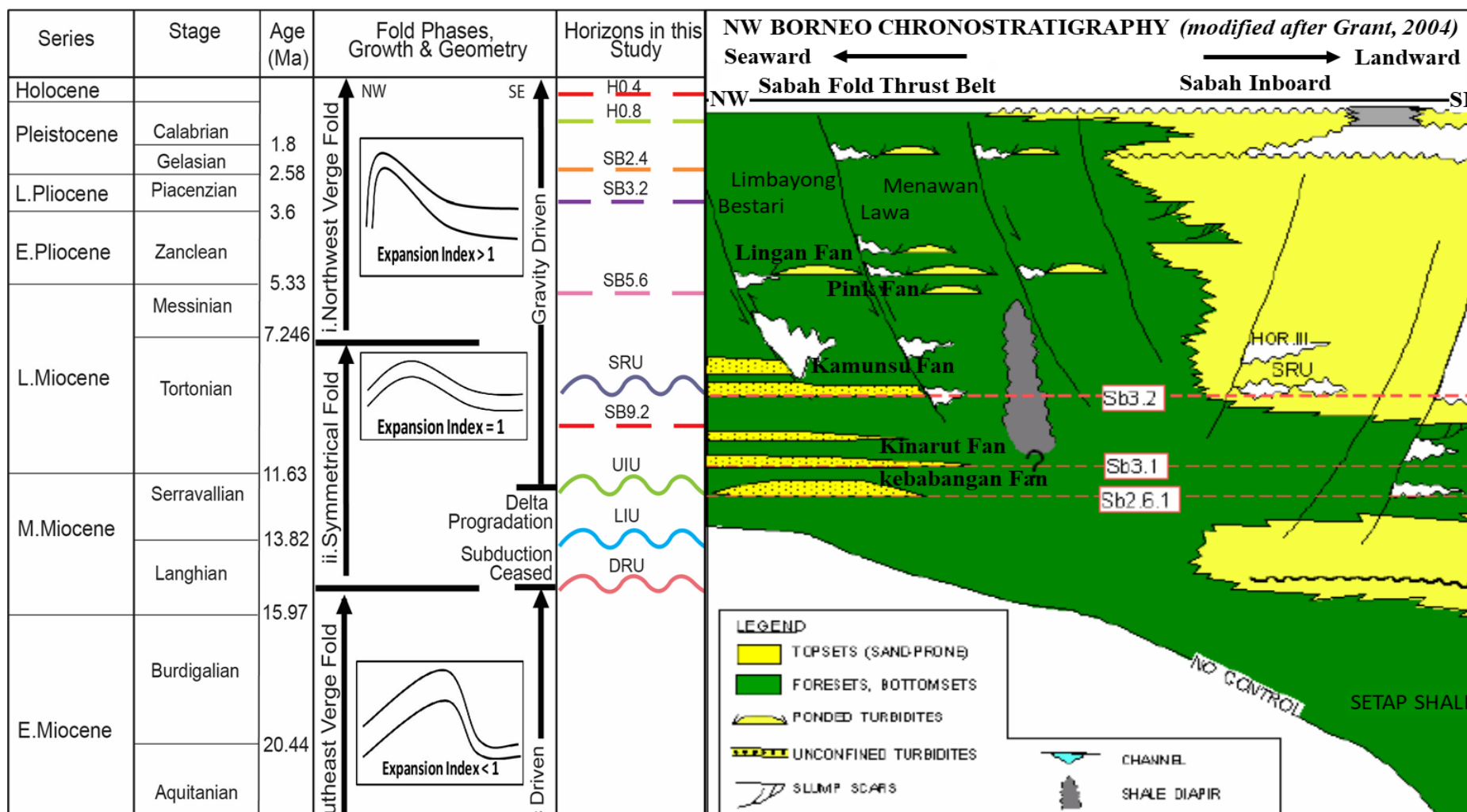
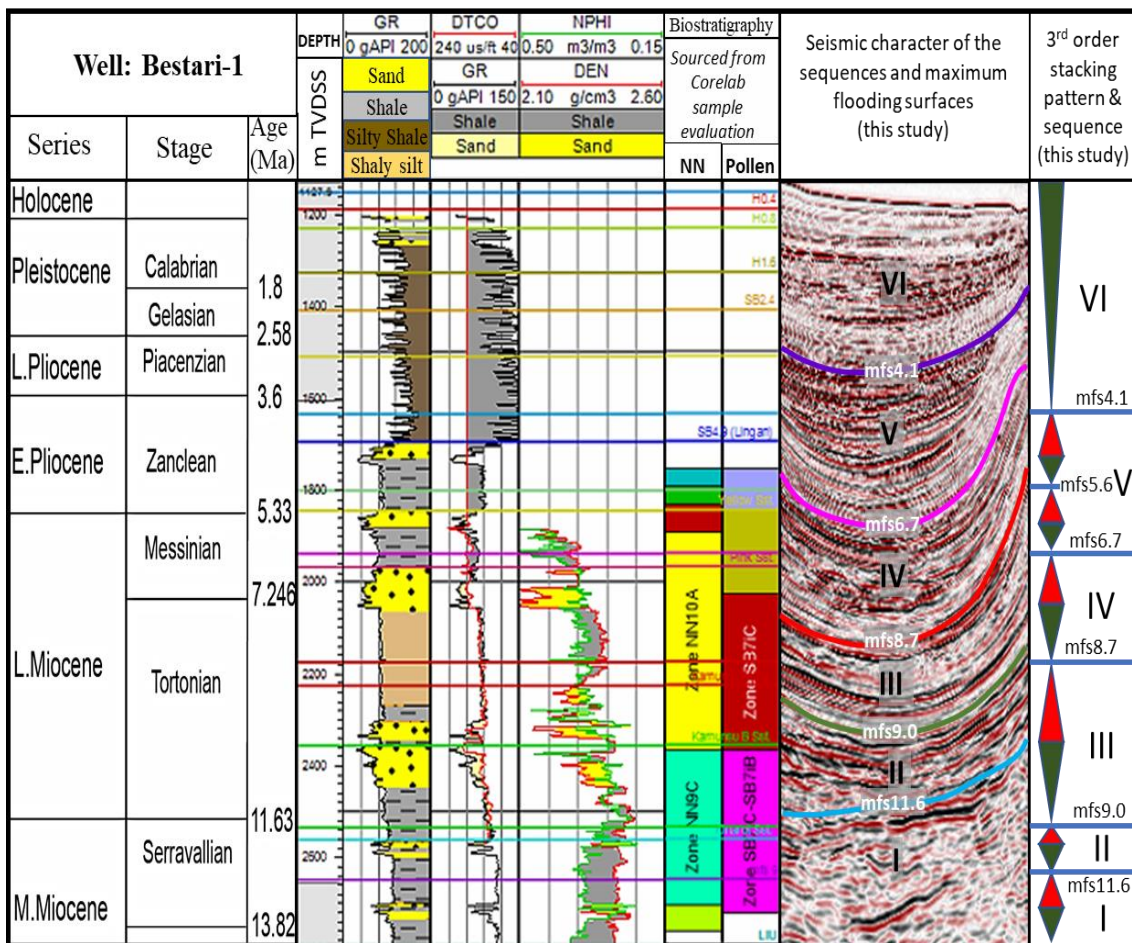


Figure 5-2: Deep-water NW Borneo fold-and-thrust belt evolution and the horizons correlated in this study with the regional NW Borneo chronostratigraphic (Modified from Grant, 2004).



System tract	
	Prograding Complex
	Transgressive system tract

Figure 5-3: Log signature interpretation of the stratigraphic systems tracts and associated facies. Gamma-ray (GR) log is cut off at 80 API applied on to differentiate shale, and 70 API to separate silt from sand. The GR is calibrated with lithology description from cuttings and core sample. DTCO cross over with GR and density with Neutron log to confirm the lithology changes and shale baseline trend.

Similarly, when sediment supply is sufficient to push deltas to the edges of shelves, deep-water deposition can ensue independent of sea-level fluctuations (Burgess & Hovius 1998, Carvajal *et al.* 2009). The study area in the SW Sabah Ramp Margin is a less developed sand-prone and mixed mud-sand deep marine fan systems and dependent on multiple entry point as the proximal deltas at the shelf developed huge accommodation space particularly in the Champion delta in offshore Brunei (Grant, 2004).

5.4.1 Deposition accommodation

Prather (2000 & 2003) divided the accommodation settings in the deep-water submarine slope based on the topography of the depositional surface (Figure 5-4):

5.4.1.1 *Ponded accommodation*

Structural movement due to sediment loading of gravity-tectonic formed thrust folds within intra-slope basins typically related to mobile substrates such as salt or shale (Prather *et al.*, 1998). The substantial topography such as steep and high fold anticline blocked the sediment down-slope route and caused major diversion of the submarine channel orientation (Mayall *et al.*, 2006). This expression could be observed in the sea-floor topography of the study area, as sediment deposition concentrated in the synclinal area between folds and elongated parallel to the fold orientation forming a confined ponded fan.

The syn kinematics sedimentation of submarine fan facies was abundant and accumulated next to and above each thrust / fold. The submarine fan sedimentation filled the available

accommodation space and can form incised channels and /or canyons cutting the growth fold tips, transporting sediment further outboard. If the sediment supply is less than the space provided by the fold-growth, the submarine channel flows around the growth folds high towards the basin floor and flow expansion is commonly recognised (Figure 5-6).

5.4.1.2 Healed slope accommodation

Defined as the space above the stepped-equilibrium profile and higher angle equilibrium profiles associated with wedge-shaped slope deposits that tape both landward and seaward (Prather, 2000 and 2003; Prather et al., 1998). A stepped profile can be formed across series of the filled ponded basins if the sediment flux exceeds rates of the intra-slope subsidence.

The healed slope accommodation usually formed on the top of the filled ponded accommodation, the sediment formation of a younger fan sequence with possible wider distribution seaward of formed a series of submarine fans linked on the top of the growth fold stepping down to the basin floor.

5.4.1.3 Incised submarine valley accommodation

Submarine canyon accommodation created by submarine erosion filled with a variety of channel deposits, dip- oriented U-shape to V-shape erosional features by significance unconformities.

5.4.1.4 *Slope accommodation*

The space between the highest stable graded-slope angle and the top of healed-slope accommodation or other older lower-grade depositional profiles (Prather, 2000). Slope accommodations appears to have little associated sand (Prather, 2003) and in this study area might be associated with the by-pass zone in the proximal from sediment source, just adjacent to the shelf break.

Figure 5-5 and 5-6 shows the accommodation settings type adopted to the sea-floor topography in the study area and the possible variation of facies distribution of the settings. The relationship and understanding from the present-day seabed profile will be useful in understanding the deeper reservoirs as the same process and depositional settings of the gravitational-loading towards the deep-water fold-and-thrust belt from Middle Miocene to present-day.

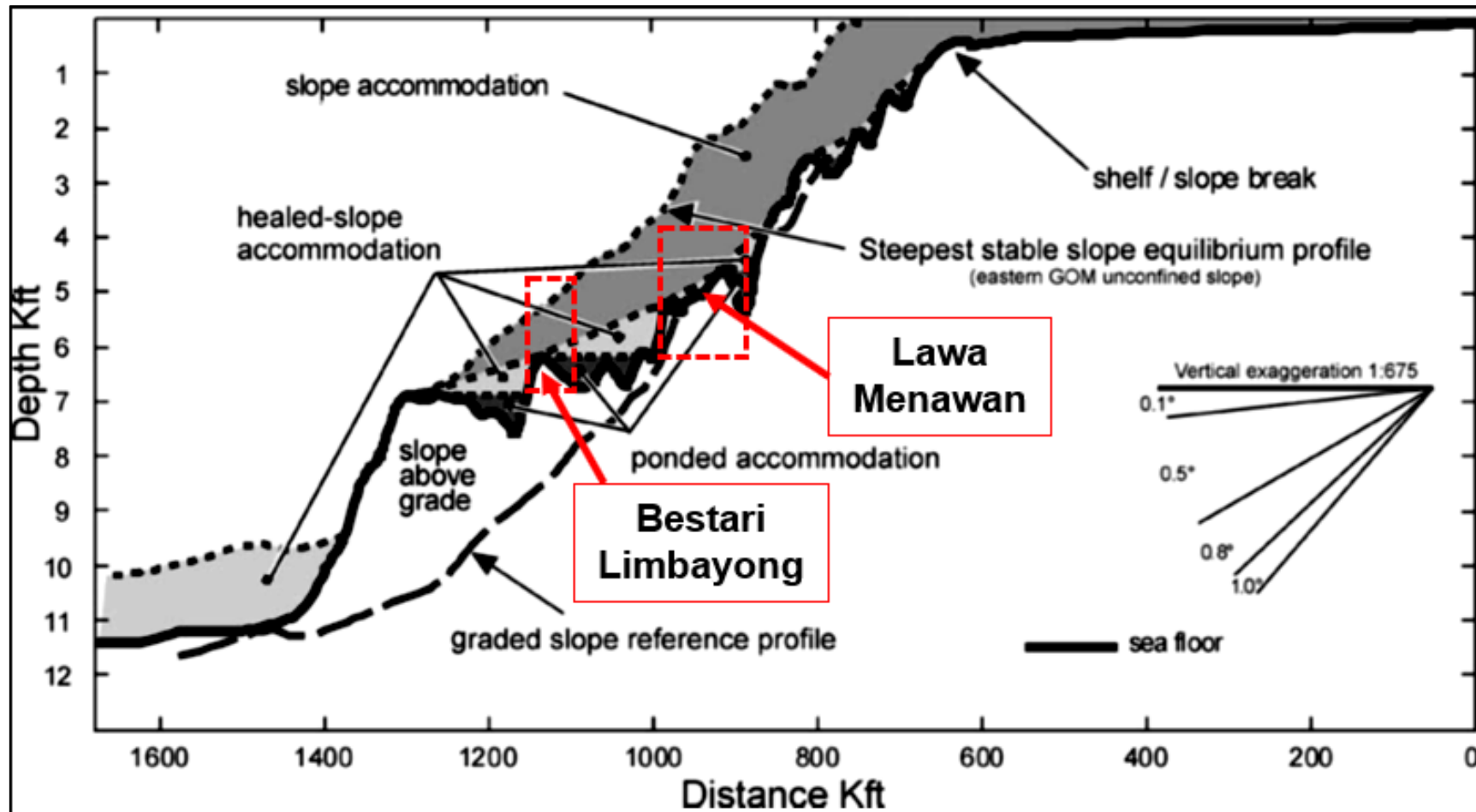


Figure 5-4: Various accommodation settings of seafloor profiles from the central Gulf of Mexico by Prather (2000, 2003).

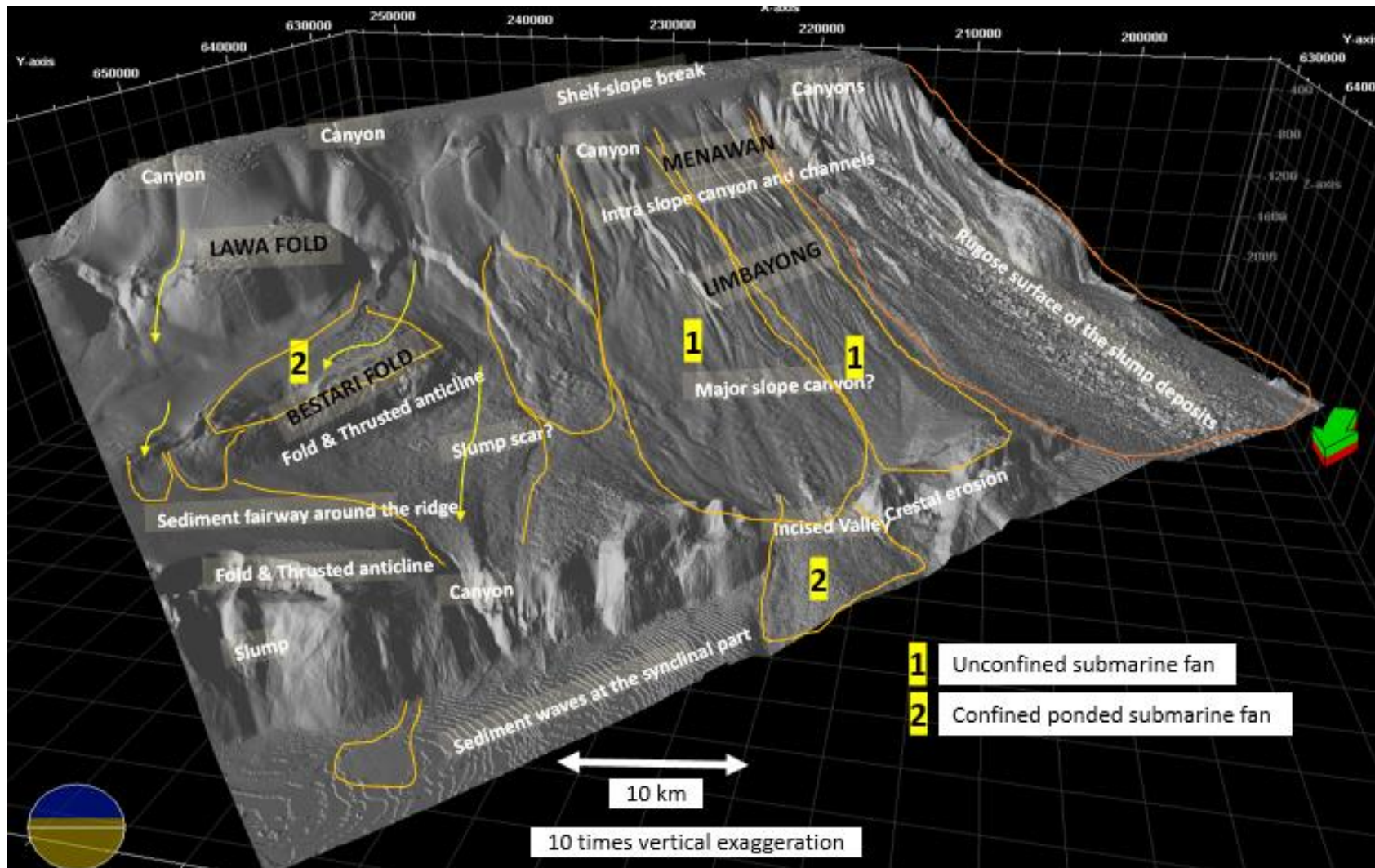


Figure 5-5: Seabed topography of the study area showing the variety of accommodation space of the slope and intra-basin settings in deep-water fold-and-thrust belt of NW Borneo.

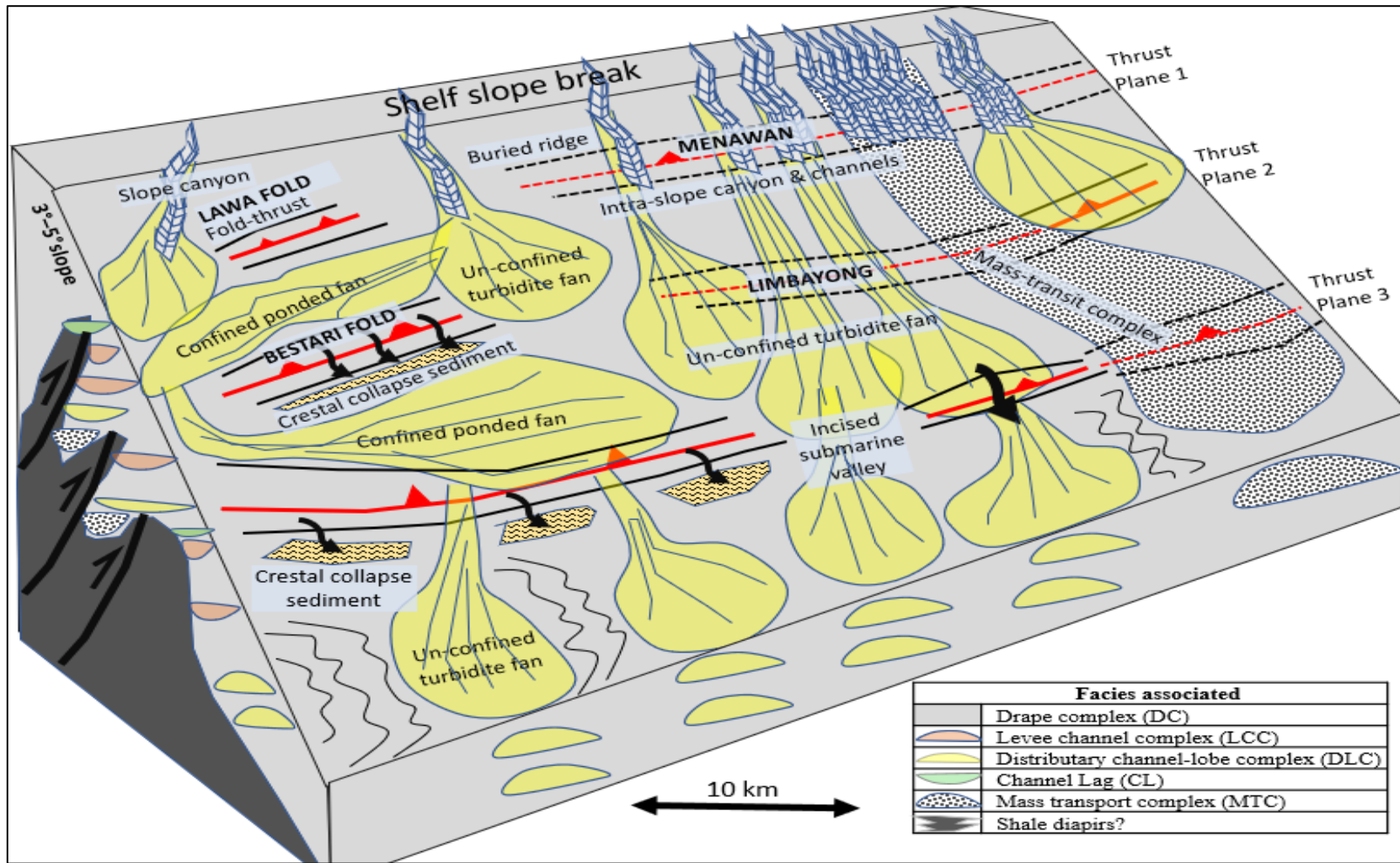


Figure 5-6: Accommodation space model of the study area based on the topography of the seabed. The model is applicable for the deposited fan systems from Middle Miocene to present-day as the process and depositional settings are the same.

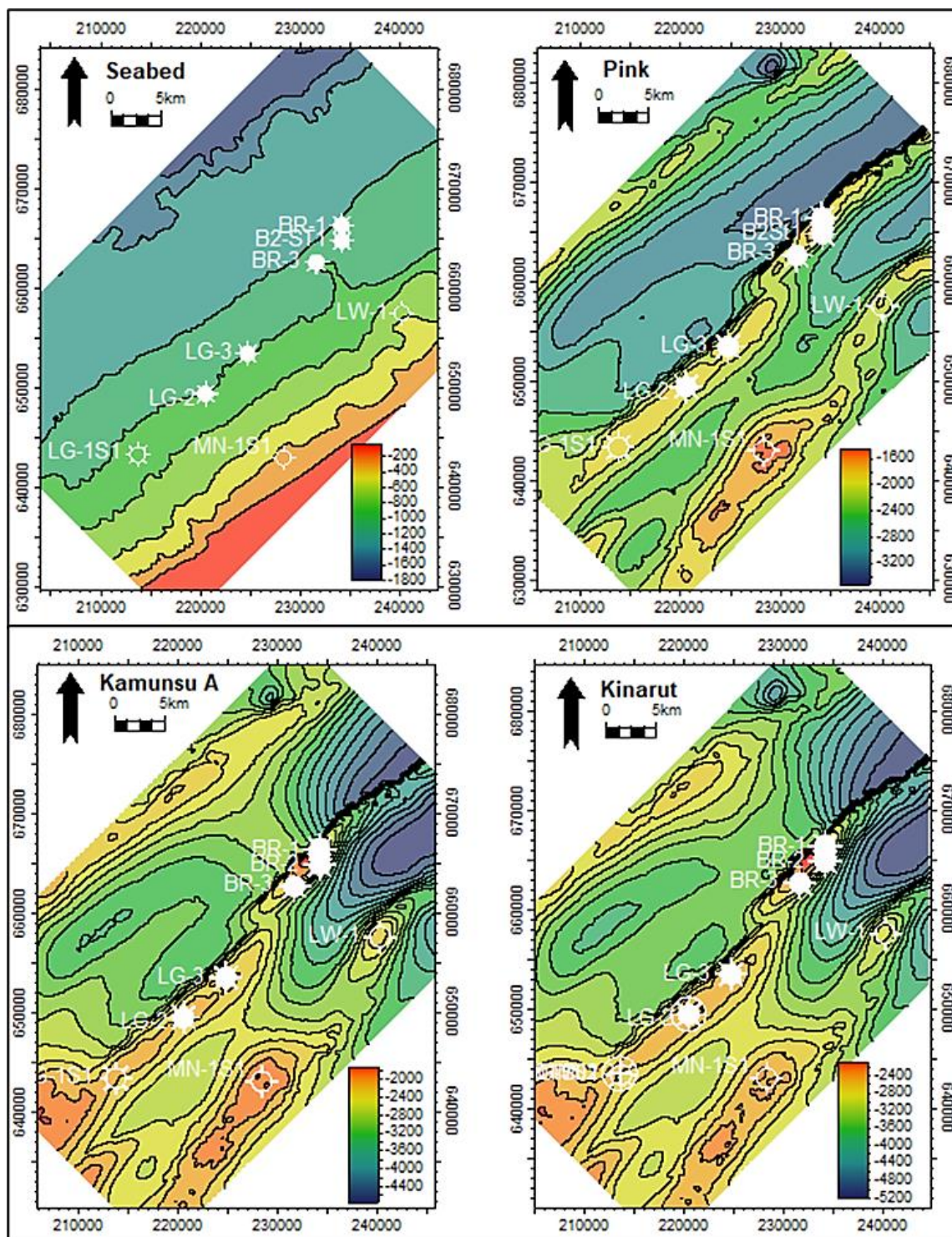


Figure 5-7: Depth structural map figure (Pink, Kamunsu and Kinarut map) to show the well locations based on structural trap optimized location. This figure highlights the challenges in modelling the lateral depositional settings and facies particularly at the synclinal parts of the area.

5.4.2 Deepwater depositional facies

Vertical patterns of well log signatures, particularly using Gamma Ray (GR) together with cuttings and recovered core are used to establish the deepwater depositional facies of the study area. The stacking patterns are calibrated with characteristics of the seismic amplitude, continuity and frequency to enable the seismic identification in the area without well control. It is important to highlight the challenges of facies identification in this area, and commonly in the fold-thrust belts worldwide. In many cases deep-water wells are usually drilled at the crestal part of the growth folds. This focus does provide less detail and seismic controls for the off-crest, down-dip and synclinal parts of the fold (Figure 5-7). Mayall et al. (2000) classified the facies in deep-water turbidite sub-marine channels variability into four main facies (Figure 5-8); (1) basal lags; (2) slumps and debris flows; (3) high Net to Gross (N: G) stacked channels and (4) low N: G channel-levee.

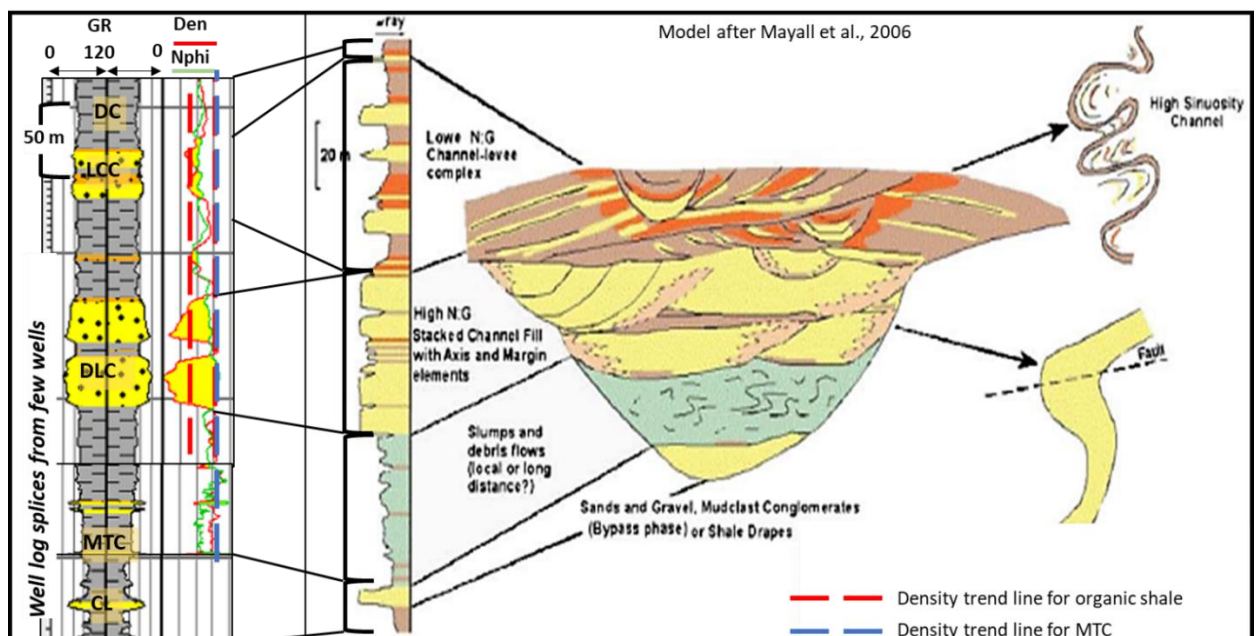


Figure 5-8: Well log expression of the facies penetrated by well in the area and the lithology and facies types as classified by Mayall et al., 2006.

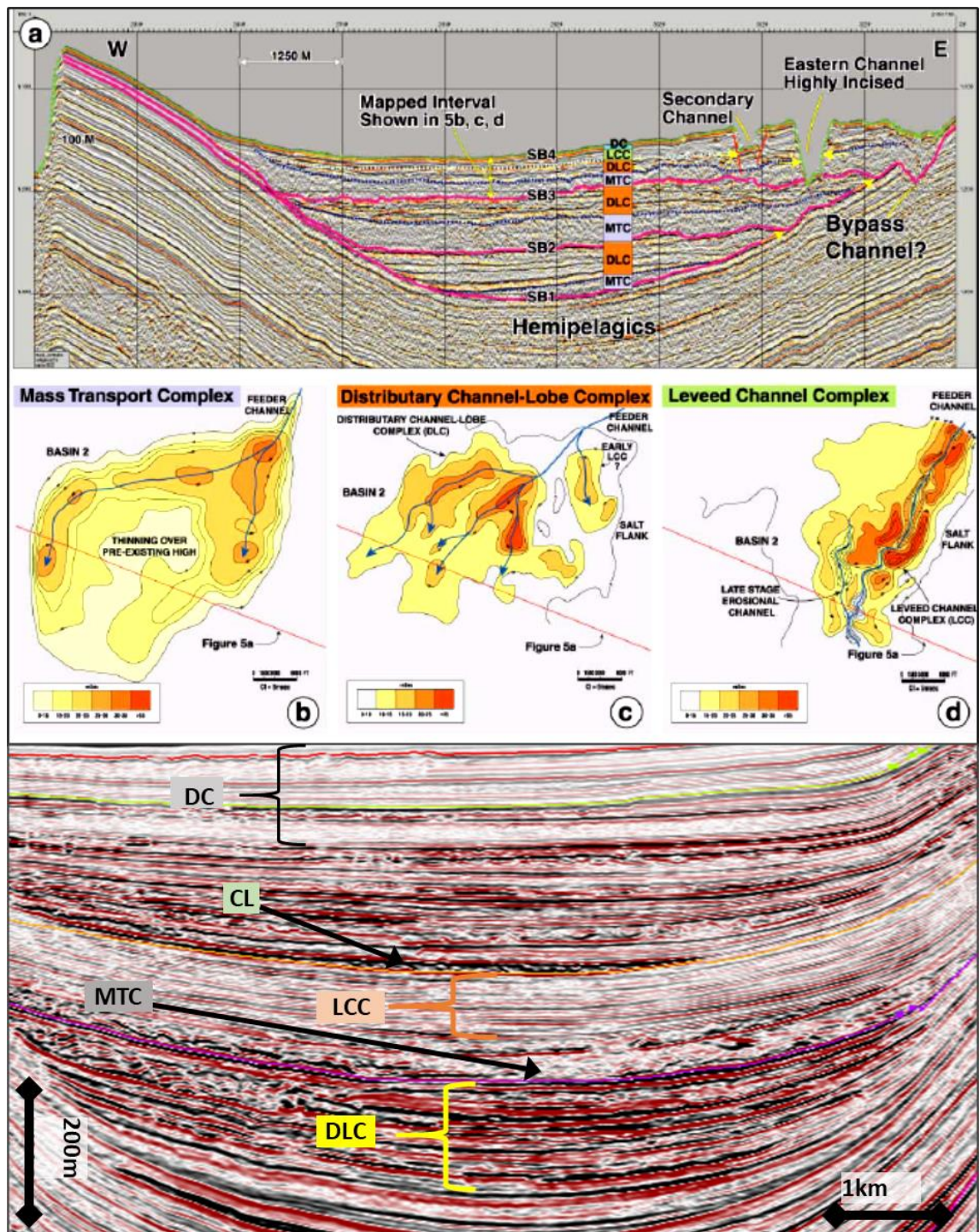


Figure 5-9: Seismic characterization of the facies based on Beaubouef et al., 2000 classifications of the facies in the deep-water submarine fan settings (Figure 5-9a, b, c & d) and the seismic cross section example from this study (Figure 5-9e). Abbreviations; Drape Complex (DC), Levee channel complex (LCC), Distributary channel-lobe complex (DLC), Channel Lag (CL) and Mass Transport Complex (MTC).

An alternative presented by Beaubouef et al. (2000) classified the facies filling up the intra-slope basin based on the seismic characteristic's succession of the undeformed, thin flat lying units and onlap toward the steeply dipping hemipelagic facies at the basin margin. The hemipelagic facies characterized by highly reflective, parallel, and continuous seismic amplitude deposited prior to salt withdrawal / fold growth or basin subsidence. Beaubouef et al. (2000) classified seismic stratigraphy basin fills into four major classes (Figure 5-9); (1) low amplitude, chaotic units; (2) high to moderate amplitude units with moderate to high reflection continuity that onlap or thin along basin margins; (3) low to moderate amplitude units with high reflection continuity that downlap and thin away from a central channel; (4) thin, highly continuous units of either low, or high amplitude reflection character.

Both the Mayall et al. (2000) and Beaubouef et al. (2000) classifications address similar facies variations filling up the intra-slope basin with submarine channel successions. In this study, both classifications are applied in defining and describing the facies and depositional settings in the study area. The facies identified can be identified in each deltaic fan systems of the Lingan, Yellow, Pink, Kamunsu and Kinarut even though the repetition is not identical in each fan systems separated by sequence boundary and maximum flooding surfaces. This suggests that the basin fill accommodation space and sediment supply temporally varied. Localized variation of seabed topography during deposition caused the facies difference between well vertical successions. Both temporal and spatial (topography related) localised variations in this area were controlled by the fold-thrust belt evolution as discussed in Chapter 3.

The facies classification used in this study can be classified into four groups, combined from Mayall et al. (2000) and Beaubouef et al. (2000) classifications: (1) Drape complex (DC); (2) Levee channel complex (LCC); (3) Distributary channel-lobe complex (DLC) and (4) Mass transport complex (MTC).

5.4.2.1 Drape Complexes (DC)

The DC is the hemipelagic mudstones deposited during sediment starvation and abandonment, characterised by thin, continuous seismic either high or low amplitude (e.g., Beaubouef et al., 2000). The high or low impedance seismic with uniform thickness is muddy turbidites to condensed section and pelagic to hemipelagic drape in the deepest basin during deposition (Prather et al., 1998). Mayall et al. (2000) however in his classification DC is one of the three types of basal lag deposits at the base of the channel-fills. Apart from shale drape, the other two types in this group are the coarse sand and conglomerates, and the mud-clast conglomerates that usually occur at the base of the channel fills.

DC is observed in each of the fan system sequences, interpreted as the deepest sea level rise represents by deposition of the marine shale with high radioactivity reading measured by the GR log. It is important in differentiating the DC from MTC as both usually tend to be formed at the deepest part of the basin or sequences during deposition. From well log, the density trend of the DC is lower compared to that of the MTC, and from seismic, the differences are obvious with the parallel and continuous reflectors widespread at the bottom of the sequences as opposite to chaotic features of the MTC. The seismic response as observed in this area for the DC is mainly transparent and relatively lower amplitude

with common high frequencies seismic attributes for shale layering and some silty and sandy bedded units.

The DC is a good marker between the well and seismic for correlation control, as it is distinctive from the well log trend and marks the change from the transgressive system tract (TST) to the prograding complex (PGC). It is picked as the MFS and matched with the biostratigraphy where it displays the highest abundance of foraminifera. In seismic section, it can be picked with confidence as it displays continuous sharp contrast of the top two layers and displays a much higher amplitude than either MTC's or the channel turbidite sequences.

5.4.2.2 *Leveed Channel Complexes (LCC)*

The LCC is characterized by low amplitude, highly continuous, down-lapping seismic reflector of the mud-rich overbank low-density turbidity flows (Beaubouef et al., 2000). The mud-rich system is associated with few thin bedded turbidite sandstone (Prather et al., 1998). The thin turbidite sandstone in LCC however, is widespread over the slope fan apron and composed of many thin sands (Mayall et al., 2000). The typical "gull wing" shape associated with LCC, is not clearly shown in the seismic sections for this study. This is in part due to compactional effects and possibility that the channel levee system was reflected by interbedded sandstone and mudstone (e.g., Mayall et al., 2000). From the wireline logs, the LCC tend to give a higher API for Gamma-ray readings indicating the occurrence of thin bedded sands in mud-rich settings helping identify the LCC.

Seismic data illustrates the amplitude is moderate particularly in the centre of the syncline area. The amplitude is higher than DC but lower when compared to the thick turbidite channelised complexes. It is easily differentiated with the other facies as the thin bedded sandstones is widely spread throughout the area and common to see numbers of these layers in one LCC.

The LCC will be a good potential as a reservoir target in the down-dip part of the structure as the onlap towards the overbank of the levee could provide a lateral permeability barrier for the trapping. The shale layering on top is a good top seal for the thin layers and provides enough overburden for the thin sandstone reservoir.

5.4.2.3 Distributary channel-lobe complexes (DLC)

DLC's are sand-rich, turbidite dominated systems and represent the most reservoir-prone in the basin, characterised by high amplitudes and continuous reflectors. The DLC's typically overlie the seismically chaotic MTC's and exhibit lobate or distributary fan patterns with often internally channelised proximal parts (Beaubouef et al., 2000). DLC's are associated with sand-rich submarine-fan complexes with sand sheets, leveed channels, and ponded mass flows (Prather et al., 1998). DLC's can have thin mud clast conglomerates or coarse pebbly lags marking the channel base and in most recognised occurrences fine-up into hemipelagic mudstones.

DLCs can be identified easily by the thick sand units marked with abrupt changes from high to very low Gamm-ray readings in strong contrast to the 'clean' sandstones of the turbidite channels. The radioactivity of the gamma-ray reading is commonly lower than

LCCs and the thickness difference distinctive. The neutron-density cross plots show a large separation reflecting the high porosity and clean nature of the sandstone with high net to gross ratios (N:G). In the study area, the DLC's are recognised from the Pink fan and deeper and characteristically underlain by MTCs.

The abrupt changes of the coarsening upwards facies of the DC's or MTC's, to the fining upwards of the submarine turbidite channel marks the sequence boundary. This contrast can be imaged as high amplitude seismic of the impedance differences.

The seismic characteristic of DLCs in the study area shows a low frequency interlayering amplitude, with possible "gul-wing" features preserved even-though the magnitude seems to be lowered by the overburden sediment loading. Seismic contrast of the DLCs facies sequence with the bottom and top layers is easily recognised due to the very high amplitude and common continuous thick sand layers.

5.4.2.4 *Mass transport complex (MTC)*

The MTC is a deposit formed from coherent slides, slumps and incoherent debris flows processes derived either from localised slumping and sliding from the adjacent canyon or channel walls. MTC's sediments can be derived from much further upslope and even direct from the shelf, as the complex usually contains extra-formational clasts different from the material usually seen in the sandy channel systems (Mayall et al., 2000; Moscardelli et al. 2006).

The MTC units consists of muddy matrix and muddy sands to clean sands. Internal complex contorted geometries of reflectors reflect the weak to moderate amplitude, while incoherent reflection indicates the poorly organized impedance structure with minor impedance contrast (e.g., Beaubouef et al., 2000 and Mayall et al., 2000).

The MTC in well logs may be confused with DC as both show high radioactivity and a high GR value. However, in the correlated density trend the MTC commonly shows higher density as compared to DC.

To distinguish the facies, lithology descriptions from cuttings, sidewall core or conventional core will be used to highlight the obvious difference. It is expected that MTC will have transported clasts from outside the channel system. In the study area, it is common to see mixture of carbonaceous flakes, dolomitic parting or lenses, coal fragments and quartz granules.

The occurrence of MTC in the study area is generally located at the level of the deeper fan systems of the base of Pink, Kamunsu and Kinarut. In seismic, the MTC could be picked up confidently as the chaotic image with the low amplitude background and the mixture of mid to high amplitude of the debris in the unit is easily differentiated from the other facies in the basin fills.

It is important to note that MTCs have traditionally been identified as seals although they can also act as migration pathways or cannibalise and compartmentalise adjacent reservoirs.

5.5 Results

5.5.1 Well penetration: vertical stacking pattern

Individual wells in each growth fold structure were studied to establish the vertical stacking pattern of the facies based on the log response, lithology, and seismic response. Interpretation of the possible depositional environment associated with the facies observation will provide an understanding of the facies distribution for each individual fold structure and the relationship to the overall depositional settings in the study area.

5.5.1.1 *Menawan structure (Figure 5-10)*

Menawan-1 & ST-1 well is the only well drilled on the Menawan structure. It is the most proximal anticline towards the shelf edge and the canyon complex at the shelf break of slope. The Menawan-1 & ST1 well targeted the Middle to Late Miocene submarine fan reservoirs of the Pink, Kamunsu and Kinarut and Keabangan. The well location was at 398 m water depth and drilled down to 3171 m TVDSS. The well was drilled with the same exploration model as the outboard Limbayong-1& ST1 discovery on the basis it might share the same source rock kitchen located between the two folds. However, being proximal to the sediment source, the Menawan-1 & ST-1 encountered mostly shale without significant reservoirs in any of the submarine fan systems.

The lithology descriptions from cuttings described the mudstone encountered throughout the well with minor rafted material such as carbonaceous specks, mica flakes, trace of pyrite, calcite, dolomite, and debris with occasionally thin laminated intervals of siltstone

and sandstone. Based on core characterisation the succession encountered is interpreted as a slump or mud-rich debrite of the MTC. This is supported by the seismic expression at the seabed (Figure 5-5). Seismic character at the well locations shows chaotic bright high amplitude at the top section of the Stage VI, as this is corresponded to the GR log indicated the high mixture of sandstone and silt in the MTC and the presence of layers of CL facies due to a new canyon located closer to the seabed as a result of the temporal and seasonal slope failure at the seabed. The rest of the seismic section shows low amplitude chaotic reflectors with very low connectivity except at the top of the Pink Fan which shows high continuous amplitude indicating LCC or CL deposits.

The sandstones encountered in the well are very fine to medium grained, occasionally very fine and coarse grained, subangular to subrounded, poorly to moderately well sorted with coal, carbonaceous debris, and coal particles. The lithologies are interpreted either as CL deposits at the bottom of the canyon fill or part of LCC as the submarine channel migrated downslope.

5.5.1.2 Lawa structure (Figure 5-11)

Lawa fold is located to the northeast of Menawan structure sharing the northeast-southwest fold trend, and is proximal to the shelf edge and adjacent to the canyons of the shelf break. From the seabed expressions, the Lawa structure is not severely affected by the intra-slope canyon complex as compared to Menawan. This might be because Lawa is located further to the north away from the shelf deltaic sediment sources. The difference of sediment supplies due to the location of the folds explains the presence of the Lawa fold at the Present-day seabed, while the Menawan fold only can be seen from

the subsurface where it has been drowned in sediment flux over the last 1 Ma. Lawa-1 is the only well on the structure. It was drilled at 666.4 m water depth and targeted the Kamunsu and Kinarut submarine fans at the crestal part of the structure. The well is located 10 km inboard of the Bestari-1 well discovery, on the adjacent fold to the northwest. The well was drilled on the prediction of having a good chance in finding the same sand fairway as discovered in Bestari-1 well. Lawa-1 drilled down to the final total depth at 3577 m TVDSS, with only very thin sandstone layers and lenses encountered with insignificant reservoir potential.

The lithological descriptions from cuttings from the Lawa structure recognises mudstone, with thin sand and siltstone lenses and/or layers throughout the well interval. The mudstone is soft to firm, blocky to sub-blocky, occasionally sub-platy, elongated and irregular shaped, with presence of silt, traces of pyrite, mica, calcite, and carbonaceous specks. In the Langan, Yellow and Pink submarine fan formations, the sandstone encountered is argillaceous, silty to fine-grained, loose to friable, poorly sorted, sub-angular to sub-rounded, dominated by quartz with traces of carbonaceous material, pyrite and some patchy calcite. However, at the bottom part of the Pink formation and in the Kamunsu formation, dolomite traces occur in the sandstone. The Kamunsu and Kinarut submarine fans contains sandstone and traces of white kaolinite occurred in the claystone. Thin layers or lenses of dolomite and limestone occurrence with average of 1 m thickness in the bottom part of Kamunsu.

Seismic character at the well location mainly shows a bright high amplitude reflector at the top Stage VI corresponding to a gamma ray response indicating a mixture of sandstone and siltstone in the Drape Complex, with some interlayering of hemipelagic material. The

Lingan and Yellow submarine fan formations are characterized by interlayering of high amplitude and low amplitude reflectors and channel shaped reflectors of Channel Lag complexes. The rest of the seismic section shows a low amplitude with chaotic reflection with very low connectivity suggesting MTC deposition from the bottom part of the Pink submarine system downwards.

5.5.1.3 Limbayong structure (Figure 5-10)

The Limbayong structure is located to the northwest outboard of Menawan fold separated by a slope sub-basin elongated northeast to southwest. Three wells have been drilled on the structure, targeting different parts of the 25 km elongated thrust fold.

Limbayong-1 & ST-1 wells were drilled in 959 m water depth, to test the 30 km² structural closure targeting the Kamunsu, Kinarut and Keabangan submarine fans. The well encountered more than 300 m reservoir from the Pink, Kamunsu and Kinarut submarine fans and were mainly gas bearing except for the water filled Lower Kinarut.

The discovery was then appraised by the Limbayong-2 well, located 9 Km to northeast of Limbayong-1 and ST-1 well at 925 m water depth. A total of 123 m oil bearing reservoirs encountered in the Upper and Lower Kinarut fan system, contradict the water bearing sand in Limbayong-1 and ST-1.

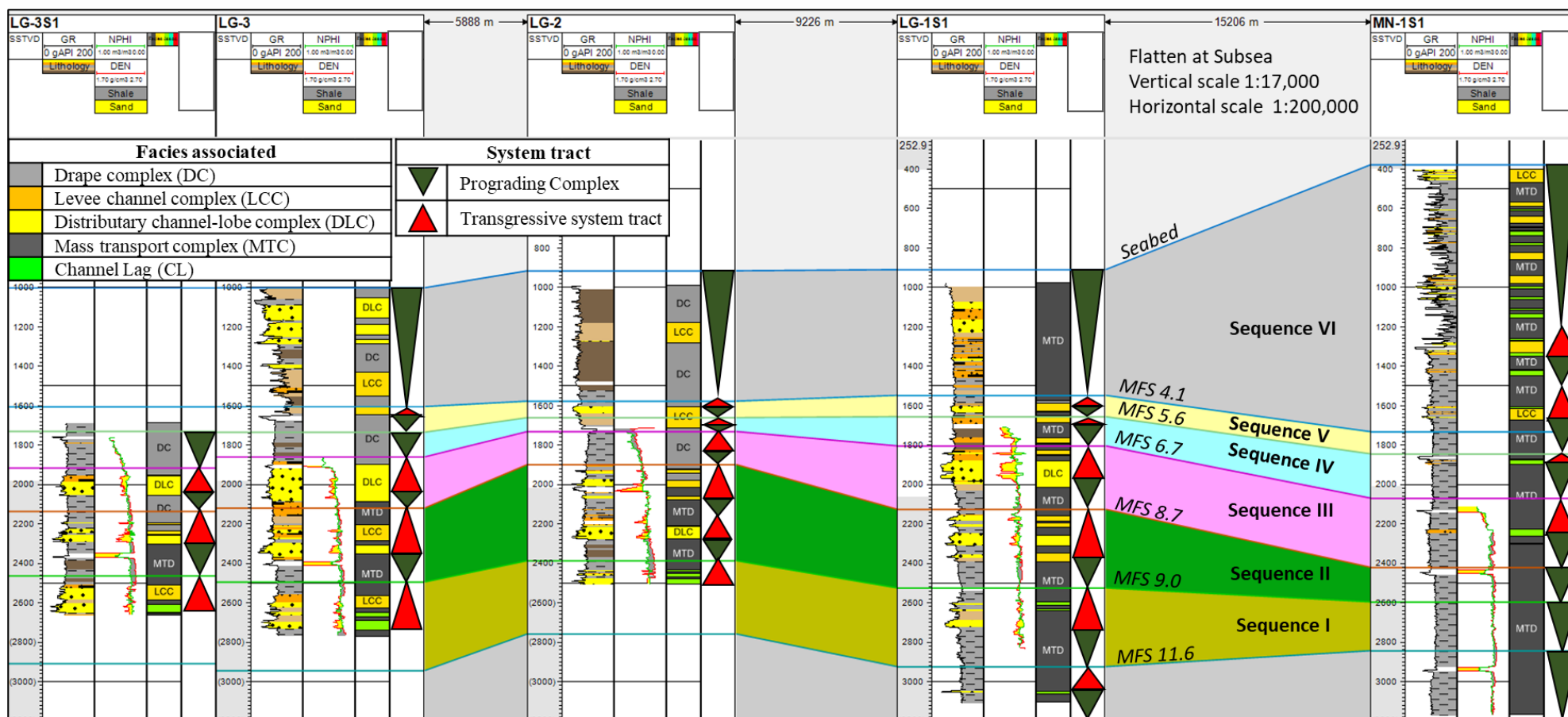


Figure 5-10: Well correlation of Menawan-1S1 and the wells in Limbayong structure with the correlated sequences and the maximum flooding surfaces (MFS) picked as the correlation marker in this study. The facies associated with the well log response and lithology description are defined and matched with the second order sequence stratigraphy system tract.

The third well on the fold drilled to 5.7 km to the northeast of Limbayong-2 well, at the Northeast Culmination further appraised the discovery in the previous two wells. The Limbayong-3 and ST-1 located at 1007 m of water depth and drilled down to 2766 m TVDSS (Limbayong-3) and 2661 m TVDSS (Limbayong-3 ST1). A side-track of the wells was drilled up dip of the original hole to find out the upside potential of the reservoirs encountered in Limbayong-3 and the hydrocarbon contact of the Pink, Kamunsu and Kinarut reservoirs. The wells encountered gas with a water contact in Pink fan system at 90 m in Limbayong-3 and 60 m in the ST-1 well. 200 m and 100 m of reservoirs encountered in Limbayong-3 and the ST-1 hole respectively with GOC and OWC penetrated in Limbayong-3 while GOC penetrated in the ST-1 hole. For the Kinarut fan system, 160 m and 120 m reservoirs encountered in Limbayong-3 and the ST-1 holes respectively, with both penetrated the OWC.

The lithological description from each well shows that the sandstone encountered by the wells generally being described as transparent to translucent, predominantly loose quartz grains, consistent of very fine to fine grains with occasionally medium to coarse, sub-angular to sub-rounded, poor to moderately well sorted, with poor visible porosity and slightly calcareous with intermittently traces of argillaceous matrix, pyrite, glauconite, dolomite fragments, coal fragments, shell fragments and fossil. The mudstone in Limbayong-1 and ST-1 well shows a similarity with Menawan-1 and ST-1 well from top to bottom, with possible MTC deposition throughout the well. The same facies were observed in the bottom part of limbayong-2, and Limbayong-3 and ST-1 wells in Kamunsu and Kinarut submarine fan formations. For the shallower part of both wells, from the Pink fans up section, mudstone with none or very small appearance of debris and mixed detrital fragments characterized the hemipelagic material of the DC deposit.

The density log trend shows a high value in the deeper MTC claystone as compared to the DC claystone. Seismic characteristics shows bright amplitudes, continuous and low frequency reflecting sandstone facies and with high contrast and low amplitude for the mudstone intervals. The MTC and DC mudstone could be easily differentiated based on the chaotic character of the MTC as compared to the interlayering hemipelagic.

5.5.1.4 Bestari structure (Figure 5-11)

The Bestari structure was the most actively explored and appraised in recent years with six wells drilled including the mechanical and geological side-track to assess the petroleum system and commerciality of the fold. The wells are the Bestari-1, Bestari-2, Bestari-2-ST-1 and ST-2, Bestari-3 and Kacak-1. In this research however, only five of the wells will be available as the Kacak-1 was just completed recently with the data and official findings yet to be released. The structure is located to the northwest outboard of Lawa structure on the same trend as the Limbayong fold. The wells drilled on the structure were targeting the same Middle to Late Miocene deep water submarine fans of the Pink, Kamunsu and Kinarut.

The first well drilled on the structure was the Bestari-1 well, at 1156 m of water depth on the front limb of the thrust-fold targeting the fault bounded three-way closure trapping mechanism. The well reached a final total depth at 2794 m TVDSS with 76 m of net sand encountered from the Pink, Kamunsu and Kinarut. The sands are gas and oil bearing, without any water contact penetrated. Bestari-2 (2099 m TVDSS total depth) located at 1106 m TVDSS water depth, 1.5 km to the south of Bestari-1 well, on the back limb of the fold, was the first appraisal of the hydrocarbon bearing reservoirs discovered by

Bestari-1 well. Bestari-2 ST-1 (2593 m TVDSS total depth) was a mechanical side-track, whilst Bestari-2 ST-2 (2379 m TVDSS total depth) was a geological side-track up-dip of the Bestari-2 and ST-1 to find the possible OWC between the Bestari-1 oil bearing reservoirs and the water bearing Bestari-2 and ST-1. Unfortunately, the up-dip Bestari-2 ST-2 encountered reservoirs that were water filled in all the sub-marine fans turbidite reservoirs. A total of 68 m of the Pink sand and 73 m of the Upper Kamunsu sand was encountered by the Bestari-2ST1 well, and the Bestari-2ST2 hole penetrated 54 m Pink sand, 43 m each from the Upper and Lower Kamunsu sands. Bestari-3 then was drilled 4.4 km and 3.3 km to southwest of Bestari-1 and Bestari-2/ST-1/ST-2 at 1096 m TVDSS water depth and reached a total depth at 2183 m TVDSS. The well was meant to appraise the hydrocarbon accumulation discovery in Bestari-1 after the disappointment seen in the Bestari-2 wells. The Pink sand with total gross thickness 50 m turned out to be water bearing, and the 2 sand packages encountered in the Upper Kamunsu had a total gross thickness of about 50 m with a possible OWC in the bottom sand.

The diachronous deposition of the submarine fan systems from the Middle Miocene to the Present day was proven by the lithology penetrated by the wells drilled on the structures. The sandstone generally showing the same characters from the description of the cuttings except for the occurrence of different debris and minerals such as dolomite, coal, calcite, and fossils. The wet sand mostly described as translucent to transparent, very fine to fine, occasionally medium, and coarse in parts, loose to friable, poor to moderately sorted with dominant of quartz. Quartz overgrowth observed in the Kamunsu turbidite sands and deeper in Bestari-2/ST-1/ST-2 well. The seismic reflection penetrated by the well shows the sandstone will correspond to high reflectivity, with obvious contrast between the above and below shale layers. The seismic reflector seems to be limited to

the crestal part of the structure with compartmentalization between the sand body. The mudstone, as described from cuttings mainly soft to moderately firm, occasionally hard, becoming more compacted, sticky and plastic with depth. Other than presence of trace of Pyrite, mica, calcite and carbonaceous specks, the presence of dolomitic and coal fragments in Kamunsu and Kinarut fans increased with depth. The density log reading for the claystone shows different trend of the shallower with average of 2.20 g/cm³ while the deeper section with ranges from 2.30 to 2.45 g/cm³. The changes of the density value of the mudstone, could be observed mainly below the Pink sandstone. These changes in density trend coincide with the chaotic seismic reflections with the low amplitude seismic reflectors.

5.5.2 Characteristics of the basin fills

Seismic characteristics (Figure 5-9) was used in identifying the seismic facies for the basin fields, mainly in the synclinal part between of the inboard and outboard thrust-fold structures. The seismic facies were calibrated with the well log signature to precisely model the depositional setting and associated facies. However, due to the magnitude of the fold growth, mainly at the third phase of the fold development when the fold growth is higher than the ability of the sediment supply to fill up the structure to the structure high, most of the facies seems to onlap the older of deposition sequences. Seismic characteristic will be the used to determine the possible depositional setting and facies associated with the seismic character.

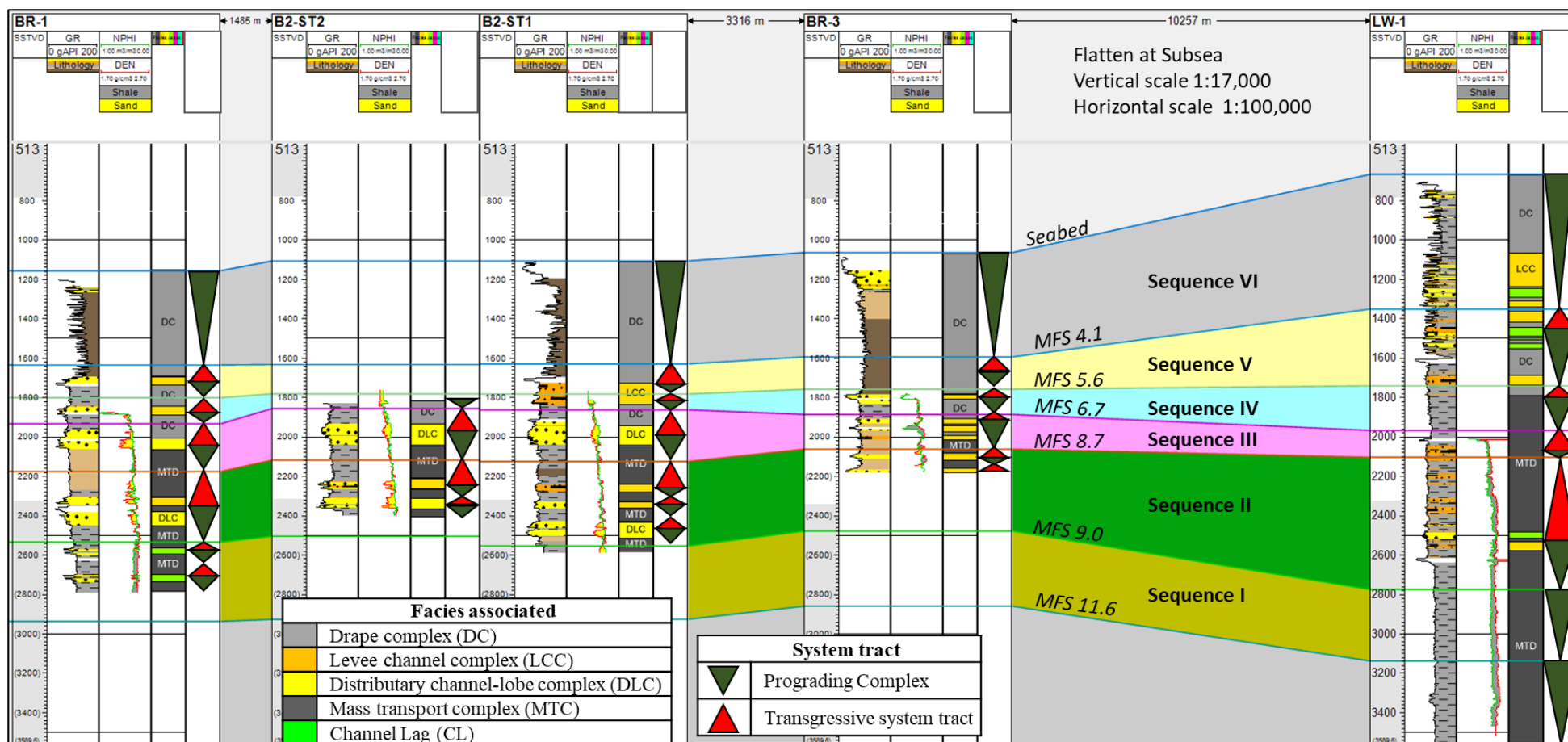


Figure 5-11: Well correlation of Lawa-1 and the wells in Bestari structure with the correlated sequences and the maximum flooding surfaces (MFS) pick as the correlation marker in this study. The facies associated with the well log respond and lithology description defined and matched with second order sequence stratigraphy system tract.

The characteristics of the depositional setting will be defined based on the sediment fairway, from the point source of the deep-water submarine fans at the shelf break, mainly dominated by the slope canyon crossing the inboard structure towards the basin. Therefore, two trends of main pathway in the study area will be analysed for this purpose:

5.5.2.1 Menawan-Limbayong trend

The amount of sediment supplied to the basin is relatively high as compared to the northern part of the area. This can be seen from the seabed seismic expression (Figure 5-6) of the presences of numerous canyon complexes at the shelf break at the southern that decrease towards the north. The huge sediment supply transported by the intra slope submarine canyons and channels towards the basin caused severe erosion of the growth-fold anticline and at the same time buried the structural high and was the most-likely factor why the growth ceased. The huge load of sediment transported to the shelf and the canyon complexes caused the MTC severe slope failure in the southern area shown by the more rugose surface of the MTC deposits on the seabed. The submarine channel developed by the canyon systems is very high density in the southern and decreased towards the north.

The seismic expression of the basin fill shows a thin, high frequency bright amplitude overlying low amplitude seismic of Sequence VI. This is interpreted as the DC consisting of hemipelagic deep-water shale deposits interlayered with sandstone or silt layers either deposited by the submarine channel or cohesive movement of the MTC. In the lower half of the sequence, despite the dominant hemipelagic deposit, a series of high amplitude

with low frequency layers could be observed in this sequence and corresponds to highly interbedded sand and shale interpreted as possible DLC facies deposition, on the GR log.

The anticlinal part of the structure mainly shows low amplitude chaotic features for most part of the high, in both Menawan and Limbayong folds except in the interval with sand deposition of the submarine fans as can be seen in the Limbayong well penetrations. The high amplitude seismic reflection, either interpreted as the LCC or DLC, seems to be compartmentalized along the Limbayong structure high based on the reflector continuation between the area penetrated by the wells. The high amplitude sand reflection in Menawan anticline however only can be seen in the Pink fan system as the deeper fan systems of the Kamunsu and Kinarut are dominantly covered by chaotic and low amplitude seismic reflection.

In the synclinal area of the intra-slope basin between the Menawan and Limbayong folds, from Sequence V downwards, different facies of submarine fan turbidite deposits can be interpreted from the seismic response. Sequence V and IV is dominated mainly by the chaotic and low amplitude seismic reflection, which can be interpreted as a MTC derived from the Menawan fold that onlaps towards the Limbayong structure high. A thick sand facies of possible DLC on the Top of Sequence V is correlated as the Ligan sand, with another thinner sand package to the bottom of the sequence believed to be the Yellow sand, limited to the synclinal part, as it seems to pinch out and onlap towards the structural highs. The Pink sandstone that was not encountered in both the Menawan-1 & ST-1 well and in Limbayong-2, interpreted as being the CL facies of the bypass zones, can be seen deposited in the syncline in Sequence IV and onlap towards the MTC.

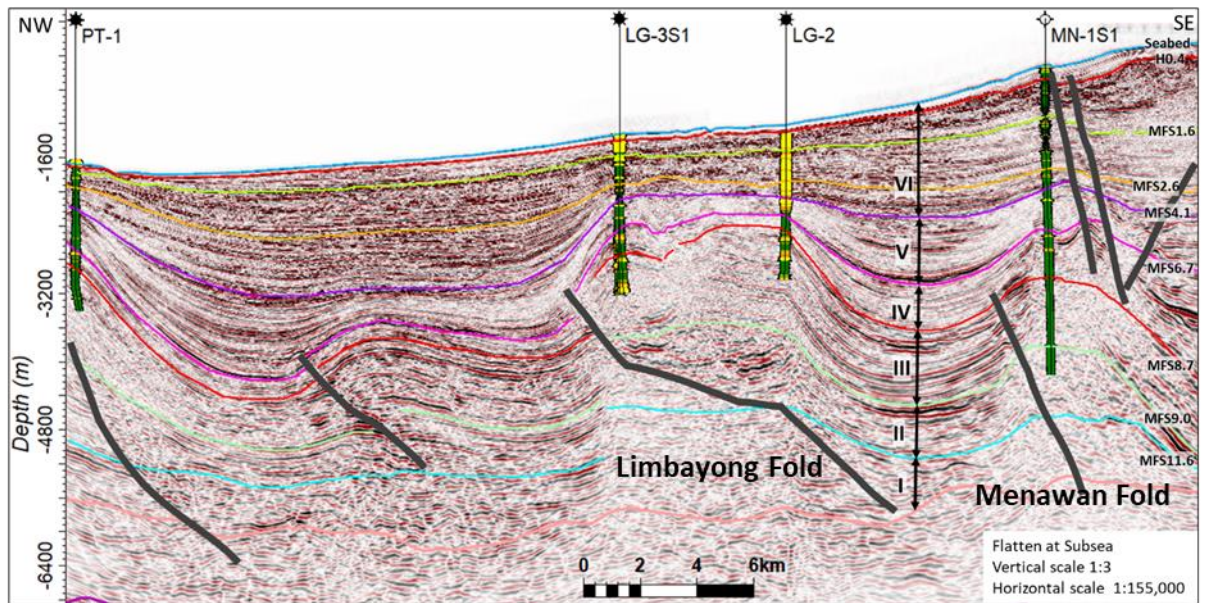


Figure 5-12: Seismic cross section of the Menawan-Limbayong-Petai structures with the sequences and interpreted horizons show the seismic amplitude characteristic differences defining the interlayering sequences in the synclinal area and the anticline of the fold- thrust structure.

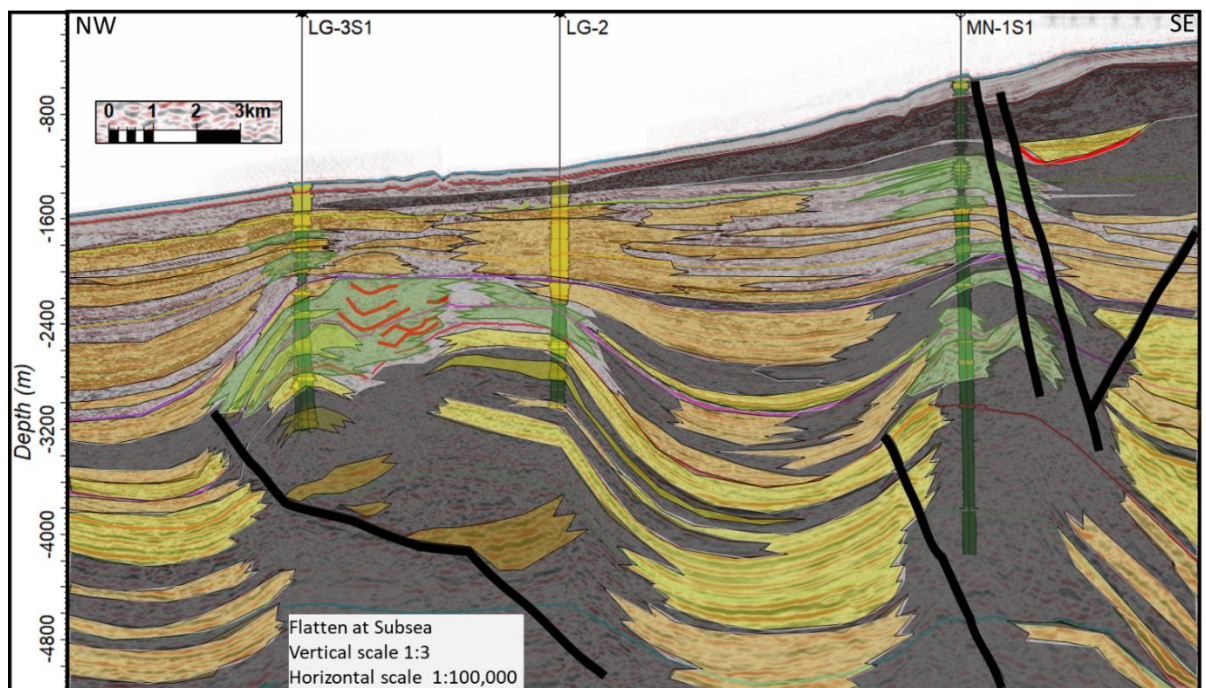


Figure 5-13: Interpreted section of the Menawan-Limbayong section with the facies associated with the seismic characteristics calibrated with the facies defined from wells.

Sequence III and II, with proven hydrocarbon bearing Kamunsu and Kinarut sandstones was encountered in the Limbayong wells show a trend turbidite deposition in the synclinal part and extends up towards the crestal part of the Limbayong structures. The seismic facies in the syncline shows a thick, low frequency with bright amplitude reflections especially at the Kinarut level. The LCC and DLC facies pinched out towards the MTC at both Menawan and Limbayong high. Apart from the Kamunsu and Kinarut sands, Sequence III and II are dominated by the chaotic, mostly low amplitude signal interpreted as the MTC.

5.5.2.2 Lawa-Bestari trend

The seabed expression in the Lawa towards the Bestari folds is much gentler compared to the Menawan-Limbayong structures. The shelf break consists of only a few canyon systems and submarine channels with the flow diverted around the Lawa fold towards the outboard and Bestari fold. The amount of sediment transported to the basin in this part might not be large enough to suspend the growth fold. However, erosion at the crest of the Bestari structure can be observed and associated crestal collapse sedimentation.

Due to the lower amount of sediment carried down by the canyon turbidites and submarine fans from the shelf, the shallower Sequence VI is dominated by DC hemipelagic deposition with interbedded sandstone and siltstone units of turbidite flows. The high amplitude, continuous and high frequency seismic facies of the interpreted LCC seems to be deposited in the more to the proximal part of the basin, based on the continuous, high frequency and high amplitude seismic characteristics commonly found associated with the Lawa structure. However, at the crestal part of Lawa fold, the seismic

amplitude become more disconnected due in part to extensional faults occurring at the crest of the fold. This discontinuous amplitude, calibrated with the gamma-ray log from the Bestari wells, correspond to shaly sediments with occasionally thin sand or silt units, interpreted as the bypass zone and the high amplitude reflectors as channel lag deposits. The turbidite deposit of LCC, DLC and MTC can be seen deposited in the synclinal area in between the folds and pinch out and onlaps towards the hemipelagic shale of the Bestari anticline. The crestal part of the Bestari structure seems to be a bypass zone with channel lag deposit represents by the high amplitude seismic facies.

From Sequence V downwards, as proven by well penetrations on the Bestari structure, the sand associated with LCC or DLC deposited to the structural high, is compartmentalized based on formation pressure and this can be seen from the seismic facies' connectivity. Different submarine channel bodies from the same submarine fan system deposited different turbidite sandstone in different parts of the structure. Another possible reason for the compartmentalization is the faulted crest of the fold formed during fold growth, supported by the changes of dip between the back and front limb of the fold. However, the normal fault is beyond the seismic resolution and is masked by the uneven mounded shaped of the submarine channel with short connectivity on top of the structure. Occurrence of the turbidite submarine channel sand on the top of the Bestari structure, is a thin extension of the thick to very thick turbidite channel complex filling up the intra-slope basin between Menawan and Bestari fold.

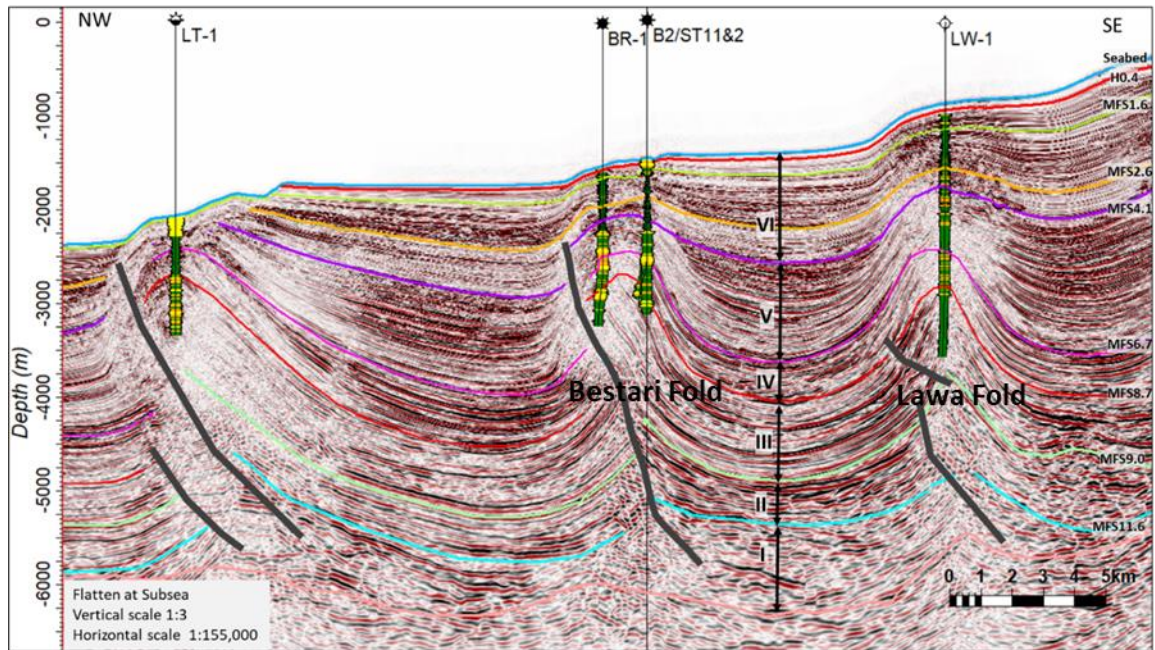


Figure 5-14: Seismic cross section of the Lawa-Bestari-Lumutan structures with the sequences and interpreted horizons show the seismic amplitude characteristic differences the interlayering sequences and between the synclinal area and the anticline of the fold- thrust structure.

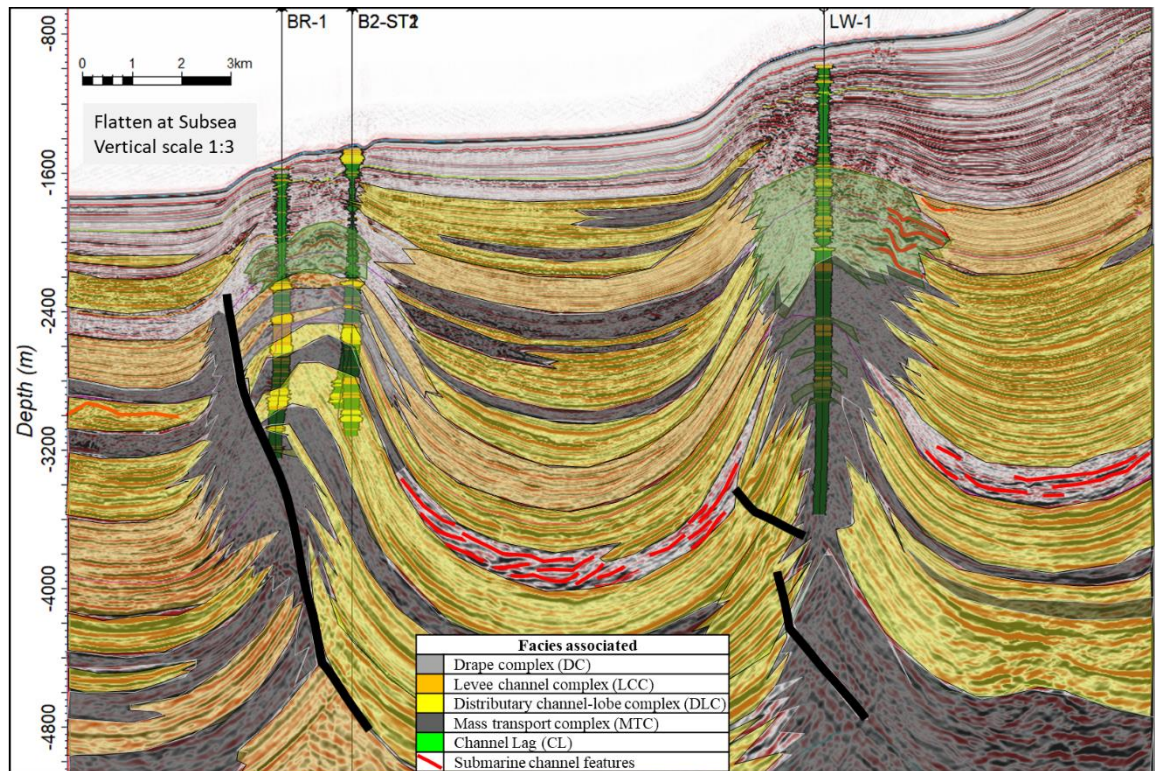


Figure 5-15: Interpreted section of the Lawa-Bestari section with the facies associated with the seismic characteristics calibrated with the facies defined from wells.

These thick interpreted LCC and DLC is based on the seismic characteristics, as observed from the Sequence VI, becoming very dominant going further from the Lingan, Yellow, Pink, Kamunsu, Kinarut and Keabangan submarine fan systems. Apart from continuous thin or thick bright amplitude and high contrast LCC or DLC, the “gull-wing” channel features with limited connectivity can be observed filling up the basin. The submarine channel systems separated by the chaotic and low amplitude seismic image of the MTC, in the syncline become the dominant features of the structural high in both folds. The MTC associated facies was mainly deposited in the Menawan fold section as only thin, low N: G sand or silt associated with the bypass zones channel lag.

5.5.3 Seismic attribute and facies distribution

Seismic attribute extraction on time and horizon slices was performed on the 3D seismic survey to identify the seismic attribute response of the area and fan system penetrated by the wells, the variations and lateral distribution of the identified facies in the deep-water fold-and-thrust belt structure and the intra-slope basin in between the inboard and outboard folds. The objective of the seismic attribute extraction in this study was focused mainly on the lithology, to address the distribution of the facies.

5.5.3.1 *Time slices attribute comparisons*

Root mean Square (RMS) time slices attribute extractions was conducted using PETREL software. As the topography in the deep-water slope settings is deepening outboard to the deeper water and shallowing steeply in both limbs of the thrust folds in each time slices intersects different age strata. In general, older formations are intersected towards the

outboard region, and younger formations intersect at the intra-slope basin compared to the bounding inboard and outboard anticline of the fold (Figure 5-14).

To understand the attribute response in the area, the proven production fields of Kikeh, Gumusut and Kakap were used as the attribute calibration to compare the seismic response of the proven present of thick submarine fan sandstone compared to the sand penetrations in the Limbayong, Bestari, Lawa and Menawan structures. The fields proved the presence of thick sandstone on the deep-water submarine fan in the NW Borneo fold-and-thrust belt as shown by Kikeh as an example, with net hydrocarbon sand of 190 m from the first three exploration and appraisal wells drilled. A range of between 115 m to 150 m sand penetrated in each submarine fan formation in Kikeh-1 exploration well, was proven to be extensive through-out the structure by the appraisal and production well drilled, supported by pressure data and hydrocarbon production from the field.

The RMS attributes extraction cross section and time slice at 3760 ms, intersect the Kinarut submarine sandstone (Figure 5-14a and a') shows the high RMS amplitude of the sandstone formations in the Yellow, Pink, Kamunsu and Kinarut. The net sand encountered by the wells in the field as proven by the well, correspond to the high RMS amplitude and appeared to be to be three to four stacked sand layers in the Kamunsu and Kinarut producing a solid bright and continuous response from the crestal part penetrated by the well going down-dip to the flank of the structure (Figure 5-14a). The time slice at 3760 ms (Figure 5-14a') shows the bright yellow response of the high RMS amplitude, at the Kikeh structure bounded by a sharp northeast-southwest thrust fault of the shale ridge, represent by the green, low amplitude RMS attribute. The same response can be seen in the Kakap and Gumusut structure as well, even though it is not as bright, and

continuous as Kikeh Field, as the time sliced focusing on Kikeh well penetration. At this level, the Bestari, Limbayong, Menawan and Lawa all showing low RMS amplitude at the anticline, except in the synclinal of the intra-slope basin, shows a high amplitude response.

To relatively compare the response seen in the production fields and the well penetration in the other folds, seismic section and time slices with RMS attribute extraction focusing on the submarine fan of the Kamunsu and Kinarut were completed. In the Bestari and Lawa structure (Figure 5-14b and b'), the seismic section from the Lawa to the Bestari fold, reflected the lithology penetrated by the well as described previously from cuttings and well log acquired from the well with the low RMS amplitude, of the green colour very dominant at the Lawa fold. The formations penetrated by Lawa-1 well, correspond with the claystone lithology penetrated by the well of the possible bypass zone with occasionally present of very thin sand interpreted as the CL. While for Bestari, the sections show low to moderately high to high RMS amplitude at the Pink, Kamunsu and Kinarut submarine fans level. The attribute however is limited in terms of continuity between the crest down to the flank of the structure. This can be clearly seen by the time slice at 2194 ms showing the Kamunsu submarine fan system at the crest of the Bestari fold, showing possible lateral connectivity between the wells based on the amplitude continuity and presence of shale between the high amplitude that corresponds to the sand. In the synclinal area between the Lawa and Bestari fold, a series of bright RMS amplitude can be seen from near seabed down to the deeper section of the Kamunsu, At the shallower level down to the Pink submarine fan system, the ponded features of the potential sand prone facies lap on to the shale facies on the crest of both limbs of the inboard and outboard folds. For the Kamunsu submarine fan, continuation of the high

RMS amplitude can be seen in one or two layers of possible sand prone facies from the anticline towards the syncline of the structure.

The same features as seen in the Lawa and Bestari can be observed in Limbayong and Menawan structure based on the RMS attribute extraction, focusing on the Kinarut sandstone seismic time slice at 2658 ms (Figure 5-14c and 14c'). Bright and high RMS amplitude can be seen to be more prominent and wider in the southwest of the Limbayong-1, as compared to the Limbayong-2 middle section, in a small and limited area of the northeast part of the Limbayong fold. This shows the lateral continuation between the wells drilled in Limbayong structure to be very unlikely, proven by the well correlation and pressure system. The continuation from the crestal to the syncline area is slightly better in Limbayong as compared to Bestari, with Kamunsu and Kinarut potentially having continuous layers from the crest to the down-dip, even though the thickness seems to be much lower than then the proven penetration in the Kikeh field. The RMS attribute response in Menawan fold, is a mixture of shale and sand which seems to be a bit chaotic and might be response to the widespread MTC deposition in Menawan, as described from the cuttings and well logs.

5.5.3.2 Seismic horizons attribute blending

Seismic attribute extraction based on the interpreted and correlated horizons in this study was conducted using the Paleoscan software, to extract the RMS and RGB attribute from the seismic on the horizon slices and the blending of both attributes to enhance the geological features, mainly using the azimuth to display the structure variations and the RMS with Channels colour scheme to enhance the lithology and facies trend and

distribution in the area. Variations of depositional setting and pathways distributed in the area could be seen from the seabed down to the deepest reservoir penetration of the Kinarut submarine fan. These variations, apart from being controlled by the sediment supply from the deltaic fans at the shelf, which are known to be a significantly high throughout the temporal period of the established fan systems of the Lingan, Pink, Kamunsu and Kinarut have proven to be not the main risk, but relate more to the topography of the seabed and accommodation space during deposition of the submarine fan in the basin (Figure 5-17). The present-day seabed expression of the seismic attribute horizon blending enhanced the identified seabed features from the interpreted seismic at seabed (Figure 5-6).

The blending attributes at the seabed (Figure 5-18) shows in the southern area covering Kikeh, Gumusut, Kakap and Limbayong-1 area, the presence of bright amplitude of the coarser material dominated MTC with rugose and chaotic features of the shale prone MTC to the outboard of the basin. Between 500 to 700 m below the seabed, at Mfs2.6 horizon (Figure 5-19), the attribute blending shows an interesting expression of the unconfined and confined settings. Limbayong and Menawan fold growth ceased at this stage, and the submarine channel flowed on top of the folds, forming a submarine lobe further outboard. The deposition of the LCC dominated the submarine channel path, while the DLC towards the fan lobe and the proximal part, in the Menawan area seems to be the bypass zone with shale dominated by the coarser material of the CL deposit. Towards the Bestari and Lawa structures however, the presence of the structural high of the fold, acted as a barrier and confined the depositional path from the shelf. Proximal to the shelf, in the synclinal area of Lawa structural high, a bright attribute records ponding of sandy fan and turbidity currents.

The submarine channel flowed around the Lawa structural high and flowed in two directions afterwards, the first is towards the unconfined part to the southwest of Bestari structure, and the second forming a submarine fan lobe at the basin intra-slope between the Lawa and Bestari folds. The bright amplitude at the footwall of Bestari thrust fold, might be the eroded Bestari crestal or the crestal collapse material due to erosion of the sediment overflow from the submarine fan lobe deposit. Further outboard, towards the younger growing fold, the deposition seems to be confined by the structural high and most of the sediment deposited at the syncline between the fold.

The attribute blending for Lingan (Figure 5-20), Yellow (Figure 5-21) and Pink (Figure 5-22) submarine fans show the deep-water depositional setting for different magnitude of fold-growth, as the Limbayong and Menawan fold magnitude become higher going deeper from Lingan to Pink. The gentler magnitude in Lingan, causing the submarine fan to overflow over and through the high and possibly forming a submarine canyon on the high, making it shale prone and deposited the sand and silty sediment further outboard as submarine fan lobe.

The submarine fan lobe from the Limbayong structure high is seen at the Yellow and Pink fans, but not at the entire structure high. Both the high magnitude and steep highs of Lawa and Bestari, the sediment deposition is concentrated mainly at the down-dip part of the syncline area and flows around the high making the well location prone to being bypass zone, with exception of possibly an event of large enough sediment transport to the basin with high energy enabling it be able to reach the crest of the structure, as possibly happened in Pink fan at Bestari.

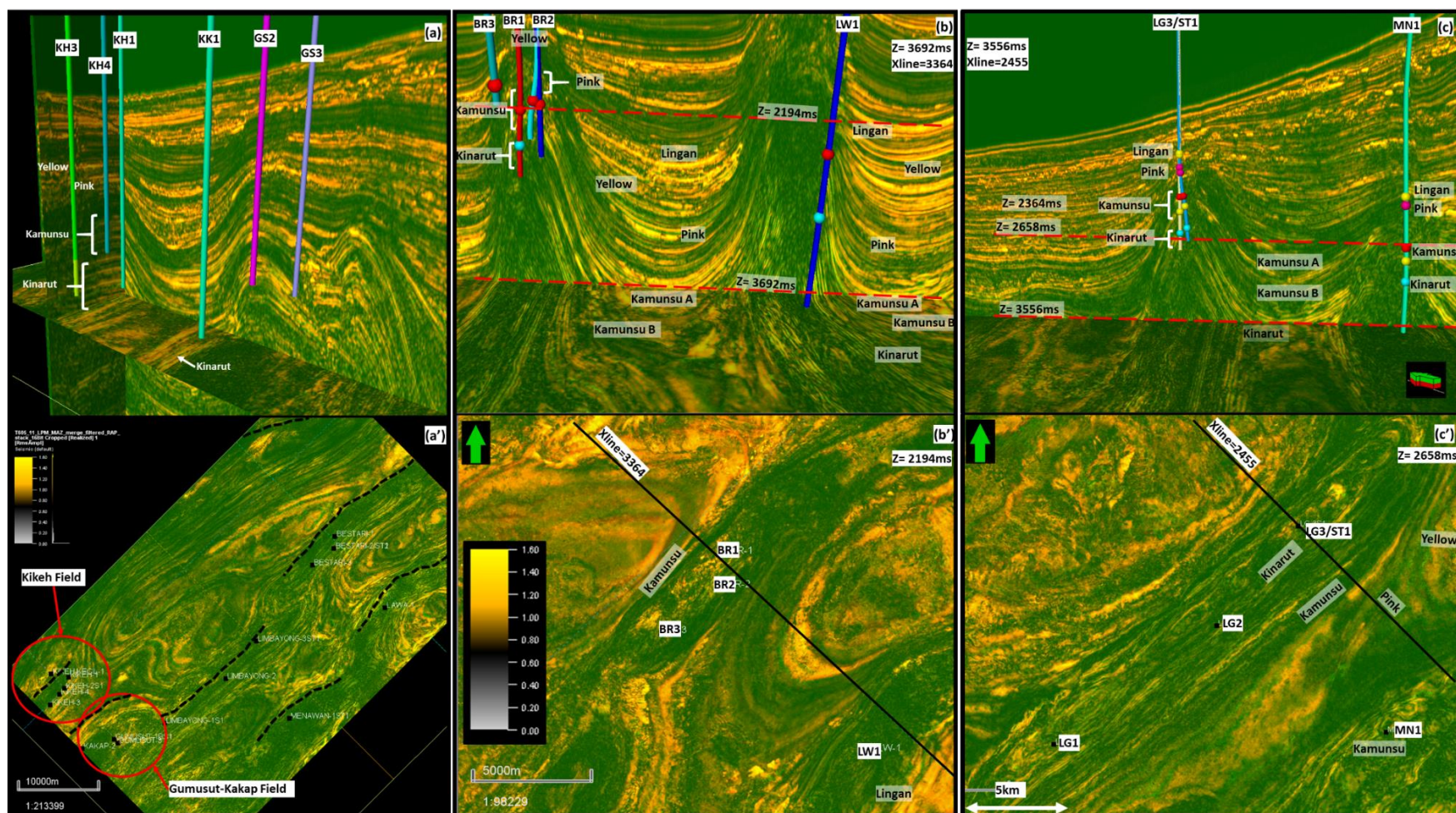


Figure 5-16: (a and a') Seismic slices at 3760 ms at proven Kikeh and Gumusut-Kakap Fields seismic attributes at production reservoirs shows high amplitude at the field area. (b and b') and (c and c') show the Bestari and Limbayong cross sections with time slices at 2194 and 2658 ms each shows the RMS amplitude response at the reservoir penetrated by the wells in each structure high.

Open

The deeper, Kamunsu and Kinarut submarine fan systems, with merely symmetrical fold geometry as the gravitational effect of the huge sediment supply from the shelf just taking place in Middle Miocene, show the depositional style to be dependent on the kinematics of the structured high at each location. The sediment depositional trend elongated parallel to the structural high is still dominant in the syncline, whilst the deposition on top of the structural high by the submarine channel flowing from the shelf will be very dependent on the amount of sediment, influencing the energy of the flow. At the Upper Kamunsu (Figure 5-23) and Lower Kamunsu (Figure 5-24), a huge amount of sediment was transported from the shelf, at the proximal Limbayong fold as compared to Bestari.

The flow of the submarine channel by individual stream system flow through the Limbayong structural high, seems to be fairly widely distributed especially in the Limbayong-1 area but was becoming limited at the Limbayong-2 and Limbayong-3ST1 and ST2. A large series of submarine fan lobes could be seen outboard of Limbayong fold, in the intra-slope basin with high probability of thick sand deposition based on the bright attribute response. The Limbayong-2 and Limbayong-3ST1 and ST2 might be in the LCC setting or possibly at the bypass zone, due to lesser amount of sand reaching these locations.

At the Bestari fold, a submarine channel could be observed flowing directly from the shelf through Lawa fold bypass zone, producing sand prone deposition at the footwall of the Lawa structure and thinning towards the Bestari high. As the seismic resolution on the crest of Bestari is not high enough for the extraction, it is unknown how widespread this submarine channel is on top of the structure.

For the Kinarut fan system (Figure 5-25), even though sediment in Limbayong is still higher than Bestari, the overall high sediment supply at this stage can be seen distributed widely in the area, filling up the syncline of the basin intra-slope. The structural high of Limbayong seems to have received a good amount of wider sediment, as the fold magnitude is not as high as Bestari, and a large amount of sediment was deposited over the fold throughout the structure. This might not be the case for Bestari, as the fold magnitude seems to be higher, and the sediment thins towards the anticline. However, individual submarine channel with high energy flow might still be able to reach the crestal part of the structure, but the distribution limited to individual stream systems.

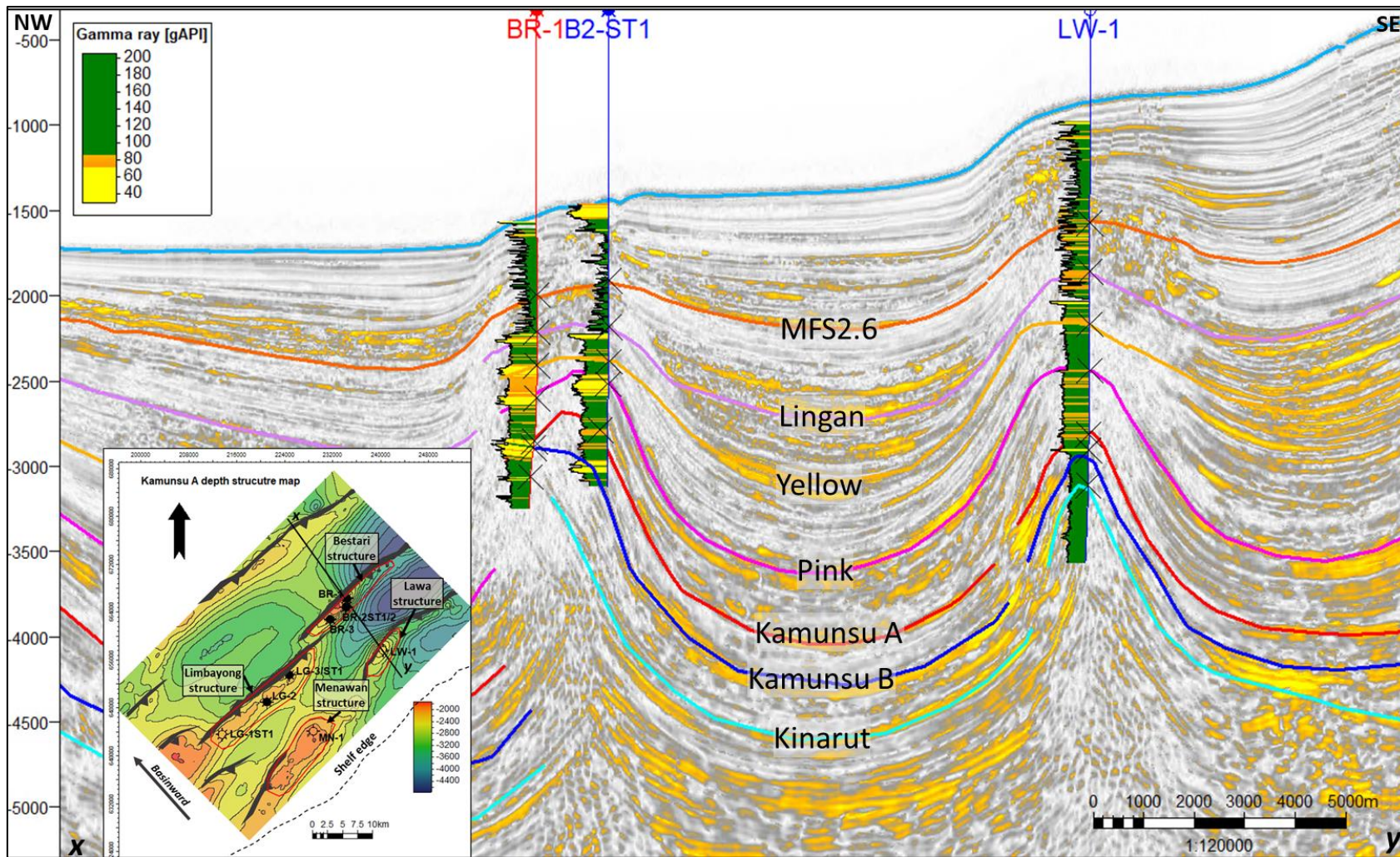


Figure 5-17: Seismic cross section with Sweetness attribute extraction, showing the horizons used to extract the RGB and RMS blending attributes (Figure 5-18 to Figure 5-24).

Open

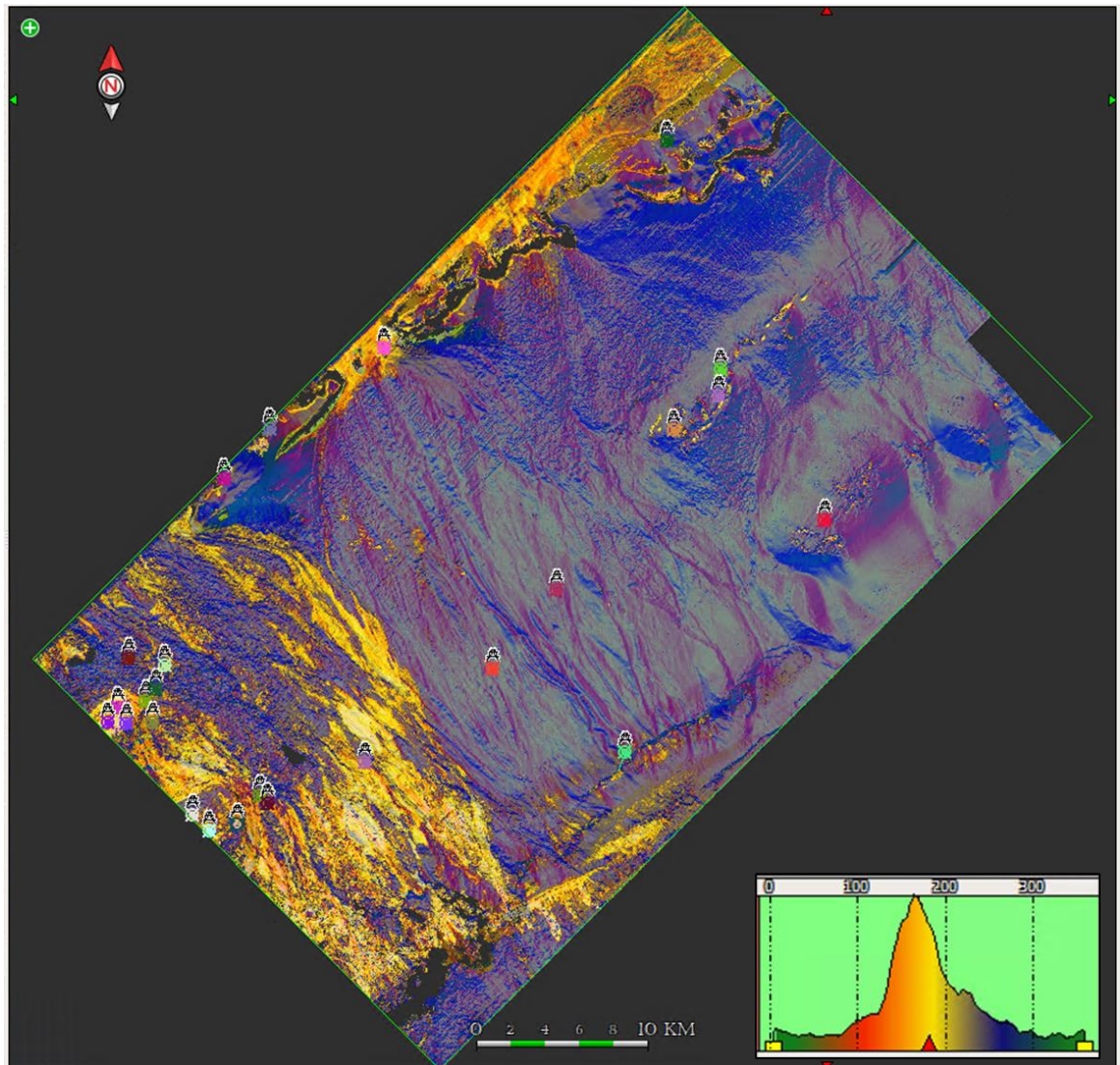


Figure 5-18: Seabed attribute of the blending of RMS, and sweetness attribute of the present-day seabed shows the submarine channels flowing down from the shelf-break in the southeast of the area. The obvious difference, between the southern area, with presence of bright yellowish attribute, represents the mixture, with coarser materials carried down in the MTC from the canyon complexes. In contrast the northern area with darker attribute indicates shale prone deposits.

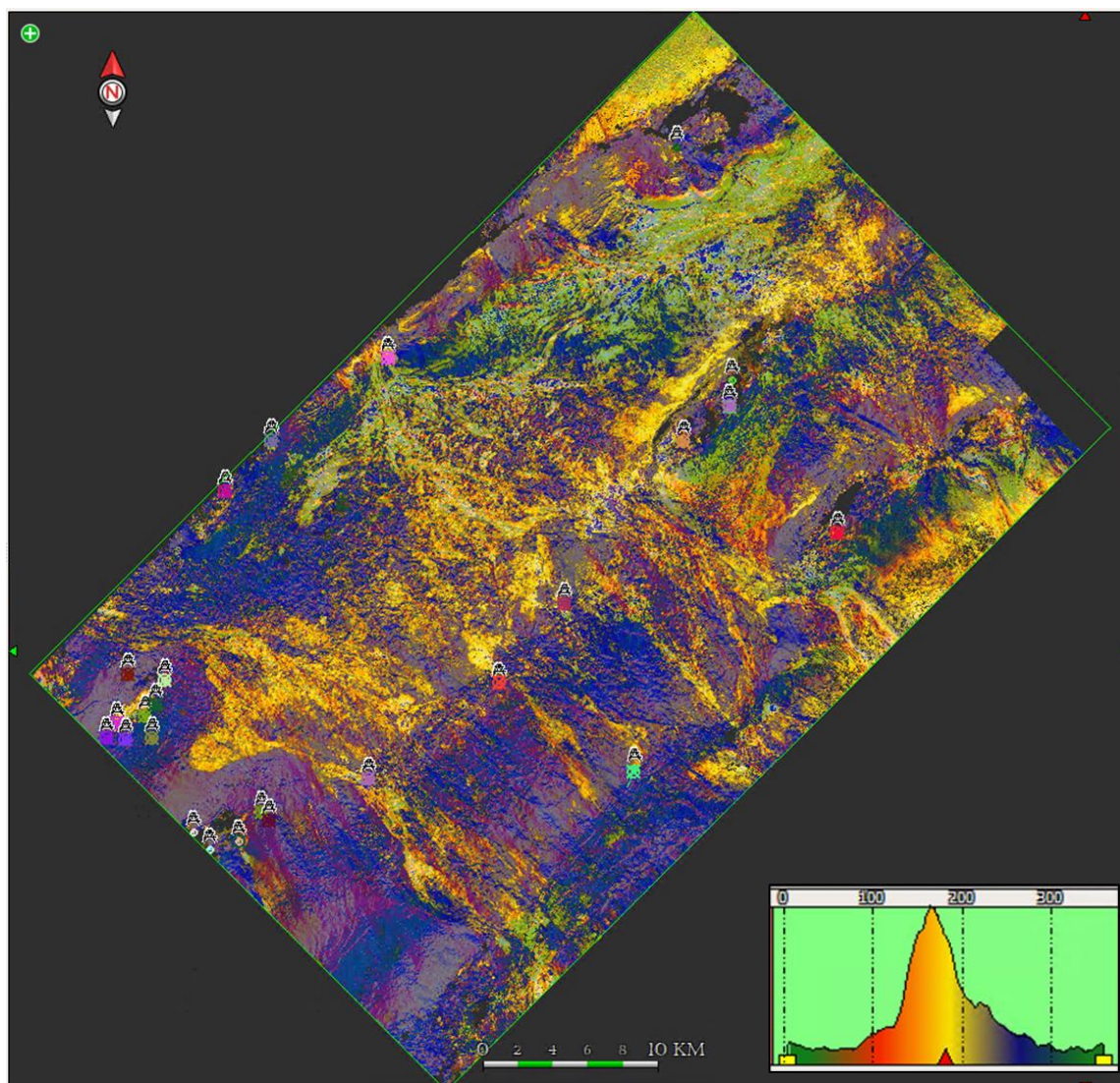


Figure 5-19: MFS 2.6 horizon attribute blending, 500 m below the present-day seabed, shows an obvious difference between the unconfined and confined depositional settings. In the southern area of the Limbayong fan a series of submarine channels flowed down from the intra-slope canyons towards the basin in an unconfined setting and formed a submarine fan lobe further outboard. Whilst in the northern area at the Lawa-Bestari structures, confined accommodation spaces near the fold ridge caused the change in direction of the sediment flow towards the northeast, parallel to the fold trend.

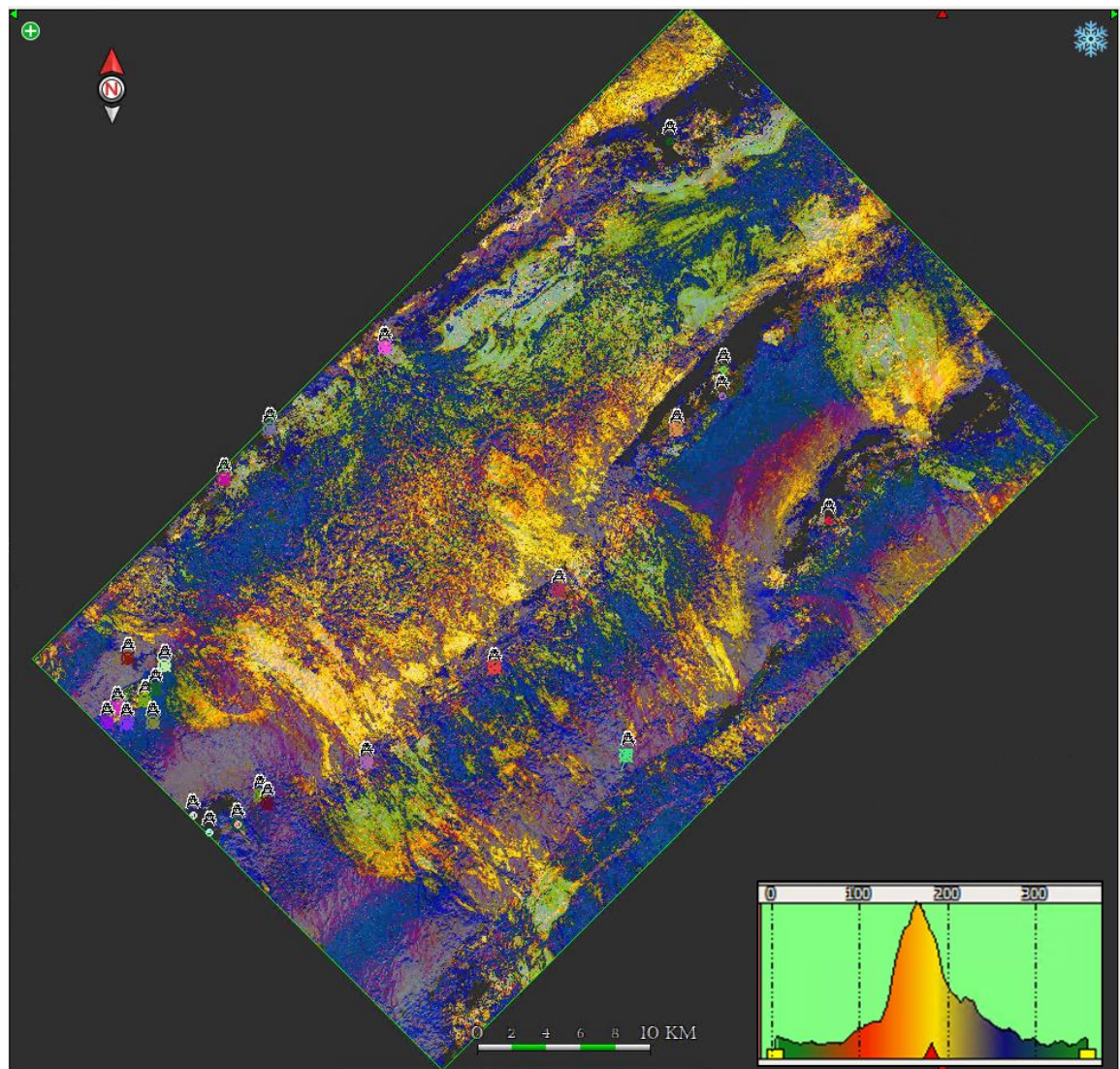


Figure 5-20: Lingan submarine fan horizon attribute blending shows three dominant submarine channel systems flowing down to the basin from the southeast in between the fold highs. The sediment supply at this time is believed to be not huge, to accommodate and fill up the accommodation space available in the basin. Submarine channels flowing through the folds in Menawan and Limbayong could be seen making the high a bypass area, and deposited the sandstone in the footwall of the Limbayong structure. Lesser sediment in the Lawa-Bestari trend caused the sandstone to be deposited mainly in the footwall of Lawa fold; a small amount reached the northern flank of Bestari fold.

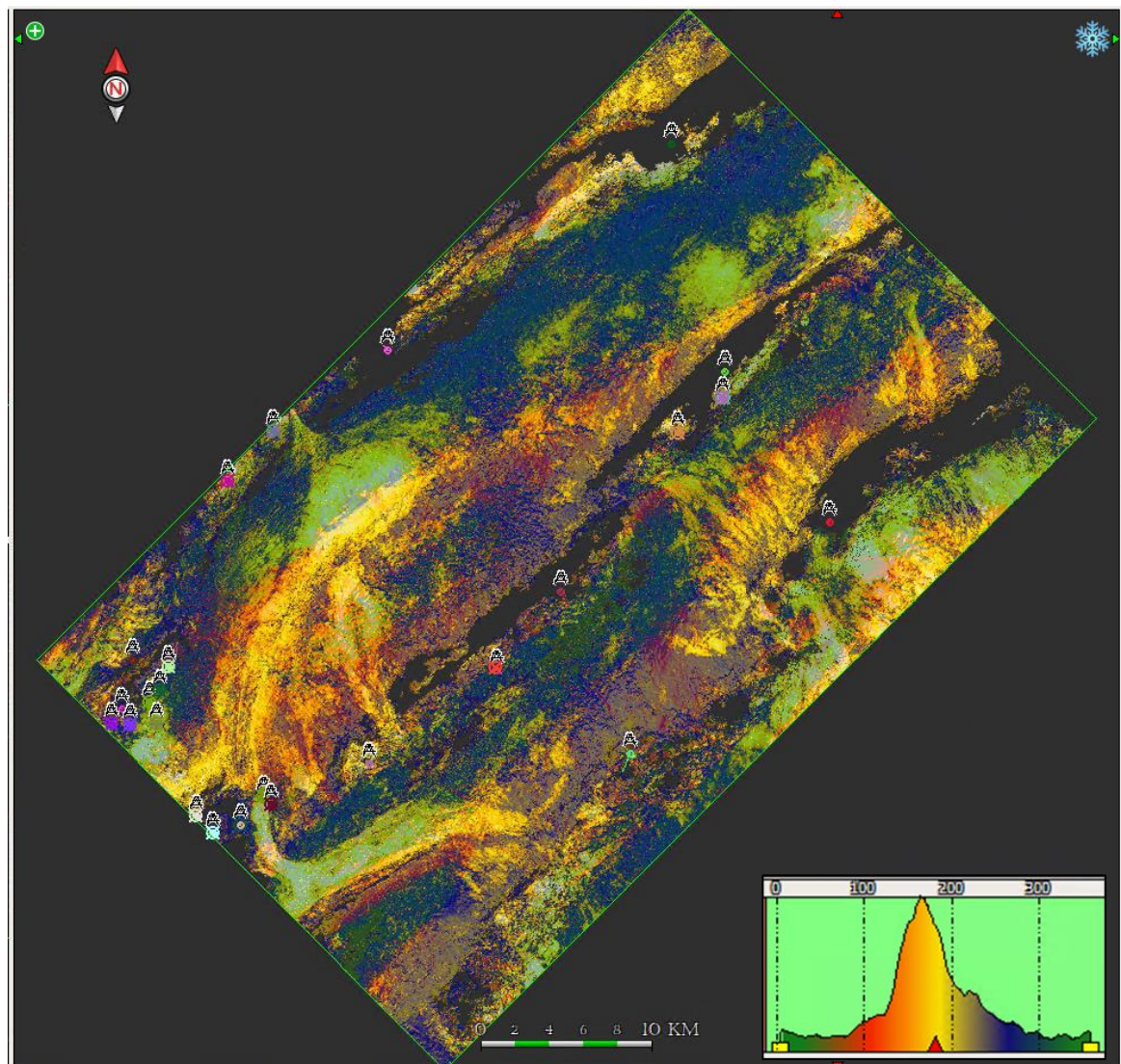


Figure 5-21: The horizon attribute blending at the Yellow submarine fan displays the submarine flow around the Limbayong structural high, and forms a submarine fan in the intra-slope basin area. Increased sandstone deposition in the synclinal area of the Lawa footwall could be seen as the submarine channel flow across the bypass zone at the Lawa fold. A thinner submarine channel could reach the Bestari structural high, particularly at the Bestari-3 area, as shown by the amplitude colour response.

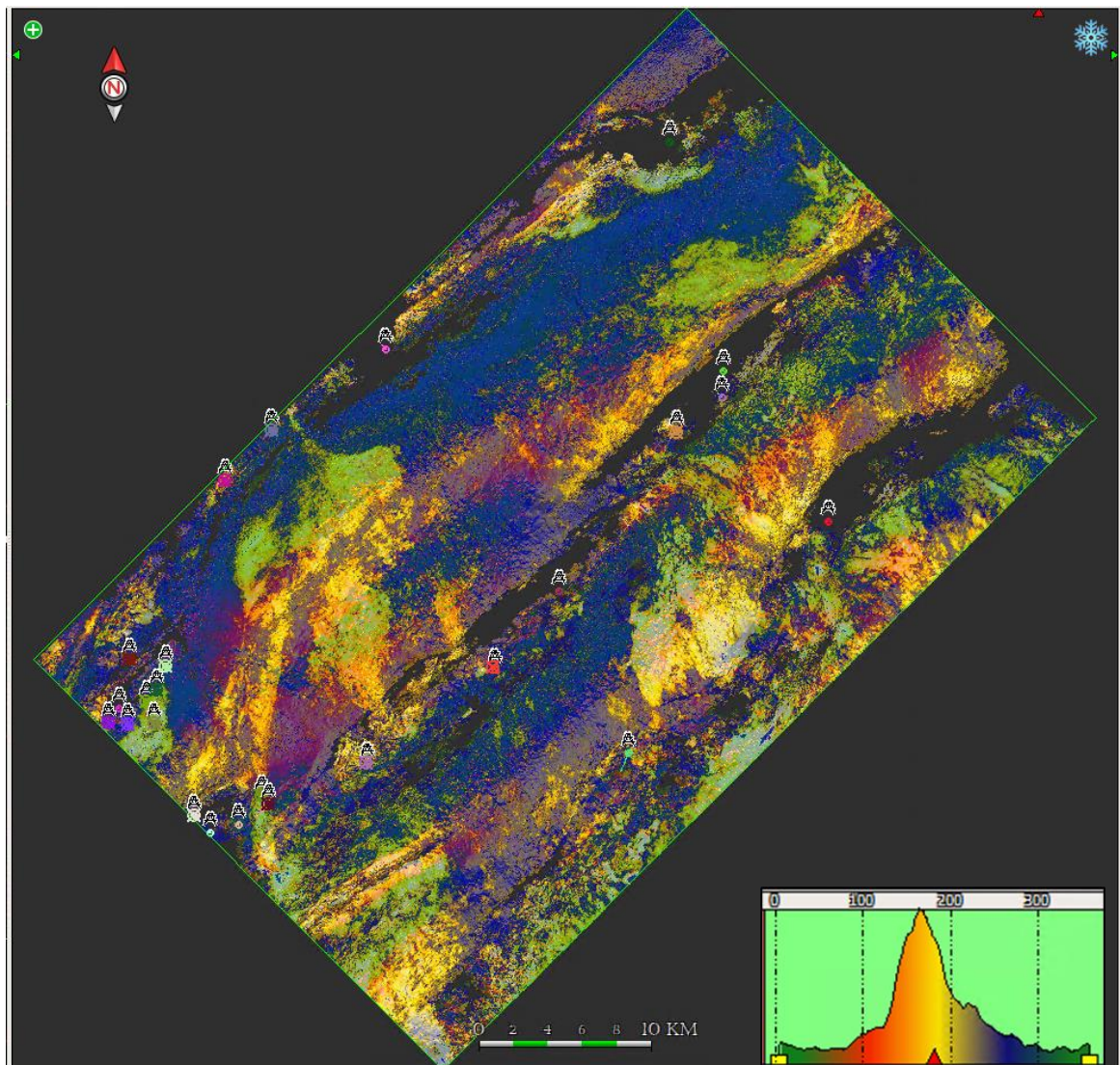


Figure 5-22: Pink submarine fan horizons attribute blending indicates increased sandstone at the Lawa and Bestari structures, with submarine fan lobes developed in the syncline in between the folds in the Lawa footwall inter-slope basin. However, the wells in Bestari might be receiving a different system of submarine channel sediment, as lateral continuity seems to be poor between Bestari-3 and Bestari-2. There is a sharp contact between the sand body and a possible MTC in the intra-slope basin at the footwall of Menawan. The sand prone submarine channel might be sourced from the southwest, and cut by the MTC deposition from the southeast.

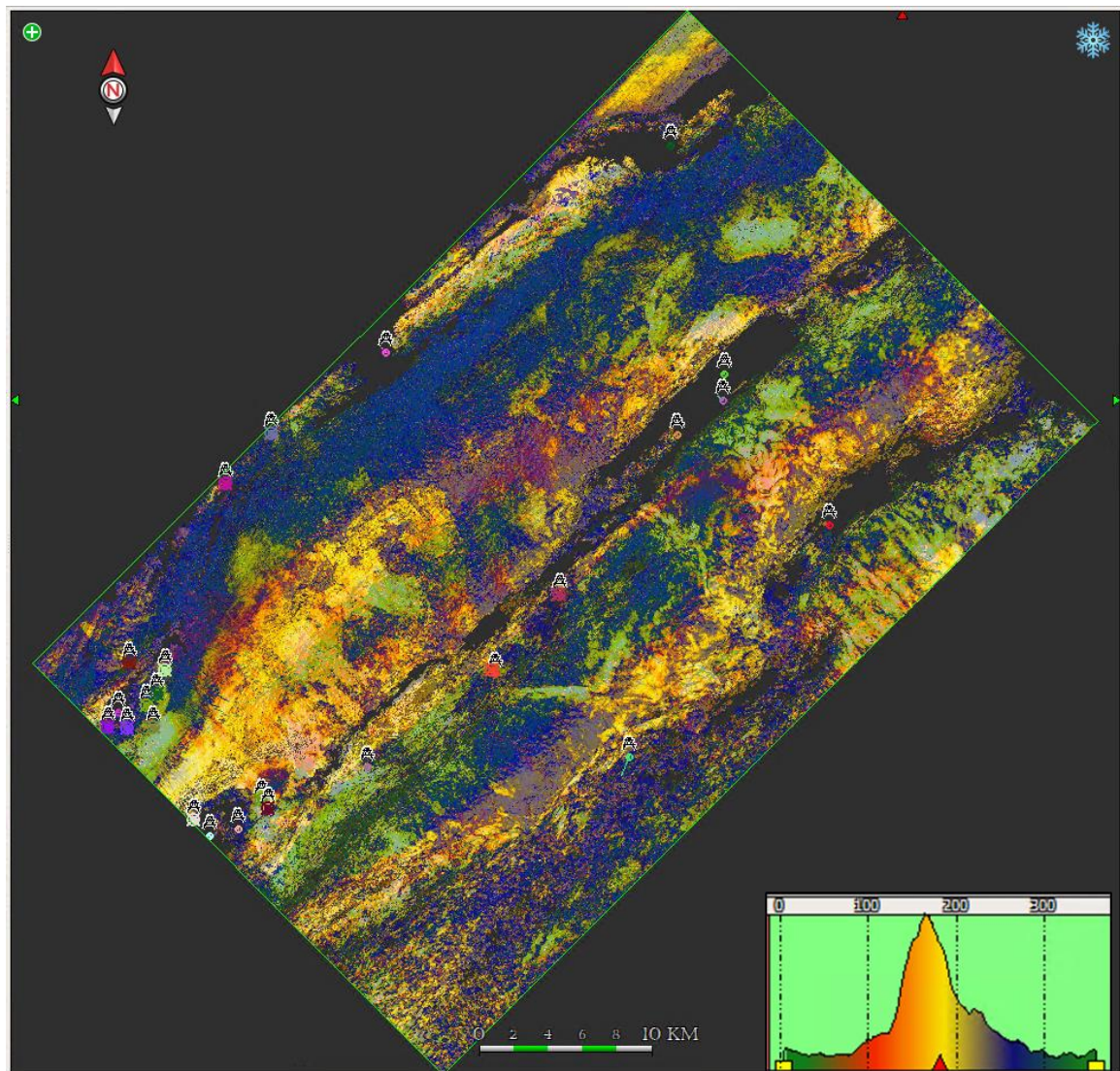


Figure 5-23: Upper Kamunsu reservoir seems to be well developed on top of the Limbayong southwestern culmination, covering the Limbayong-1 well location, decreasing towards Limbayong-2 and totally separated from Limbayong-3/ST1/ST2. Even though the sand covers the crestal part of the structure, it still depends on individual submarine channel system deposition, making it laterally separated between the three well penetrations in those three areas in the Limbayong structure. In Bestari, the deposition was mainly in the intra-slope basin syncline area, and thins towards the crestal part of the structure.

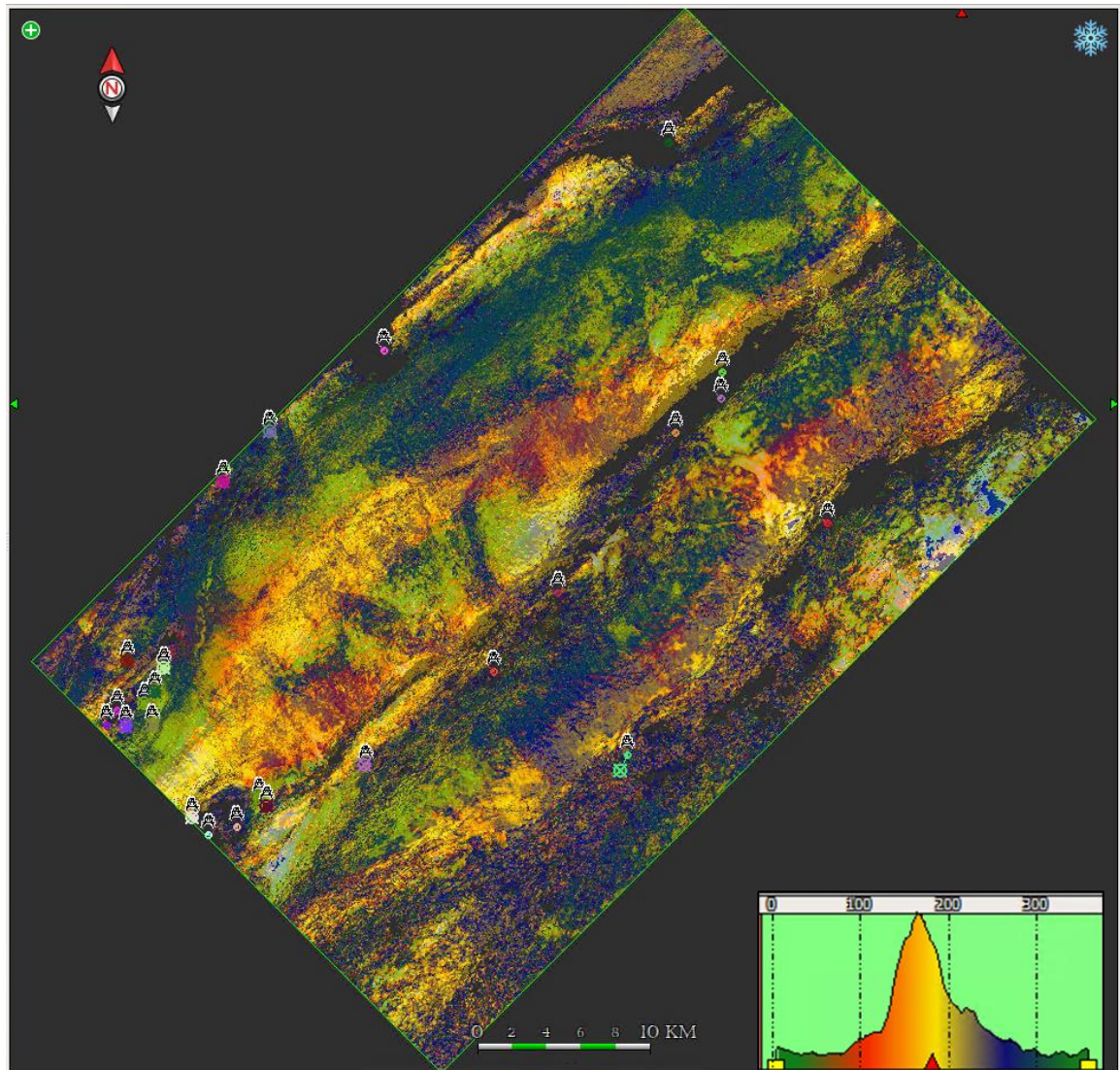


Figure 5-24: Lower Kamunsu reservoir is well developed on top of the Limbayong southwestern culmination, covering the Limbayong-1 well location, decreasing towards Limbayong-2 and totally separated from Limbayong-3/ST1/ST2. Even though the sand covers the crestal part of the structure, it still depends on individual submarine channel system deposition making it laterally separated between the three well penetration in those three areas in Limbayong structure. In Bestari, the deposition was mainly at the intra-slope basin syncline area, and thins towards the crestal part of the structure.

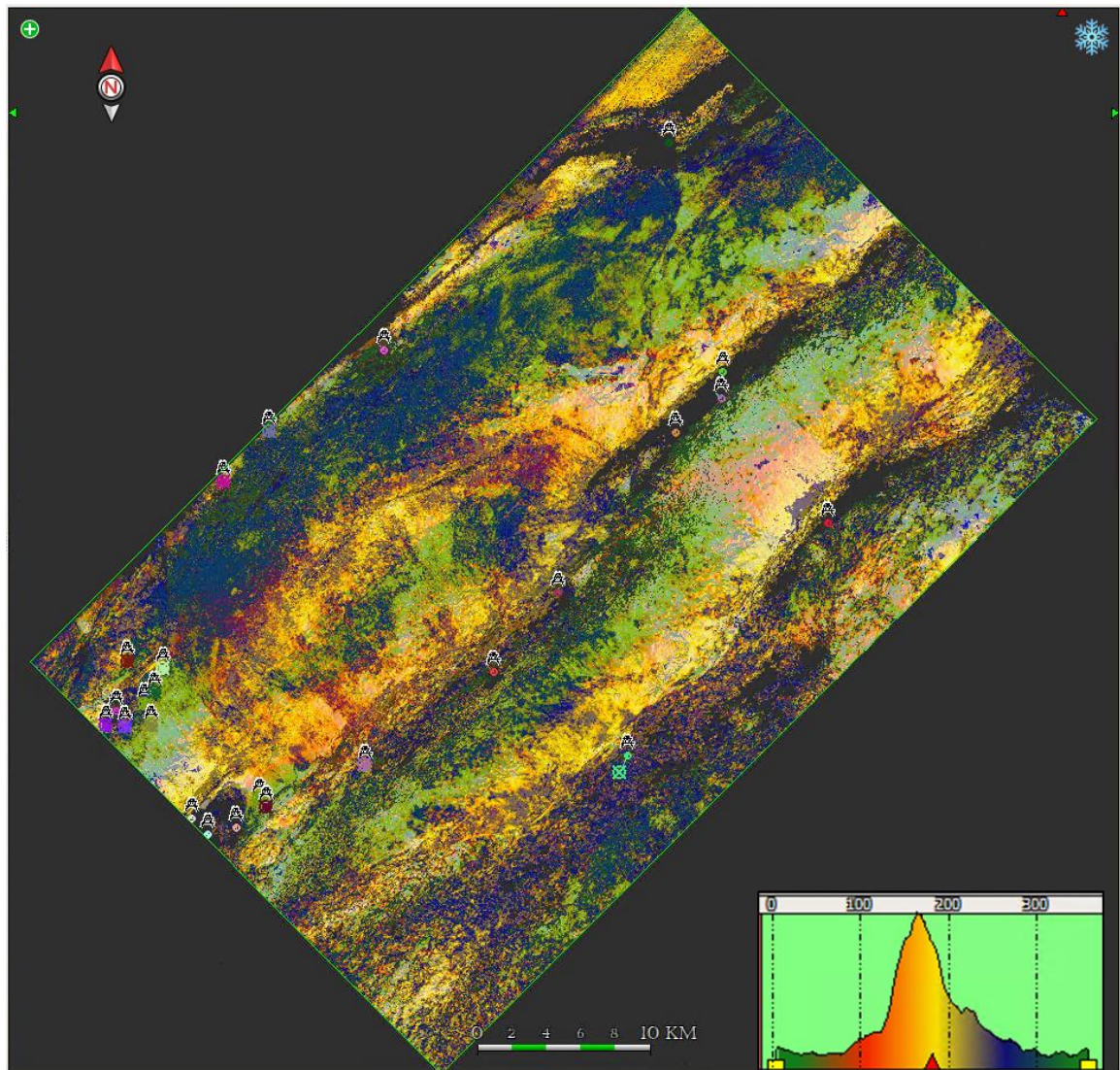


Figure 5-25: The horizon attribute blending of RMS and Sweetness attribute for the Kinarut submarine fan shows a rich reservoir sand being supplied to the basin, with a good spread of the bright amplitude in the synclinal part, thinning towards the crest of Bestari but possibly developed better in the Limbayong structure. However, it is still difficult to prove the lateral continuity of the submarine channel system in between the wells drilled in Limbayong and Bestari, as each area was charged by different submarine channel system, except for possibly the sand deposited in the syncline, and flowed as one single huge stream in the southwest to northeast direction.

5.6 Discussion

5.6.1 Depositional settings and facies distribution controlling factor

The well penetrations in the study area proved the complexity of the depositional setting in the deep-water fold-and thrust belt setting in the slope area. By integrating the well log signature, lithological description, seismic characteristics, and the seismic attribute horizons blending we should be able to understand the variations seen in the wells and the controlling factors for the differences or similarity. It is important to note, the confusion of modelling the depositional system based on the RMS attribute solely, as the bright amplitude in the footwall, elongated parallel with the fold along the syncline as seen in Bestari can easily be mistaken as being directly connected to the bright amplitude in the footwall of Lawa. It could be modelled as the same fan system, based on assumption at the crest of Bestari that the same bright amplitude absence is due to seismic image being degraded by the shallow gas and hydrate at shallower level. Therefore, integrating the attribute extraction with other data such as well logs, lithology description from cuttings and core and use of formation pressure (see Chapter 6) is important to avoid the oversimplification in deep-water submarine fan depositional settings.

In this chapter, the depositional settings and facies associated can be summarised:

5.6.1.1 Sediment supply to deep-water submarine fan systems

There is no doubt that the sediment supply is a major external control on a shelf margin growth and supply for deep-water fold thrust belts. Conceptually, the so-called

accommodation to supply ratio (A/S) explicitly acknowledges the importance of sediment supply for shoreline migration and delta front migration often to the shelf edge (Carvajal et al., 2009). Using data from modern deltaic systems, other researchers (Muto & Steel 2002; Porebski & Steel 2006) have highlighted that given sufficient sediment supply deltas are capable of prograding to the shelf edge during rising sea level within a characteristic short transit time (<100 ky).

Studies of modern river-delta systems have also emphasised the importance of supply by quantifying sediment flux to the ocean based on drainage-basin area, relief, climate, bedrock lithology, etc. (Milliman and Syvitski, 1992; Hovius, 1998; Syvitski and Milliman, 2007). Furthermore, there has been a continued focus on sea level in efforts to predict the delivery and formation of sandy deep-water deposits (Catuneanu et al., 2009a,b; Helland-Hansen, 2009) despite the likelihood that supply; 1) can be the key driver for shelf-margin progradation and delivery of deep-water sand even during rising sea level (Burgess and Hovius, 1998; Pinous et al., 2001; Muto and Steel, 2002; Carvajal and Steel, 2009) and 2) may also allow the prediction of sediment bypass to deep-water areas.

It is obvious that the sediment supply to the DWFTB of NW Borneo has been critically controlled by the progradation of the large Baram and Champion deltas. These two wave-dominated deltaic systems filled in much of the Brunei shelf during the Late Miocene to present-day and significantly contributed to by-pass of sediments from the shelf into deep-water (Sidi et al. 2003). The Champion delta prograded approximately 40 km during the Late Miocene and 12 km in the Pliocene (see Sidi et al. 2003). Carvajal et al (2009) indicate that in progradational margins, progradation rates tend to correlate with sediment

supply, and that increasing rates of progradation commonly imply increased volumes of sand being brought to the deep-water basin floor.

Furthermore, it seems that over time scales greater than 1–2 Ma, sediment supply is the key limiting variable controlling the volume of sandstone in the slope and basin floor. This is a conclusion in agreement with studies of modern/Quaternary systems that demonstrate fan volumes to be directly related to river discharge (Sømme et al., 2009).

5.6.1.2 Sediment provenance

The difference of the amount of sediment affects the shelf-break submarine canyons development. The differences are obvious between the southern part of the area, with numerous submarine canyons developed because of huge amount of sediment transported down from the shelf. The area located proximal to provenance of sediment of the Baram and Champion deltas and the presence of submarine channel systems connecting the fans in the inboard to this area might be the reason for this.

Apart from the sediment supplied from the southeast of the area, the seismic attribute shows a possible sediment migration from the southwest, parallel with the fold directions. This particularly can be seen in the deeper fans of Kamunsu and Kinarut. This might be explaining the thick reservoir encountered in the Kikeh, Gumusut and Kakap fields and the thicker reservoir seen in Limbayong wells as compared to the wells in the Bestari structure.

5.6.1.3 Seabed topography during deposition

The topography of the seabed during sediment deposition affecting the accommodation spaces and the submarine channel pathway. The steeper slope at the Menawan and Limbayong make the stream flowed energy higher than the causing the area to become a bypass zone as submarine channel and canyons cut through the structure with CL deposits at, he based of the channel.

The huge amount of sediment towards Limbayong, at the Lingan submarine fan upwards to the present-day seabed, either eroded the crest of the anticline or ceased the growth of the fold due to the rapid sedimentation on top of the structure. This causing the MTC deposition and submarine channel to be deposited in unconfine settings as compared to the confine settings in Bestari. The high magnitude with steeper limb of Bestari fold, restricted the submarine channel ability to reach the crestal part of the structure, and causing the submarine channel to flow around the fold. This might be the reason for the poor reservoir development in Bestari as compared to the lower magnitude Limbayong fold.

5.6.1.4 Individual submarine channel deposition

The expected a fan lobe setting in this area deposited mostly at the footwall of the more unconfine setting of the folds. The targeted crestal of the folds, being the targeted location for the wells either cut through by submarine channel resulting in stacking channel of the DLC or LCC. However due to the kinematics of the submarine channel deposition with

the fold growth magnitude, most of the channel deposit thinning out or fade off to the top of the structure.

The expectation of having a connected sand system throughout the structural high is proven to be unlikely as the folds are fed by different submarine channel bodies (Figure 5-26, 5-25 and Figure 5-27).

5.6.1.5 Inter-pod depositional models

The depositional setting of the submarine channel and fans seems to be concentrating towards the synclinal area of the intra-slope basin area in between of the inboard and outboard folds at the footwall of the folds (Figure 5-28). The seismic characteristics, attribute extraction of the time slices and horizons attribute blending shows the common northeast-southwest elongated features parallel with the fold direction in an inter-pod depositional model.

The high and continuous seismic amplitude, with bright high attribute suggested the thick sandstone of the possible stacking channels with DLC might dominated this pod as usually expected in the basin floor fan.

Due to none of the well ever penetrated the synclinal part to test the pod of bright attribute, it will be possible future target for exploration target for possible stratigraphic trap play with the sand pond seems to be pinching out on-lap on the MTC.

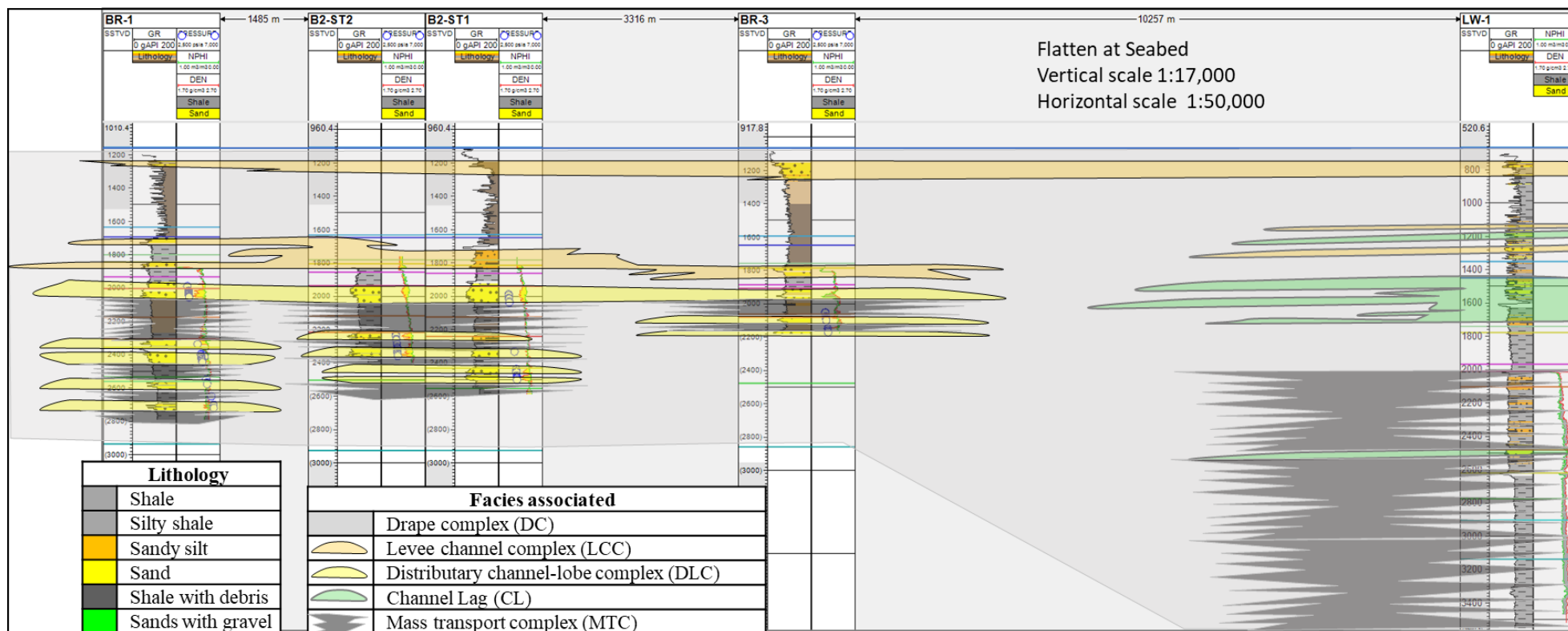


Figure 5-26: Well correlation interpretation sections for the Lawa and Bestari wells, flattened at seabed, integrating information from the well log, lithology description, seismic facies and formation pressure. Data suggest a bypass zones dominated by either the MTC or “shale diapirs” at the Lawa-1 well, whilst at Bestari the sand encountered is proven to be charged by a different submarine channel stream.

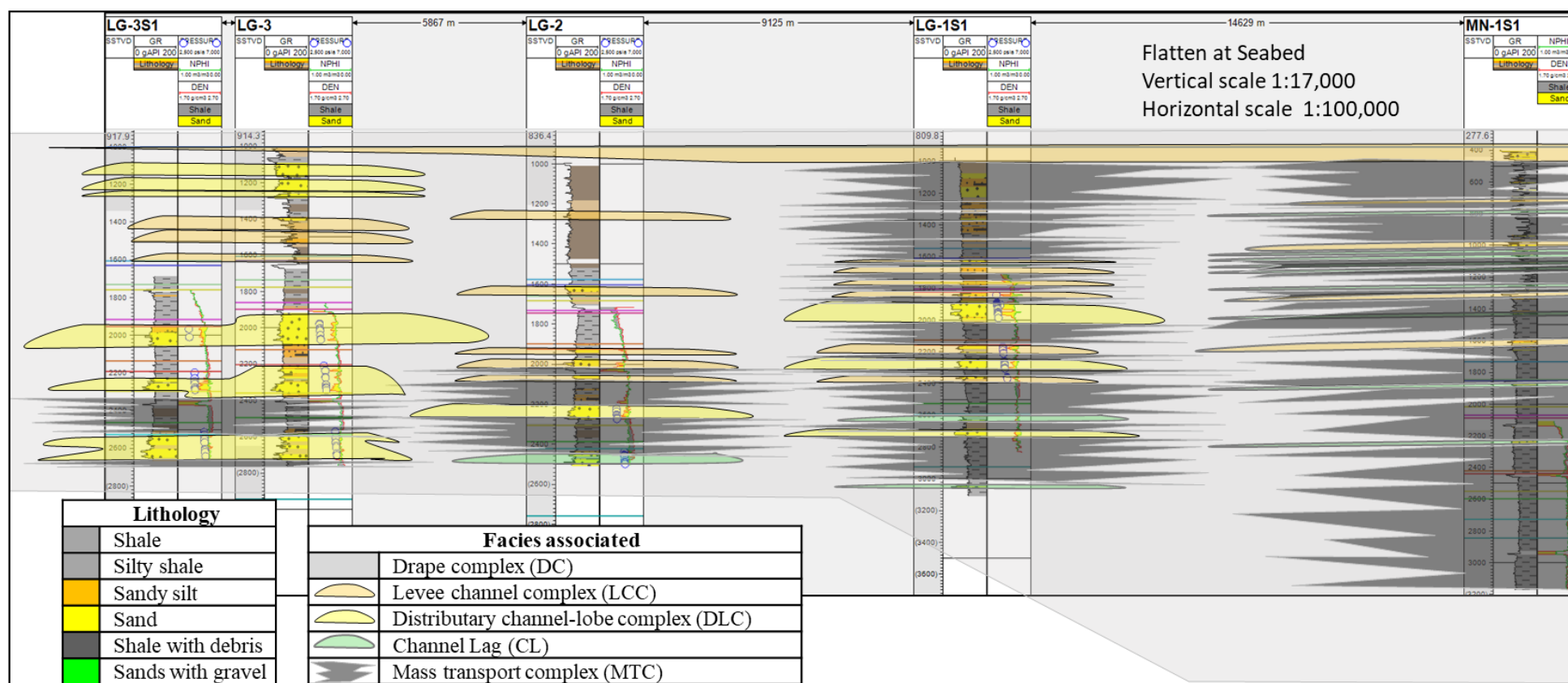


Figure 5-27: Interpreted correlation of Menawan-1ST1 and the wells in the Limbayong structure, flattened at seabed. The sand deposition in Limbayong is thicker, with more layers as compared to Bestari due to the closeness to the source of the sediment. The upper part of Menawan-1ST1 and Limbayong-1 was dominated by MTC deposition from the multiple submarine canyons at the shelf-break. From below the Kamunsu reservoir and deeper, there are possibly the “shale diapirs” popping up from the deeper Setap Shale formation.

5.6.2 Chronostratigraphic correlation

The deep-water fold-and-thrust belt of NW Borneo depositional setting proven to be varied not only between the fold, but also between the area from the same fold. This proven by the trend showed by well drilled in both folds, even though not very far apart, less than 5 km like the well in Bestari, of only 1.5 km apart between Bestari-1 and Bestari-2/ST-1/ST-2. However, generally the trend of the regional shale, still reliable as the anchor for correlation (e.g., maximum flooding surfaces) as the seawater fluctuation affecting the area could be seen all over the wells and seismic respond.

As the provenance and magnitude of the fold growth difference between Bestari and Limbayong, the different in the chronostratigraphic between the wells and folds could be established. The chronostratigraphic charts for a cross section between Menawan and Bestari-1 (Figure 5-29) and Lawa towards Limbayong-2 (Figure 5-30) displayed the differences from the well and seismic analyses in this study. The differences in the amount of sediment, especially reservoir transported to the Menawan-Limbayong fold could be seen very dominant not only at the shallower fan systems, but also in the Kamunsu and Kinarut. The difference of the accommodation spaces in the Pink submarine fan and upwards could be seen clearly as in Menawan-Limbayong trend, the fold growth ceased and provided an unconfined setting for the depositional from the shelf, whilst in the Lawa-Bestari trend, the fold anticline can still be seen at the present-day seabed expression, due to the fold growth still very dominant until above the Lingan submarine fan in the end of Late Pliocene.

The sediment deposit of the submarine channel could be seen mainly very thick and dominant in the inter-slop basin of the syncline in the footwall of the fold could be seen in both cross sections. The Menawan-Limbayong shows a thicker sand presence due to the sediment been supplied from two different provenance, the southeast and the southwest as compared to the Lawa-Bestari only received a sediment supply from the southeast and located more proximal than the Menawan-Limbayong structures.

The claystone, defined into two different types, the deep-water shale of the DC and the MTC with the presence of high percentage debris, coincide with the chaotic seismic characteristics. The assumption of the chaotic claystone or shale features seen in seismic as all of the MTC facies associated, could be not all true after considering the overall seismic features of the body consist of the same features, It might be true for the interlayering MTC with the sand in the syncline area, but for the chaotic features in the fold, or forming the shale core and becoming a shale ridge of the fold, it might be a shale from the deeper formations being pushed up as shale diapirs as can be seen widely present in the shelf of the inboard area of the NW Borneo.

It is quite convincing, looking at the “Christmas-tree” shape of the shale when tracing the boundary of the body of the chaotic features in the seismic as can be seen in the seismic cross section (Figure 5-28). From lithological description of the cuttings and core samples however, it is almost impossible to differentiate the difference between the MTC deposited from the shelf due to the cohesive movement of the sediment in the canyons and the possible shale diapirs from the deeper shale and older shale of the most-likely Setap Shale as seen in the other area in NW Borneo.

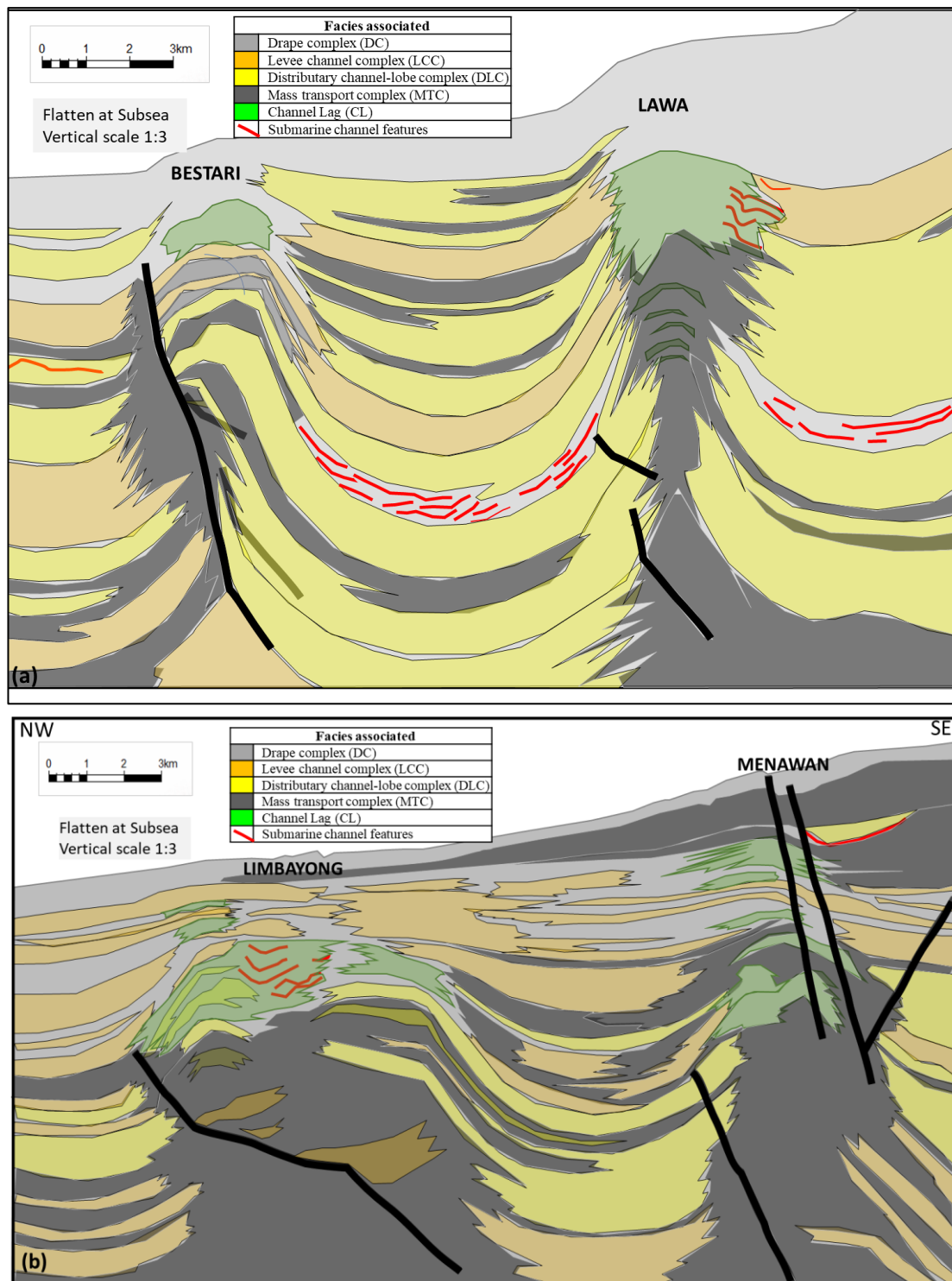


Figure 5-28: Interpretation from seismic section crossing (a) Lawa-1 and Bestari-1 and (b) Menawan-1ST1 and Limbayong-2 wells, showing the dominance of sand deposition at the synclinal area, forming a possible inter-pod depositional model, thick at the syncline and getting thinner towards the crest. The “Christmas tree” shaped of the possible shale diapirs could be seen in all structures, popped out higher at Lawa and Bestari, lower but wider at Limbayong and Menawan.

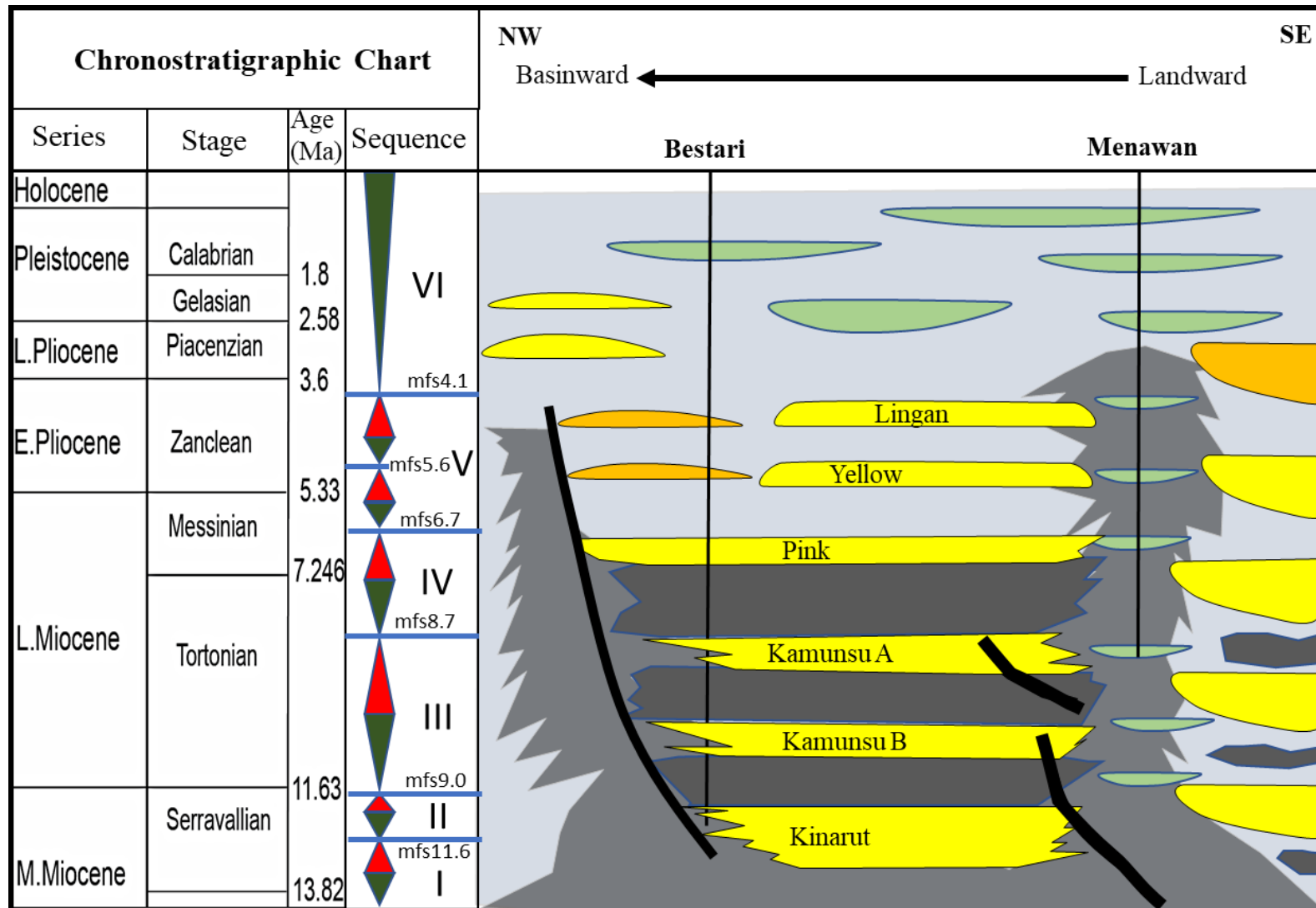


Figure 5-29: Chronostratigraphic chart of Lawa and Bestari structures, summarizing information and analyses, results of the well logs, lithology, seismic facies, and attribute extractions.

Open

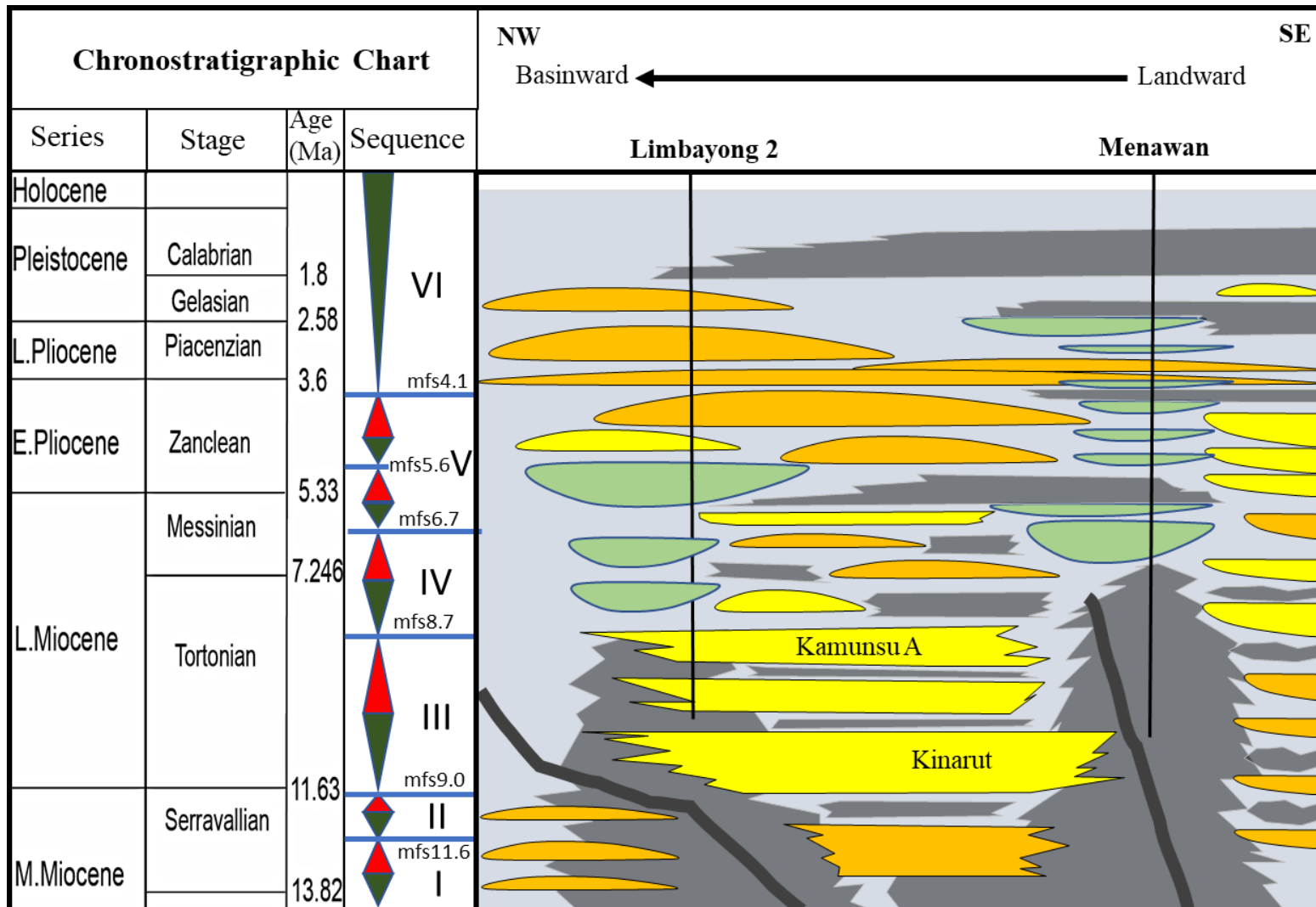


Figure 5-30: Chronostratigraphic chart of Menawan and Limbayong summarizing information and analyses result of the well log, lithology, seismic facies, and attribute extractions.

Open

5.7 Conclusion

1. Previous attempts at correlating submarine fan facies across the deep-water fold thrust belt has been unsuccessful as the facies have used biostratigraphy based upon chronostratigraphic of the shelfal sediments and of course these are reworked into by the MTC and submarine fans – there is also a strong diachroneity across the structures. In this study, sequence stratigraphy redeveloped based on a revised understanding of the facies, lithologies and use of high-quality seismic data sets.
2. This study recognized a whole suite of submarine facies and packages used to help understand the sedimentary processes and drive the correlation of the different fans.
3. This study established robust correlations-based sequence stratigraphy, seismic correlation and formation pressure and then used to reconstruct the development of the deep-water submarine fans and MTC histories using time slices.
4. Change from isolated submarine fans and turbidity channel fills that were strongly controlled by the sea floor topography and fold growth to larger submarine fans that are sediment supply controlled and have inundated the structures in many parts over the last 1 Ma. Change from a tectonically driven sedimentary system to one that is sediment supply and perhaps climatically controlled.

5. This study has shown the tectono-stratigraphic control the differences of the depositional setting and the facies distribution. The amount of sediment supply interactively be the controlling factor of the fold growth as proved by the fold growth ceased earlier in Limbayong as compared to Bestari, due to the proximity of Limbayong to the provenance, with addition of extra provenance from the southwest for the deeper hydrocarbon prolific Kamunsu and Kinarut submarine fans.
6. The different in sediment supply amount from the shelf break, affected the depositional settings with more submarine canyons developed at the slope as can be seen in Limbayong and caused huge MTC body deposited in the basin, in the unconfined settings due to the cessation of the fold growth. This not seen in Bestari, as the location is farther away from the provenance.
7. The seabed topography is a very important control of the depositional settings as the accommodation space in the deep-water intra-slope basin changes abruptly due to steep changes near the fold. The structural high act as a barrier if the submarine channel flows caused it to flow around the structural high, limited the ability of the reservoirs to deposited on top of the anticline. The presence of possible shale diapirs, as described as MTC might change the approach of hydrocarbon exploration and development of the area. The thick reservoir at the synclinal area, could be the interesting target of finding thicker and high net to gross sand, with potential trap bounded by the shale diapirs at folds inboard and outboard of the area

Chapter VI:

Overpressure occurrence and
impact on reservoir quality in
submarine fan systems of a NW
Borneo deep water fold-and-
thrust belt

*This chapter has been submitted to the Geological Society of London Journal
Petroleum Geoscience and will form part of a thematic set of papers on geopressure.*

6.1 Introduction

The NW Borneo deep-water fold-and-thrust belt offshore Sabah, southern South China Sea (Figure 6-1), contains a structurally complex region with several seafloor ridges outboard of the shelf slope break. As identified in Chapter 5 of this thesis (Figure 5-28, 5-29 and 5-30), have suggested the seafloor ridges formed either above shale diapirs produced by mass movement of overpressured shales (i.e., mobile shale) or above an imbricate fold-and-thrust array. However, syn-kinematic sedimentation interactions with growing folds, high sedimentation rates associated with MTD's and large submarine fan systems and, near-surface strains provide a challenging environment for prediction of subsurface sandstone reservoir quality. The NW Borneo deep-water fold-and-thrust belt is classified as a linked extensional-compressional system, with zones of inter- or intra-continent convergence involving gravity sliding or differential loading with far-field lithospheric stresses (Morley et. al., 2011). The gravity influence upon fold development began in the Middle Miocene and became prominent at the end of Late Miocene (Chapter 4), separate from the mainly tectonic driven structuration from the Late Oligocene, marked by the South China Sea spreading as mentioned by Hutchinson, (2004). Data from the Bestari and Limbayong folds (Figure 6-2) demonstrate three phases of fold development from the early tectonic phase until Middle Miocene, the beginning of the gravitational phase, and finally the gravitational phase with around 2500 m of submarine fans and MTD sediments deposited in less than 10 Myrs (Figure 6-4). The fold growth is further complicated by the development of four contemporaneous submarine fans called the Kinarut, Kamunsu, Pink and Yellow fans (Figure 6-3) and are the focus of this study with particular attention to the Bestari growth fold.

Hydrocarbon producing basins that display early onset and maintenance of high pore fluid pressure (i.e., low vertical effective stress (VES)) have been shown to preserve anomalously high porosity (>30%) by lessening the impact of mechanical compaction during burial (e.g. Grant et al., 2014; Nguyen et al., 2013; Sathar and Jones, 2016; Stricker et al., 2016). The NW Borneo deep-water fold-and-thrust belt offshore Sabah displays a complex interrelationship between the structural evolution, high sedimentation rates and overpressure development and evolution. The nature of the overpressure and overpressure distribution are examined in this chapter. A model is presented that integrates the overpressure distribution and potential reservoir quality of the submarine fan sandstones. These challenges are commonly encountered amongst other deep-water fold-and-thrust belt settings globally and the research presented here has important implications for prediction of reservoir quality and close association to anomalous compartmentalized overpressures encountered in deep water fold-and-thrust belts and structurally complex regions.

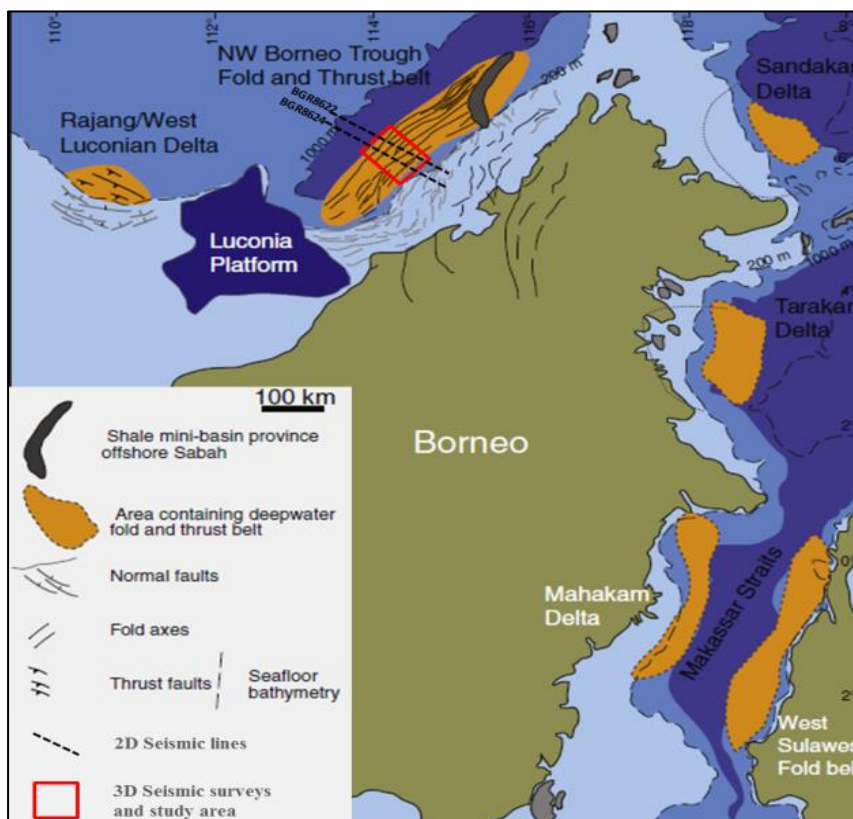


Figure 6-1: The study area is in the middle part of the NW Borneo deep-water fold and thrust belt aligned parallel with Sabah coast. Offshore Borneo is the location of at least 4 other deep-water fold-and-thrust belts. Figure modified after Morley et al. (2011).

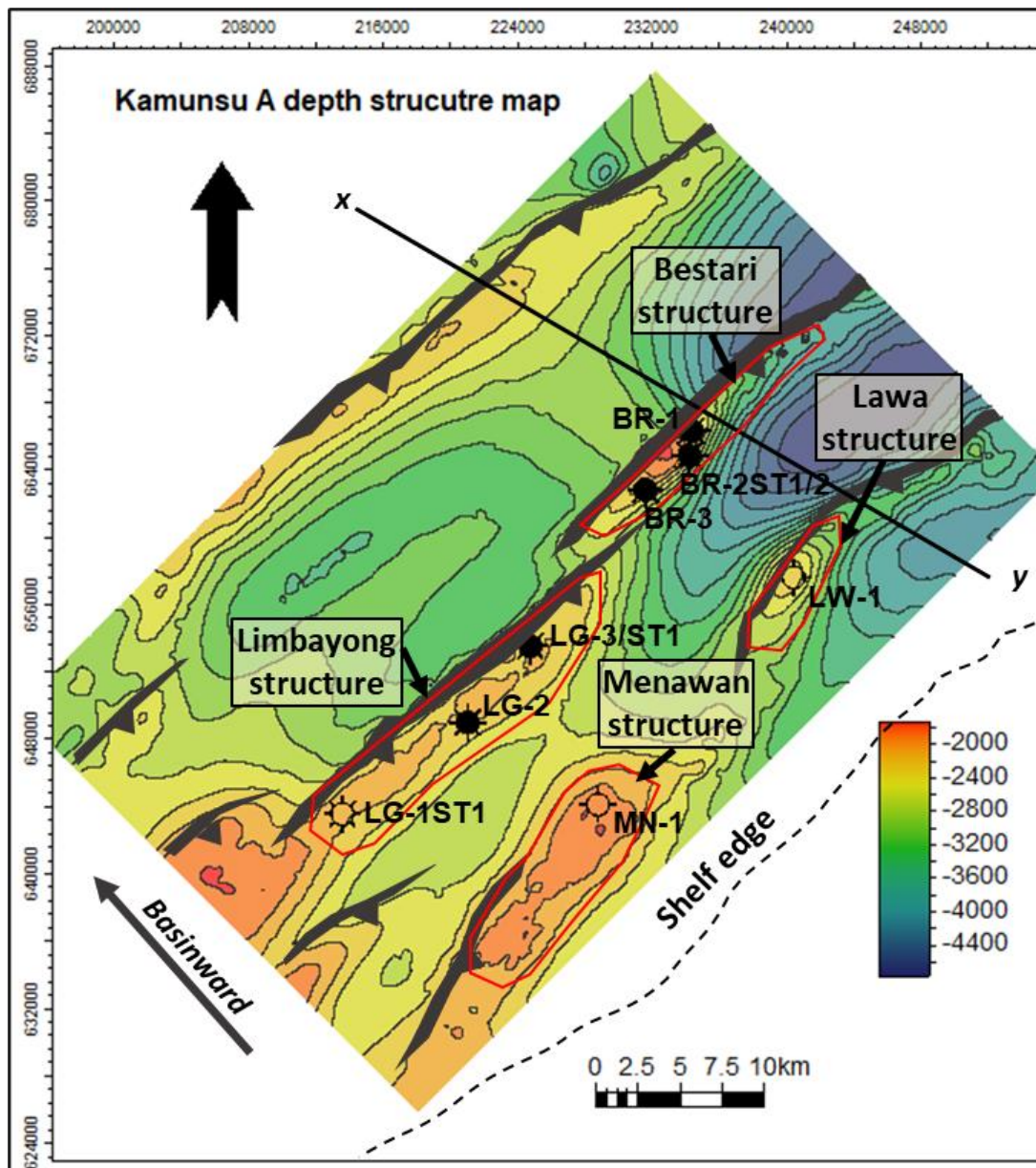


Figure 6-2: Depth structure map of Top Kamunsu shows the study area with the location of the thrust folds. The well data used in this study are located along the crest of the structures and are among the latest drilled in the deep-water fold and thrust belt province and the area covered by the 3D multi-azimuth seismic.

6.2 Tectono-stratigraphy

The deep-water NW Borneo fold-and-thrust as defined in Chapter 3 is divided into three phases of fold development confirmed by the burial history of the Bestari-1 well (Figure 4-11). The first phase was controlled by the tectonic activity of the Dangerous Ground subduction towards Borneo from Late Oligocene to Early Middle Miocene. The second phase, from Middle to Late Miocene, shows the changing trend of the burial history with increased sediment supply into the basin due to the uplift of the Crocker Ranges.

The gravitational tectonics outboard of Sabah drove the development of the thrust-and-fold belt with a change of vergence towards the northwest. The third phase from Late Miocene to Present-Day, records the transition to high sediment supply from the shelf and coastal plains of NW Borneo. The large volumes of sediment supplied to the shelf directly fed a series of submarine fans and MTD's and significantly contributed to gravity driven fold-growth in the complex deep-water fold-and-thrust belt of NW Borneo at Present-day. Submarine fans, the terminal portion of sedimentary source-to-sink systems, are amongst the largest and most rapidly deposited sedimentary accumulations on the planet with recent monitoring in Congo Submarine Canyon and Channel shows a turbidity current ran out for 1,150 km into the deep-sea carrying in excess of cubic kilometre of sand and mud flowing for two whole days (Talling et al., 2007, 2021). Shaped by sediment gravity flows which deliver a range of sedimentary deposits in deep-water environments, they provide an invaluable record of Earth's climate and tectonic history, and the dispersal of sediment. Both external

and internal processes control the morpho-dynamic evolution and stratigraphic record of submarine fans.

The external controls including climate, sea-level and tectonics are responsible for the large-scale variations in the rate and volume of sediment supplied to the sediment routing systems. In comparison the internal controls driven by self organisation of the submarine fans include channel avulsion, levee growth and compensational stacking (i.e., preferential deposition in topographic lows) of lobes and their constituent building blocks; 'lobe elements'. There have been many investigations of the interrelationship between external and internal forces, but fewer studies have considered the direct relationship of deep-water fold growth, rapid sediment supply and deposition and development of overpressure in the basin.

The basin floor submarine fan systems and MTD's of the study area consist of at least seven turbidite fan formations regionally identified and mapped from inboard towards shelf edge in the form of slope channels and bypass assemblages, further outboard to the deeper water mainly deposited as sandy basin floor systems (Ingram et al., 2004). The important sub-marine fan complexes are the Ligan Fan (youngest), Pink Fan, Kamunsu Fan, Kinarut Fan and Kebabangan Fan (oldest) correlated by seismo-stratigraphy with unconformities on the shelf and are interpreted as related to a combination of sea-level changes, enhanced by penecontemporaneous tectonic movements inboard. Seismic analysis has identified both confined and unconfined basin floor fans, base-of-slope and slope fans, as well as associated turbidite feeder systems.

6.3 Overpressure and vertical effective stress

The prediction of pore fluid pressure (overpressure) in sedimentary basins is often addressed using one-dimensional methods (e.g., Daniel, 2001; Hennig et al., 2002; van Ruth et al., 2002; Zhang, 2013), assuming that mechanical compaction is solely driven by the vertical effective stress exerted by the overburden (Hubbert & Rubey, 1959; Terzaghi, 1923). Even in cases where pore pressure evolution is modelled using basin models which incorporate 2-D or 3-D fluid flow, porosity loss is generally considered as being a simple function of vertical effective stress (e.g., Allwardt et al., 2009; Flemings & Lupa, 2004). In this way, porosity is a function of vertical effective stress, which then allows pore pressure to be estimated.

In addition, even state-of-the-art basin modelling software is not capable of modelling structural development as a result of tectonic activity, instead using prescribed geometries at specified geological times (Neumaier et al., 2014). These approaches to pore pressure evolution are unlikely to be sufficient in basins dominated by active tectonics such as fold-and-thrust belts or basins associated with salt diapirs, due to the contribution of lateral deformation and lateral stresses on compaction and overpressure generation (e.g., Couzens-Schultz & Azbel, 2014; Obradors-Prats et al., 2016). However, even advanced coupled, critical state, geomechanical-fluid flow simulation models as presented by Obradors-Prats et al. (2017, 2019) require a robust understanding of the input parameters relating to the sediment petrography (grain size, grain types, maturity, clay content), porosity and permeability evolution and potential compartmentalisation of overpressure due to lateral facies changes and/or faulting and folding of the stratigraphy.

Furthermore, there is a growing number of studies that have recognised the role of fluid pressure and enhanced porosity in sandstones. It has been suggested that overpressures can limit or prevent significant quartz cementation by forestalling the onset of intergranular pressure solution thereby eliminating a primary source of silica (e.g., Oye et al., 2018, 2020; O'Neill et al., 2020; Stricker & Jones 2018; Stricker et al., 2016a, b).

This study will further analyse the overpressure generation mechanism in the area, with particular attention paid to the Bestari growth structure, based on the evidence from drilled well data and the relationship of overpressure generation with the tectono-stratigraphy. The maintenance of porosity and its direct influence on the reservoir quality, especially the deeper submarine fan sands, will be appraised.

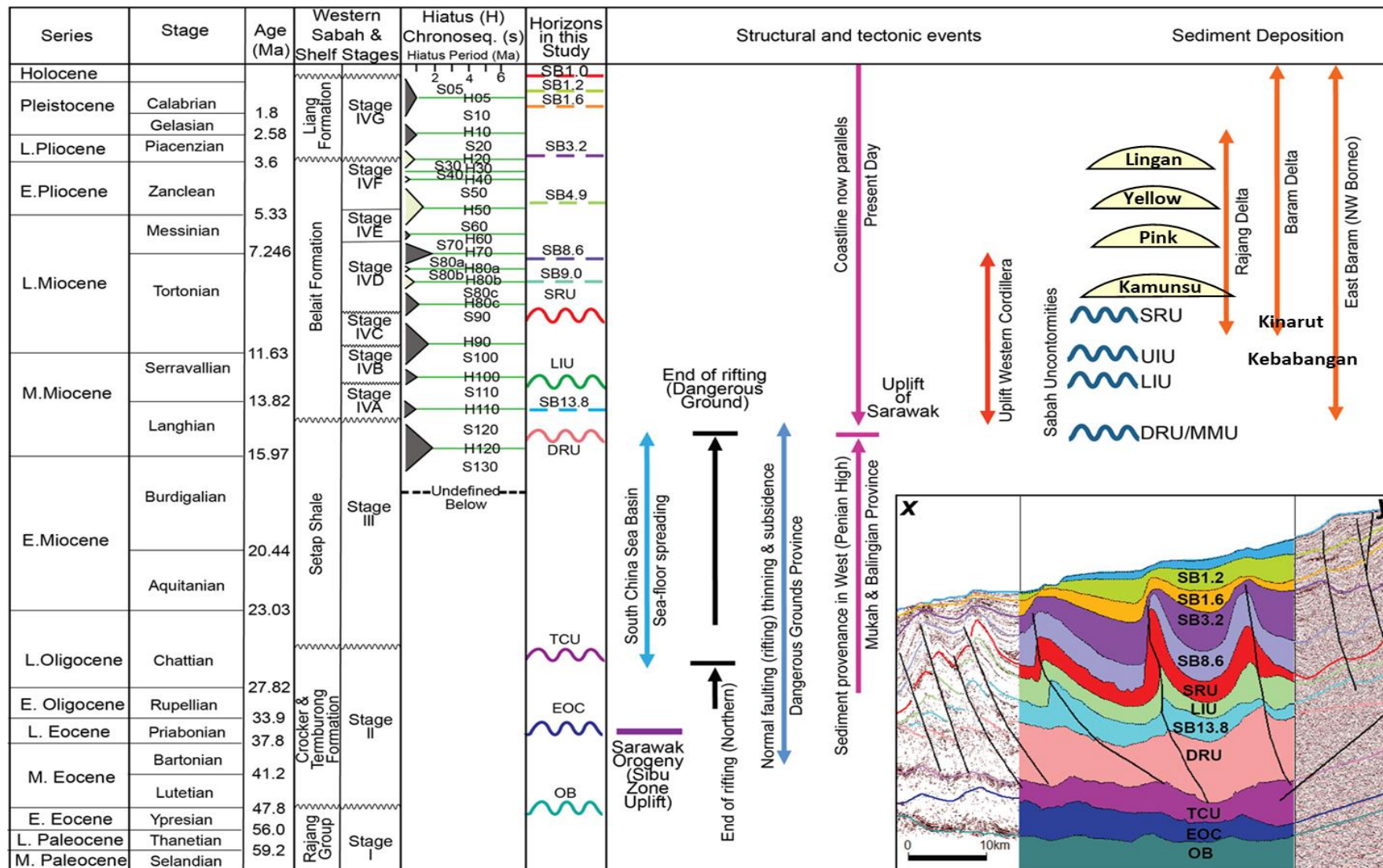


Figure 6-3: NW Borneo stratigraphy chart with the highlighted reservoir of interest in this study.

Open

6.4 Methodology

Data utilized in this study primarily was sourced from drilled wells in the study area, along the thrust folds of Bestari, Limbayong, Menawan and Lawa structure (Figure 6-2 and Table 6-1). A standard well log and pressure measurement acquired mostly by direct measurement including MWD/LWD and wireline logging being used for the well correlation and to analyse the pressure mechanism. This is further combined with well sample analysis from side-wall cores and conventional cores provided by PETRONAS and undertaken by CORELAB. Multi-Azimuth three-dimensional seismic data and two-dimensional regional seismic lines interpreted and incorporate with horizons from well for well correlation and generating the horizon maps.

No.	Wells	Well log					Pressure Data			Well Sample Analysis			
		GR	RHOB	RDEEP	DTC	Temp.	Formation	LOT	Mud Weight	Thin Section	XRD	SEM	RCA
1	B1	X	X	X	X	X	X	X	X	X	X	X	X
2	B2ST1	X	X	X	X	X	X	X	X	X	X	X	X
3	B2ST2	X	X	X	X	X	X	X	X	X			
4	B3	X	X	X	X	X	X	X	X				
5	L1ST	X	X	X	X	X	X	X	X				
6	L2	X	X	X	X	X	X	X	X				
7	L3	X	X	X	X	X	X	X	X				
8	L3ST1	X	X	X	X	X	X	X	X				
9	Mn1	X	X	X	X	X	X	X	X	X	X	X	
10	Lw1	X	X	X		X		X	X	X	X	X	

Table 6-1: Well data availability used in this study. A total of 10 wells were analysed across 4 growth folds.

Pressure data from different sources acquired during well drilling, pre-drilling for pressure prediction and post-drilling analysis were used to obtain a comprehensive pressure data set for the structures. The fracture pressure data come from well Leak of Test (LOT) and Formation Integrity Test (FIT), whilst formation pressures were obtained mostly from wireline logging operation of the Modular Formation Tester (MDT) and Repeat Formation Tester (RFT). In some of the recent wells such as Bestari-1, formation pressure was also acquired by the Logging While Drilling (LWD) formation-pressure testing (TESTRAK).

6.4.1 One dimensional burial history modelling

Pore pressure evolution within the stratigraphy intersected by the Bestari-1 well was modelled in one dimension using Schlumberger's PetroMod (V. 2015) software. One-dimensional modelling provides a good insight into overpressure build-up by disequilibrium compaction (Stricker, 2016), which is regarded as the principal driver in NW Borneo DWFTB. PetroMod is based on a forward modelling approach to calculate the geological evolution of a basin from its burial history (Hantschel and Kauerauf, 2009).

However, the models do not include other mechanisms for generating excess pore pressure, such as hydrocarbon cracking, gas generation or load transfer (Lahann and Swarbrick, 2011) and are only able to account for vertical stress. 1D modelling will also not show the potential discrepancies in overpressure between reservoir and shales

caused by lateral fluid flow, but this can be calibrated using measured reservoir pressure data where available.

The generation and dissipation of pore pressure is a 3D process, which is not captured in a 1D system. Fluid flow in the form of lateral drainage, lateral transfer and fault related flow have been identified in the NW Borneo DWFTB (see Couzens et al., 2014) and must be taken into consideration when interpreting modelling results.

The burial model uses present-day well stratigraphy provided for the Bestari-1 well and lithologies created from mud log cuttings data from well completion reports provided by the drilling operator (Table 6-2). The model was calibrated against a corrected bottom hole temperature, measured formation pressures and helium porosity from core samples (Figure 6-5).

Porosity reduction was calculated using the Sclater-Christie (Athy) exponential-decay equation. Porosity optimization was performed using PetroMod Mechanical Compaction options by adjusting the Athy's factor (Athy, 1930 and Ruth et al., 2002). The heat flow and temperature for the model were derived from Formation Tester (MDT), Repeat Formation Tester (RFT) and log-derived temperatures. An average of 6 °C were used for the surface temperature for all the wells run in the model as the average surface temperature recorded in the seabed. The temperature correction method used was based on a calibration study carried out in the Malay Basin which is valid for depths up to about 3500 m (Waples et al., 2001). To test the validity of the input for the model, the corrected temperature, pressure, and porosity from the wells need to be calibrated with the model output (Figure 6-5).

To get calculated temperature profiles in the model calibration to fit with the measured temperature data involved adjustment of heat flow or conductivities via lithologies, mineralogy and porosities.

As this model not utilized for source rock evaluation, no further attention of the hydrocarbon generation and expulsion was considered in this modelling. For pressure and porosity optimization, the model involved optimization mainly for conductivities using a lithology-based approach (Table 6-2).

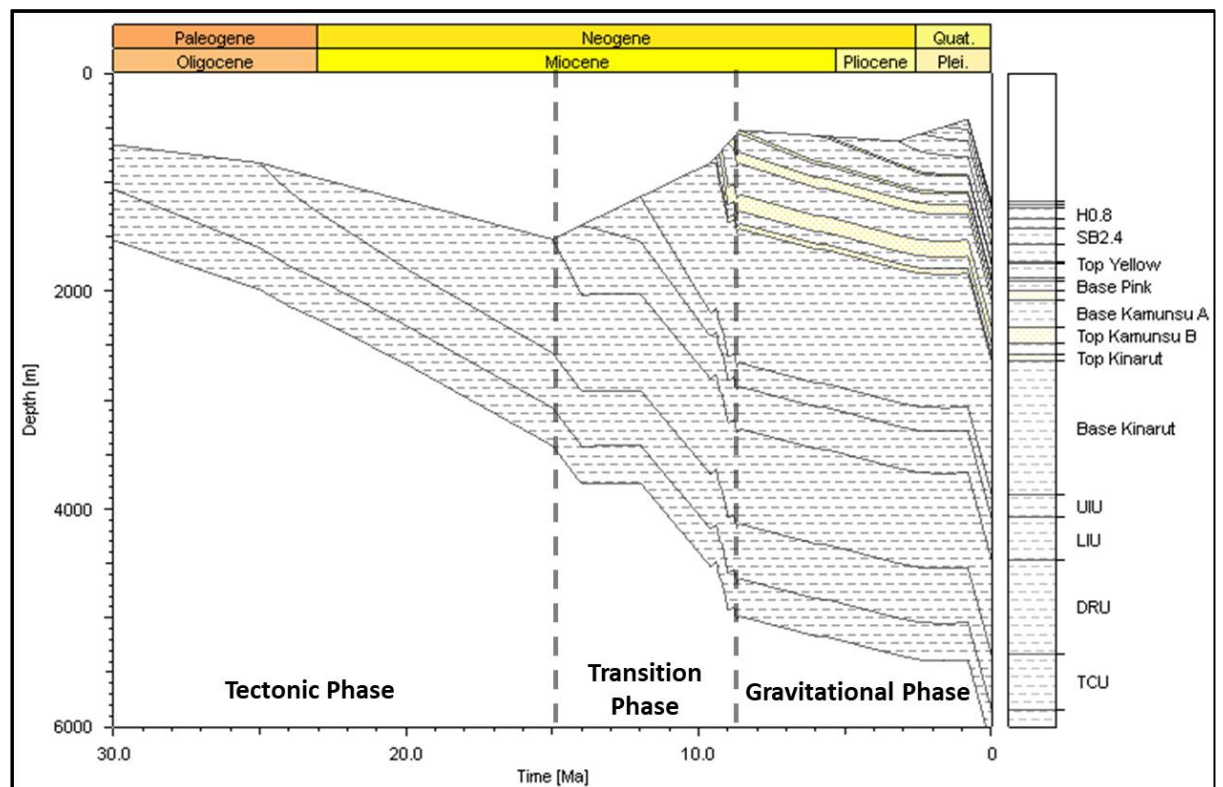


Figure 6-4: Burial history of Bestari-1 well located on the crest of the Bestari growth structure (See Figure 6 2 for locations). Three phases of the fold evolution from tectonic phase, symmetrical phase, and gravitational influence are recognised. Over 2000 m of submarine fan sediments have been deposited in the basin in the last 5 Ma.

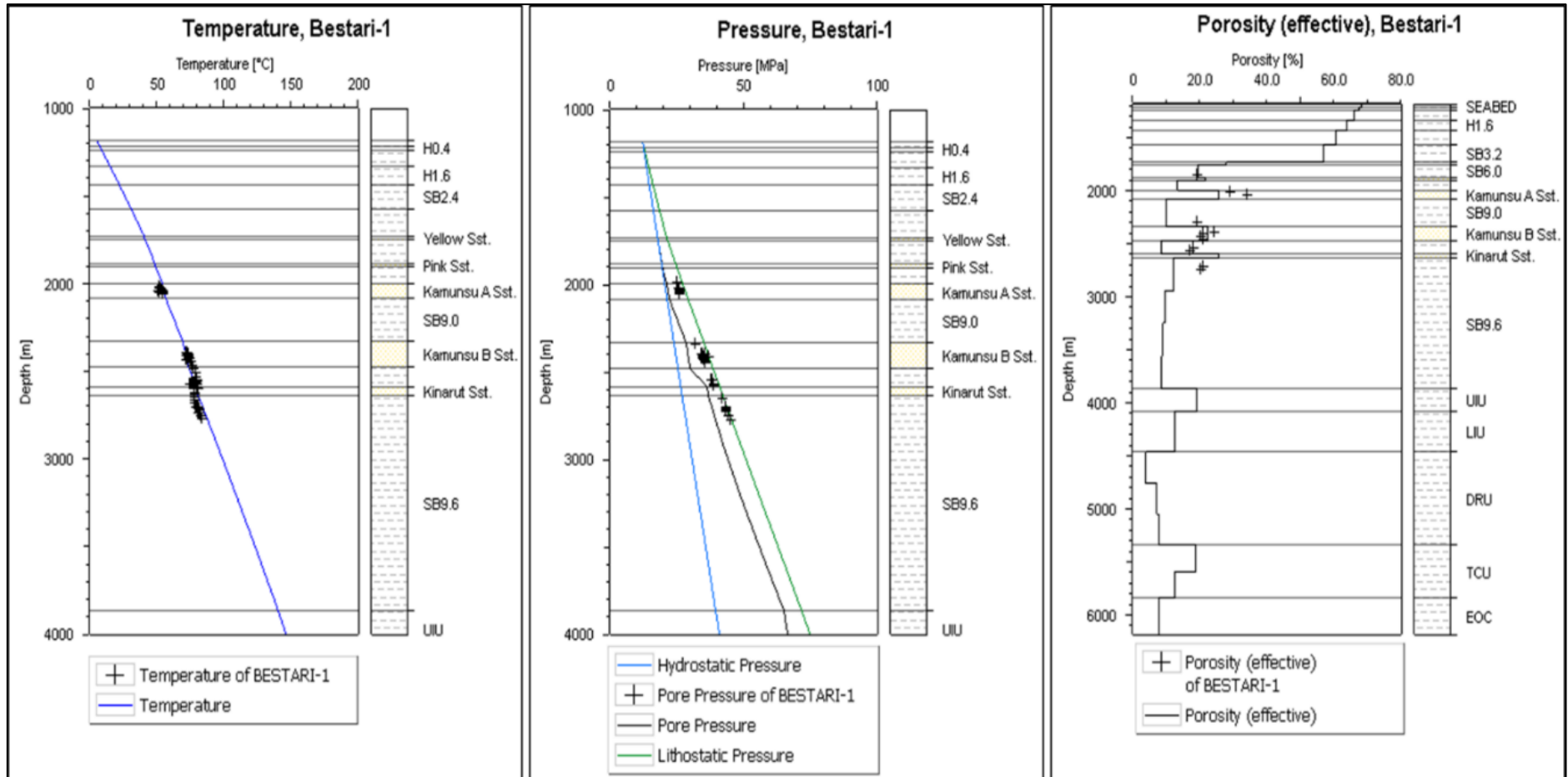


Figure 6-5: Model calibration for Bestari-1 well for the porosity, pressure, and temperature. The porosity calibration matches well with the model. However, even after optimization the pressure and temperature show a higher trend in the well as compared to the model.

Horizons	Age	Bestari-1		Bestari-2/ST1		Bestari-3		Limbayong-1ST1		Limbayong-2		Limbayong-3/ST1	
	(Ma)	Thick (m)	Lithology	Thick (m)	Lithology	Thick (m)	Lithology	Thick (m)	Lithology	Thick (m)	Lithology	Thick (m)	Lithology
Seabed	0	31	Shale	21	Shale	50	Shale	103	Shale	120	Shale	48	Shale
H0.4	0.4	30	Shale	46	Shale	52	Shale	189	Shale	188	Shale	136	Shale
H0.8	0.8	90	Sandy Sh.	167	Shale	225	Shale	204	Shale	213	Shale	200	Shale
H1.6	1.6	100	Sandy Sh.	216	Shale	163	Shale	300	Shale	276	Shale	262	Shale
SB2.4	2.4	140	Silty Sh.	150	Shale	111	Shale	150	Shale	157	Shale	121	Shale
SB3.2	3.2	161	Shale	176	Shale	133	Shale	106	Shale	99	Shale	142	Shale
Top Yellow	5.6	15	Silty Sst.	157	Silty Sh.	132	Shale	129	Shale	138	Shale	136	Shale
Base Yellow	6	133	Shale	133	Shale	114	Shale	122	Shale	152	Shale	114	Shale
Top Pink	8.6	23	Silty Sst.	223	Shaly Sst.	186	Shale	183	Shale	156	Shale	272	Sandy Sh.
Base Pink	8.7	91	Shale	209	Shale	151	Shale	175	Shale	160	Shale	265	Shale
Kamunsu A	8.8	87	Sandstone	116	Sandstone	95	Sandstone	149	Sandstone	67	Sandstone	130	Sandstone
Base Kamunsu A	9	246	Shale	194	Silty Sh.	226	Silty Sh.	141	Silty Sh.	171	Sandy Sh.	169	Sandy Sh.
Kamunsu B	9.2	147	Sandstone	274	Shaly Sst.	311	Sandy Sh.	149	Sandy Sh.	261	Sandy Sh.	426	Sandy Sh.
Base Kamunsu B	9.3	109	Shale	62	Shale	76	Shale	29	Shale	62	Shale	206	Shale
Kinarut	9.4	49	Sandstone	85	Sandstone	95	Sandstone	64	Sandstone	120	Sandstone	157	Sandstone
Base Kinarut	9.6	1217	Shale	996	Sandy Sh.	1089	Shale	432	Shale	482	Shale	222	Sandy Sh.
UIU	12	213	Shale	292	Shale	182		890	Sandstone	521	Shale	576	Shale

Table 6-2: Lithology type and respective thickness of the modelled layers for the 1D Basin Modelling input.

6.4.2 Pore pressure history and wireline analysis

During mechanical compaction, increasing effective stress pushes the grains closer together as water escapes from the pore space, reducing porosity and permeability. When water cannot escape fast enough to remain in hydrostatic equilibrium as burial proceeds, overpressure is said to be generated by disequilibrium compaction. The retention of excess water necessarily means that the porosity is greater than it would be if the pore water were in hydrostatic equilibrium.

To be able to recognise the occurrence of overpressure wireline log data and wireline log trends has been analysed for each of the wells using combination of deep resistivity, sonic, and density (Figure 6-6; Bowers 1994). The approach used in this study very much follows that of the work of Bowers (1995, 2001), Dutta (2002, 2016), Sargent et al. (2015) and Ramdhan et.al., (2017). Bowers (1994 and 2002) divided shale deformation behaviour by the formation stress history (Figure 6-7). Pore pressure data acquired by the drilled wells were used to calculate the vertical effective stress using the Terzaghi (1925) expression:

(Equation 2):

$$\text{Vertical effective stress } (\sigma^1) = \text{Lithostatic stress } (\sigma) - \text{Pore pressure (Pp)}$$

The first type is in non-decreasing effective stress states, with the sediment compaction, and their density, resistivity and sonic velocity asymptotically approach limits set by the properties of the sediment grains resulting of the normal compaction curve or referred as the virgin curve (Figure 6-8 and Figure 6-9).

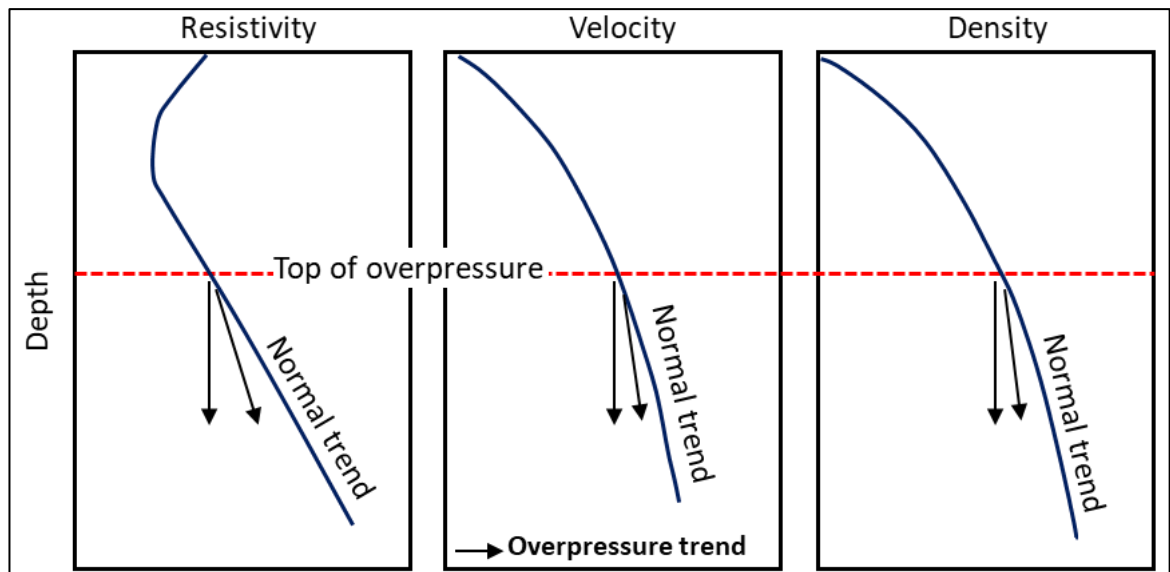


Figure 6-6: The wireline logs as indicators of the top of overpressure in wells (modified after Bowers, 1994).

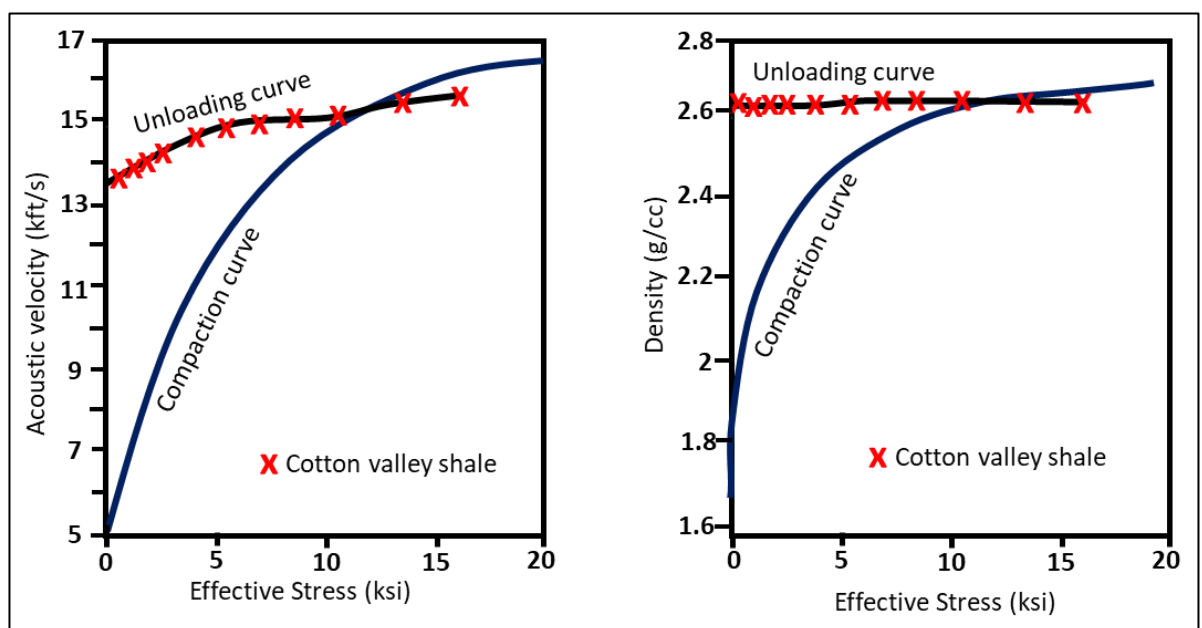


Figure 6-7: Response of formation acoustic velocity and density to effective stress (modified after Bowers, 1994). The same approach is used to analyse the dataset in the study area, to investigate the trend, and the possibility of generating overpressure other than disequilibrium compaction.

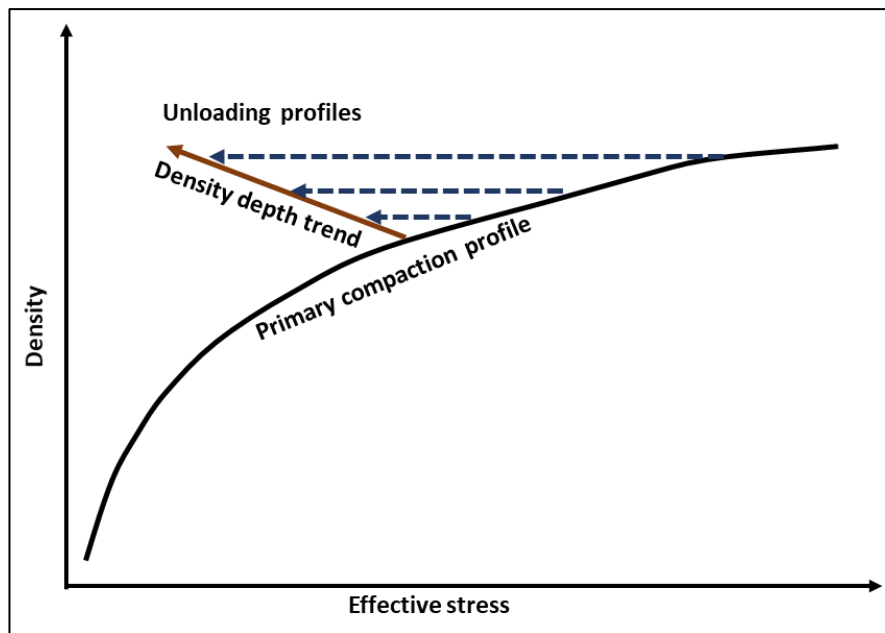


Figure 6-8: Density relationship with effective stress. Normal compaction or primary compaction profile, of the loading trend relationship shows increasing trend of effective stress to increase in density. The unloading profiles, however, display the opposite trend with increased density resulting in decreased effective stress. Multiple unloading profiles can potentially exist in one well (modified after Lahann et al., 2011).

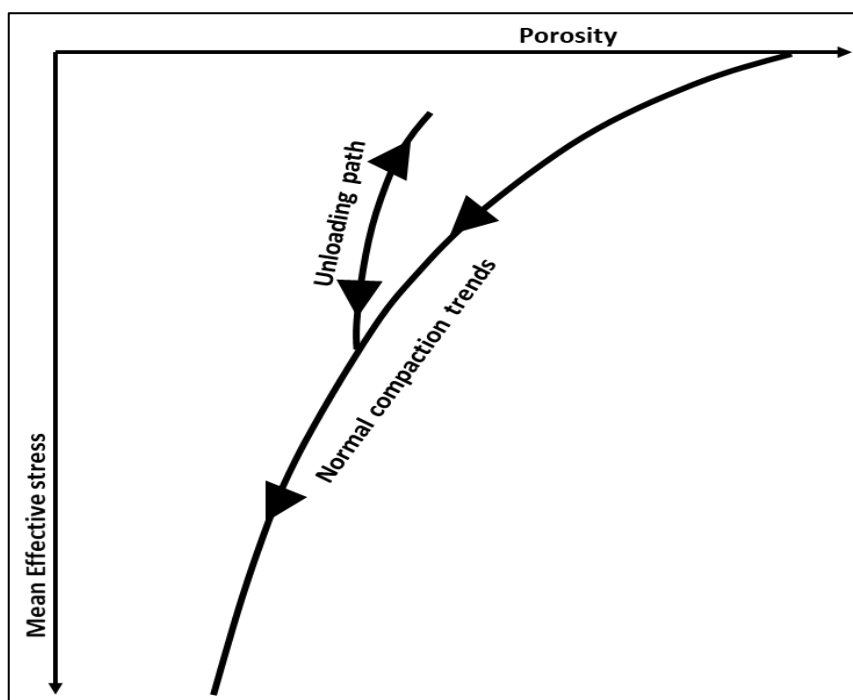


Figure 6-9: Relationship between porosity with effective stress (Modified after Gouly et al., 2012).

The second type is the states of effective stress reductions, with compaction is predominantly an inelastic process. Only small amount of elastic rebound occurs with the effective stress reduce or known as unloading. This relationship will be used to analyse the history of the deformation behaviour of the formation in the study area. This will lead to the assessment of possible anomaly in the effective stress respond towards the log respond as the area known to be merely in normal compaction trend due to the rapid burial due to the high sediment supplied by the deltaic fan from Middle Miocene towards the basin.

In this study, the method applied by using wireline log overpressure indicators, with shale resistivity, sonic velocity, and density data fall below their normal trends. Other than used to divide the pressure into clusters or regimes, the wireline logs trend will be used to be calibrated to the well correlation as the connectivity of the facies between wells might be indicated by the logs respond.

6.4.3 Petrography and sampling

Sidewall and conventional core sampling had been acquired in Bestari-1 and Bestari-2 wells. Thirteen core samples were collected from both wells from predominantly the sandy intervals (Table 6-3). Samples were analysed using transmitted-light microscopy on impregnated thin sections and modal analysis was undertaken on all samples to ascertain mineralogy (300 counts per section). Thin sections of these were produced for transmitted light microscopy and SEM analysis by Corelab, as well as rock chips for x-ray diffraction analysis.

All thin sections were highly polished to 30 μ m and coated with 30nm of carbon before analysis by a Hitachi SU-70 field emission scanning electron microscope (SEM) equipped with an energy-dispersive detector (EDS). Backscatter scanning electron microscopy of thin sections was conducted at acceleration voltages of 15 kV with a beam current of 0.6nA. The SEM-EDS assembly was used for rapid identification of chemical species and their orientation in the sample. Scanning electron microscopy was undertaken on selected samples, providing additional information on the pore-system geometry, authigenic mineralogy, and paragenetic relationships. The analysis was undertaken on gold palladium coated; freshly broken samples glued onto aluminium stubs with silver paint. Cathodoluminescence analysis was undertaken on selected thin sections using a Gata MonoCL system with a panchromatic imaging mode operated at 15kV. SEM–EDS was used for rapid identification of chemical species and orientation on the sample.

X-ray diffraction (XRD) analysis (semiquantitative bulk rock and clay fraction) was conducted by Corelab and has been used to identify the clay mineral quantities, composition and diagenetic alterations within the samples from both Bestari wells chosen for this study.

Well (Core type)	Sample	Depth (m):	Lithology:	Rock Classification (Folk 1980)
B1 (Sidewall Core)	1	2437.00	Sandstone	Feldspathic Litharenite
	2	2447.20	Argillaceous Sandstone	Feldspathic Litharenite
	3	2451.20	Argillaceous Sandstone	Feldspathic Litharenite
	4	2457.00	Siltstone	Feldspathic Litharenite
	5	2481.50	Sandstone	Feldspathic Litharenite
	6	2488.70	Argillaceous Sandstone	Feldspathic Litharenite
	7	2490.20	Silty Claystone	-
	8	2755.70	Sandstone	Feldspathic Litharenite
	9	2757.50	Sandstone	Feldspathic Litharenite
	10	2758.50	Sandstone	Feldspathic Litharenite
	11	2767.00	Argillaceous Siltstone	Litharenite
	12	2769.00	Slightly argillaceous Siltstone	Feldspathic Litharenite
	13	2771.20	Slightly argillaceous Siltstone	Feldspathic Litharenite
B2 (Conventional Core): Core 1	1	2010.24	Argillaceous Sandstone	Feldspathic Litharenite
	2	2013.56	Slightly argillaceous Sandstone	Feldspathic Litharenite
	3	2021.29	Sandstone	Feldspathic Litharenite
	4	2024.36	Sandstone	Sublitharenite
	5	2027.79	Sideritic Claystone	-
	6	2029.86	Sandstone	Sublitharenite
B2ST1 (Conventional Core): Core 2	7	2497.02	Slightly argillaceous Sandstone	Feldspathic Litharenite
	8	2501.29	Sandstone	Feldspathic Litharenite
	9	2503.12	Sandstone	Feldspathic Litharenite
	10	2506.18	Argillaceous Sandstone	Litharenite
	11	2507.08	Sandstone	Feldspathic Litharenite
	12	2508.30	Sandstone	Feldspathic Litharenite
	13	2510.44	Sandstone	Feldspathic Litharenite

Table 6-3: Samples from Bestari-1 and Bestari-2 wells were sampled for thin section, SEM, and XRD analyses by using side-wall core plugs and conventional core recovered from both wells.

6.5 Results

6.5.1 Well correlation and formation pressures

Correlating the horizons in the deep-water fold-and-thrust belt is never an easy task due to the diachronous submarine fan facies deposition. Well location is critical for correlation as proven by each well drilled in the Menawan and Lawa growths folds (Figure 6-2) and demonstrated to be unexpectedly to be shale prone as a shelf-slope by-pass depositional setting (Jong et al., 2016). Sand to sand correlation usually leads to correlation between different sand bodies due to simplification of the modelling of facies distribution. Furthermore, it has been demonstrated that deep-water sand delivery can occur during any stage of relative sea level position and across a large range of values of rate of relative sea-level change (see Harris et al., 2018).

Increased uncertainty with correlation of sand-bodies is also contributed to by the location of the wells drilled in the deep-water fold belt. Many wells drilled in NW Borneo to date have targeted the crestal parts of the growth anticlines. This results in a very limited lateral distribution across the growth anticlines for seismic calibration and facies correlation. As mentioned by Jong et. al., (2016), the seismic image quality over the large anticlinal crest commonly deteriorates due to steep dips, uniform shale core lithologies and common occurrence of shallow gas, compounding the correlation of sand bodies further in these regions.

To address the high uncertainties in the analysis for sand-body distribution and connection due to their complexity and heterogeneity the use of formation pressures has been used (Figure 6-10). The clusters of the sand bodies formation pressure compared well with the well correlations that were tentatively established (Figure 6-11). The use of pressure data can be used directly to reduce stratigraphic uncertainty and establish a new channel sand-body correlation strategy.

The sand body correlation based on the formation pressure seems can be well constrained for the well located on the Limbayong structure, as the pressure increment, and overpressure trend is almost at the same magnitude. The trend at Limbayong, correlates well with the trend observed at Bestari-3 well, at least until Kamunsu A level with the pressure increase with depth and jump significantly in every deeper sand package. However, for Bestari fold, the trend is more complicated as the pressure trend illustrating particularly different trends for Kamunsu A and Kamunsu B submarine fan sand facies. Bestari-1 well shows an increasing trend of overpressure, Bestari-2 has the consistent trend parallel with the hydrostatic and Bestari-3 is highly overpressure but decreases with depth for each of the pressure regimes. The formation pressure is a reflection of fluids in the formation as the Bestari-2, Bestari-2ST1 and Bestari-2ST2 wells are proven to be water bearing, based on the pressure plot gradient and formation fluid samples from the borehole. Apart from the different in the fluid filling up the formation, the pore pressure is different between the sand bodies in between the wells shows possible compartmentalisation between the sand bodies.

The correlation of the sand body connectivity between the wells by using the pressure magnitude and trend as shown by the dashed trendlines proven to be beneficial in

establishing the lateral connectivity between the well. Bestari-2/ST1 well shows pressure trend parallel with the hydrostatic gradient (0.43 psi/ft) throughout the wells from Pink Sandstone and going deeper at Kamunsu A and Kamunsu B sandstones. The pressure different at Pink sandstone is roughly around 50 psia from Bestari-1 and Bestari-3 thus make it possibly laterally connected throughout the structure. This take into consideration the thickness of the Pink sandstone is more than 1000m in all the wells. As of the other sand bodies in Bestari structure hardly sharing the same pressure system due to the big difference between each other.

The usage of pressure data in correlation is well known for faulted compartmentalised reservoirs, but is not commonly used in identifying compartmentalisation due to facies variation. This is very useful to further understand the spatial and temporal distribution of the reservoir sandstones (Figure 6-12).

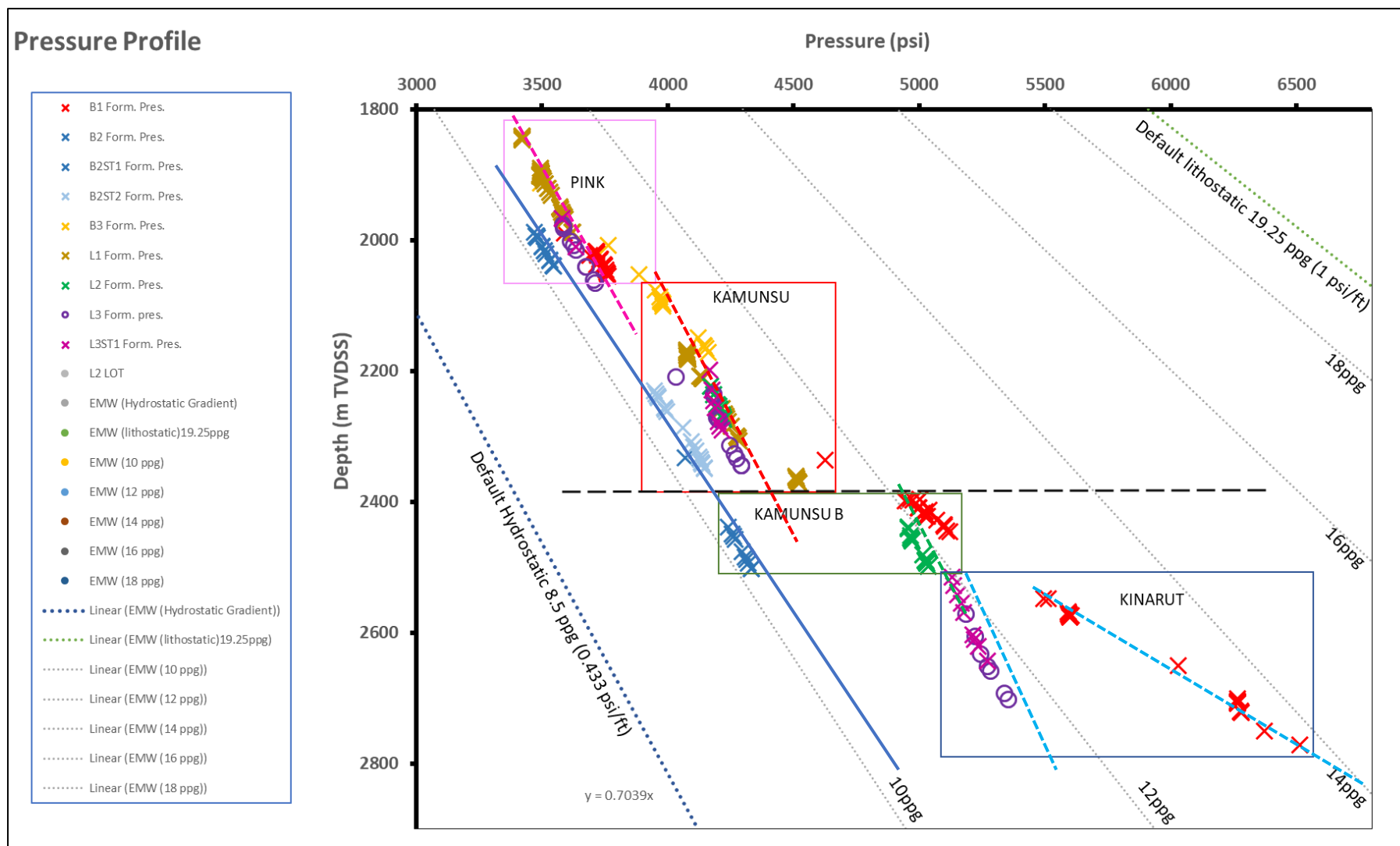


Figure 6-10: Formation pressure divided into reservoirs (submarine fan systems).

Open



Figure 6-11: Well correlation combining well log trends, seismic interpretation, biostratigraphy, and formation pressure data.

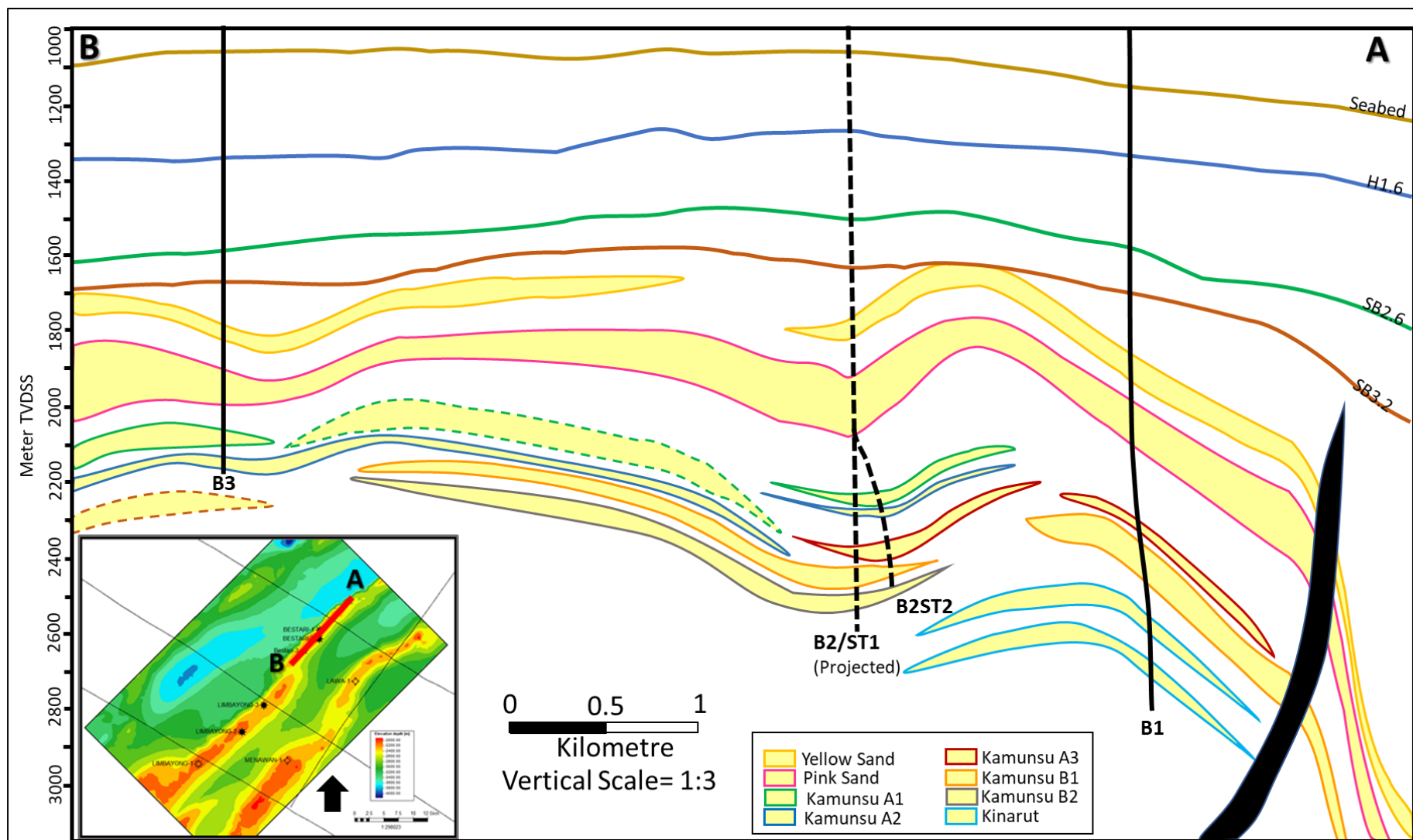


Figure 6-12: Schematic cross-section of the reservoir spatial and temporal distribution.

Open

6.5.2 Burial history and overpressure evolution

6.5.2.1 *Burial History*

Burial history of the wells in each structure shows rapid burial from 9 Ma of the reservoir indicating the deposition into deeper parts of the basin was associated with rapid subsidence and maintenance of high sediment supplies direct from the Shelf and slope break. From 8.5 Ma the burial rate changed to an average of 200 to 250 meters per 1 Ma (Figure 6-13).

Both Limbayong and Bestari show generally the same burial history and could be divided by the three-phase development of the fold-thrust structures, with a change from tectonic towards gravitational controls on the structuration and sediment deposition. This can be easily distinguished by the abrupt change of the steep burial history trend in Middle Miocene and Late Miocene.

The difference between the folds is mainly the growth rate, which directly affected the water depth and the sediment accommodation space during submarine fan deposition. Limbayong is consistently in deeper water depth as compared to the Bestari fold from the Eocene until late Miocene. This will lead to the difference in syn-kinematic sediment deposition onlapping the folds.

Limbayong structures will likely have experienced the deep-water turbidite deposition on the structure, and might have overflowed towards the deeper part of the basin. This might explain the proven Kikeh Field further outboard from the shelf and distal from

Limbayong. This will lower the risk of reservoir presence or distribution towards the crest of the structure as compared to Bestari fold which is a greater magnitude structure compared to Limbayong. This might cause the deltaic fan to be distributed around the structure towards the flank and along the synclinal valley and canyon between the folds. This will probably lead towards the different quality of reservoir of the two folds, which might to be shaly and mud rich in Bestari as compared to Limbayong.

6.5.2.2 Pore fluid pressure generation and histories

The data show generally a similarity of the pressure history of the wells in the Bestari and Limbayong structures in the turbidite formation. The only obvious exception is the higher overpressure of Bestari-1 well at Kinarut Sandstone level (Figure 6-14). Generally, even though the pressure increased over time, there is strong evidence of disequilibrium compaction because of rapid burial of sediment since Middle Miocene. However, for Bestari-1 well, pressure ramp-up occurs from ~2 Ma ago. This increase in pressure can be attributed to the location of the Bestari-1 is closest to the fault (Figure 6-14).

There is potential for high pore fluid pressures to be generated at greater depths associated with the mobile shale of the Setap Formation (Figure 6 13 and 5-30 in Chapter 5) and gas generation. The Setap Formation fulfils the typical role of mobile shales in large deltaic provinces: it forms the overpressured fine-grained unit at the base of a thick, rapidly prograding sequence of shelfal, shallow marine to continental sediments. In response to sediment loading the shale underwent viscous flow creating growth faults, overpressured shale intrusions into the overburden, and toe folds and

thrusts. It is these growth faults that could act as a conduit for pressure transfer (e.g., Waples et al., 1998; Moreley 2003). Therefore, further assessment of the overpressure in Bestari-1 well needs to consider the possibility of lateral transfer of pressure from deeper levels with relatively very high overpressure especially at Kamunsu B and Kinarut reservoirs. This form of overpressure cannot be identified by well logs, which makes the pore pressure prediction more complex.

The additional pressure in the Bestari-1 well and other wells in the study area could be explained due to lateral pressure transfer. For the deeper level, i.e., Kinarut reservoir, comparison between Bestari-1 and Limbayong-1/ST1 is different, with again possible fluid transfer caused by unloading and diagenesis, compared to Limbayong-1/ST1 that displays a hydrostatic parallel trend and disequilibrium compaction can be attributed to the pressure generation.

6.5.2.3 Temperature history

Generally, both wells show a similar trend of low temperature of ~30 - 50 °C at the depth range of 500 to 1000 m below seabed until the Kamunsu A reservoir level (Figure 6-14). However, going deeper to Kamunsu-B and Kinarut reservoirs, Bestari-1 shows slightly higher temperature from the end of Late Miocene to Recent. Temperature-driven changes in grain-to-grain contact relationship, will have a range of effects in pore-pressure, as outlined by Swarbick (2012) including (1) Cement precipitation, reducing porosity, (2) Rock grains dissolution, reducing porosity, (3) Rock grains weakening, ductile behaviour, (4) Mineral transformation, smectite and kaolinite to illite.

In this study possible clay mineral transformations, as highest temperature recorded in the wells, at the reservoir level only in the range of between 60 - 80 °C which is too low for cement precipitation, grain dissolution and weakening.

The mineral transformation is kinetically controlled and occurring over temperatures in the range 80 - 150 °C. Therefore, there is small possibility that clay mineral transformation has added to the overall overpressure encountered in the Kamunsu B and Kinarut reservoirs of the Bestari-1.

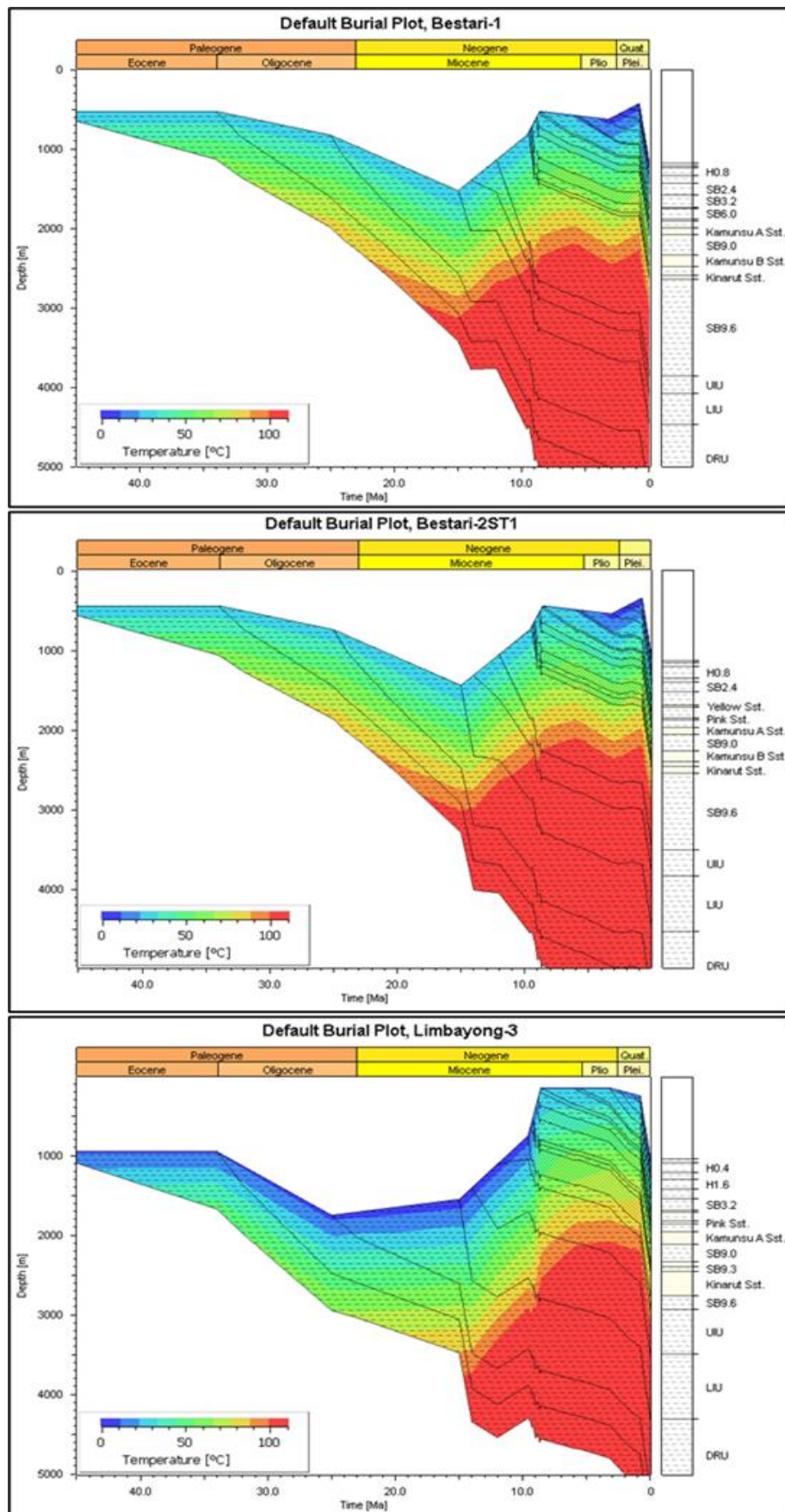


Figure 6-13: Burial history temperature plot for (a) Bestari-1 and (b) L3. Each model shows the folds have three phases of evolutions with the Limbayong structure seeming to be in the deeper part of the basin from the Eocene to Late Miocene. Both structures show temperature history of less than 100 °C for the reservoir level.

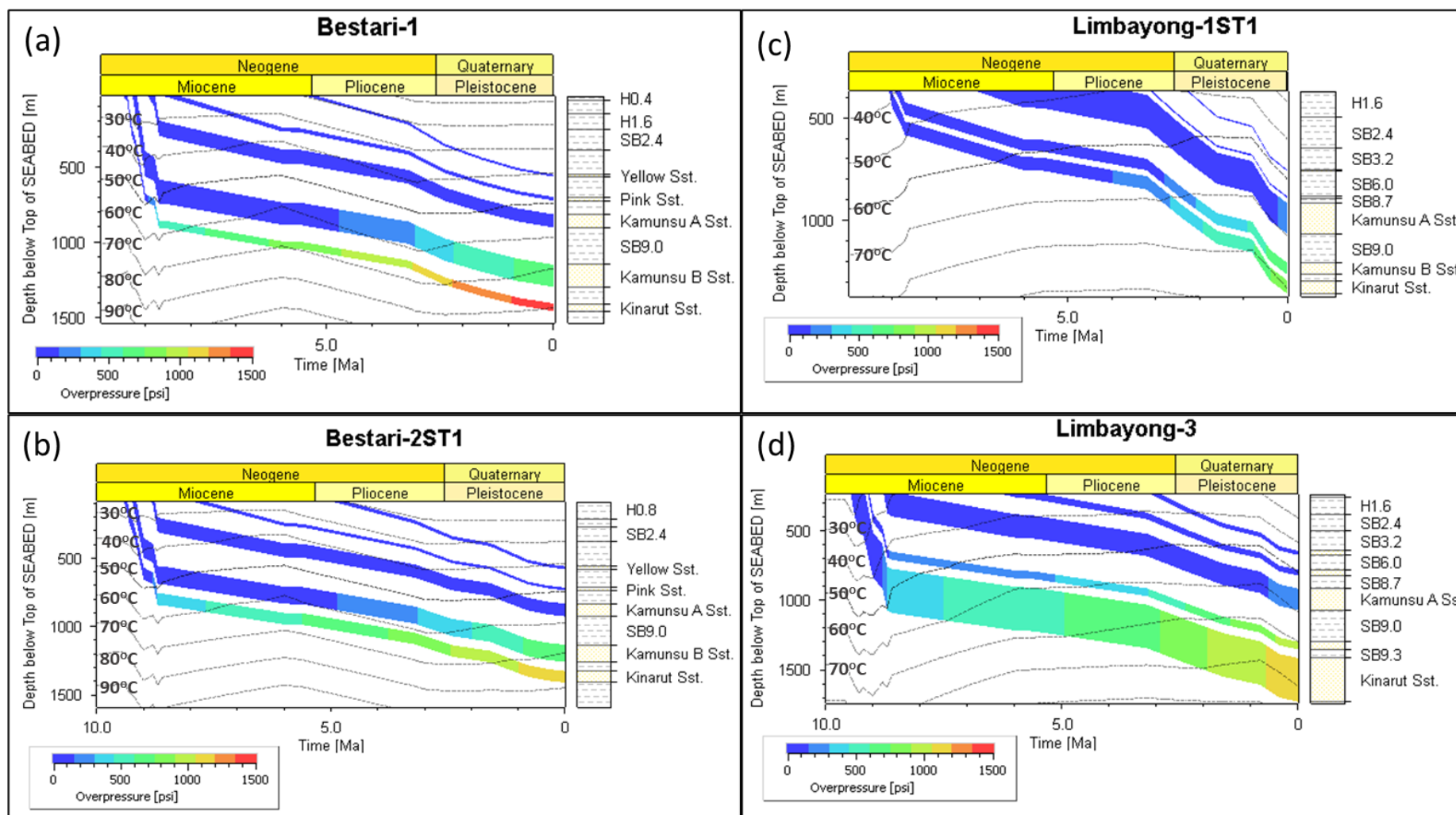


Figure 6-14: Pressure and temperature (isoline) history of wells in the Bestari and Limbayong structures for the submarine fan reservoirs.

6.5.3 Overpressure zones

All wells in both Bestari and Limbayong structures are overpressured especially at the Kamunsu and Kinarut reservoirs with different magnitudes (700, 1000 and 1500 psia) and profiles (see Figure 6-15). The pressure data set consists of three different trends of pressure gradient, (1) hydrostatic parallel trend, (2) lithostatic parallel gradient and (3) pressure gradient increasing trend towards lithostatic in the wells. The pressure plot (Figure 6-10) and overpressure trend plot for each well is shown in Figure 6-15. This enables the overpressure to be divided into groups: (1) hydrostatic parallel trend showing almost constant overpressure of ~700 psia for most of the wells at the shallower depth, which correlate to the Pink reservoir. At deeper level of Kamunsu A and B, only Bestari-2ST1 and Bestari-2ST2 maintaining the trend with other wells show increment of overpressure. (2) lithostatic parallel trend with constant overpressure of ~1000 psia mainly for Kamunsu A and ~1500 psia Kamunsu B and Kinarut reservoirs. (3) The increasing trend only observed in Bestari-1 well, with increasing overpressure value for the Kinarut reservoirs from ~2000 psia at 2550 m to almost ~2500 psia at 2750 m. These clusters or groups of geopressured are further supported by the wireline log - depth plots (see Figure 6-16). The example, Bestari-1 and Bestari-2 are distinctively different in the magnitude of overpressure and pressure trend but equally illustrate the same trend with resistivity, sonic velocity, and density logs. In Bestari-1, the changes of the pressure regimes from Group 1 to Group 3 could be pick up by the trend changes display by the wireline logs. Whilst for Bestari-2, it is hardly any changes from the shallower depth going deeper except for slight changes around 2250 m, which might cause by non-pressure related mechanism. The depth of the trend changes from the logs together with the overpressure and pressure Group

depth, will be used in defining of possible occurrence of different overpressure mechanism in the well.

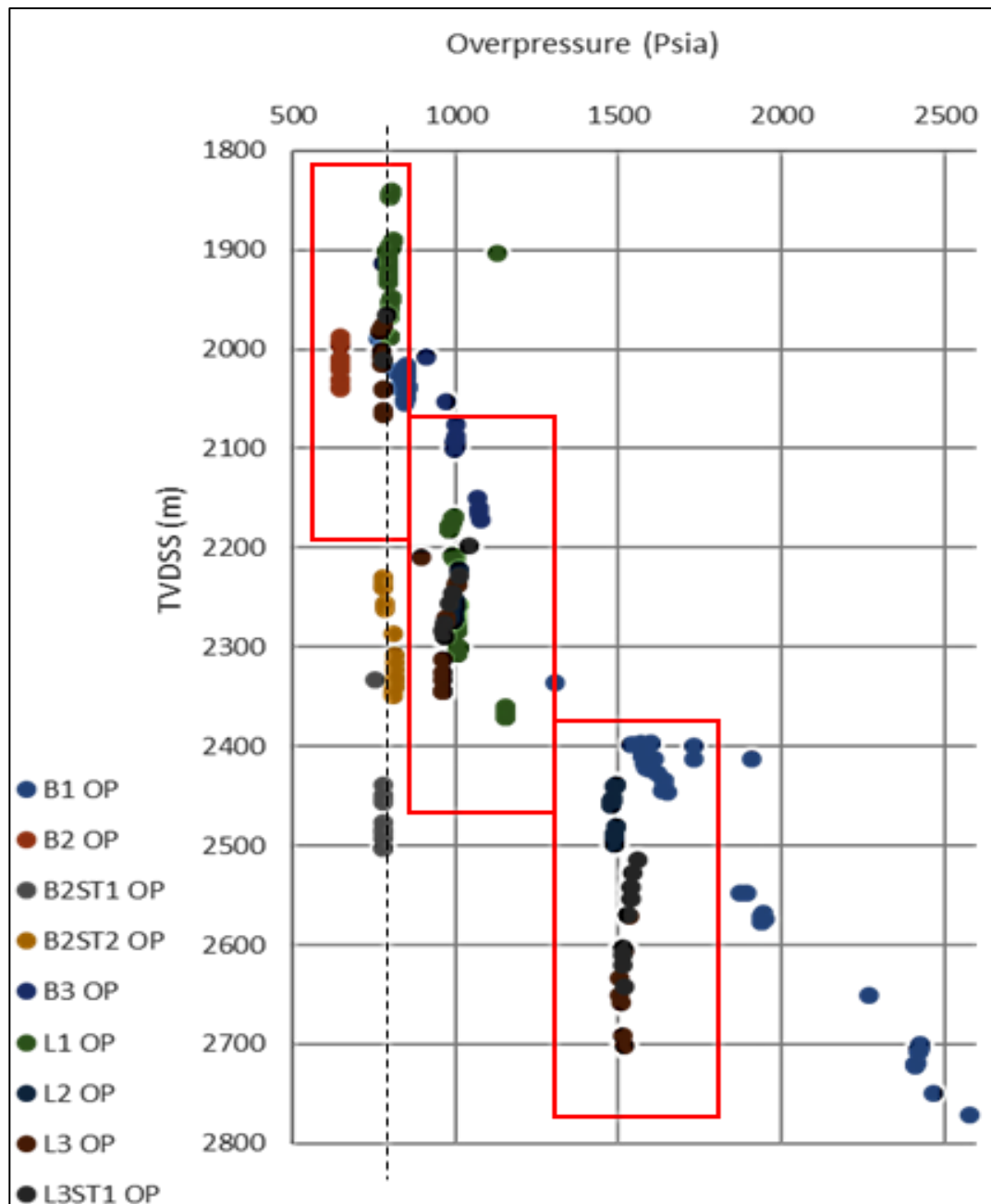


Figure 6-15: Overpressure trend of the wells in both folds generally shows an increase with depth, with an exceptional trend of the Bestari-2/ST1/ST2 holes. Overpressure ramp-up from the Bestari-2/ST1/ST2 trend around 200 psia at 2200 m TVDSS and a significant 700 psia increment at 2400 m TVDSS. The Bestari-1 well, however, displays exceptional continuous increment of overpressure through depth as compared to the other wells.

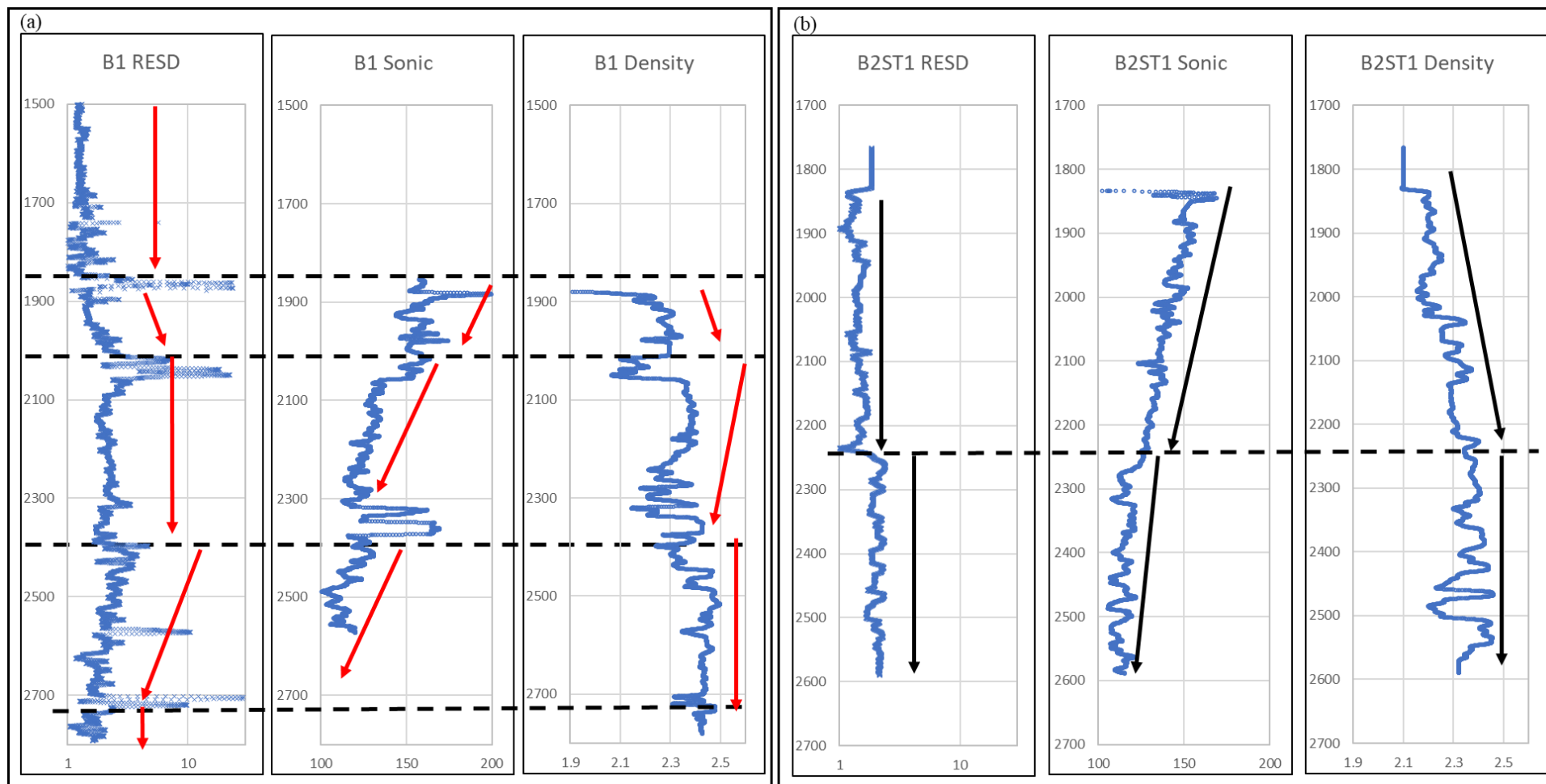


Figure 6-16: Bestari-1 well logs (a) show changes in at least three depths in all the logs whilst Bestari-2/ST1/ST2 well logs (b) only show two possible trends throughout the well.

6.5.4 NW Borneo DWFTB Overpressure mechanism

6.5.4.1 Disequilibrium compaction

Relationship of vertical effective stress with compressional velocity and density of sediment used in identifying the cause of overpressure in the area as Bowers (1994) suggested normal compaction trend or the disequilibrium compaction will be reflected by the loading curve trends, whilst others such as load transfer (Tingay et al., 2009) or fluid expansion (Bowers 2002; Yassir et al., 1996), clay mineral transformation (Figure 6-8; Lahann et al., 2011) and tectonic compression (Yassir et al., 2002) are reflected by the unloading curve trends. Generally, the disequilibrium compaction is the obvious mechanism for overpressure generation for all the wells in both Bestari and Limbayong folds as supported by compressional velocity and density plot against vertical effective stress (Figure 6-17a and b). This is further supported by the compressional velocity plot against the density value of sediment (Figure 6-17c). A faster velocity trend could be seen with an increase of effective stress and relative increase of sediment density. The disequilibrium compaction is commonly expected for the deltaic fan depositional environment in fold-thrust belt setting as the rapid sedimentation filling up the NW Borneo deep-water offshore average rate was at 200 to 250 m/Ma. This gives a total of ~2.5 km of sediment in less than 9 Ma. Apart from the loading trends of the disequilibrium compaction, unloading trend of relatively very small increment of compressional velocity and almost constant density with decrease in vertical effective stress can be seen for Bestari-1 well. This will need further analyses on the possible unloading mechanism, but due to the pressure trends appears to represent a mix of load transfer (from deeper depths) and fluid expansion (from gas charging) most likely.

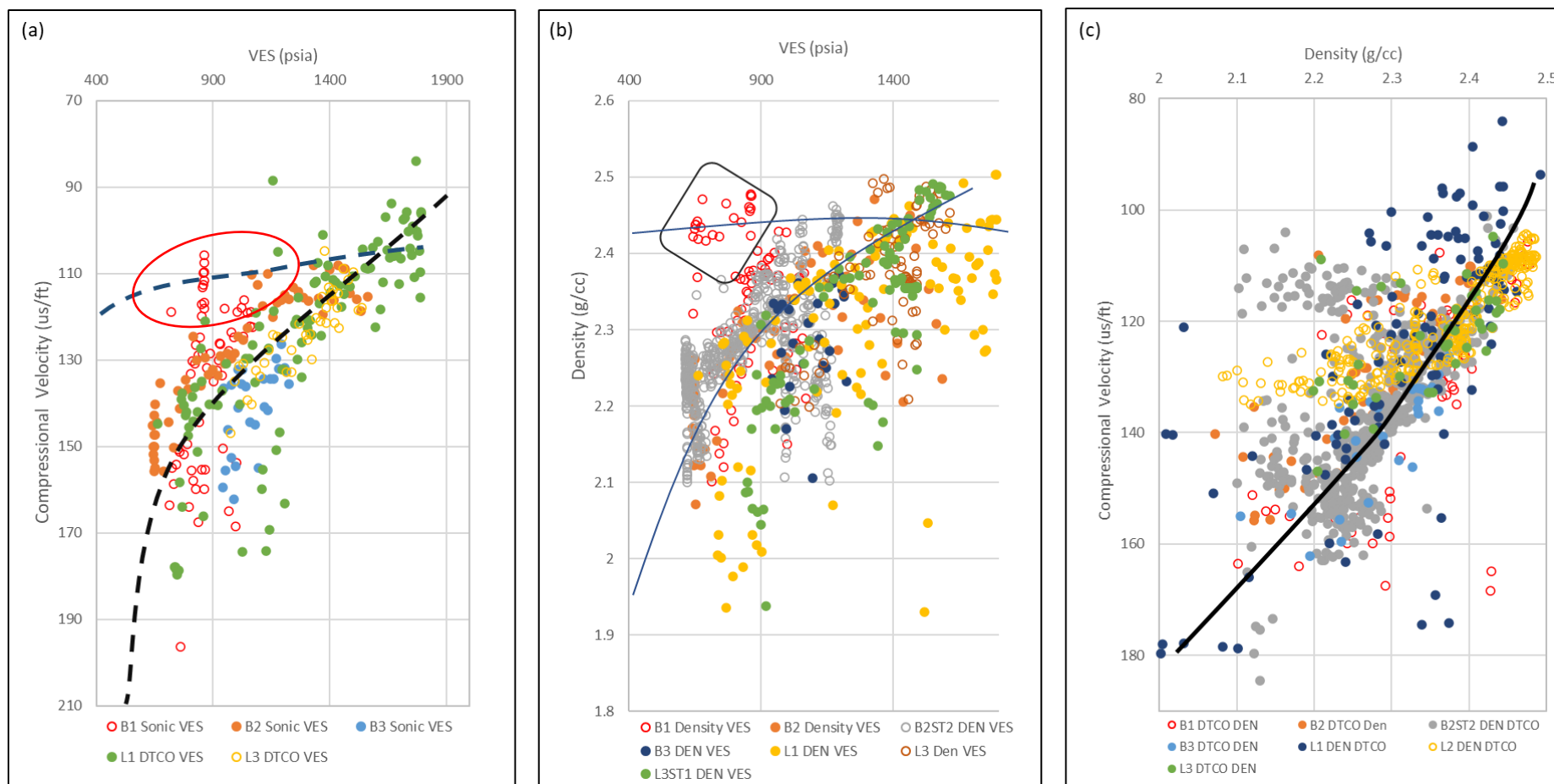


Figure 6-17: Relationship between VES and acoustic/density of different overpressure mechanism and the acoustic velocity-density cross plot shows mainly a loading trend of disequilibrium compaction and an unloading trend in the Bestari-1 well.

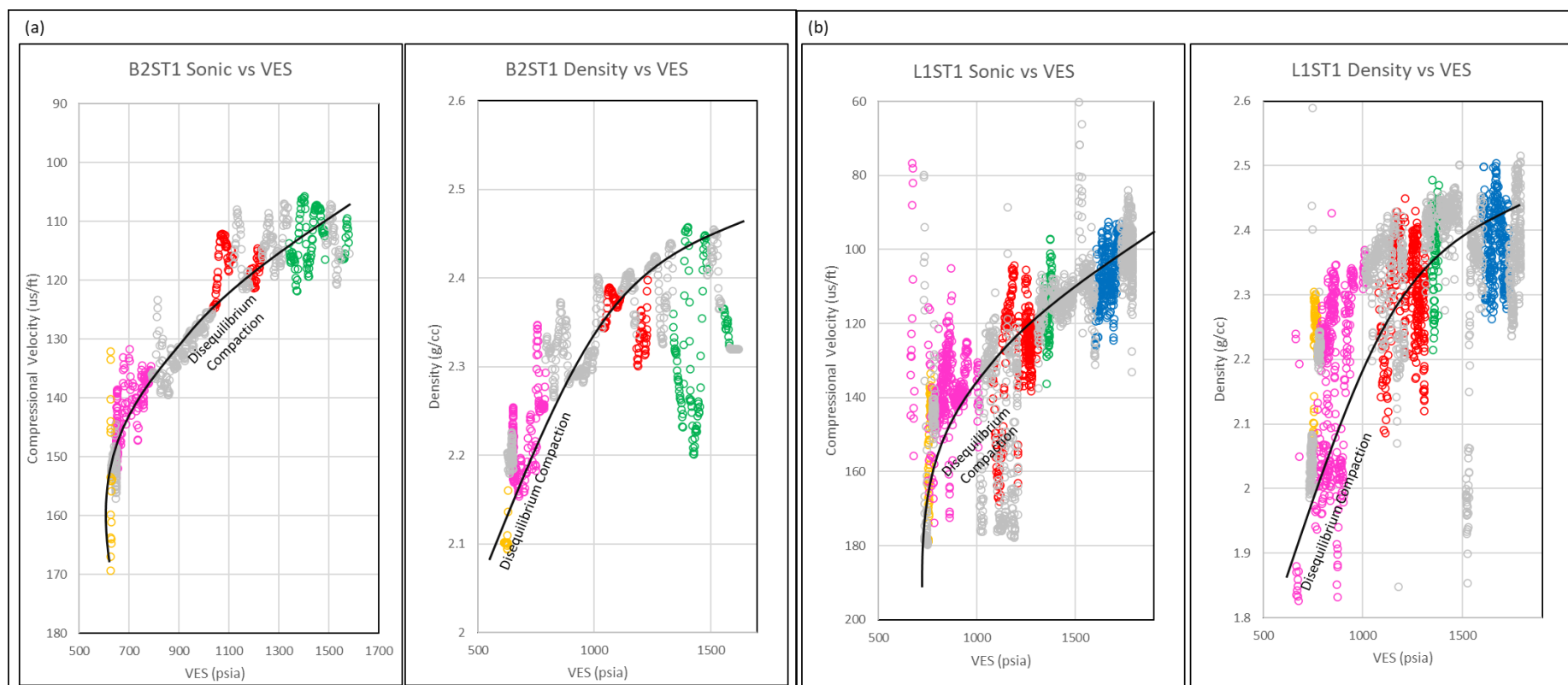


Figure 6-18: Compressional velocity and density plots against vertical effective stress segregated by reservoirs for Bestari-2/ST1/ST2 and Limbayong-1ST1. Both wells are representative of wells in the Bestari and Limbayong structures, except for the Bestari-1 well, and show a disequilibrium compaction trend without any unloading trends as the overpressure generation mechanism.

6.5.4.2 Unloading trends

All the wells in the study area except for Bestari-1 well, indicate no unloading trend could be established apart from the disequilibrium compaction. This is shown by the compressional velocity and density log plots against the vertical effective stress (Figure 6-18).

In the NW Borneo fold-and-thrust belt, as the well drilled mostly at the crestal part of the structures, the possibility of lateral transfer causing relatively very high and increasing trend of overpressure as seen in Bestari-1 is very likely. However, it is also worth considering other possible overpressure generating mechanisms for the unloading trend.

Interesting trend of relative porosity ranges between 15% to 25% in relation to low VES range between 400 psia to 600 psia could be seen from Bestari-1 well for the Kinarut and Kamunsu B reservoirs (Figure 6-19a). The porosity ranges are higher as compared to some of the Pink at much shallower depth. The black filled green and blue circle in Figure 6-19a is a representative of the samples analysed for petrographic and Scanning Electron Microscopy for any possible clay mineral transformation.

The compressional velocity and density plots versus vertical effective stress (Figure 6-19b and c), display both disequilibrium compaction trends for the shallower formation from Yellow, Pink, and upper part of Kamunsu B. The unloading trend could be seen at compressional velocity ~ 120 us/ft and density ~ 2.3 to ~ 2.5 g/cc, with vertical effective stress between ~ 600 to 700 psia. This unloading trend mainly at

Kinarut and Kamunsu B reservoir level. Even though the porosity trend is higher from the regional porosity trend, it is a similar trend with the disequilibrium compaction trend at shallower depths. This might indicate the possible leaking of the shale formation on top of the reservoirs as the increase in pressure due to the lateral migration exceeded the sealing capacity.

1. Lateral transfer

Lateral transfer is a migration of pressure through fluid or gas from another high overpressure zone up-dip through conduit as faults, dipping sand enclosed in shale (Bowers, 2002; Yardley and Swarbrick, 2000). High pore pressures closing the fracture pressure can be generate for the overpressure lateral transfer especially with huge gas column (Bowers, 2002). Bestari-1 well location at the front limb of the thrust-fold, relative around 1 km from the active thrust fault, make it to very likely influence by lateral transfer of fluids or gas from deeper shale formation through the fault as main conduit.

The Setap shale, underneath the Mid Miocene sequence known to be very high pressure proven by drilling exploration in the inboard part of NW Borneo offshore. This might explain the high-pressure anomaly of increasing towards the lithostatic and fracture gradient especially at the Kamunsu B and Kinarut level.

The gas seepage above the crestal part of the structure (Figure 6-23), might as well explain the possible effect of lateral transfer, as the pressure is increasingly high to the level of the shale fracture pressure.

2. Fluid expansion

Heating, hydrocarbon maturation, migration and expulsion could be generating overpressure due to sediment matrix constraining the pore fluid to increase the volume, known as fluid expansions (Bowers, 1995, 2002). Fluid expansions tend to decrease the effective stress as burial continues (Bowers, 2002).

In the case of the Bestari-1 well, as of the triggering factors for the fluid expansion mechanism involving hydrocarbon maturing which require temperature at least at 95 °C (Pepper and Corvi, 1993) make this factor to be very unlikely as the temperature recorded in Bestari-1 is lower than 90 °C.

3. Clay mineral transformation

The Bestari-1 well density plot against vertical effective stress will be the main reference to discuss the possibility of clay mineral transformation of either smectite to illite or kaolinite to illite in the unloading trend of Kinarut sandstone level, the deepest reservoir penetrated by this well.

The density -vertical effective stress of Bestari-1 well (Figure 6-19c) shows similarity with the primary compaction and the unloading profile by Lahan et al., 2011 (Figure 6-8). At least three level of unloading curve could be established at the Kinarut sandstone level with a possible illitic compaction trend as suggested by Lahann et al. (2001)., as the model suggested the increased in density with velocity reduction is not consistent with fluid expansion mechanism.

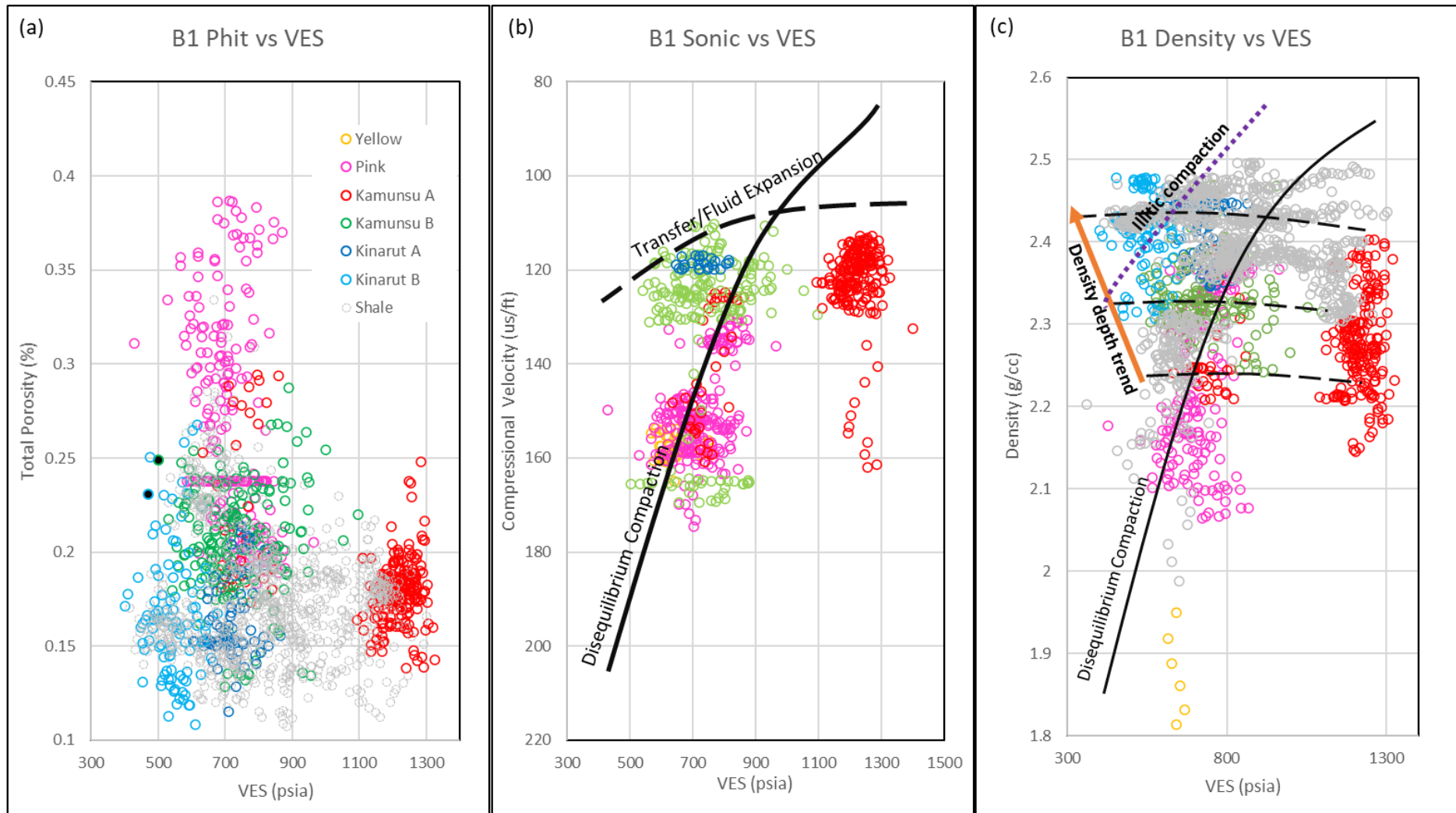


Figure 6-19: Bestari-1 well porosity, compressional velocity and density plots against vertical effective stress, showing both disequilibrium compaction and unloading curve.

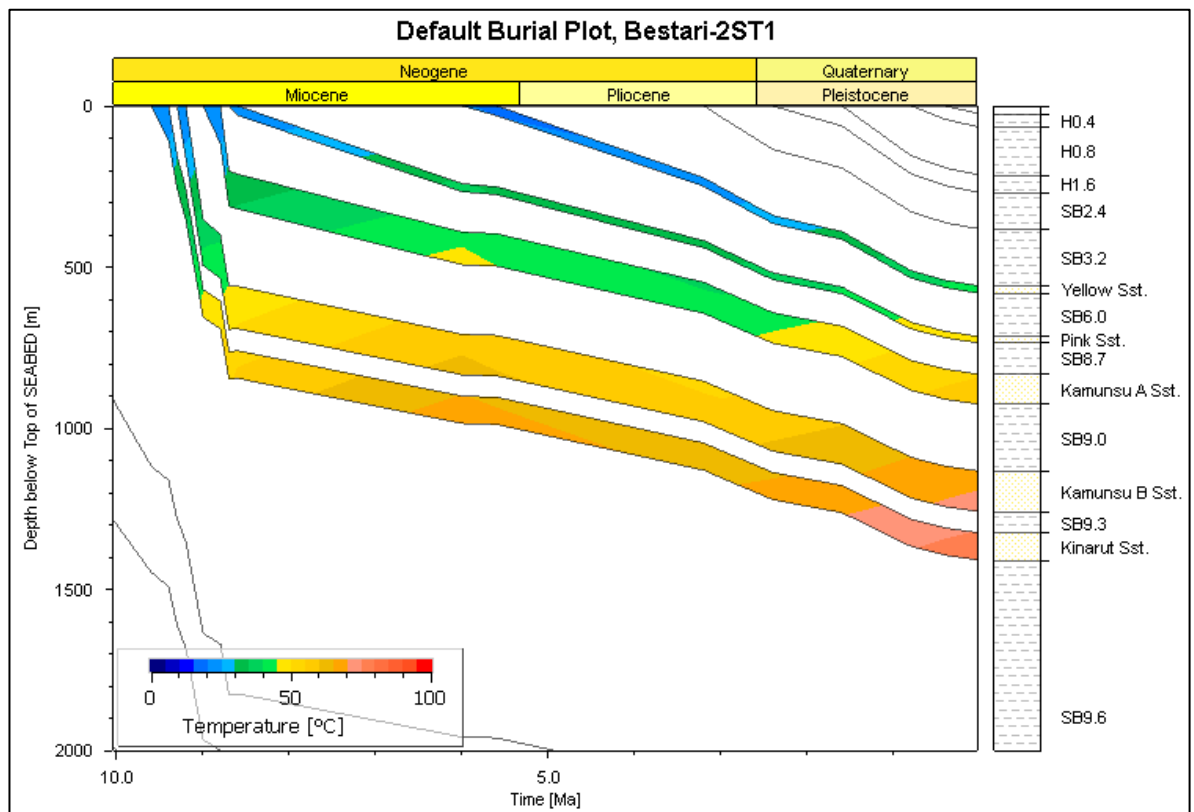
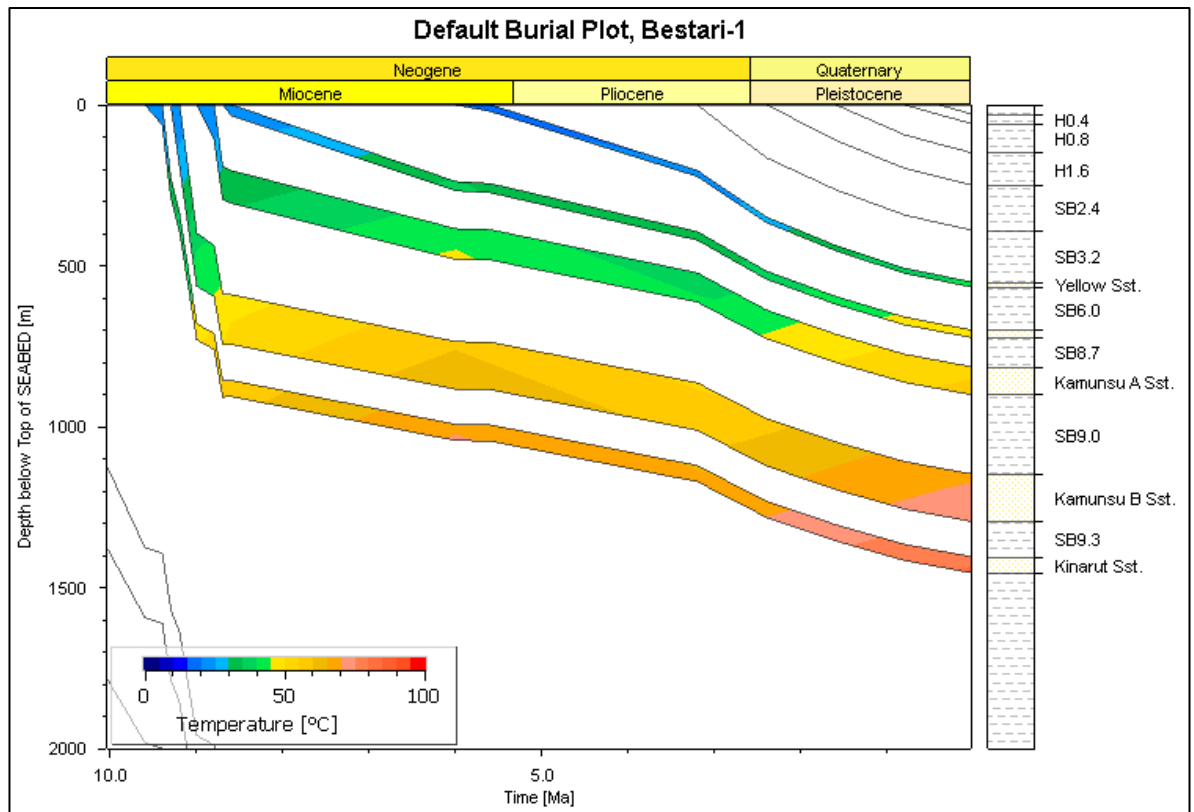


Figure 6-20: Temperature history of Bestari-1 and Bestari-2/ST1/ST2 wells for the deltaic fan reservoirs.

As shown by the Kinarut sandstone level at Bestari-1 well, the velocity is reduced with reduction of vertical effective stress and slightly increased in density, align with the density depth trend (Figure 6-19c). increased in density and stress coupled with velocity reduction may be due to illite formation (Lahann et al., 2011).

Other factors to be seriously considered for clay transformation is the temperature of the Kinarut sandstone. At the depth of ~1400 m from seabed, the temperature is hardly reach 90 °C (Figure 6-14 and Figure 6-20). Diagenetic transformation of clay mineral especially smectite to illite, starting at temperatures around 65 °C, and kaolinite to illite starting at around 120 °C (Goultly et al.,2012; Giorgetti et al.,2000; Nadeau et al., 2002). Therefore, there is a possibility of mineral transformation from smectite to illite in Bestari-1 well.

Petrography, Scanning Electron Microscopy (SEM) and X-ray Powder Diffraction (XRD) analyses for the deltaic fan's reservoirs sample from Bestari-1 and Bestari-2/ST1/ST2 wells (Figure 6-21 and Figure 6-22) being look into details to see if there is any evidence of any clay mineral transformation, especially smectite to illite in any of the sample especially for the Kinarut sandstone in Bestari-1.

The sample from the shallower formation, which now know to be most-likely only influence by burial of disequilibrium compaction, will be used as to compare the percentage of the clay mineral and the transformation. Two samples from Bestari-1 well, each from Kamunsu B (Figure 6-21b) and Kinarut sandstone (Figure 6-21c) level, and two samples from Bestari-2/ST1/ST2 from each Pink (Figure 6-22b) and Kamunsu B (Figure 6-22c) sandstone chosen for this purpose.

The sample number 9 from Bestari-1 well, at 2704 m TVDSS the deepest sample available from both Bestari and Limbayong folds, pick at Kinarut sandstone with low VES of 472 psia and porosity of 23%. The sample is sandstone with feldspathic litharenite with moderate sorting and fine sand mean grain size of 0.14 mm. Quartz is dominant mineral with 84.7% of the total sample from XRD analyses, follows by Plagioclase 2.9%, K-Feldspar 1.5%, Calcite 1.2%, Pyrite 0.6% and clay mineral 9.2%. The clay mineral consists of 2.8% illite/smectite, 3.7% illite and mica, 1% kaolinite and 1.7% chlorite. There is evidence of smectite-illite transformation as it is only left with 20-30% of smectite left in the total of illite/smectite.

As for sample number 4 at the depth of 2414 m TVDSS from Bestari-1, the sample pick from Kamunsu B level. It is classified as siltstone of feldspathic litharenite with 0.06 mm grain size in moderate sorting. Total quartz in the sample is 81.46%, 6.4 feldspar, with various lithic fragment 0.6% and total clay mineral of 11.6% from XRD analyses. A total of 3.2% illite/smectite, 5.3% illite and mica, 1.2% kaolinite and 1.8% chlorite. Similar with the Kinarut sample, the percentage of smectite in the lump illite/smectite is 20-30%.

As for Bestari-2/ST1 well sample, the deepest was acquired from Kamunsu B at the depth of 2483 m TVDSS with 30% porosity and 1400 psia vertical effective stress. The second sample is pick from the Pink sandstone at the depth of 1983 m TVDSS with porosity of 30% and VES of 700 psia. The Kamunsu B sample, a sandstone with feldspathic litharenite classification, 0.09 mm very fine sand grain and moderately sorting. XRD analyses give a total of 54.2% quartz, 7.9% feldspar, 0.6 siderite and total clay of 35.9%. The clay consists of 15% illite/smectite, 15.4%

illite and Mica, 2.3% kaolinite and 3.3% chlorite. 20-25% smectite identified from the illite/smectite. As there is no XRD analyses performed on the Pink, the mineralogy percentage was acquired from petrography point-counting. The quartz total in 44.4%, 11.2% feldspar, 12% rock fragments, 4% of other minerals and total of 10% clay matrix.

The comparison of all the samples above from both wells, indicated even-though there is evidence of smectite-illite transformation, it could be rule out as the mechanism of overpressure for the unloading trend in Bestari-1 as the same amount of transformation are happening as well in the shallower disequilibrium compaction of the Kamunsu B and even in the hydrostatic parallel of shallow Pink sandstone and the Kamunsu B reservoir in Bestari-2/ST1/ST2.

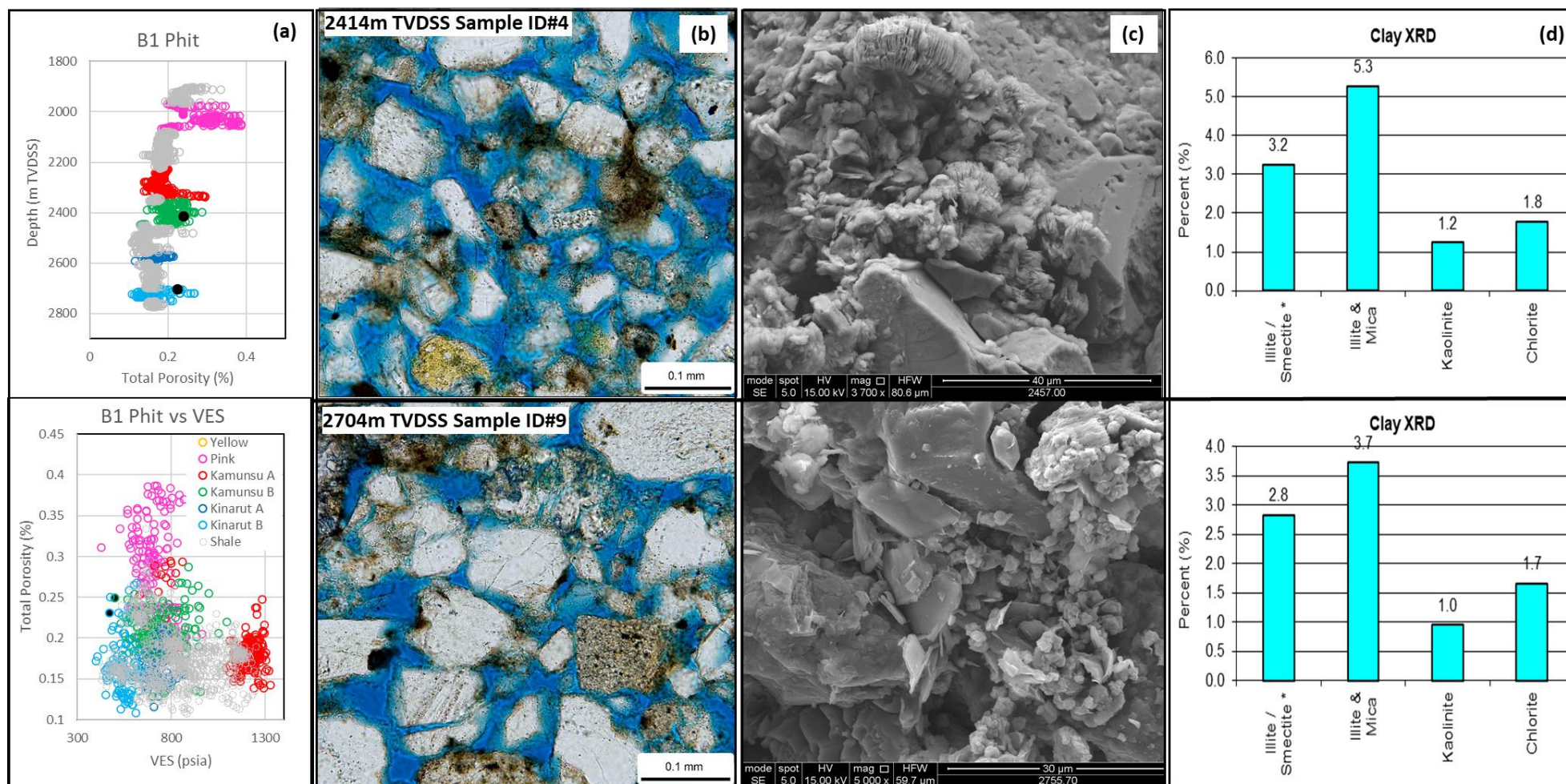


Figure 6-21: Bestari-1 well thin section and SEM (modified from Corelab Bestari-1 post evaluation report) sample, representative of the Kamunsu B sandstone and Kinarut sandstone. The black filled circle in (a) is the sample chosen to be looked in detail for the petrography, SEM and XRD for the clay mineralogy transformation.

Open

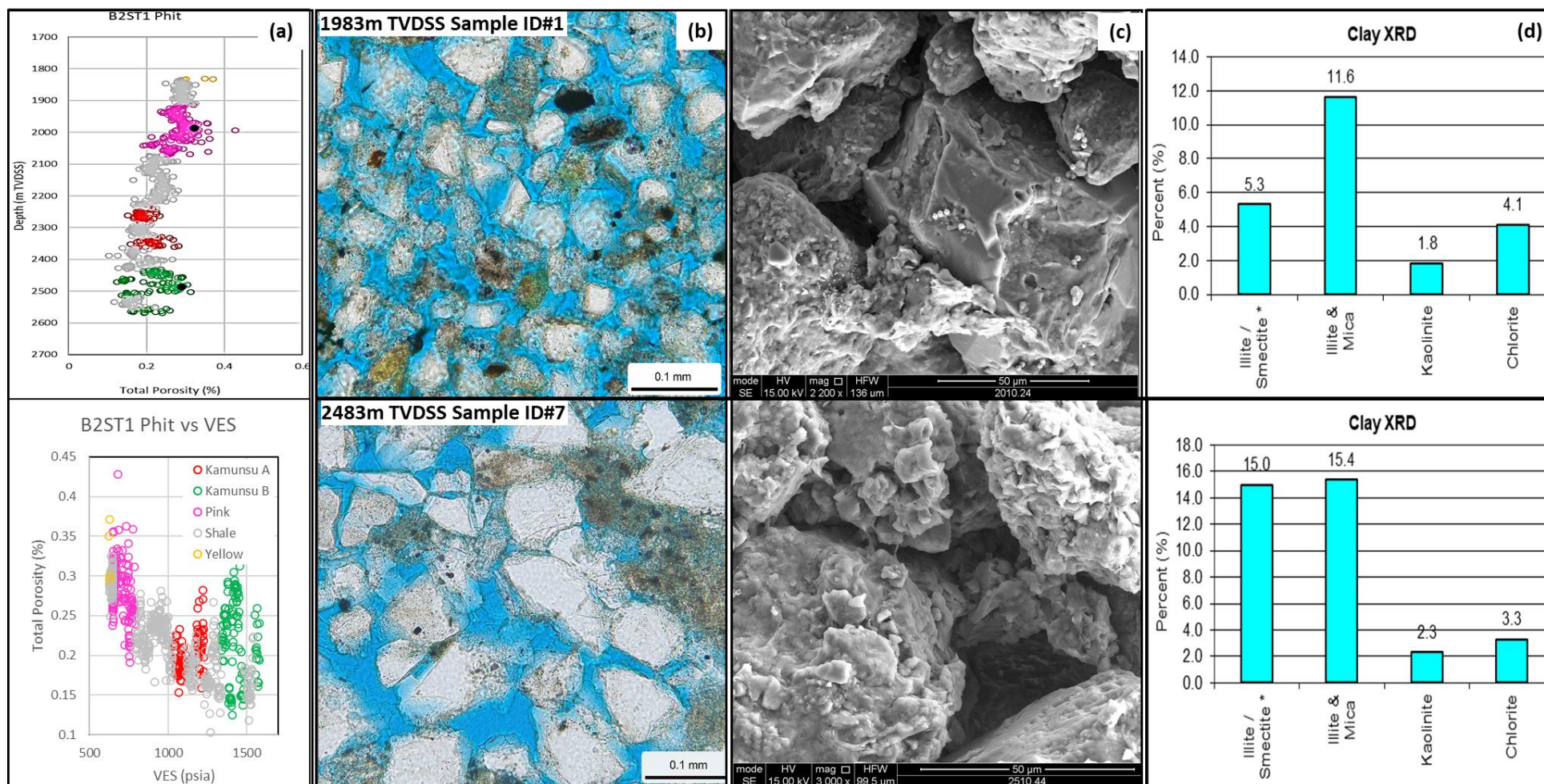


Figure 6-22: Bestari-2/ST1/ST2 well thin section and SEM micrographs (modified from Corelab Bestari-1 post evaluation report). Sample representative of the Pink sandstone and Kamunsu B sandstone. The black filled circle in (a) is the sample chosen for petrography, SEM and XRD analyses.

Open

6.6 Discussion

6.6.1 Geopressure compartmentalization

The complex interactions between fold growth and surrounding sediments makes assessment of potential prospects and drilling in these deep-water plays particularly challenging. Geopressure compartmentalisation has already been recognised in salt basins where complex interactions between salt and sediment occur, for example, in the Gulf of Mexico where Tertiary to Quaternary salt basins are created by a mix of rapid sediment loading and active movement of salt (see Shaker 2004; Luo et al., 2017; Sathar & Jones 2017; Heidari et al., 2019).

In the complicated diachronous synkinematic depositions of the submarine fan in the NW Borneo deep water fold-and-thrust belt, the application of pore pressure to assist in correlating the stratigraphy has proven to be successful. The correlation by using the wireline log respond, lithology, biostratigraphy and seismic will be remain the crucial part of the initial correlation. However, with the deep-water environment with the slope failure deposits, canyon, turbidity, Mass Transit Complex (MTC) and the submarine fans facies co-exist in a very short period of time, in the case of NW Borneo fold-and-thrust belt, in less than 10 Ma and more than 2.5 km thick of sediment, correlation by using the usual technique is definitely challenging and confusing.

Usually, biostratigraphy and heavy mineral will be decisive in correlating even a very complicated strata, however with the lack of in-situ sample and mixture of the transported sediment contain foraminifera, nannofossil, pollen and heavy minerals

from the shelf or scoured along the pathway towards the well make it almost impossible to accurately correlate based on biostratigraphy zonation or mineralogy. The approach of doing this will result in inaccurate zonation where strong diachroneity exists across all of the fold structures outboard of the shelf slope break.

Therefore, the approach of using the geopressure clustering of the pore fluid pressure data sets is a useful tool for deciphering the complex stratal packages and potential for connectivity of isolation of the submarine fan facies (Figure 6-10). This is especially useful in avoiding oversimplification of correlating the sand bodies between wells along and off strike of the growth folds. It is very common mistake in this challenging deep-water setting, that the sand bodies can be correlated between wells in a very simplified way using log characteristics alone, especially for wells with distances less than 5 km, and in some case less than 2 km apart as can be seen in the Bestari structure (Figure 6-11). The recognition of different overpressure zones for the Bestari and Limbayong structures is important for understanding submarine fan deposition, where structurally controlled sea-floor topography may result in submarine fans being deflected, diverted, constricted or blocked (Clark & Cartwright, 2009; Kneller & McCaffrey, 1995; Oluboyo et al., 2014). Although considerable attention continues to be focused on the fold kinematics and contemporaneous submarine fan deposition, including in this study (see Chapter 4), the importance of the role played by overpressure in these tectonically active deep-water systems in controlling the reservoir properties needs to be better appraised. This study has identified the importance of overpressure in defining isolated early depositional sand bodies compared to younger laterally extensive and connected sand bodies that have been viewed as potential better targets for exploration. Furthermore, as in this study for the

Bestari structure other mechanisms may enhance or top-up the disequilibrium compaction generated overpressure, in particular tectonic compression, cracking of kerogen to gas and vertical/lateral transfer.

6.6.2 Tectono-stratigraphy influence on overpressure

The subdivision of the NW Borneo deep-water fold-and-thrust belt development into three phases based on the structural geometry using 3D seismic data (see Chapter 4) was also applied to studying the relationship of the tectono-stratigraphy with overpressure in the region. The three phases of tectonically influenced, transitional and gravitational phases are agreeable with the 1D burial history modelling, which is directly calibrated with the pressure, temperature, and porosity inputs from the wells across the Bestari and Limbayong structures.

The burial history modelling timeline and depth allow the rate of deposition and thickness of overburden through time to be calculated, which crucial in understanding the overpressure development and supporting the overpressure mechanism especially the disequilibrium compaction (Figure 6-13). The lateral transfer mechanism as for the Kinarut sandstone in Bestari-1 well suggestion from the density plot against vertical effective stress (Figure 6-18), supported by the temperature history plot derived from the burial history (Figure 6-13).

The lithology assignment from the cuttings and core description on developing the model is crucial in get a properly calibrated the burial history model to the pressure, temperature, and porosity. Thus, understanding of both tectonic and stratigraphy

relationship with the overpressure development in the NW Borneo fold-and-thrust belt is merely important in justifying the findings from the logs and stress method. As for the study area, the well location on the fold, in the case of Bestari-1 well, closer to the active thrust fault and at the fold front limb, as compared to the other well proven to be having different triggering mechanism for the high and increasing trend of overpressure. By this understanding, Bestari-1 well will be useful in future well planning or pressure modelling.

6.6.3 Pore fluid pressure and porosity

Three clusters of overpressures data were classified in the datasets from the wells in the study area. The first group is the hydrostatic parallel trend (Figure 6-10) with almost constant overpressure ~600 - 700 psia for all the deltaic fan reservoirs, from Pink to Kamunsu B sandstones. This trend only observed in Bestari-2/ST1/ST2 wells reservoirs which proven to be water bearing from the pressure gradients and fluid sampling. The overpressure-depth plot (Figure 6-15) shows clearly the trend is distinctive from the other trends as only slight increment of overpressure could be seen. This suggests the influenced of hydrocarbon towards the overpressure. Even though, all the reservoirs in this trend are already in higher pressure zones than the hydrostatic trend, however the overpressure is lower as compared to the hydrocarbon bearing reservoirs. This is a good indication of the equilibrium compaction generating the overpressure and the relationship of burial and overburden to the formation pore fluid pressure. The porosity for this cluster shows a trend higher than the average regional trend of 20 - 25% even in the deeper part of Bestari-2/ST1/ST2 well at ~2500 m TVDSS. This is direct evidence of how overpressure due to rapid burial in deep-

water fold-and-thrust belt can actively arrest porosity loss from burial compaction effects (Stricker et al., 2016; Sathar & Jones 2017; O'Neill et al., 2018; Oye et al. 2018; Oye et al., 2020).

The second cluster is the mostly lithostatic parallel trend (Figure 6-10) with increasing overpressure trend from ~700 psia at Pink sandstone level, to ~1000 psia at the Kamunsu A level and increased to ~1500 psia in Kamunsu B and Kinarut sandstone levels. This trend could be seen in all the Limbayong wells, Bestari-3 well and for Bestari-1 in all the reservoirs except for Kamunsu B and Kinarut sandstones. This trend is a representative for the disequilibrium compaction effect towards the hydrocarbon bearing formations. The increment of overpressure contributed by both burial effect and pressure from the hydrocarbon. The porosity trend shows similarity with the first group as both groups' porosity preservation was due to the overpressure from the same equilibrium compaction mechanism.

The third group is only observed in Bestari-1 well deeper reservoir level of the Kamunsu B and Kinarut sandstones. The pressure trend shows a high magnitude increment towards the lithostatic gradient from ~1500 psia to more than ~2500 psia of overpressure. In relationship with porosity, even though this group is in the deepest reservoir penetrate by the well, the porosity is still reaching 20% at 2700 m TVDSS. As the overpressure for this group is believed to be caused by lateral transfer of high pressure migrated fluids or gas from deeper formation, this shows a role of overpressure in preserving the porosity caused by unloading.

Each of the groups identify the role played by overpressure in aiding reservoir quality of submarine fan sandstones. When looked at carefully, it is clear that other influences, beside overpressure (vertical effective stress), can play a key role in determining reservoir quality. Chlorite coatings and the presence of microquartz rims (e.g., Osborne and Swarbrick, 1999, Stricker et al., 2016; Oye et al., 2020; Charlaftis et al., 2021) dictate the ability of authigenic quartz cements to form at detrital grain surfaces and potentially occlude porosity. Low vertical effective stress due to overpressure development helps retard pressure solution and thus restricts the amount of locally sourced silica available to enter into solution. In the absence of significant cementation, compaction is left to play its over-arching role.

6.6.4 Implications for overpressure in NW Borneo Deep-Water Fold Belt

Structural analysis of the growth folds by Wu *et al.*, (2020). shows that the poorly imaged seismic zones within the NW Borneo deep-water fold belt (e.g., growth fold centres) can be reconciled as thrust imbricates above multiple detachments. Wu *et al.* (2020) ascribe those mobile shales are not required to explain deformation in the NW Borneo region. However, what is apparent from this study, is the importance of the spatial and temporal relationships between the submarine fan sandstones, MTD's and contemporaneous fold growth to strongly compartmentalise the facies and resulting overpressures. There is seismic evidence for fluid escape features above fold crests (Figure 6-23). Fluid escape features have also been seen within the Brunei sector from outcrop (Morley, 2003) and seismic studies (Warren et al., 2014).

Overall, for the wells in both Bestari and Limbayong structures, all the wells are in overpressure states mainly from Pink sandstone level as can be observed from pressure and porosity plots. This is also proven by the well logs with the logs changing direction as a respond of pressure system changes. Disequilibrium compaction is the main the mechanism for overpressure generation in the area for all of the wells from the Pink down to Kinarut sandstone level. The exception being the Bestari-1 well, which has higher overpressures that are attributed to lateral and vertical transfer. The recognition of additional sources of overpressure is an important result from this research. Previously, the recognition of increased overpressures was attributed to greater sand thicknesses and in the Champion delta region enhanced overpressures correspond to regions of inversion anticlines with uplift adding to the pressure system (Morley et al. 2008). One potentially important impact of the recognition of lateral or vertical transfer of pressure from deeper sources is the potential for previously unrecognised hydrocarbons with the deeper and older submarine fan sandstones potentially acting as transient traps for hydrocarbons and pressure on their route to younger reservoirs. Similar occurrences have been previously recognised in the Taranaki Basin, New Zealand (see Webster et al. 2011; O'Neill 2018).

In comparison the younger submarine fans (Late Miocene) of the Pink, Yellow and Lingan have a better-connected network with a higher net-to-gross and in part reflects the recent higher sediment flux from the shelf causing many of the growth folds to become 'drowned' where sediment supply outstrips localised uplift rates. The high sedimentation rates have directly led to disequilibrium compaction, but overpressures are readily dissipated due to the connected nature of the depositional facies and shallower depths.

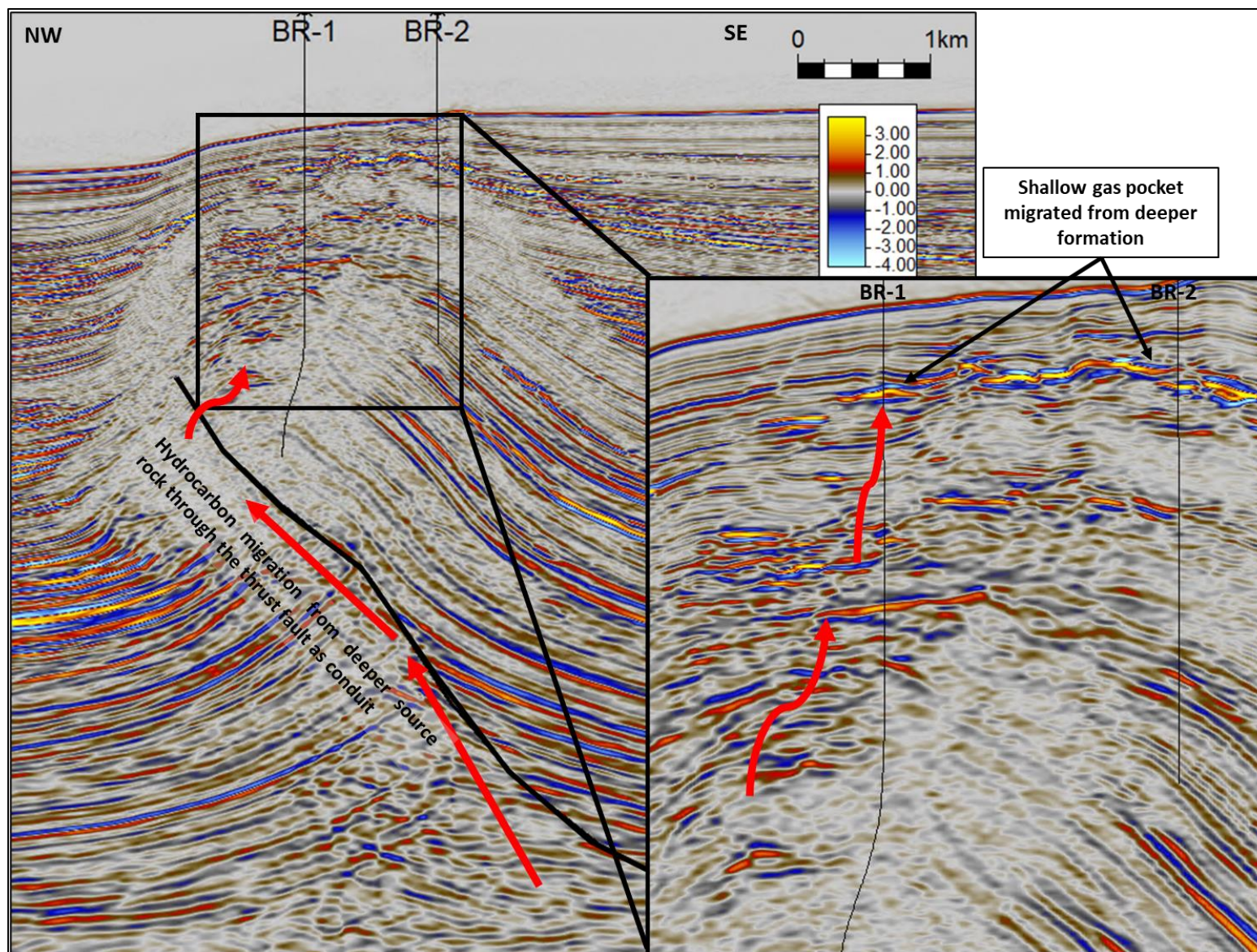


Figure 6-23: Dip line seismic section crossing Bestari-1 and Bestari-2/ST-1/ST2 well locations, showing the gas pocket at the shallow level close to seabed migrated from the deeper level, through the thrust fault.

Open

6.7 Conclusions

1. The usage of pressure and pressure clusters as a tool in correlating the complex diachronous submarine fan facies in deep-water fold-and-thrust belt proven to be effective. It directly as it helps in defining the lateral and vertical connectivity of the sand bodies between the wells.
2. Burial history from 1D Basin Modelling confirmed the three-phases of the fold-and-thrust development of the tectonic phase from Eocene to Middle Miocene, the transition phase from Middle Miocene to end of Middle Miocene and the gravitational phase from end Middle Miocene until present day.

The accuracy of the model was depending on the optimization towards the formation pressure, temperature and porosity calibration shows how those parameters are related to the tectono-stratigraphy history.

3. Rapid burial of the deltaic fan towards the deep-water of NW Borneo from Middle Miocene until recent with an average of ~250 m sediment thickness in per 1 Ma, a total of ~2.5 km of sediment deposited in less than 9 Ma. This rapid sedimentation was the main cause of the disequilibrium compaction overpressure in the basin.
4. The deltaic fans of interest of the Pink, Kamunsu and Kinarut sandstones temperature history generally in average of 50 °C with maximum of less than 90 °C. Therefore, this make the unloading mechanism of mineral transformation from

smectite to illite, fluid expansion and hydrocarbon generation are not contributing to causing the overpressure in the area.

5. Three groups of overpressures could be identified from the wells in the area, first group is the hydrostatic parallel pressure trend with constant overpressure of ~600 -700 psia. This trend is observed in the water bearing reservoirs with porosity preservation in the Kamunsu sandstone up to 20 - 25% due to the disequilibrium compaction causing overpressure in the system without influenced of hydrocarbon presence.

The second group is the lithostatic parallel pressure trend with overpressure increased from ~700 to ~1500 psia. This trend observed in the hydrocarbon bearing wells with porosity preservation similar with the first group, giving porosity of 20 - 25% in the deepest part of Kinarut sandstone in the depth of ~2700 m TVDSS.

The third group is only observed in the Bestari-1 well, at the Kinarut sandstone level from 2500 to 2800 m TVDSS with pressure trend of increasing towards the lithostatic, approaching the fracture pressure. This trend is due to unloading mechanism of the most-likely lateral transfer due to overpressure fluid or gas from deeper formation through the active thrust fault. The trend show similarity with the deepest penetration of the reservoir shows porosity of 20 – 25% at 2700 m TVDSS similar with the other previous group. This similarity is due to the leak in the top seal of the overpressure as indicated by the gas chimney above the reservoir level, causing the porosity preservation was only due to the

disequilibrium compaction without any additional preservation even though the pressure is increasing.

6. The finding from this paper, will be useful for future well exploration in de-risking the reservoir presence and properties, by using pressure prediction modelling in relation to facies vertical and lateral continuity. The three groups of overpressures will be beneficial in well drilling operation planning with high and increasing pressure should be expected at the front-limb of the fold and increased with distance to the active thrust fault.

Chapter VII:

Discussion, conclusions, and
future work

7.1 Synthesis

This study has used integrated approaches to understand the external controls acting upon submarine channel and fan facies, and the occurrence and geopressure development in the Deep-water NW Borneo fold-thrust belt. Available data and information from wells and two and three-dimensional seismic surveys enables various methods to be adopted in understanding the fold evolution and growth history (Chapter IV), depositional settings and facies (Chapter V) and porosity preservation and compartmentalization (Chapter VI). A discussion and conclusions are presented in this chapter followed by suggestions for further work as a way forward to address many aspects of complex deep-water sedimentary environments.

7.1.1 Structural evolution: control on reservoir distribution and quality

The study provides new, balanced interpretations of regional, three-dimensional (3-D), multichannel seismic-reflection profiles, that allow for the quantitative interpretation of tectonic shortening throughout the deep-water fold-and-thrust belt of NW Borneo (Figure 4-4).

The use of 3D seismic surveys in this study in the qualitative and quantitative analysis of the gridded horizons and dip-azimuth measurement, horizons flattening for simple restoration and expansion index trends, enables the identification of tectonic and gravitational factors in controlling fold evolution in the NW Borneo deep-water fold-and-thrust belt (Figure 4-8). The 3D seismic image quality makes it possible to analyse fold evolution through time, tracking the growth history of the folds. This is critically

important in order to understand the controlling factors, magnitude and timing of the fold-and-thrust belt (Figure 4-9).

A key result of this is the recognition of three phases of fold evolution that have been spatially and temporally defined using these new datasets (Figure 4-11). Phase one was dominantly influenced by the subduction of the Proto-South China Sea towards Borneo in a Northwest to Southeast direction. This phase is marked by asymmetrical folds that verge towards the Southeast, and tectonic thickening of pre-folding strata.

Phase two occurs from the end of the Middle Miocene to the end of the Late Miocene, and is characterized by symmetrical fold geometry, with multiple thrust geometries and detachment surfaces. This phase is identified as the early onset of gravitational sediment loading and sediment supply from the shelfal and coastal plains of NW Borneo.

Phase three records continued fold growth from the end of the Late Miocene until Recent, and is characterized by strong, asymmetrical, fold growth with Northwest-ward vergence and abrupt upward growth. Phase three folds are dominantly influenced by gravitational sediment loading and strongly influence routing of channelized turbidite flows and submarine fan evolution.

This research highlights the importance of creating accurate spatial and temporal frameworks to reconstruct fold growth in complex deep-water fold-and-thrust belts, particularly where there are very large volumes of sediment deposited in the basin from proximal shelfal and prograding deltaic margins. Fold evolution is crucial in controlling the facies distribution in the deep-water settings, as the accommodation space for sediment deposition and pathways from the shelf (transported by submarine channels) are

directly related to the magnitude of the folds and the unconfined or confined settings of the basin, as discussed in Chapter V (Figure 5-2).

7.1.2 Sequences and associated facies in the study area

The well penetrations in the study area proved the complexity of the depositional setting in the deep-water fold-and thrust belt. By integrating the well log signatures, lithological descriptions, seismic characteristics, and the seismic attribute horizons blending, we can understand the variations seen in the wells and the controlling factors for the differences or similarities.

By using a sequence stratigraphic approach on correlating the wells with calibration of seismic interpretation and formation pressure, six sequences are identified in the study area (Figure 5-3):

1. Sequence I, the deepest penetrated sequence by the wells, bound by the MFS11.6 at the top of the sequence. The Keabangan Fan has the reservoir potential in this sequence, with bright and continuous amplitude from the seismic that could be related to turbiditic sand presence.
2. Sequence II extends from MFS11.6 to MFS9.0 and includes the Kinarut Fan. Associated deposition is marked by dim and discontinuous seismic amplitudes at the bottom part, interpreted as possible Mass Transport Complexes (MTC). Continuous and bright amplitudes are interpreted as turbiditic sandstones on the top of the sequence.

3. Sequence III, from MFS 9.0 at the bottom to MFS8.7, is marked by the Shallow Regional Unconformity (SRU) right on top of the sequence and associated with the Kamunsu fans deposition.
4. Sequence IV is associated with the Pink fans and extend from MFS8.7 to MFS6.7.
5. Sequence V is bounded by MFS6.7 at the bottom, MFS5.6 in the middle and MFS 4.1 at the top. This sequence is a combination of two sequences; the bottom part associated with the Yellow fans and the top part with the Lingan fans.
6. Sequence VI is the Pleistocene and Holocene sediment fill, mainly pelagic shale with thin layers of sand.

The present-day seabed topography mapped in this study (Figure 5-5), is used as an analogue for modelling the accommodation space for the deep-water fold-and-thrust belt in the subsurface, as the thrust-fold structure and sediment has formed by the same processes and sources since ~12 Ma.

The accommodation space identified in the area includes settings in canyon complexes at the shelf breakout area, unconfined space from the shelf breakout towards the basin, confined space bounded by the thrust folds and incised valleys as a result of submarine erosion in between folds forming further outboard canyons in the deeper water areas (Figure 5-6).

Associated facies characterised by the well log and seismic signature are identified (Figure 5-8 and Figure 5-9):

1. Drape complex (DC) of the deep-water marine hemipelagic shale.
2. Levee channel complex (LCC) of thin and low net to gross turbidite sand.
3. Distributary channel-lobe complex (DLC) of the thick and high net to gross turbidite sand.
4. Mass transport complex (MTC) of the slump deposit with chaotic and poorly sorted mixed lithology.

7.1.3 Depositional setting controls in the Deep-water NW Borneo fold-and-thrust belt:

1. Location with respect to sediment source

The sediment supply affects the shelf-break submarine canyon development. The differences are obvious between the southern part of the area, with numerous submarine canyons developed because of huge amount of sediment transported down from the shelf. The area is located close to the Baram and Champion deltas, and the presence of submarine channel systems connecting the fans to this area is the reason for this regional difference in sediment supply (Figure 3-5).

2. Seabed topography during deposition

The steeper slopes at the Menawan and Limbayong folds cause bypass zones, as submarine channels and canyons cut through the structure, with channel lag (CL)

deposits at the base of the channel. The huge amount of sediment towards Limbayong, at the Lingan submarine fan upwards to the present-day seabed, either eroded the crest of the anticline or swamped the growth of the fold due to the rapid sedimentation on top of the structure. This caused MTC deposition, and submarine channel sediments to be deposited in unconfined settings, as compared to the confined settings in Bestari. The high magnitude, steeper limb of the Bestari fold restricted the submarine channel ability to reach the crestal part of the structure and caused the submarine channel to flow around the fold (Figure 5-28).

7.1.4 Compartmentalization

The sand body correlation based on the formation pressure seems to be straightforward for the wells in the Limbayong structure as the pressure increment and overpressure trends are almost at the same magnitude (Figure 5-27). The trend at Limbayong correlates well with the trend observed at the B3 well, at least until the Kamunsu A level, with the pressure increase with depth, and significant jumps in every deeper sand package. However, for the Bestari fold, the trend is more complicated as the pressure has different trends for the Kamunsu A and Kamunsu B submarine fan sand facies (Figure 6-10).

The formation pressure is a reflection of fluids in the formation, as the Bestari-2, Bestari-2ST1 and Bestari-2ST2 wells are proven to be water-bearing, based on the pressure plot gradient and formation fluid samples from the borehole. Apart from the differences in the fluid filling up the formation, the pore pressure differences between the sand bodies from the different wells shows possible compartmentalisation between the sand bodies (Figure 6-11).

7.1.5 Porosity preservation with overpressure

Three clusters of overpressure data can be classified in the datasets from the wells in this area (Figure 6-15). The first group is the hydrostatic parallel trend, with almost constant overpressure ~600 - 700 psia for all the deltaic fan reservoirs, from Pink to Kamunsu B sandstones. The porosity for this cluster shows a trend higher than the average regional trend and tends towards the high porosity trend of 20 - 25%, even in the deeper part of the B2ST1 well at ~2500 m TVDSS (Appendix 9). This is good evidence of how overpressure due to rapid burial in deep-water fold-and-thrust belt could preserve the porosity in the sediment.

The second cluster is the mostly lithostatic parallel trend with increasing overpressure trend from ~700 psia at Pink sandstone level, to ~1000 psia at the Kamunsu A level and increased to ~1500 psia in Kamunsu B and Kinarut sandstone levels. The porosity trend shows similarity to the first group as both groups' porosity preservation was due to the overpressure from the same equilibrium compaction mechanism.

The third group is only observed in the Bestari-1 well, at the deeper reservoir level of the Kamunsu B and Kinarut sandstones. The pressure trend shows a high magnitude increment towards the lithostatic gradient from ~1500 psia to more than ~2500 psia of overpressure. In relationship with porosity, even though this group is in the deepest reservoir penetrated by the well, the porosity still reaches 20% at 2700 m TVDSS. As the overpressure for this group is believed to be caused by lateral transfer of high pressure migrated fluids or gas from deeper formation, this shows a role of overpressure in preserving the porosity caused by unloading.

7.2 Conclusions

1. The amount of sediment supply is a controlling factor of the fold growth, as shown by the fold growth ending earlier in Limbayong as compared to Bestari, due to the proximity of Limbayong to the sediment source, with addition of an extra source from the southwest for the deeper Kamunsu and Kinarut submarine fans.
2. The difference in sediment supply amount from the shelf break affected the depositional settings, with more submarine canyons developed at the slope as can be seen in Limbayong. This caused huge MTC bodies to be deposited in the basin, in the unconfined settings due to the cessation of the fold growth. This is not seen in Bestari, as the location is farther away from the sediment supply.
3. The seabed topography is a very important control of the depositional settings as the accommodation space in the deep-water intra-slope basin changes abruptly, due to steep changes near the fold. The structural high acted as a barrier if the submarine channel had to flow around the structural high, limiting the ability of the reservoir sands to be deposited on top of the anticline.
4. The thick reservoirs at the synclinal area could be an interesting target to find thicker and high net to gross sand, with potential traps bounded by the shale diapirs at folds inboard and outboard of these areas.
5. The presence of possible shale diapirs, as previously described as MTC, might change the approach of hydrocarbon exploration and development of the area.

6. The usage of pressure and clusters of overpressures as an additional tool in correlating the complicated, diachronous, deltaic fan facies in deep-water fold-and-thrust belt are proven to be effective. This approach helps in defining the lateral and vertical connectivity of the sand bodies between the wells.
7. There was rapid burial of the deltaic fan towards the deep-water of NW Borneo from Middle Miocene until recent, with an average of ~250 m sediment thickness in per 1 Ma, a total of ~2.5 km of sediment deposited in less than 9 Ma. This rapid sedimentation was the main cause of the disequilibrium compaction overpressure in the basin.
8. The three-groups of overpressures, based on the pressure and overpressure trends, are related to a ramp up in pressure going deeper in the subsurface due to disequilibrium compaction. The exceptional high overpressure in Bestari-1 well is due to pressure migration from deeper formations, through the thrust fault.

7.3 Implications of this study

The findings of this research should be of broad interest those studying deep-water facies distributions and depositional setting in other fold-and-thrust belts (e.g., Mahakam Delta, South Caspian Basin; Niger Delta,) and deep-water submarine settings in general (e.g., Congo Submarine Canyon, Gabon North and South Basins, Guyana-Suriname Basin).

The implications of this study are as follows:

1. Depositional environment and facies distribution models for the deep-water fold-and-thrust belt setting involve controls by regional and localised tectono-stratigraphic evolution.

Therefore, methods used in this study by integrating well data, seismic and formation pressure in modelling the facies, should be used in understanding the variations in the depositional setting and facies distributions. Generalised and simplified models should not be used in this complicated structure and diachronous stratigraphy.

2. Compartmentalisation due to different submarine channel system on a structure is very likely to be the case for the structures further away from the provenance and the steep syn-kinematic folds.

This should be considered in modelling the reservoir for resource estimation, to avoid over-estimation.

3. Stratigraphic trap plays in the intra-slope basin, with high sandstone concentration deposited by the submarine channel in the confined setting, should be targeted in future exploration, with de-risking process by detailed seismic attribute and quantitative analyses.

These plays may have thick and high net to gross distributary channel lobe (DLC) facies bounded by the low permeability MTC and hemipelagic deep-water shale with source rock potential from the deeper Setap shale other than the transported intraformational source rock from the Sabah onshore and shelf. The stratigraphic

play if successful, will open up huge upside potential in NW Borneo deep-water fold-and-thrust belt and in other part of the world sharing the same settings.

4. The identification of formation pressure and overpressure clusters will be beneficial in well drilling operation planning. High and increasing pressure should be expected at the front-limb of the fold and increasing with distance to the active thrust fault.
5. The facies depositional model, and the method used in defining the facies distributions in this study, should be applicable in Carbon Capture and Storage (CCS) as the thick reservoir in the offshore deep-water could be ideal for CCS with lower risk to the environment, health, and safety.

7.4 Future work

1. Shale mineralogy and provenance studies, to differentiate between potential shale diapirs in the fold cores and the units previously described as Mass Transport Complexes (MTC).

This objective could be done by comparing the mineralogy between the shale in the chaotic and dim seismic forming the “Christmas tree” features usually observed in shale and salt diapirs. Hence, comparisons of the samples with outcrop mineralogy of the deeper Setap shale and MTC could be carried out, as both outcrops could be found in Sabah and Sarawak.

Differentiating the shale diapirs and MTC in the core of the thrust fold is critical in studying the reservoir quality in deep-water NW Borneo. This could be a very significant external factor affecting the reservoir quality of the submarine channel bodies.

2. Detailed mapping of possible faulted crestal folds, by using higher resolution seismic images to confirm the facies versus fault compartmentalisation. By using high resolution seismic acquisition or processing to enhance the image quality as at the core of the thrust folds, will answer a lot of questions regarding the observed compartmentalisation between wells from same structure as seen from this study.

Improving the seismic resolution will allow quantitative imaging, modelling, and rock physics by using seismic velocity. The modelling of the seismic facies and definition of the depositional settings will be higher confidence. The de-risking process of the petroleum system could be made more accurate, and the proposal of drilling a stratigraphic play well at the intra-slope basin at the synclinal area will be more justifiable.

Improving the seismic resolution will address the possible presence of shale diapirs in the deep-water NW Borneo fold-and-thrust belt, currently believed to be non-existent, and the thrust folds to be underlain by active-inactive toe thrusts (Sandal, 1996).

3. In this study, the three-phases of the fold evolution identified (Figure 4-11) changed directions of the sediment supply into the basin. The attribute extraction

maps (Figure 5-22 - Figure 5-25) show the possibility of different sediment pathways towards the Limbayong and Bestari structures.

Identifications of the provenance of the sediments from each sediment pathway will be useful in defining the reservoir quality, similarity or difference. The effects of provenance can be matched to the facies distribution and depositional settings of the three wave-dominated deltas of the Early Miocene Meligan Delta, Middle to Late Miocene Champion Delta and Pliocene to Present-Day Baram Delta (Koopman, 1996).

Scientifically, more provenance studies (e.g., using detrital zircons or chemostratigraphy) could tie the deposited sands to different source areas, and so look at changing sediment pathways over time. With possibly deeper well penetration in the future to the Eocene to Middle Miocene formations, the same provenance study could be carried out for the sediment deposition from the Dangerous Ground at the Northwest of the fold-and-thrust belt.

4. As well as Vertical Effective Stress relationship with reservoir quality, the Horizontal Effective Stress might affect the reservoir quality distribution in the deep-water fold-and-thrust belt setting and would be worth detailed evaluation and modelling. Modelling geomechanical fluid flow to assess the lateral deformations in sediment compaction and overpressure generations and analysing the relationship of the Horizontal Effective Stress with reservoir quality will be useful for de-risking process of the stratigraphic play in the synclinal area of the basin.

5. The methods used in this study, should be tested in other deep-water fold-and-thrust belt setting in other part of the world such as the South Caspian Basin, Gabon Basins and Guyana-Suriname Basin, in modelling the depositional setting and facies distribution for the reservoirs, de-risking and finding potential plays and traps for hydrocarbon exploration and Carbon Capture and Storage (CCS). No doubt similar studies have been done by exploration teams in these areas; it would be good to have more cross-comparison of methods and results, with conclusions made available for general use.

Linking progradation rates from the shelf deltaic systems to occurrence and frequency of deep-water sand facies. This would require regional 3D seismic from the shelf into deep-water to allow detailed chronostratigraphic correlations.

Appendices

Appendix 1A: 3D seismic survey coverage available for the research

Appendix 2A: Synthetic seismogram of the Lawa-1 well

Appendix 3A: Time - depth relationship of checkshot and VSP from the wells drilled in the area

Appendix 4A: Seismic time slices at different depths showing geometry and verge of the folds

Appendix 5A: Variance cube time slices at different depths showing the fold trends and variations

Appendix 5B: Variance cube time slices at different depths showing the fold trends and variations

Appendix 6A: Streonet plot of the azimuth and dip of the Limbayong and Menawan

Appendix 6B: Streonet plot of the azimuth and dip of the Bestari and Lawa

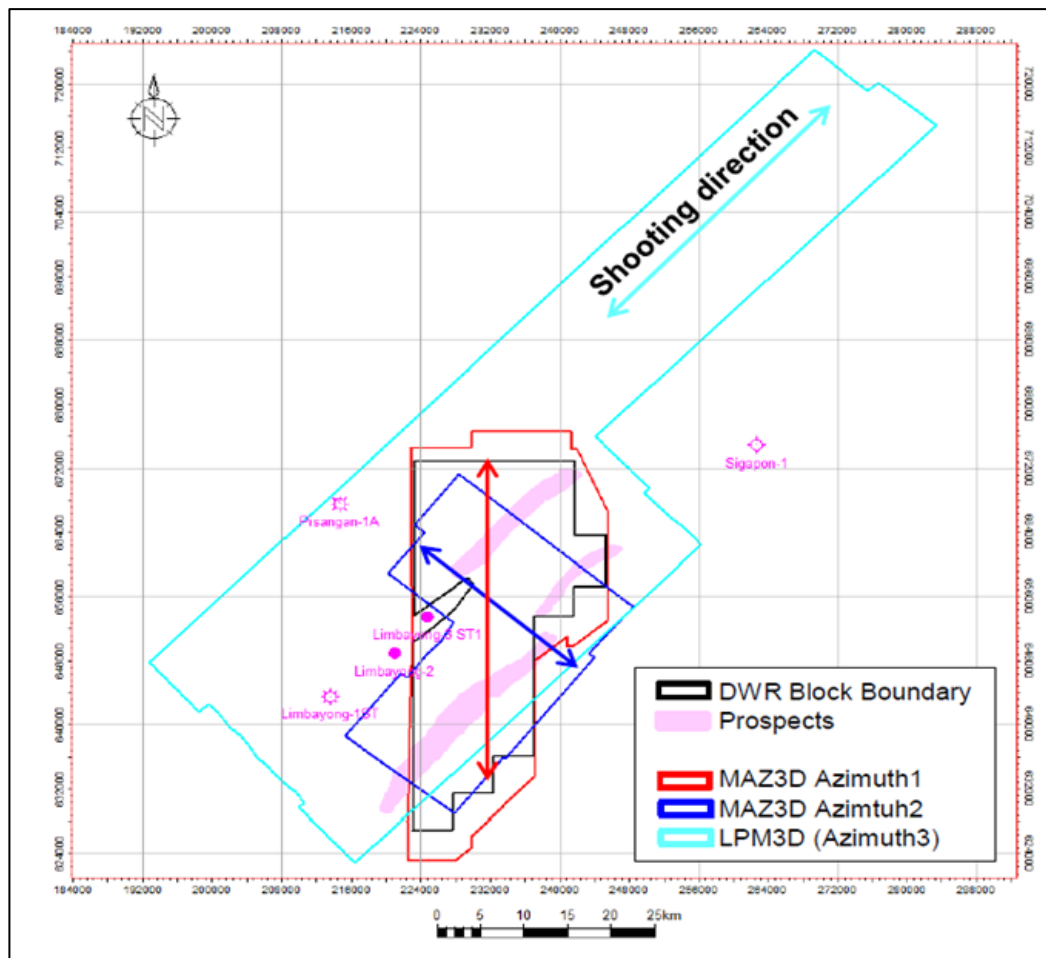
Appendix 7A: RGB, RMS attribute and blending of both attributes for Seabed and Lingan submarine fan

Appendix 7B: RGB, RMS attribute and blending of both attributes for Yellow and Pink submarine fans

Appendix 7C: RGB, RMS attribute and blending of both attributes for Kamunsu A and Kinarut submarine fans

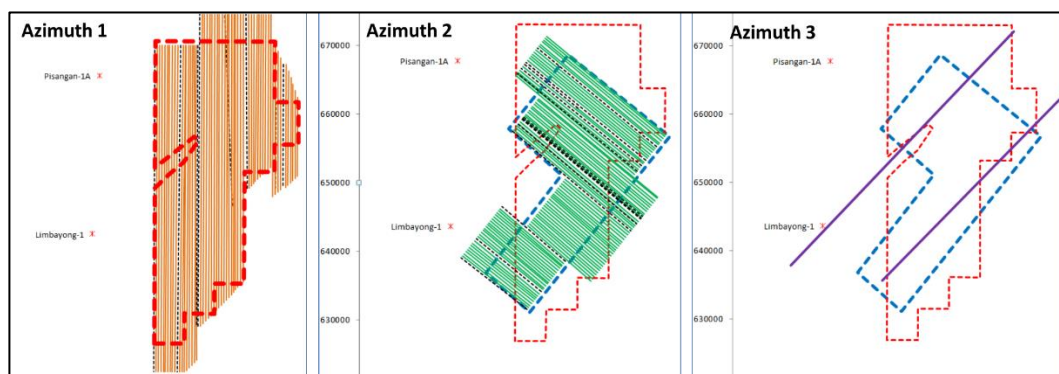
Appendix 8A: RGB attribute blending of the 10Hz, 20Hz and 41Hz band pass for seabed

Appendix 9A: Porosity plot obtain from well logs (density and sonic) and side-wall core and conventional core thin section point counting and Helium injection.

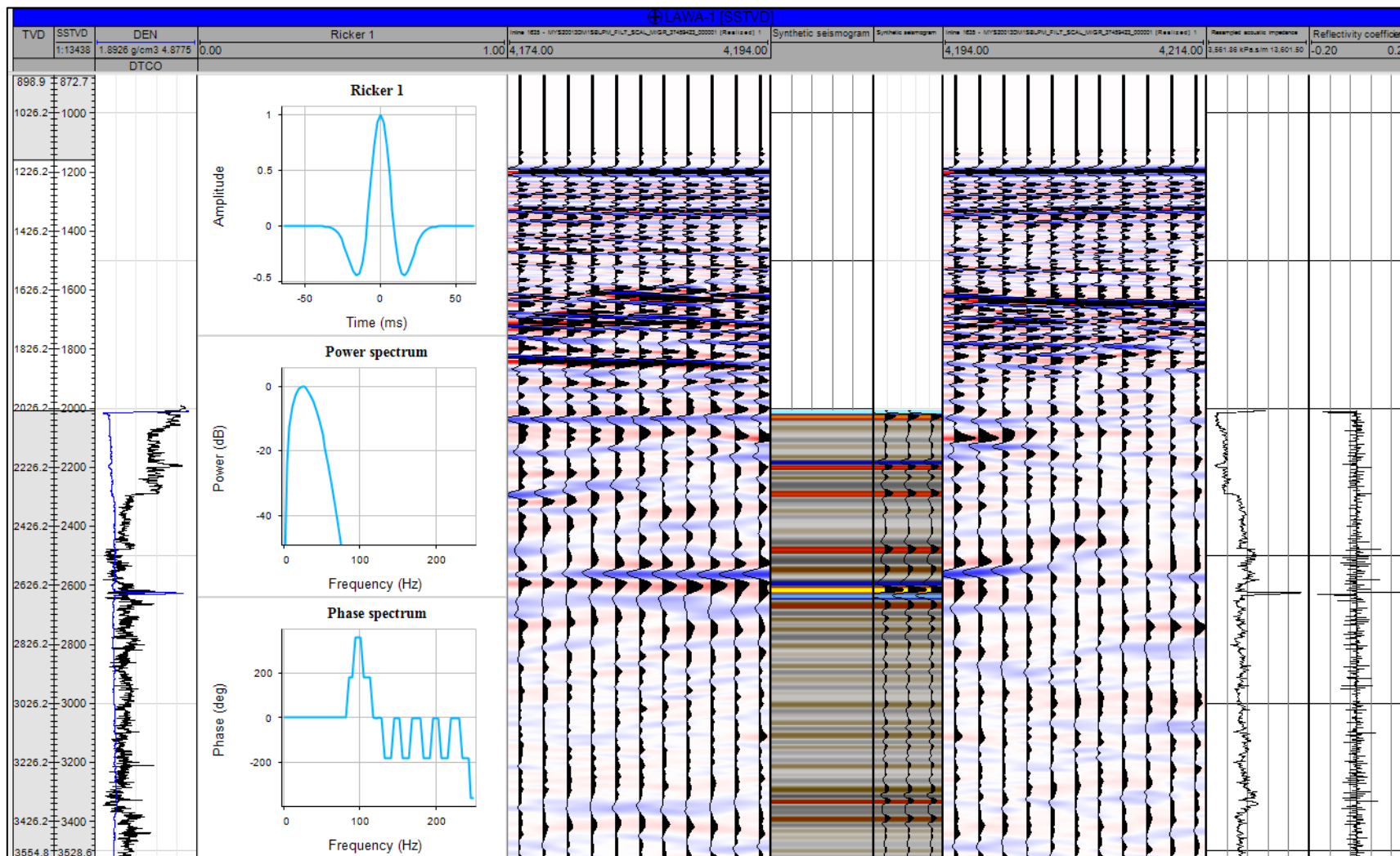


SEISMIC DATA:

1. 2013 DWR MAZ3D (Azimuth 1 & 2)
 - Acquired by JX Nippon (2012)
 - Broadband & Multi-azimuth acquisition
 - Processed to PSTM & PSDM
2. LPM3D (Reprocessed 2013, Azimuth 3)
 - Acquired by Shell (2001)
 - Conventional acquisition
 - Processed to PSTM (2013: PSTM & PSDM)

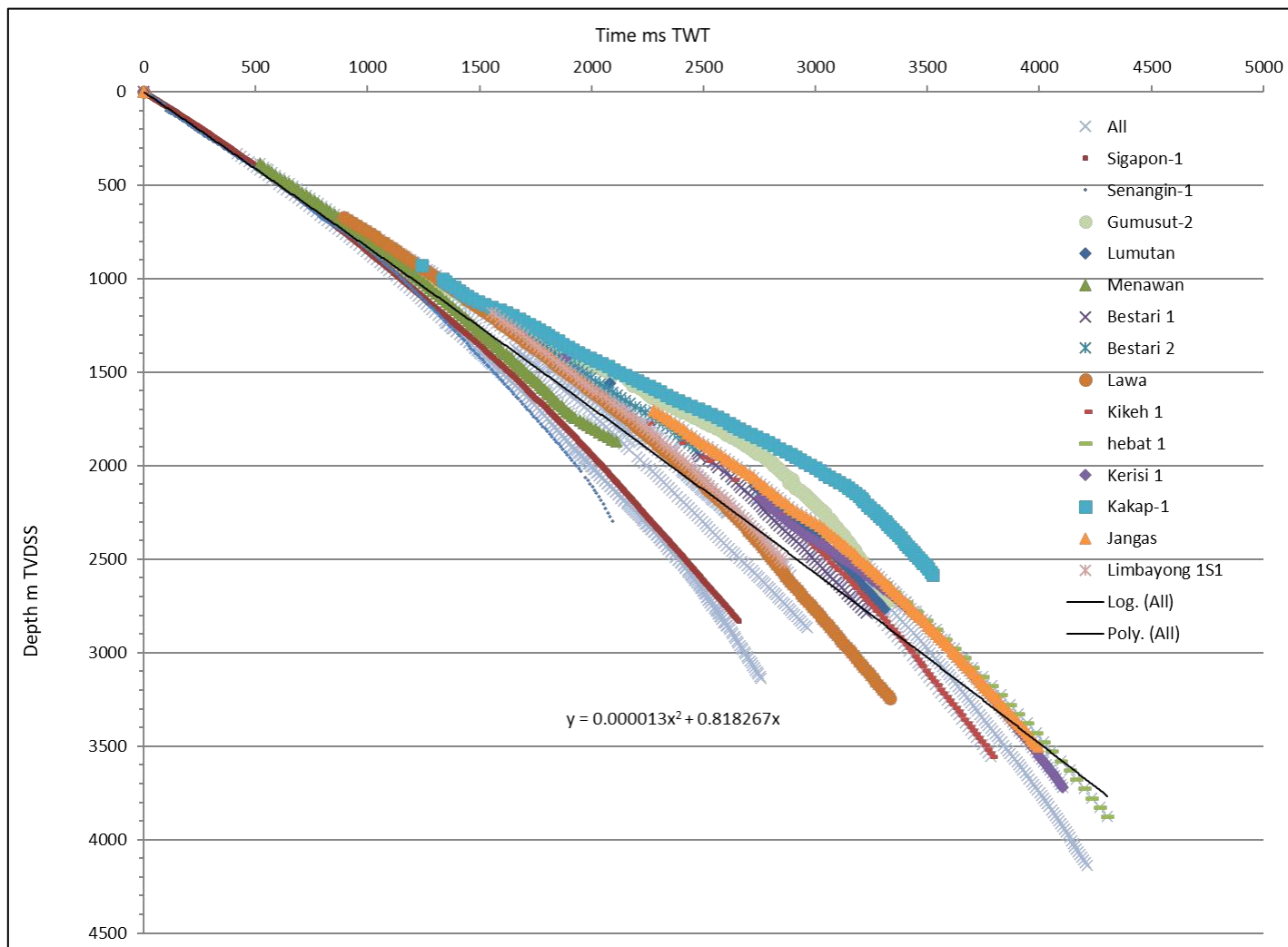


Appendix 1A: 3D seismic survey coverage available for the research

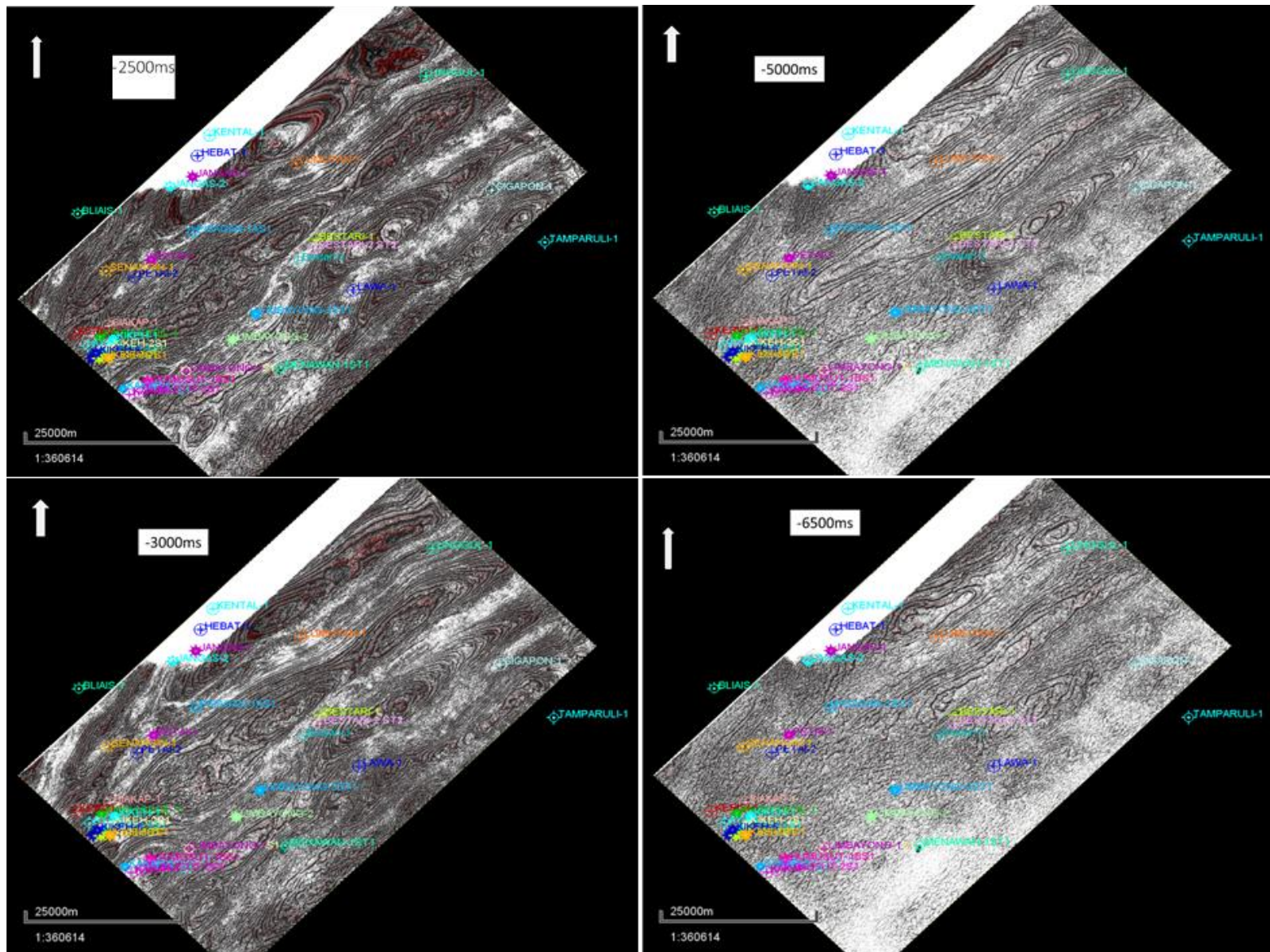


Appendix 2A: Synthetic seismogram of the Lawa-1 well

Open

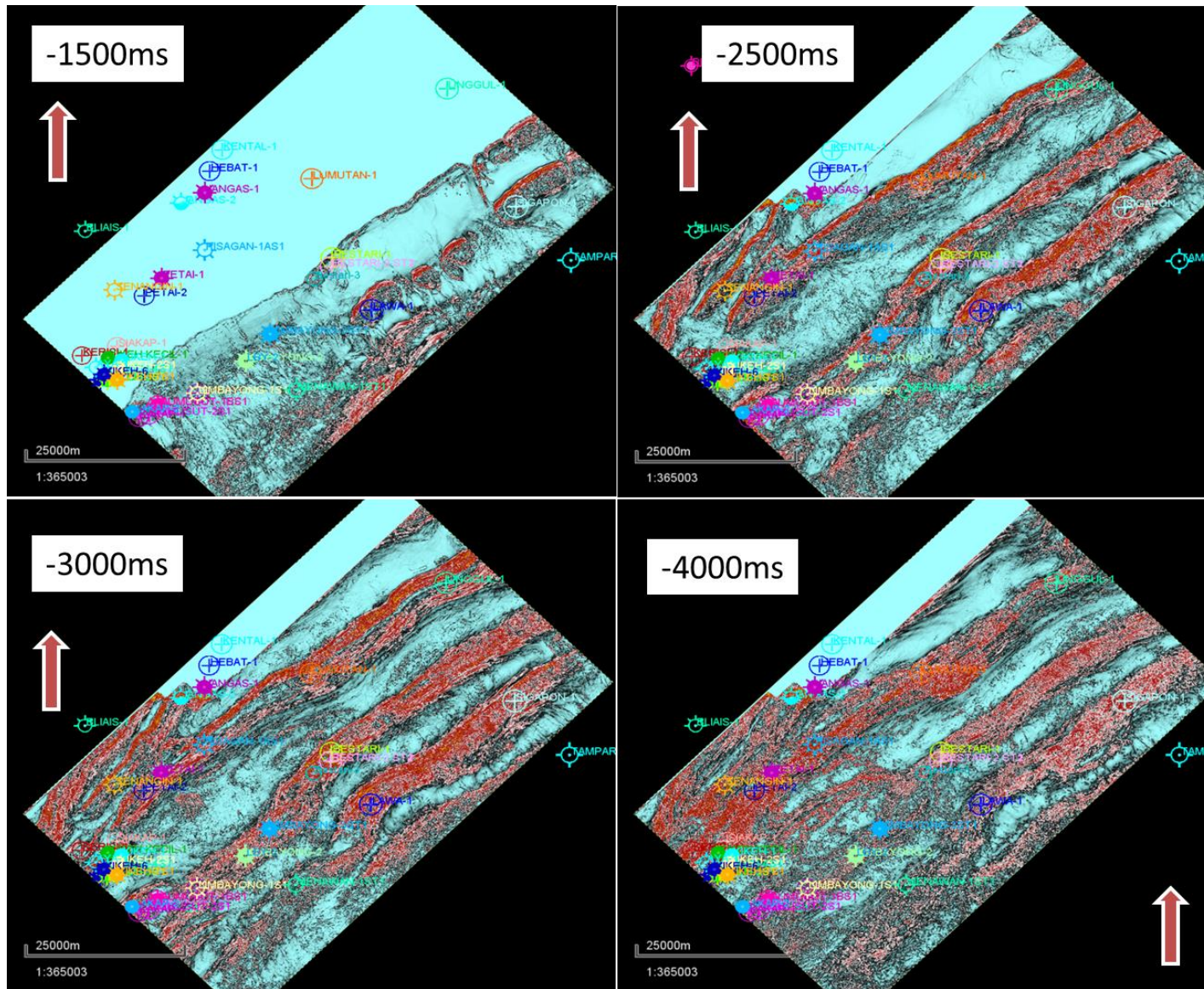


Appendix 3A: Time - depth relationship of checkshot and VSP from the wells drilled in the area



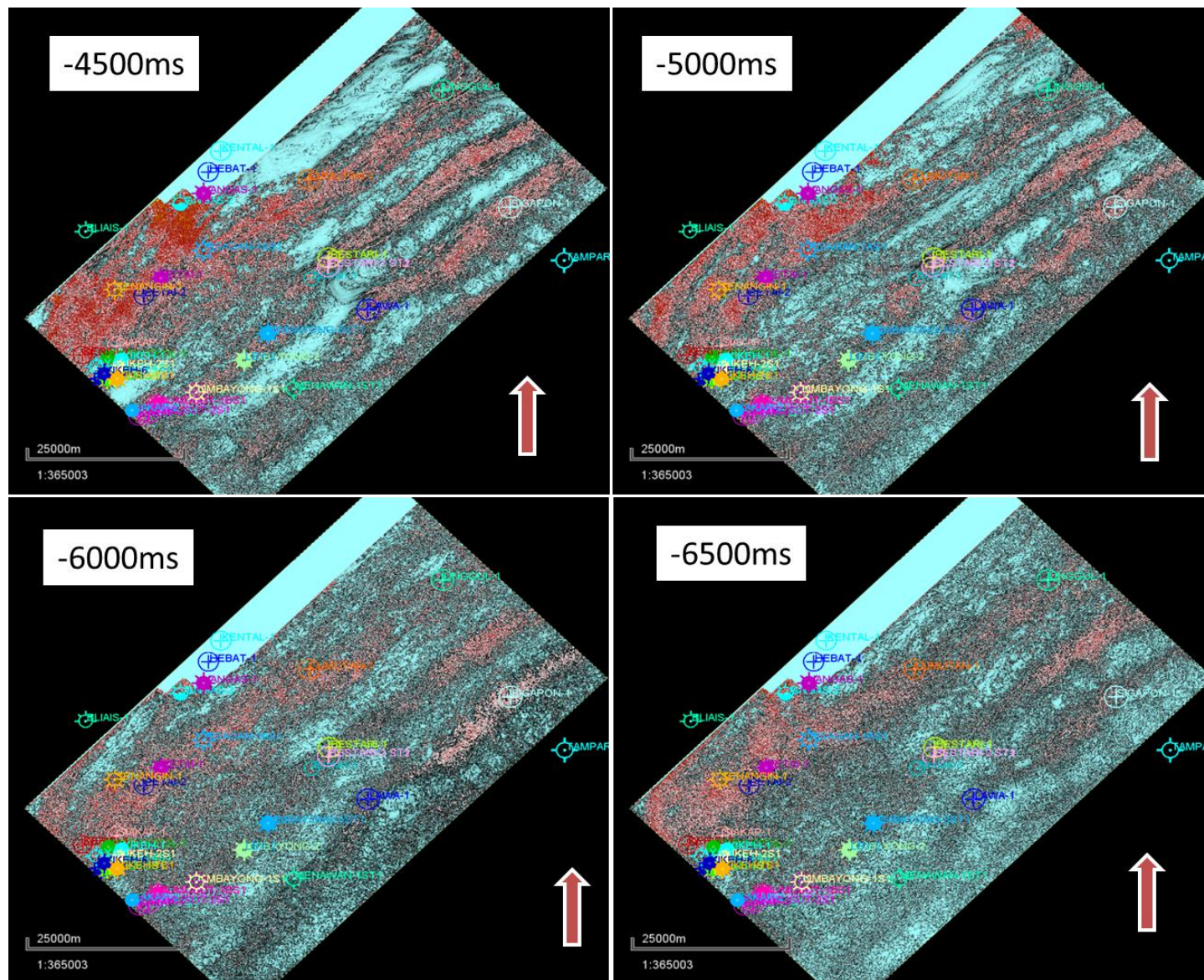
Appendix 4A: Seismic time slices at different depths showing geometry and verge of the folds

Open



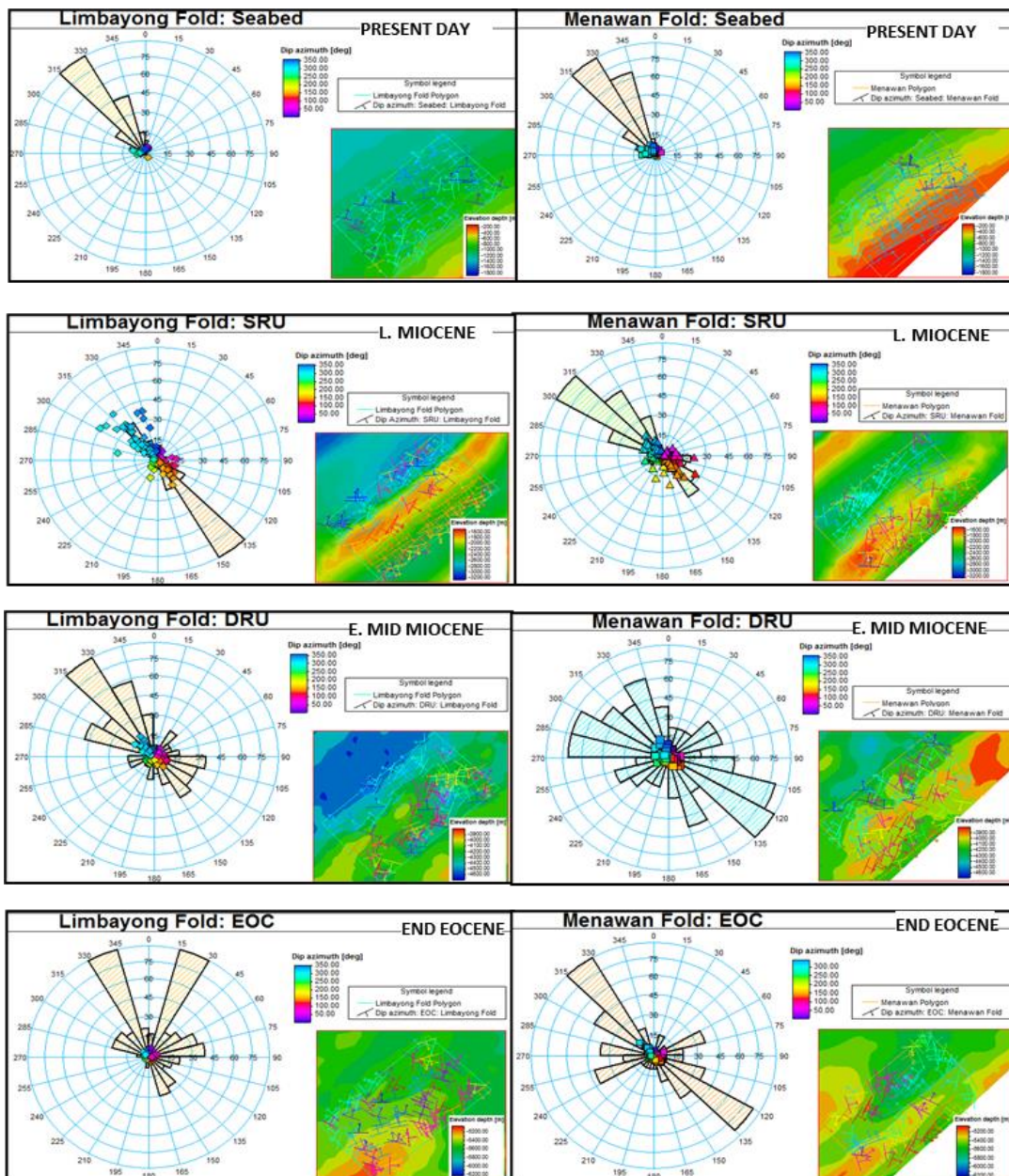
Appendix 5A: Variance cube time slices at different depths showing the fold trends and variations

Open

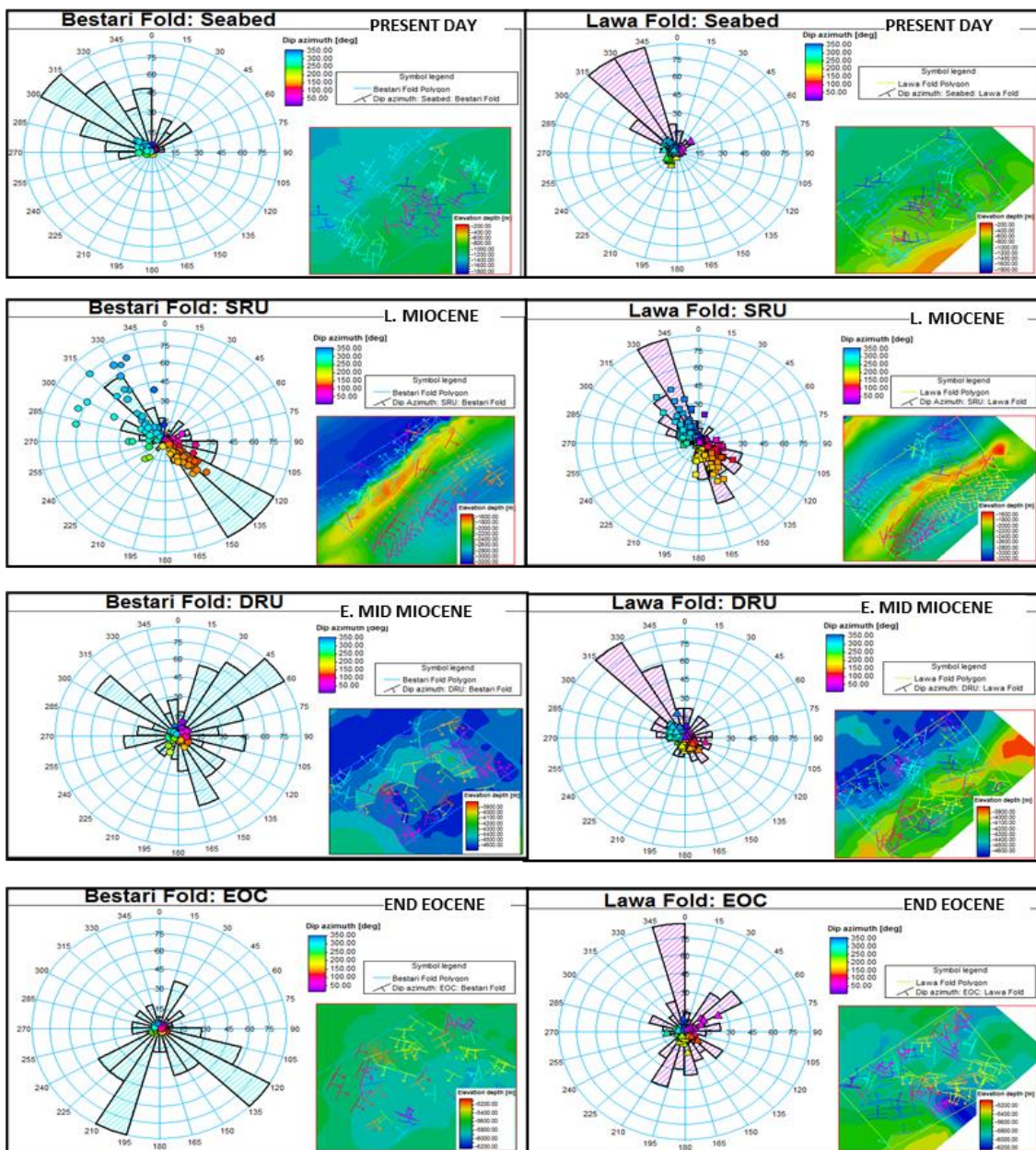


Appendix 5B: Variance cube time slices at different depths showing the fold trends and variations

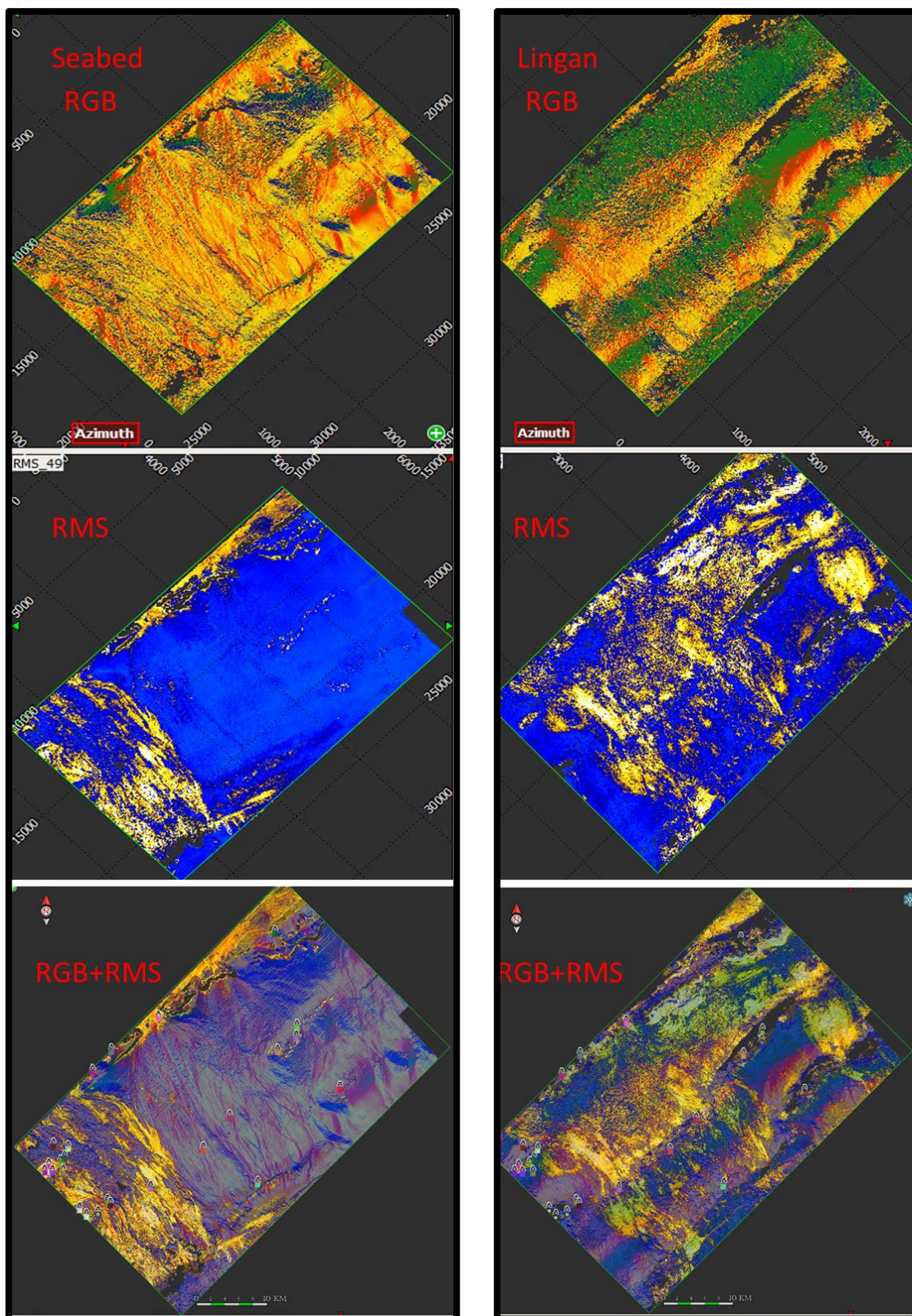
Open



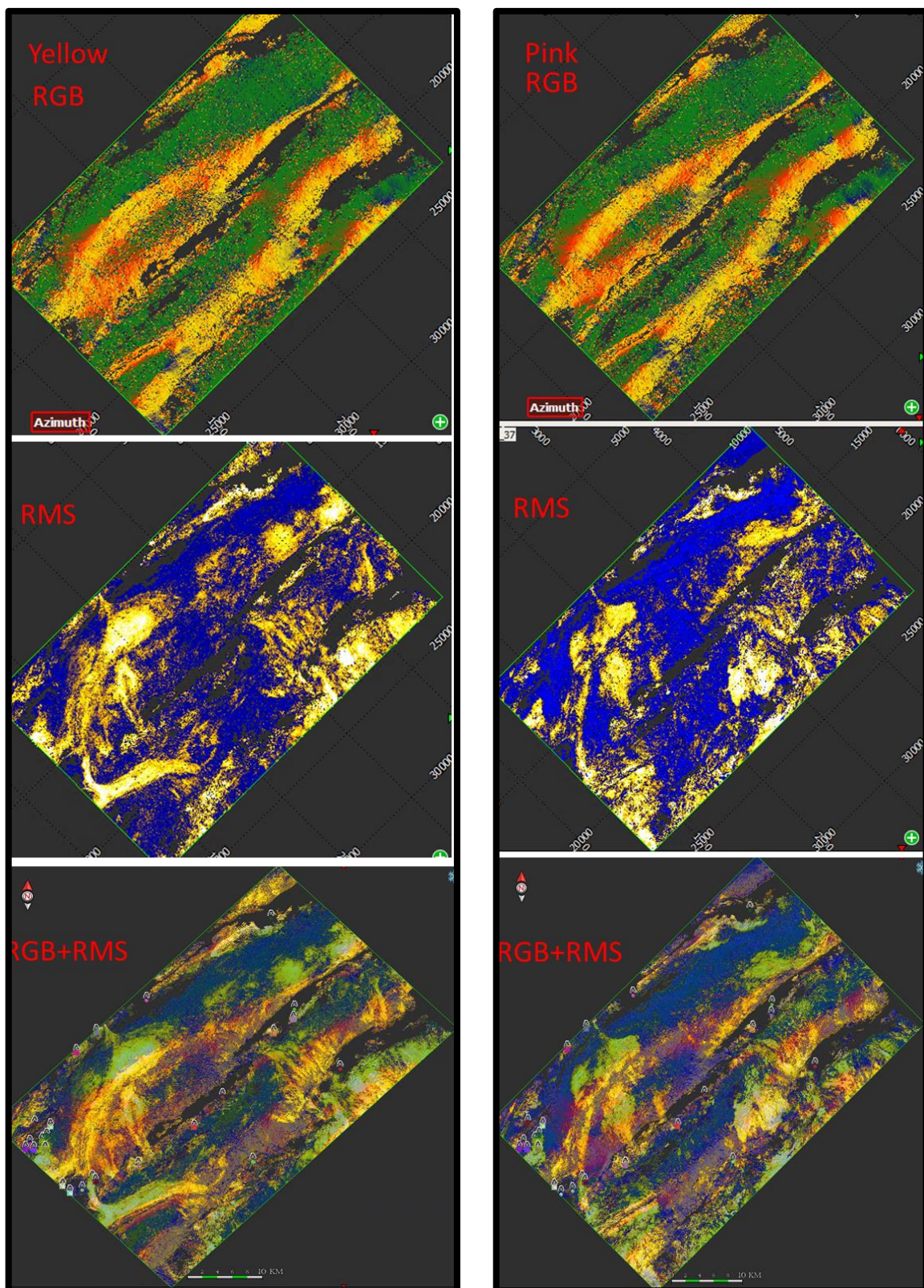
Appendix 6A: Stereonet plot of the azimuth and dip of the Limbayong and Menawan



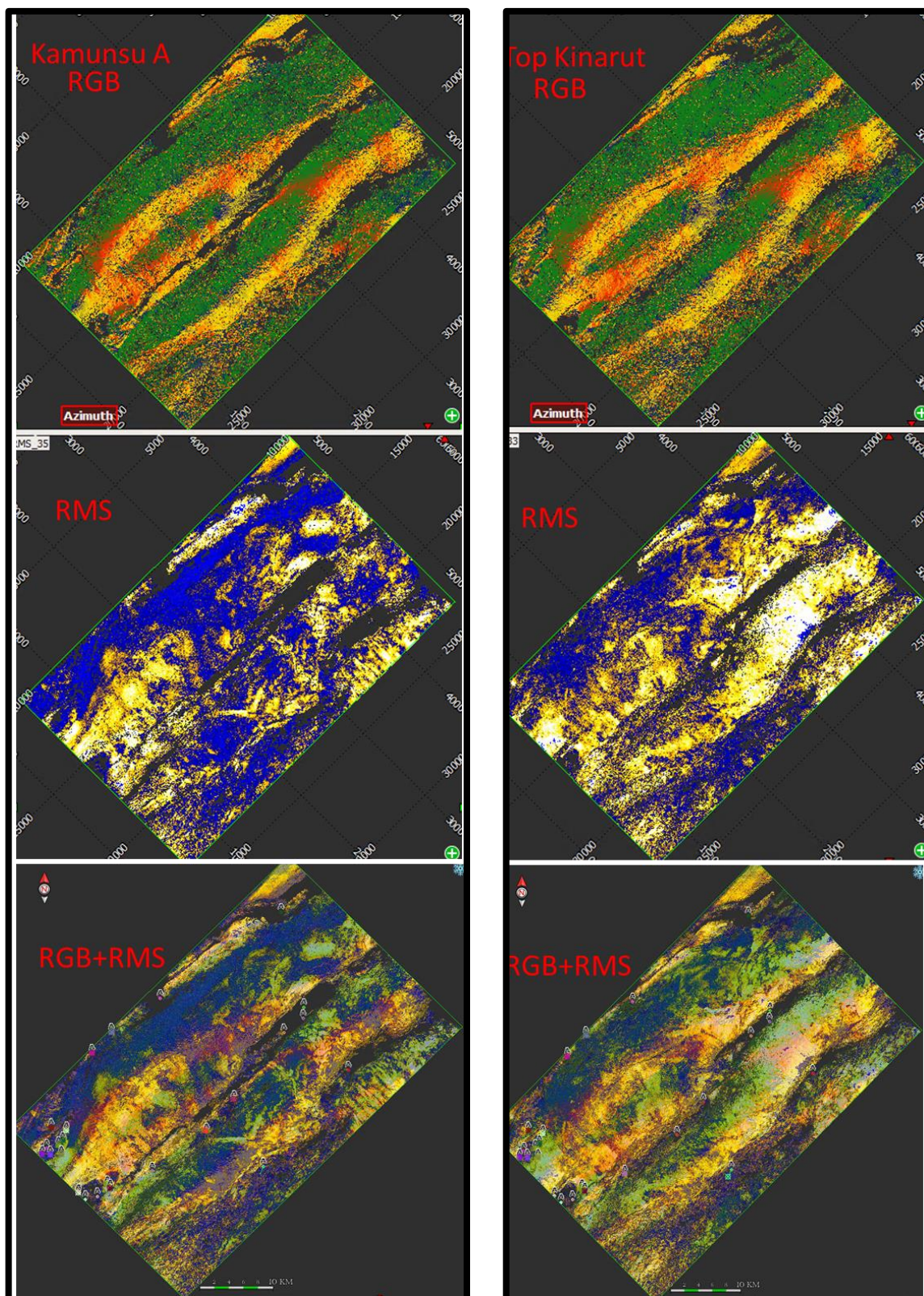
Appendix 6B: Stereonet plot of the azimuth and dip of the Bestari and Lawa



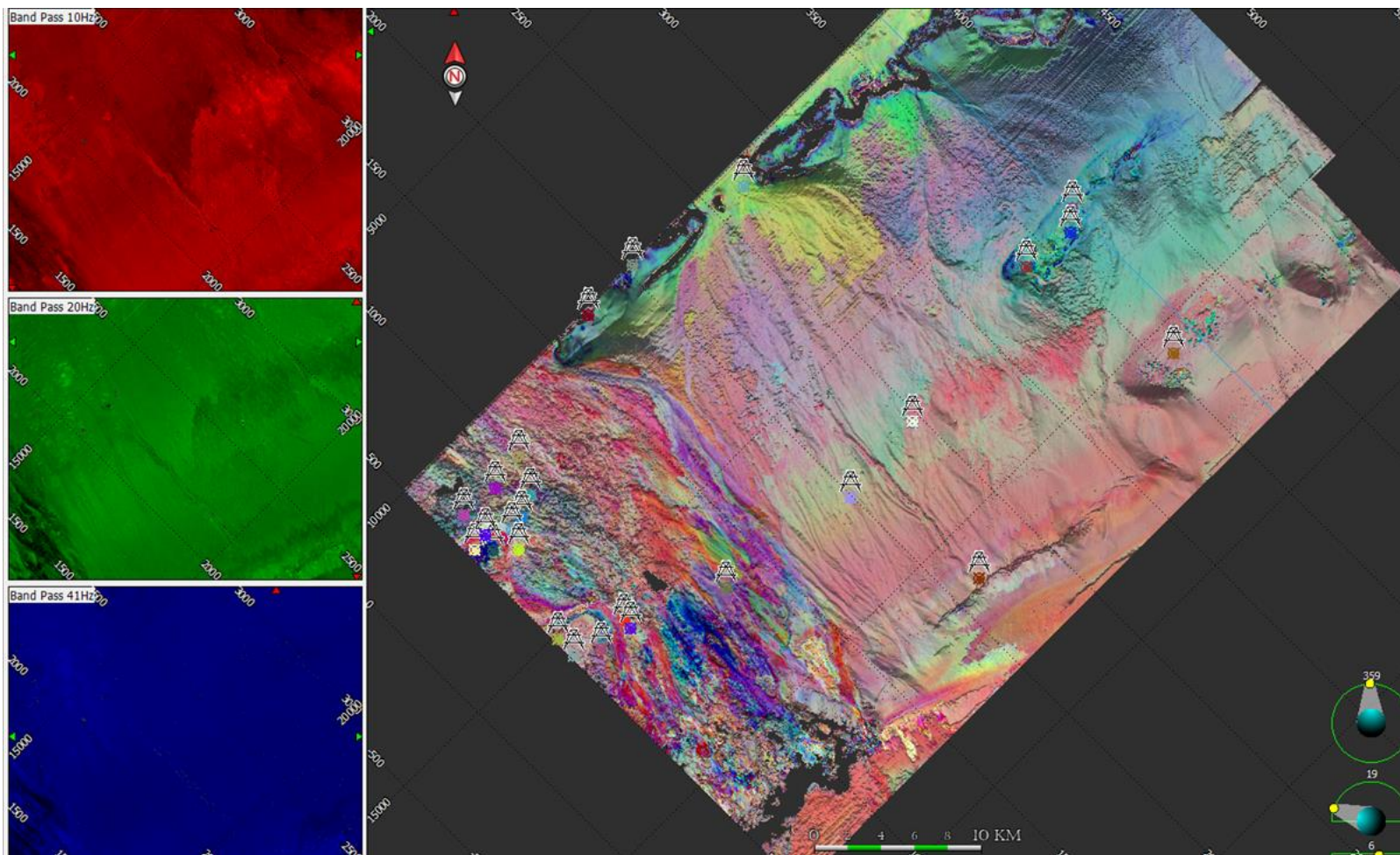
Appendix 7A: RGB, RMS attribute and blending of both attributes for Seabed and Lingan submarine fan



Appendix 7B: RGB, RMS attribute and blending of both attributes for Yellow and Pink submarine fans

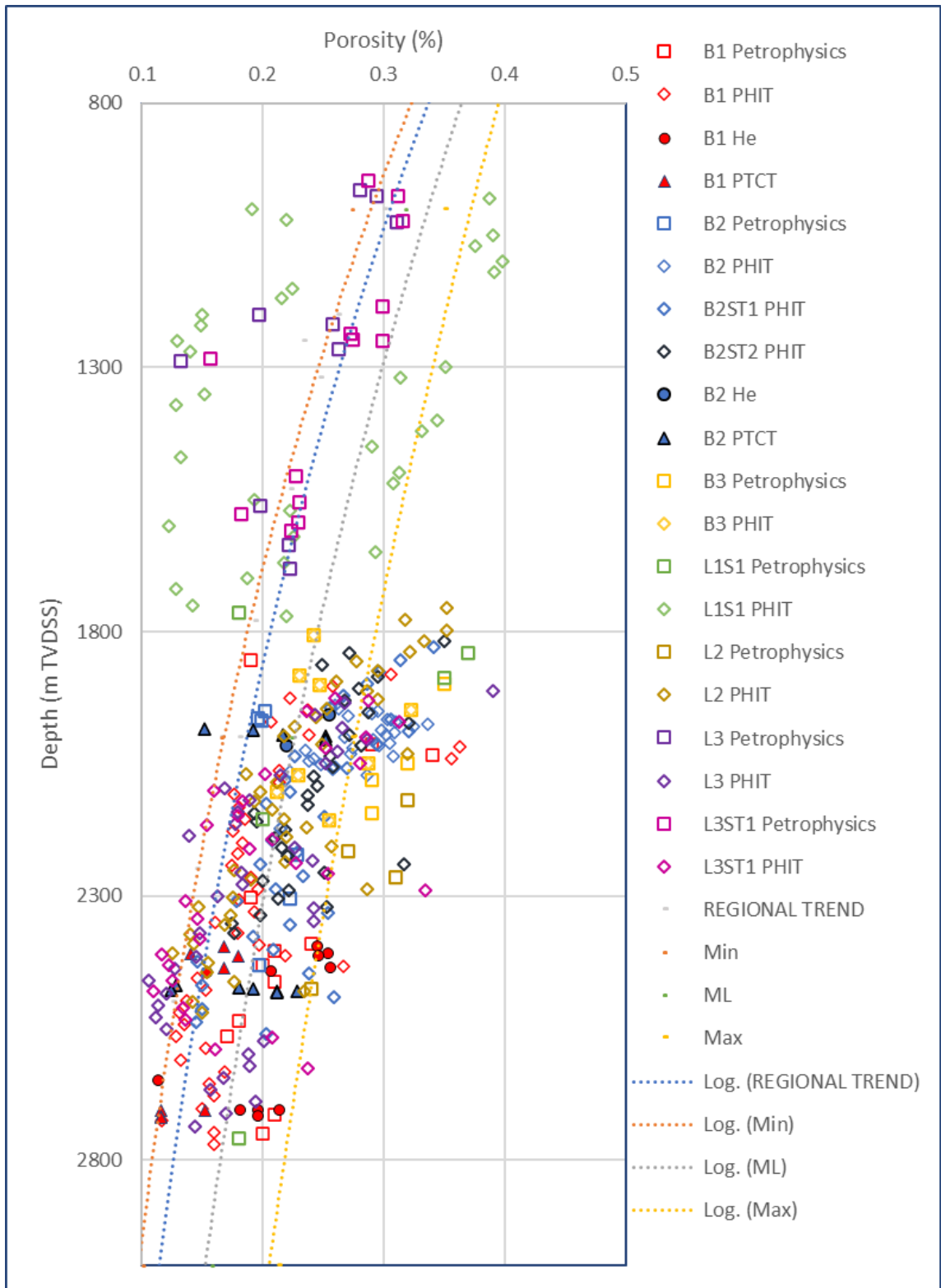


Appendix 7C: RGB, RMS attribute and blending of both attributes for Kamunsu A and Kinarut submarine fans



Appendix 8A: RGB attribute blending of the 10Hz, 20Hz and 41Hz band pass for seabed

Open



Appendix 9A: Porosity plot obtain from well logs (density and sonic) and side-wall core and conventional core thin section point counting and Helium injection.

Bibliography

Abdullah, W.H., Togunwa, O.S., Makeen, Y.M., Hakimi, M.H., Mustapha, K.A., Baharuddin, M.H., Sia, S.G., Tongkul, F., (2017) ‘Hydrocarbon source potential of Eocene-Miocene sequence of Western Sabah, Malaysia’. *Marine and Petroleum Geology* 83, 345–361.

Allwardt, J. R., Michael, G. E., Shearer, C. R., Heppard, P. D., & Ge, H. (2009). 2D modeling of overpressure in a salt withdrawal basin, Gulf of Mexico, USA. *Marine and Petroleum Geology*, 26(4), 464–473.

Athy, L.F., 1930. Introduction to petrophysics of reservoir rocks. *AAPG Bulletin*, 34, 943–61.

Azlina Anuar, Abdul Jalil, Muhamad, (1997) ‘A comparison of source rock facies and hydrocarbon types of the Middle Miocene sequence, offshore NW Sabah Basin, Malaysia’. In: Howes, J.V.C., Noble, R.A. (Eds.), *Proceedings of the IPA Petroleum Systems of SE Asia and Australasia*. Indonesia Petroleum Association, Jakarta, pp.

Back, S. et al. (2005) ‘Stratigraphic development of synkinematic deposits in a large growth-fault system, onshore Brunei Darussalam’, *Journal of the Geological Society*, 162(2), pp. 243–257.

Backé, G. et al. (2009) ‘Two-dimensional geomechanical reconstruction of a deepwater fold and thrust belt: the Baram Delta System, NW Borneo’, *AAPG Hedberg Conference “Deepwater Fold and Thrust Belts”*, October 4-9, 2009, Tirrenia, Italy.

Balaguru, A. and Hall, R. (2009) ‘Tectonic evolution and sedimentation of Sabah, North Borneo, Malaysia’, *American Association of Petroleum Geologists*, 30084(1990), pp. 1–7.

Balaguru, A., Nichols, G. and Hall, R. (2003) 'Tertiary stratigraphy and basin evolution of southern Sabah: implications for the tectono-stratigraphic evolution of Sabah, Malaysia', *Bull. Geol. Soc. Malaysia*, 47, pp. 27–49.

Barckhausen, U. et al. (2014) 'Evolution of the South China Sea: Revised ages for breakup and seafloor spreading', *Marine and Petroleum Geology*. Elsevier Ltd, 58(PB), pp. 599–611.

Beaubouef, R.T., Rossen, C., Zelt, F.B., Sullivan, D.C., Mohrig, D.C., Jennette, D.C., 1999. Deep-water sandstones, Brushy Canyon Formation, West Texas: AAPG Continuing Education Course Notes Series, 40pp.

Booth, J. R., A.E. DuVernay III, D. S. Pfeiffer, and M. J. Styzen, 2000, Sequence stratigraphic framework, depositional models, and stacking patterns of ponded and slope fan systems in the Auger Basin: central Gulf of Mexico slope, in P. Weimer, R. M. Slatt, J. L. Coleman, N. Rosen, C. H. Nelson, A. H. Bouma, M. Styzen, and D. T. Lawrence, eds., *Global Deep-Water Reservoirs: Gulf Coast Section SEPM Foundation 20th Annual Bob F. Perkins Research Conference*, p. 82-103.

Bowers, G. L., 1994, Pore pressure estimation from velocity data: Accounting for overpressure mechanisms besides under-compaction: Presented at the 1994 International Association of Drilling Contractors/SPE Drilling Conference, 515–530.

Bowers, G. L., 1995, Pore pressure estimation from velocity data: Accounting for overpressure mechanisms besides under compaction: *SPE Drilling & Completion*, v. 10, no. 2, p. 89–95, doi:10.2118/27488-PA.

Bowers, G.L., 2001. Determining an appropriate pore pressure estimation strategy. In: OTC 13042 Paper Presented at OTC Conference, Houston, TX, April 30 - May3, 2001.

Bowers, G.L., 2002. Detecting high overpressure. *Lead. Edge* 21 (2), 174-177.

Burgess, P.M., Hovius, N., 1998. Rates of delta progradation during highstands: consequences for timing of deposition in deep-marine systems. *Journal of the Geological Society of London* 155, 217e222.

Carvajal, C., Steel, R., Petter, A., 2009. Sediment supply: the main driver of shelf- margin growth. *Earth-Sci. Rev.* 96, 221e248.

Casson, N. et al. (1998) 'Modern morphology - ancient analogue: insights into deep water sedimentation on the active tectonic margin of West Sabah (abs.)', In: GEOSEA '98, Ninth Regional Congress on Geology, Mineral and Energy Resources of Southeast Asia, (August), pp. 141–143.

Casson, N. et al. (1999) 'Modern morphology - ancient analogue: insights into deep water sedimentation on the active tectonic margin of west Sabah', *Bulletin of the Geological Society of Malaysia*, 43(August), pp. 399–405. doi: 10.7186/bgsm43199940.

Catuneanu, O., Abreu, V., Bhattacharya, J.P., Blum, M.D., Dalrymple, R.W., Eriksson, P.G., Fielding, C.R., Fisher, W.L., Galloway, W.E., Gibling, M.R., Giles, K.A., Holbrook, J.M., Jordan, R., Kendall, C.G.S.C., Macurda, B., Martinsen, O.J., Miall, A.D., Neal, J.E., Nummedal, D., Pomar, L., Posamentier, H.W., Pratt, B.R., Sarg, J.F., Shanley, K.W., Steel, R.J., Strasser, A., Tucker, M.E., Winker, C., 2009. Towards the standardization of sequence stratigraphy. *Earth-Science Rev.* 92, 1–33. <https://doi.org/10.1016/j.earscirev.2008.10.003>

Catuneanu, O., Bhattacharya, J.P., Blum, M. D., Dalrymple, R.W., Eriksson, P. G., Fielding, C. R., Fisher, W. L., Galloway, W. E., Gianolla, P., Gibling, M. R., Giles, K. A., Holbrook, J. M., Jordan, R., Kendall, C. G. St. C., Macur- da, B., Martinsen, O. J., Miall, A.D., Nummedal, D., Posamentier, H.W., Pratt, B. R., Shanley, K.W., Steel, R. J., Strasser, A., Tucker, M.E., 2010. Sequence stratigraphy: common ground after three decades of development. *First Break* 28, 21–34.

Clark, I.R., Cartwright, J.A., 2009. Interactions between submarine channel systems and deformation in deep-water fold belts: examples from the Levant Basin, Eastern Mediterranean Sea. *Mar. Pet. Geol.* 26, 1465e1482.

Couzens-Schultz, B. A. and Azbel, K. (2014) 'Predicting pore pressure in active fold-thrust systems: An empirical model for the deepwater Sabah foldbelt', *Journal of Structural Geology*. Elsevier Ltd, 69(PB), pp. 465–480.

Cullen, A. B. (2010) 'Transverse segmentation of the Baram-Balabac Basin, NW Borneo: refining the model of Borneo's tectonic evolution', *Petroleum Geoscience*, 16(1), pp. 3–29.

Cullen, A. et al. (2010) 'Rifting of the South China Sea: new perspectives', *Petroleum Geoscience*, 16(3), pp. 273–282.

Daniel, R. B. (2001). Pressure prediction for a Central Graben wildcat well, UK North Sea. *Marine and Petroleum Geology*, 18(2), 235–250.

Dimitrios Charlaftis, Stuart J. Jones, Katherine J. Dobson, Jonathan Crouch, Sanem Acikalin; Experimental study of chlorite authigenesis and influence on porosity maintenance in sandstones. *Journal of Sedimentary Research* 2021; 91 (2): 197–212. doi: <https://doi.org/10.2110/jsr.2020.122>

Ding, W. et al. (2013) 'Seismic stratigraphy and tectonic structure from a composite multi-channel seismic profile across the entire Dangerous Grounds, South China Sea', *Tectonophysics*, 582, pp. 162-167.

Dutta, N. C., 2002, Deepwater geohazard prediction using prestack inversion of large offset P -wave data and rock model: *The Leading Edge*, v. 21, no. 2, p. 193–198, doi:10.1190/1.1452612.

Dutta, N. C., 2016, Effect of chemical diagenesis on pore pressure in argillaceous sediment: *The Leading Edge*, v. 35, no. 6, p. 523–527, doi:10.1190/tle35060523.1. faulting: *Bulletin of the Geological Society of America*, v. 70, p. 115–166.

Flemings, P.B., and Lupa, J.A., 2004, Pressure prediction in the Bullwinkle Basin through petrophysics and flow modeling (Green Canyon 65, Gulf of Mexico): *Marine and Petroleum Geology*, v. 21, no. 10, p. 1311–1322.

Franke, D. et al. (2008) ‘Seismic images of a collision zone offshore NW Sabah/Borneo’, *Marine and Petroleum Geology*, 25(7), pp. 606–624.

Gee, M. J. R. et al. (2007) ‘The Brunei slide: A giant submarine landslide on the Northwest Borneo Margin revealed by 3D seismic data’, *Marine Geology*, 246(1), pp. 9–23.

Giorgetti, G., Mata, P. & Peacor, D.R. 2000. TEM study of the mechanism of transformation of detrital kaolinite and muscovite to illite/smectite in sediments of the Salton Sea Geothermal Field. *European Journal of Mineralogy*, 12, 923–934.

Goult, N.R., Ramdhan, A.M., Jones, S.J., 2012. Chemical compaction of mud-rocks in the presence of overpressure. *Petrol. Geosci.* 18, 471e479.

Grant, C. J. (2004) ‘The Upper Miocene deepwater fans of Northwest Borneo’, *Indonesian Petroleum Association Proceedings, Deepwater And Frontier Exploration in Asia & Australasia Symposium, December 2004*.

Grant, C., 2006. The Upper Miocene deepwater fans of northwest Borneo: *Indonesian Petroleum Association proceedings, Deepwater and frontier symposium*.

Grant, N.T., Middleton, A.J., and Archer, S., 2014, Porosity trends in the Skagerrak Formation Central Graben, United Kingdom Continental Shelf: The role of compaction and pore pressure history: *AAPG Bulletin*, v. 6, no. 6, p. 1111–1143.

Grech, M., Flint, S., Potts, G., Wickens, D., and Johnson, S., 2003, Partial ponding of turbidite systems in a basin with subtle growth-fold topography: Laingsburg–Karoo, South Africa: *Journal of Sedimentary Research*, v. 73, p. 603–620.

- Groshong R. (2006) Structural validation, restoration and prediction. In: 3-D structural geology: a practical guide to quantitative surface and subsurface map interpretation. Birkhäuser, Basel, pp 305–372.
- Hall, R. & Blundell, D. (eds), (1996) ‘Tectonic Evolution of Southeast Asia’, Geological Society Special Publication, 106, pp. 539-547.
- Hall, R. (1996) ‘Reconstructing Cenozoic SE Asia’, Geological Society, London, Special Publications, 106(1), pp. 153–184.
- Hall, R. (1997) ‘Cenozoic plate tectonic reconstructions of SE Asia’, Geological Society, London, Special Publications, 126(1), pp. 11–23.
- Hall, R. (2013) ‘Contraction and extension in Northern Borneo driven by subduction rollback’, *Journal of Asian Earth Sciences.*, 76, pp. 399–411.
- Hall, R. (2014) ‘The Origin of Sundaland’, *Proceedings of Sundaland Resources 2014 MGEI Annual Convention*, (November), pp. 1–26.
- Hall, R. and Nichols, G. J. (2002) ‘Cenozoic sedimentation and tectonics in Borneo: climatic influences on orogenesis’, Geological Society, London, Special Publications, 191(1), pp. 5–22.
- Hall, R., Cottam, M. a. and Wilson, M. E. J. (2011) ‘The SE Asian gateway: history and tectonics of the Australia-Asia collision’, Geological Society, London, Special Publications, 355(1), pp. 1–6.
- Hantschel, T., and Kauerauf, A.I., 2009, *Fundamentals of basin and petroleum systems modelling*: Springer-Verlag, Berlin, 1-476 p.
- Haq, B. U., J. Hardenbol, and P. R. Vail, 1987, *Chronology of fluctuating sea levels since the Triassic*: *Science*, v. 235, p. 1156-1166.

Harris, A.D., Baumgardner, S.E., Sun, T., and Granjeon, D., 2018, A poor relationship between sea level and deep-water sand delivery: *Sedimentary Geology*, v. 370, p. 42–51, <https://doi.org/10.1016/j.sedgeo.2018.04.002>.

Hart, B. S., P. B. Flemings, and A. Deshpande, 1995, Porosity and pressure: Role of compaction disequilibrium in the development of geo-pressures in a Gulf Coast Pleistocene basin: *Geology*, 23, 45–48.

Helland-Hansen, W., Hampson, G. J., 2009. Trajectory analysis: concepts and applications. *Basin Research* 21, 454–483.

Hennig, A., Yassir, N. A., Addis, M. A., & Warrington, A. (2002). Pore-pressure estimation in an active thrust region and its impact on exploration and drilling. In Huffman, A. R. & Bowers, G. L. (Eds.), *Pressure regimes in sedimentary basins and their prediction*, AAPG memoir (Vol. 76, pp. 89–105). AAPG.

Hesse, S., Back, S. and Franke, D. (2009) ‘The deep-water fold-and-thrust belt offshore NW Borneo: Gravity-driven versus basement-driven shortening’, *Bulletin of the Geological Society of America*, 121(5–6), pp. 939–953.

Hesse, S., Back, S. and Franke, D. (2010) ‘The structural evolution of folds in a deepwater fold and thrust belt - a case study from the Sabah continental margin offshore NW Borneo, SE Asia’, *Marine and Petroleum Geology*. Elsevier Ltd, 27(2), pp. 442–454.

Hodgson, D.M., Bernhardt, A., Clare, M.A., Da Silva, A.C., Fosdick, J.C., Mauz, B., Midtkandal, I., Owen, A., Romans, B.W., 2018. Grand challenges (And great opportunities) in sedimentology, stratigraphy, and diagenesis research. *Front. Earth Sci.* 6, 1–9. <https://doi.org/10.3389/feart.2018.00173>

Hoesni J (2004) *Origins of Overpressure in the Malay Basin and its Influence on Petroleum Systems*, PhD thesis. University of Durham, UK.

Hovius, N., Controls on sediment supply by large rivers, in *Relative Role of Eustasy, Climate, and Tectonism in Continental Rocks*, edited by K.W. Shanley, pp. 3–16, SEPM Society for Sedimentary Geology Special Publication, 1998.

Hubbert, M., and Rubey, W.W., 1959, Role of fluid pressure in mechanics of overthrust
 Hutchison, C. S. (1995) 'Melange on the Jerudong Line, Brunei Darussalam, and its regional significance', Geological Society of Malaysia Bulletin, in press.

Hutchison, C. S. (1996) 'The "Rajang accretionary prism" and "Lupar Line" problem of Borneo', Geological Society Special Publication, 106(106), pp. 247–261. doi: 10.1144/GSL.SP.1996.106.01.16.

Hutchison, C. S. (2004) 'Marginal basin evolution: The southern South China Sea', Marine and Petroleum Geology, 21(9), pp. 1129–1148.

Hutchison, C. S. (2010) 'The North-West Borneo Trough', Marine Geology. Elsevier B.V., 271(1–2), pp. 32–43. Hutchison, C. S. (2014) 'Tectonic evolution of Southeast Asia', Bulletin of the Geological Society of Malaysia, 60(December), pp. 1–18.

Hutchison, C. S. et al. (2000) 'A Miocene collisional belt in North Borneo: uplift mechanism and isostatic adjustment quantified by thermochronology', Journal of the Geological Society, 157(4), pp. 783–793.

Ingram, G. M. et al. (2004) 'Deepwater Northwest Borneo: Hydrocarbon accumulation in an active fold and thrust belt', Marine and Petroleum Geology, 21(7), pp. 879–887.

Ingram, G.M., Chisholm, T.J., Grant, C.J., Hedlund, C.A., Stuart-Smith, P., Teasdale, J., 2004. Deepwater Northwest Borneo: hydrocarbon accumulation in an active fold and thrust belt. Mar. Petrol. Geol. 21, 879e887.

Ismail, A., H.F. Ewida, M.G. Al-Ibiary, S. Gammaldi, A. Zollo 'Identification of gas zones and chimneys using seismic attributes analysis at the Scarab field, Offshore, Nile Delta, Egypt', Petroleum Research, 5 (2019), pp. 59-69,

Jong, J., Khamis, M. A., Wan M Zaizuri Wan Embong, Yoshiyama, T. and Gillies, D., 2016. A Sequence Stratigraphic Case Study of an Exploration Permit in Deepwater Sabah: Comparison and Lesson Learned from Pre- Versus Post-Drill Evaluation,

Proceedings of the 39th IPA Convention and Exhibition, Jakarta Convention Centre, 25-27 May 2016.

King, R. C. and Morley, C. K. (2017) 'Wedge Geometry and Detachment Strength in Deepwater Fold-Thrust Belts', *Earth-Science Reviews*. Elsevier B.V., 165, pp. 268–279.

King, R. C. et al. (2009) 'Present-day stress and neotectonic provinces of the Baram Delta and deep-water fold–thrust belt', *Journal of the Geological Society*, 166(2), pp. 197–200.

King, R. C. et al. (2010) 'Balancing deformation in NW Borneo: Quantifying plate-scale vs. gravitational tectonics in a delta and deepwater fold-thrust belt system', *Marine and Petroleum Geology*. 27(1), pp. 238–246.

King, R. C. et al. (2010) 'Present-day stress orientations and tectonic provinces of the NW Borneo collisional margin', *Journal of Geophysical Research: Solid Earth*, 115(10), pp. 1–15.

Kneller, B. C., and W. D. McCaffrey, 1995, Modeling the effects of salt-induced topography on deposition from turbidity currents, *in* C. J. Travis, H. Harrison, M. R. Hudec, B. C. Vendeville, F. J. Peel, and R. F. Perkins, eds., *Salt, sediment and hydrocarbons: Gulf Coast Section SEPM*, p. 137–145.

Kumar, A. et al. (2016) 'Origin and distribution of abnormally high pressure in the Mahanadi Basin, east coast of India Technical papers, Origin and distribution of abnormally high pressure in the Mahanadi Basin, east coast of India', (October 2018).

Lahann, R. W., and R. E. Swarbrick, 2011, Overpressure generation by load transfer following shale framework weakening due to smectite diagenesis: *Geofluids*, 11, 362–375, doi: 10.1111/j.14688123.2011.00350. x.

Lahann, R., 2002. Impact of smectite diagenesis on compaction modelling and compaction equilibrium. In: Huffman, A.R., Bowers, G.L. (Eds.), *Pressure Regimes in Sedimentary Basins and Their Prediction*. AAPG, Tulsa, pp. 61e72.

- Lahann, R.W., Lahann, C., McCarty, D., Hsieh, J., 2001. Influence of Clay Diagenesis on Shale Velocities and Fluid Pressure. Offshore Technology Conference, Houston.
- Lee, T. Y. and Lawver, L. A. (1994) 'Cenozoic plate reconstruction of the South China Sea region', *Tectonophysics*, 235(1–2), pp. 149–180.
- Legrand, X. et al. (2015) 'A new Source-to-Sink approach to petroleum systems and prospectivity evaluation in deep-water: case study from Sabah', Asia Petroleum Geoscience Conference and Exhibition, October 2015.
- Mazlan, M., Leong, K.M., Azlina Anuar, (1999) 'Sabah Basin. The Petroleum Geology and Resources of Malaysia'. Percetakan Mega, Kuala Lumpur, pp. 501-538.
- Milliman, J. D. and Syvitski, J. P. (1992). Geomorphic/tectonic control of sediment discharge to the ocean: the importance of small mountainous rivers. *The Journal of Geology*, 525-544.
- Milsom, J. et al. (1997) 'Gravity anomalies and deep structural controls at the Sabah-Palawan margin, South China Sea', Geological Society, London, Special Publications, 126(1), pp. 417–427.
- Morley, C. (2009) 'Geometry of an oblique thrust fault zone in a deepwater fold belt from 3D seismic data', *Journal of Structural Geology*. Elsevier Ltd, 31(12), pp. 1540–1555.
- Morley, C. et al. (2009) 'Present-day stress field of Southeast Asia', *Tectonophysics*, 482(1–4), pp. 92–104.
- Morley, C. K. (2002) 'A tectonic model for the Tertiary evolution of strike-slip faults and rift basins in SE Asia', *Tectonophysics*, 347(4), pp. 189–215.
- Morley, C. K. and Guerin, G. (1996) 'Comparison of gravity-driven deformation styles', *Tectonics*, 15(6), pp. 1154–1170.

Morley, C. K. et al. (2003) 'Characteristics of repeated, detached, Miocene-Pliocene tectonic inversion events, in a large delta province on an active margin, Brunei Darussalam, Borneo', *Journal of Structural Geology*, 25(7), pp. 1147–1169.

Morley, C. K. et al. (2005) 'Present-day stress orientation in Brunei: a snapshot of "Prograding tectonics" in a Tertiary delta', *Journal of the Geological Society*, 162(1), pp. 39–49.

Morley, C. K. *et al.* (2011) 'Deepwater fold and thrust belt classification, tectonics, structure and hydrocarbon prospectivity: A review', *Earth-Science Reviews*. Elsevier B.V., 104(1–3), pp. 41–91. doi: 10.1016/j.earscirev.2010.09.010.

Morley, C.K., 2003a. Mobile shale related deformation in large deltas developed on passive and active margins: review and new views. In: Van Rensbergen, P.R., Hillis, R., Maltman, A., Morley, C.K. (Eds.), *Subsurface Sediment Mobilization: Geol. Soc. Lond. Spec. Pub.*, 216, pp. 335–357.

Morley, C.K., 2003b. Outcrop examples of mudstone intrusions from the Jerudong anticline, Brunei Darussalam, and inferences for hydrocarbon reservoirs. In: Van Rensbergen, P.R., Hillis, R., Maltman, A., Morley, C.K. (Eds.), *Subsurface Sediment Mobilization: Geol. Soc. Lond. Spec. Pub.*, 216, pp. 381–394.

Morley, C.K., 2007a. Interaction between critical wedge geometry and sediment supply in a deepwater fold belt, NW Borneo. *Geology* 35, 139–142.

Moscardelli, L., Wood, L., Mann, P., 2006. Mass-transport complexes and associated processes in the offshore area of Trinidad and Venezuela. *AAPG Bull.* 90, 1059e 1088.

Muto, T., and Steel, R.J., 2002, In defense of shelf-edge delta development during falling and lowstand of relative sea level: *Journal of Geology*, v. 110, p. 421–436.

Nadeau, P.H., Peacor, D.R., Yan, J. & Hillier, S. 2002. I–S precipitation in pore space as the cause of geopressuring in Mesozoic mudstones, Egersund Basin, Norwegian continental shelf. *American Mineralogist*, 87, 1580–1589.

Neumaier, M., Littke, R., Hantschel, T., Maerten, L., Joonnekindt, J., & Kukla, P. (2014). Integrated charge and seal assessment in the Monagas fold and thrust belt of Venezuela. *AAPG Bulletin*, 98(7), 1325–1350.

Nguyen, B.T.T., Jones, S.J., Goult, N.R., Middleton, A.J., Grant, N., Ferguson, A., and Bowen, L., 2013, The role of fluid pressure and diagenetic cements for porosity preservation in Triassic fluvial reservoirs of the Central Graben, North Sea: *AAPG Bulletin*, v. 97, no. 8, p.1273–1302.

Nor Azidin, Nor Farhana, Balaguru, A., Ahmad, Nasaruddin, (2011) ‘Structural Styles of the Northwest Sabah and Sulawesi Fold Thrust Belt Regions and its Implications to the Petroleum System-a Comparison’. Conference Proceedings, PGCE 2011, Jul 2011, cp-251-00067.

O’neill, S.R., 2018, Evolution and distribution of pore pressure across the Taranaki Basin, New Zealand, Durham theses, Durham University.

O’neill, S.R., Stuart J. Jones, Peter J.J. Kamp; Diagenesis and burial history modeling of heterogeneous marginal marine to shoreface Paleocene glauconitic sandstones, Taranaki Basin, New Zealand. *Journal of Sedimentary Research* 2020; 90 (6): 651–668.

Obradors-Prats, J. *et al.* (2017) ‘Hydromechanical Modeling of Stress, Pore Pressure, and Porosity Evolution in Fold-and-Thrust Belt Systems’, *Journal of Geophysical Research: Solid Earth*, 122(11), pp. 9383–9403. doi: 10.1002/2017JB014074.

Obradors-Prats, J., Rouainia, M., Aplin, A. C., & Crook, A. J. L. (2016). Stress and pore pressure histories in complex tectonic settings predicted with coupled geomechanical-fluid flow models. *Marine and Petroleum Geology*, 76, 464–477.

Obradors-Prats, J., Rouainia, M., Aplin, A. C., & Crook, A. J. L. (2019). A diagenesis model for geomechanical simulations: Formulation and implications for pore pressure and development of geological structures. *Journal of Geophysical Research: Solid Earth*, 124, 4452–4472.

- O'Conner, S., Swarbrick, R.E., Lahann, R.W., 2011. Geologically driven pore fluid pressure models and their implications for petroleum exploration. Introduction to thematic set. *Geofluids* 11 (4), 343e348.
- Oluboyo, A.P., Gawthorpe, R.L., Bakke, K., Hadler-Jacobsen, F., 2014. Salt tectonic controls on deep-water turbidite depositional systems: Miocene, southwestern Lower Congo Basin, offshore Angola. *Basin Res.* 26, 597e620.
- Ortiz-Karpf, A., Hodgson, D.M., Jackson, C.A.L. & McCaffrey, W.D. 2018. Mass-transport complexes as markers of deep-water fold-and-thrust belt evolution: insights from the southern Magdalena fan, offshore Colombia. *Basin Research*, 30, 65-88.
- Osborne, M.J., Swarbrick, R.E., 1997. Mechanisms for generating overpressure in sedimentary basins: re-evaluation. *AAPG Bull.* 81, 1023e1041.
- Oye, O., Aplin, A.C., Jones, S., Gluyas, J., Bowen, L., Orland, I., and Valley, J., 2018, Vertical effective stress as a control on quartz cementation in sandstones: *Marine and Petroleum Geology*, v. 98, p. 640–652.
- Oye, O.J., Aplin, A.C., Jones, S.J., Gluyas, J.G., Bowen, L., Harwood, J., Orland, I.J., Valley, J.W., 2020. Vertical effective stress and temperature as controls of quartz cementation in sandstones: Evidence from North Sea Fulmar and Gulf of Mexico Wilcox sandstones. *Mar.Pet.Geol.* 115, 104289. <https://doi.org/10.1016/j.marpetgeo.2020.104289>.
- Panpichityota, N., Morley, C.K., Ghosh, J., (2018) 'Link between growth faulting and initiation of a mass transport deposit in the northern Taranaki Basin, New Zealand', *Basin Research*, 30, 237–248.
- Pepper, A.S. and Corvi, P.J., 1995. Simple kinetic models of petroleum formation. Part 1: Oil and gas generation from kerogen. *Marine and Petroleum Geology*, Vol. 12, No. 3, p 291–319.

Pickering, K.T., and Corregidor, J., 2005, Mass-transport complexes, (MTCs) and tectonic control on basin-floor submarine fans, middle Eocene, south Spanish Pyrenees: *Journal of Sedimentary Research*, v. 75, p. 761–783.

Pinous, O.V., Levchuk, M.A., Sahagian, D.L., 2001. Regional synthesis of the productive Neocomian complex of West Siberia: sequence stratigraphic framework. *American Association of Petroleum Geologists Bulletin* 85 (10), 1713–1730.

Porebski, S. J., Steel, R. J., 2006. Deltas and sea-level change. *Journal of Sedimentary Research* 76, 390–403.

Posamentier, H. W., R. D. Erskine, and R. M. Mitchum Jr., Models for submarine-fan deposits within a sequence-stratigraphic framework. In P. Weimer and M.H. Link (eds.), “Seismic Facies and Sedimentary Processes of Submarine Fans and Turbidite Systems, *Frontiers in Sedimentary Geology.*” Springer-Verlag, New York, NY. https://doi.org/10.1007/978-1-4684-8276-8_6

Posamentier, H.W., and G.P. Allen, “Siliciclastic Sequence Stratigraphy —Concepts and Applications.” *Soc. Econ. Paleo. and Mineral. (SEPM) Concepts in sedimentology and paleontology*, No. 7, (1999), 210 pp.

Posamentier, H.W., and P. Weimer, Siliciclastic sequence stratigraphy and petroleum geology — Where to from here? *Amer. Assoc. Pet. Geol. Bull.*, 77, (1993), 731-742.

Radovich, B. J., and R. B. Oliveros, 1998, 3-D sequence interpretation of seismic instantaneous attributes from the Gorgon field: *The Leading Edge*, v. 17, p. 1286–1293.

Radovich, B. J., and Oliveros, R. B., 1998, 3-D sequence interpretation of seismic instantaneous attributes from the Gorgon field: *The Leading Edge*, 17, 1286–1293.

Ramdhan, A. M., and N. R. Goultly, 2011, Overpressure and mud rock compaction in the Lower Kutai Basin, Indonesia: A radical reappraisal: *AAPG Bulletin*, 95, 1725–1744, doi: 10.1306/02221110094.

- Ramdhan, A.M., Goult, N.R., 2010. Overpressure-generating mechanisms in the Peciko Field, Lower Kutai Basin, Indonesia. *Petrol. Geosci.* 16, 367e376.
- Rangin, C. et al. (1990) 'Neogene arc-continent collision in Sabah, Northern Borneo (Malaysia)', *Tectonophysics*, 183(1–4), pp. 305–319.
- Ruth, P. J. Van, Hillis, R. R. and Swarbrick, R. E. (2002) 'Detecting overpressure using porosity-based techniques in the Carnarvon Basin, Australia'. *APPEA Journal*
- Saller, A. and Blake, G. (2003) 'Sequence Stratigraphy and Syndepositional Tectonics of Upper Miocene and Pliocene Deltaic Sediments, Offshore Brunei Darussalam', *Tropical Deltas of Southeast Asia*, pp. 219–234. doi: 10.2110/pec.03.76.0219.
- Sargent, C., P. Andras, N. R. Goult, and A. C. Aplin, 2015, Compaction and overpressure in the Sergipe-Alagoas Basin, in *GeoPOP3 Final Report: Durham*, p. 199–232.
- Sathar, S. and Jones, S. (2016) 'Fluid overpressure as a control on sandstone reservoir quality in a mechanical compaction dominated setting: Magnolia Field, Gulf of Mexico', *Terra Nova*, 28(3), pp. 155–162. doi: 10.1111/ter.12203.
- Scherer, F.C., (1980) 'Exploration in East Malaysia over the past decade'. In: Halbouty, M.T. (Ed.), *Giant Oil and Gas Fields of the Decade 1968-1978*, vol. 30. AAPG Memoir, pp. 423e440.
- Schlische, R. W. et al. (2014) 'Quantifying the geometry, displacements, and subresolution deformation in thrust-ramp anticlines with growth and erosion: From models to seismic-reflection profile', *Journal of Structural Geology*. 69, pp. 304–319.
- Scotese, C. R. and Parrish, J. T. (2004) 'A Continental Drift Flipbook', *Journal of Geology*, 112(6), pp. 729–741.

Sidi, F. H., Nummendal, D., Imbert, P., Darman, H. & Posamentier, H. W. 2003. Tropical Deltas of SE Asia – Sedimentology, Stratigraphy and Petroleum Geology. SEPM Special Publication 76

Sømme, T., Howell, J.A., Hampson, G.J. and Storms, J.E.A. (2008) Genesis, architecture, and numerical modeling of intra-parasequence discontinuity surfaces in wave-dominated deltaic deposits: Upper Cretaceous Sunnyside Member, Blackhawk Formation, Book Cliffs, Utah, USA. In: Recent Advances in Models of Siliciclastic Shallow-Marine Stratigraphy (Eds G.J. Hampson, R.J. Steel, P.M. Burgess and R.W. Dalrymple), SEPM Spec. Publ., 90, 421–441.

Steuer, S. et al. (2014) ‘Oligocene-Miocene carbonates and their role for constraining the rifting and collision history of the Dangerous Grounds, South China Sea’, *Marine and Petroleum Geology*, 58, pp. 644–657.

Stricker, S., 2016, Influence of fluid pressure on the diagenesis of clastic sediments, Durham theses, Durham University.

Stricker, S., and Jones, S.J., 2016, Enhanced porosity preservation by pore fluid overpressure and chlorite grain coatings in the Triassic Skagerrak, Central Graben, North Sea, UK: Geological Society, London, Special Publications, v. 435.

Stricker, S., Jones, S.J., and Grant, N.T., 2016a, Importance of vertical effective stress for reservoir quality in the Skagerrak Formation, Central Graben, North Sea: *Marine and Petroleum Geology*, v. 78, p. 895–909.

Stricker, S., Jones, S.J., Meadows, N., and Bowen, L., 2018, Reservoir quality of fluvial sandstone reservoirs in salt-walled mini-basins: an example from the Seagull field, Central Graben, North Sea, UK: *Petroleum Science*, v. 15, no. 1, p. 1–27.

Stricker, S., Jones, S.J., Sathar, S., Bowen, L., and Oxtoby, N., 2016b, Exceptional reservoir quality in HPHT reservoir settings: Examples from the Skagerrak Formation of the Heron Cluster, North Sea, UK: *Marine and Petroleum Geology*, v. 77, p. 198–215.

Swarbrick, R. E., 2012, Review of pore pressure prediction challenges in high temperature areas: *The Leading Edge*, 31, 1288–1294, doi: 10.1190/tle31111288.1.

Swarbrick, R.E., Osborne, M.J., 1998. Mechanisms that generate abnormal pressures: an overview. In: Law, B.E., Ulmishek, G.F., Slavin, V.I. (Eds.), *Abnormal Pressures in Hydrocarbon Environments*. AAPG, Tulsa, pp. 13e34.

Swarbrick, R.E., Osborne, M.J., Yardley, G.S., 2002. Comparison of overpressure magnitude resulting from the main generating mechanisms. In: Huffman, A.R., Bowers, G.L. (Eds.), *Pressure Regimes in Sedimentary Basins and Their Prediction*. AAPG, Tulsa, pp. 1e12.

Sweet, M.L. and M.D. Blum, 2016, Connections between fluvial to shallow marine environments and submarine canyons: Implications for sediment transfer to deep water, *J. Sediment. Res.*, 86, 1147-1162. doi: 10.2110/jsr.2016.64

Syvitski, J.P.M., and Milliman, J.D., 2007, Geology, geography and humans battle for dominance over the delivery of fluvial sediment to the coastal ocean: *Journal of Geology*, v. 115, p. p. 1–19, doi:10.1086/509246.

Talling, P.J., Amy, L.A. and Wynn, R.B., (2007b), New insights into the evolution of large volume turbidity currents; comparison of turbidite shape and previous modelling results, *Sedimentology*, v. 54, p. 737-769.

Teasdale, J. and Bon, J. (2017) ‘A new plate model for South East Asia aimed at understanding basin evolution’, SEAPEX Exploration Conference 2017, (April).

Terzaghi, K., 1925. Principles of soil mechanics, IV—Settlement and consolidation of clay. *Engineering News-Record*, 95, 874-878.

Terzaghi, K., 1943, *Theoretical Soil Mechanics*: John Wiley & Sons, Inc., Hoboken, NJ, USA.

Thorsen, C. E., 1963, Age of growth faulting in Southeast Louisiana: Gulf Coast Association of Geologists Societies Transactions, v. 13, p. 103–110.

Tingay, M. et al. (2011) ‘Origin of Overpressure and Pore Pressure Prediction in the Baram Delta Province Brunei Province’, Search and Discovery, 40709(March), pp. 65–85.

Tingay, M. et al. (2013) ‘Comparison of modern fluid distribution, pressure and flow in sediments associated with anticlines growing in deepwater (Brunei) and continental environments (Iran)’, Marine and Petroleum Geology. 51, pp. 210–229.

Tingay, M. R. P. et al. (2003) ‘Variation in vertical stress in the Baram Basin, Brunei: Tectonic and geomechanical implications’, Marine and Petroleum Geology, 20(10), pp. 1201–1212.

Tingay, M. R. P. et al. (2005) ‘Present-day stress orientation in Brunei: a snapshot of “prograding tectonics” in a Tertiary delta’, Journal of Structural Geology, 162, pp. 39–49.

Tingay, M. R. P., R. R. Hillis, R. E. Swarbrick, C. K. Morley, and A. R. Damit, 2009, Origin of overpressure and pore pressure prediction in the Baram Delta Province, Brunei: AAPG Bulletin, 93, 51–74, doi: 10.1306/08080808016.

Tingay, M.R.P., Hillis, R.R., Swarbrick, R.E., Morley, C.K., Damit, A.R., 2007. “Vertically transferred” overpressures in Brunei: evidence for a new mechanism for the formation of high magnitude overpressures. *Geology* 35 (11), 1023e1026.

Vail, P.R., R.M. Mitchum Jr., and S. Thompson III, Seismic stratigraphy and global changes of sea level, Part 3: Relative changes of sea level from coastal onlap. In C.E. Payton, (ed.), “Seismic Stratigraphy — Applications to Hydrocarbon Exploration.” Amer. Assoc. Pet. Geol. Memoir 26, (1977), 63-81.

Vail, P.R., Seismic stratigraphy interpretation using sequence stratigraphy. Part 1: Seismic stratigraphy interpretation procedure. In A.W. Bally, (ed.), "Atlas of Seismic Stratigraphy." Amer. Assoc. Pet. Geol. Studies in Geology 27, 1, (1987), 1-10.

Van Rensbergen, P. and Morley, C. K. (2000) '3D seismic study of a shale expulsion syncline at the base of the champion delta, offshore Brunei and its implications for the early structural evolution of large delta systems', Marine and Petroleum Geology, 17(8), pp. 861–872.

Van Rensbergen, P. et al. (2007) 'Structural evolution of shale diapirs from reactive rise to mud volcanism: 3D seismic data from the Baram delta, offshore Brunei Darussalam', Journal of the Geological Society, 156(3), pp. 633–650.

Van Wagoner, J.C., and G.T. Bertram, "Sequence Stratigraphy of Foreland Basin Deposits." Amer. Assoc. Pet. Geol. Memoir 64, (1995), 490 pp.

Van Wagoner, J.C., H.W. Posamentier, R.M. Mitchum, P.R. Vail, J.F. Sarg, T.S. Loutit, and J. Hardenbol, An overview of sequence stratigraphy and key definitions. In C.K. Wilgus, B.S. Hastings, C.G. St. C. Kendall, H. Posamentier, C.A. Ross, and J.C. Van Wagoner (eds.), "Sea-Level Changes — An Integrated Approach." Soc. Econ. Paleo. and Mineral. (SEPM) Spec. Publ. 42, (1988), 39–45.

Van Wagoner, J.C., Mitchum R.M., and Rahmanian, V. D. (1990) 'Siliciclastic Sequence Stratigraphy in Well Logs, Cores, and Outcrops: Concepts for High-Resolution Correlation of Time and Facies_Pt. 2', AAPG Methods in Exploration Series 7, (7), pp. 16–20.

Van Wagoner, J.C., R.M. Mitchum, K.M. Campion, and V.D. Rahmanian, "Siliciclastic Sequence Stratigraphy in Well Logs, Cores, and Outcrops." Amer. Assoc. Pet. Geol. Methods in Exploration Series No. 7, (1990), 55 pp.

Waples, D. W. and Couples, G. D., 1998, Some thoughts on porosity reduction – rock mechanics, overpressure, and fluid flow. In: DUPPENBECKER, S. J. & ILIFFE, J. E. (eds) Basin Modelling: Practice and Progress. Geological Society, London, Special Publication, 141, 73-81

Waples, D.W. and Mahadir Ramly, 2001, A statistical method for correcting log-derived temperatures, *Petroleum Geoscience*, v. 7, pp. 231-240.

Ward, C., 1995. Evidence for sediment unloading caused by fluid expansion overpressure generating mechanisms. In: Fejerskov, M., Myrvang, A.M. (Eds.), *Proceedings of the Workshop on Rock Stress in the North Sea*. SINTEF and the University of Trondheim, Trondheim, pp. 218e231.

Webster, M., O'Connor, S., Pindar, B., and Swarbrick, R., 2011, Overpressures in the Taranaki Basin: Distribution, causes, and implications for exploration: *AAPG Bulletin*, v. 95, no. 3, p. 339–370.

Weimer, P., 1987, Seismic stratigraphy of three areas of lower slope failure, Torok Formation, northern Alaska, in I. L. Tailleux, and P. Weimer, eds., *Alaskan North Slope geology: SEPM Pacific Section Special Publication No. 50*, p. 481–496.

Weimer, P., 1989, Sequence stratigraphy of the Mississippi Fan (Plio-Pleistocene), Gulf of Mexico: *Geo-Marine Letters*, v. 9, p. 185–272.

Weimer, P., 1990, Sequence stratigraphy, seismic geometries, and depositional history of the Mississippi Fan, deep Gulf of Mexico: *AAPG Bulletin*, v. 74, p. 425–453.

Weimer, P., 1991, Seismic facies, characteristics, and variations in channel evolution, Mississippi Fan (Plio/Pleistocene), Gulf of Mexico, in P. Weimer and M. H. Link, eds., *Seismic facies and sedimentary processes of submarine fans and turbidite systems: Springer-Verlag, New York*, p. 323–347.

Weimer, P., and H. W. Pettingill, 2000, Many frontiers ultra-deep-water basins have strong hydrocarbon potential: *Offshore Magazine*, Special Issue: UltraDeep Engineering, p. 26–29.

Weimer, P., and M. H. Link, 1991, Global petroleum occurrences in submarine fans and turbidite systems, in P. Weimer, and M. H. Link, eds., *Seismic facies and sedimentary processes of submarine fans and turbidite systems*: Springer-Verlag, New York, p. 9-67.

Weimer, P., and R. T. Buffler, 1992, Structural geology and evolution of the Mississippi Fan foldbelt, deep Gulf of Mexico: *AAPG Bulletin*, 76, 225–251.

Weimer, P., J. R. Crews, R. S. Crow, and P. Varnai, 1998, Atlas of the petroleum fields and discoveries in northern Green Canyon, Ewing Bank, and southern Ship Shoal and South Timbalier area (offshore Louisiana), northern Gulf of Mexico: *AAPG Bulletin*, v. 82, p. 878-917.

Weimer, P., P. Varnai, P., F. M. Budhijanto, Z. M. Acosta, R. E. Martinez, A. F. Navarro, M. G. Rowan, B. C. McBride, T. Villamil, C. Arango, J. R. Crews, and A. J. Pulham, 1998, Sequence stratigraphy of Pliocene and Pleistocene turbidite systems, northern Green Canyon and Ewing Bank (offshore Louisiana), northern Gulf of Mexico: *AAPG Bulletin*, 82., no. 5b, p. 918-960.

Weimer, P., R. M. Slatt, J. L. Coleman, N. Rosen, C. H. Nelson, A. H. Bouma, M. Styzen, and D. T. Lawrence, eds., 2000, *Global deep-water reservoirs: Gulf Coast Section—SEPM Foundation Bob. F. Perkins Twentieth Annual Research Conference*, 1104 p.

Weimer, P., R. M. Slatt, P. Dromgoole, M. Bowman, and A. Leonard, 2000a, Developing and managing turbidite reservoirs: case histories and experiences—results from the AAPG/EAGE Research conference: *AAPG Bulletin*, v. 84, p. 453–464.

Wu, J. and Suppe, J. (2018) ‘Proto-South China Sea Plate Tectonics Using Subducted Slab Constraints from Tomography’, *Journal of Earth Science*, 29(6), pp. 1304–1318.

Wu, J., McClay, K. and de Vera, J. (2020) 'Growth of triangle zone fold-thrusts within the NW Borneo deep-water fold belt, offshore Sabah, southern South China Sea', *Geosphere*, 16(1), pp. 329–356.

Yardley, G.S., and Swarbrick, R.E., 2000, Lateral transfer: A source of additional overpressure? *Marine and Petroleum Geology*, v. 17, no. 4, p. 523–537.

Yassir, N. A., and J. S. Bell, 1996, Abnormally high fluid pressures and associated porosities and stress regimes in sedimentary basins: *SPE Formation Evaluation*, 11, 5–10, doi: 10.2118/28139-PA.

Yassir, N., Addis, M.A., 2002. Relationships between pore pressure and stress in different tectonic settings. In: Huffman, A.R., Bowers, G.L. (Eds.), *Pressure Regimes in Sedimentary Basins and Their Prediction*. AAPG, Tulsa, pp. 79e88.

Zhang, J., 2011, Pore pressure prediction from well logs: Methods, modifications, and new approaches: *Earth-Science Reviews*, 108, 50–63, doi: 10.1016/j.earscirev.2011.06.001.

Zhang, J., 2013, Effective stress, porosity, velocity and abnormal pore pressure prediction accounting for compaction disequilibrium and unloading', *JMPG. Elsevier*, 45, pp. 2–11. doi: 10.1016/j.marpetgeo.2013.04.007.

Zhao, J., Li, J. and Xu, Z. (2018) 'Advances in the origin of overpressures in sedimentary basins', *Petroleum Research. Elsevier Taiwan LLC*, 3(1), pp. 1–24. doi: 10.1016/j.ptlrs.2018.03.007